PROPERTIES EVALUATION OF SOFTWOOD MODIFIED WITH MONOMERS AND NANOFILLERS

A thesis submitted in partial fulfillment of the requirements for the degree of Doctor of Philosophy

By

ANKITA HAZARIKA
Registration No. TZ121486 of 2012

School of Sciences
Department of Chemical Sciences
Tezpur University, Napaam
Assam-784 028, India
January, 2014

Dedicated

to my beloved parents

तेजपुर विश्वविद्यालय
(केंद्रीय विश्वविद्यालय)
नपाम, तेजपुर - 784 028, असम, भारत

TEZPUR UNIVERSITY
(A Central University)
Napaam, Tezpur - 784 028, Assam, India

CERTIFICATE

This is to certify that the thesis entitled "**PROPERTIES EVALUATION OF SOFTWOOD MODIFIED WITH MONOMERS AND NANOFILLERS**" submitted by Ankita Hazarika, Research Scholar of Department of Chemical Sciences, Tezpur University, Assam for the award of degree of Doctor of Philosophy to the School of Sciences, is a record of bonafide research work done under my supervision and guidance at Department of Chemical Sciences, Tezpur University. She has successfully completed the work.

She has fulfilled all the requirements for submitting the thesis for award of the degree of Doctor of Philosophy in Science.

The results embodied in the thesis have not been submitted to any other University or Institution for award of any degree or diploma.

Place: Tezpur

Date: 28/05/14

Tarun K Maji

(Prof. Tarun K. Maji)

फोन / Phone : 03712-267007 - 9 (3 lines) • फैक्स / Fax : 03712-267005, 267006 • ई-मेल / e-mail : admn@tezu.ernet.in

DECLARATION

I hereby declare that the thesis entitled "**PROPERTIES EVALUATION OF SOFTWOOD MODIFIED WITH MONOMERS AND NANOFILLERS**" is an authentic work carried out by me under the supervision of Prof. Tarun K. Maji, Department of Chemical Sciences, Tezpur University, Assam. No part of this work had been presented for any other degree or diploma earlier.

Place: Tezpur
Date:

Ankita Hazarika
(Ankita Hazarika)

ACKNOWLEDGEMENTS

At the very outset, I express my deep gratitude and sincere thanks to my research guide, Prof. Tarun K. Maji for his invaluable guidance and constant encouragement. Without his helpful, patient and encouraging advice and guidance for the solution of a number of knotty problems, it would never have been possible to finish the work successfully in time.

I acknowledge my gratitude to my doctoral research committee member, Dr. A.J. Thakur and Dr. M. Mandal, Department of Molecular Biology & Biotechnology for their valuable help and suggestion in my research work.

I would like to extend my sincere thanks to our honourable vice chancellor Prof. M.K. Choudhury for permitting me to carry out my work in the form of thesis.

I am very grateful to Prof. N. S. Islam, Prof. S. K. Dolui, Prof. N. Karak, Prof. R. C. Deka (HOD), Dr. R. Dutta, Dr. R. Borah, Dr. A. Phukan, Dr. P. Pujari, Dr. K. K. Bania, Dr. P.Bharali, Dr. N. Gogoi, Dr. B. Sarma, Dr. S.K. Das and Dr. U. Bora for their invaluable help, guidance and encouragement throughout my work.

I also express my sincere thanks to Dr. Biren Gohain, Mr. Rajen Bora, Mr. Nipu Dutta, Mr. Arup Chakrabarty, Mr. Ratan Boruah, Mr.Raju Kr. Borah, Mr. Sankur Phukan, Mr. Manuranjan Sarma, Mr. Biraj Borah, Mr. Hemanta Gogoi and Ms. Babita Das. I am also very much indebted to my lab mates, friends and well wishers, who encouraged me throughout my research work.

Words are short to express my deep sense of gratitude to Dr. B.K. Deka for his valuable suggestion at the hour of need who helped me to carry out DMA test and Raman Spectroscopy. A discussion with him was always vitalizing and encouraging for me. I would like to thank Mr. George of SAIF, North East Hill University, Shillong for TEM analysis.

A bouquet of special appreciation and high regards goes to my beloved parents, elder brother and sister-in-law for their moral support and blessings. I owe everything to them. The endless love from my nephews Sunnie and Ronnie inspired me in every step of my life.

Lastly, I sincerely acknowledge the financial support received from Tezpur University in the form of Institutional Fellowship, without which this research work would never have been possible.

Place: Tezpur University, Tezpur
Date: *(Ankita Hazarika)*

ABSTRACT

ABSTRACT

Wood–polymer composites (WPCs) are one of the most important trades of today's plastic industry. The awareness for the utilization of renewable resources is pushing in many fields of applications of polymers. As a consequence of this, composite industries are seeking more environmental friendly materials for their products. Wood is one of the best known natural engineering materials and perhaps it is also one of the most natural resources available abundantly. Though it has a pivotal role in human society, yet some unfavorable properties restrict its widespread applications. It is a heterogeneous material composed of cellulose, hemicellulose and lignin. The presence of free hydroxyl groups of cellulose and hemicellulose cause absorption of atmospheric moisture. Thus wood changes its dimension under different moisture condition and is susceptible to degradation when exposed to microorganisms.

The North Eastern part of India is bestowed with huge storage of woods. Two types of wood are available viz. hard and soft wood. Hard woods are mainly used for construction purposes. Softwoods are generally dimensional weak, lacking in strength and have poor mechanical properties which restrict their use. They are mostly used for fuel purpose. These lower grade wood can be modified through the fabrication of WPC by impregnating polymer through *in situ* polymerization to make it value added material suitable for different purposes. WPC generally exhibit remarkable improvement in properties of wood like low moisture absorption and high resistance to UV ray damage and decay, insect etc.

Various types of vinyl monomers and low molecular weight resins are used for impregnation into wood for bringing superior properties. Wood impregnated with thermosetting resin can effectively improve the properties of wood as it can penetrate in the cell wall of wood. The impregnation of wood with vinyl monomer leads to an improvement in dimensional stability, mechanical properties and water resistance. Though these monomers impart dimensional stability, they are effective in filling the cell lumen but not effective in filling the cell wall.

Crosslinking agents are used to improve penetration of this monomer into the cell wall of wood. They are bifunctional or multifunctional monomer that increase the interfacial interaction between wood and polymer and hence increases the polymer loading.

Flame retardancy is a desirable property of WPC. The high molecular weight polymeric flame retardant obtained from renewable resource will minimize leaching

problem and improve the service life of the composite. Moreover it is eco-friendly. The gum obtained from *Moringa oleifera* plant can be used as an effective flame retarding agent.

The use of nanotechnology opens up the opportunity to produce new materials with unique properties and improved products for many applications. It is a striking field to develop high-valued wood polymer nanocomposite (WPNC). Retention of homogenous distribution of the nanoparticles in the polymer matrix is essential for the nanocomposites to offer improved properties as the properties are greatly influenced by the degree of mixing between the two phases. The nanofillers used can be easily accommodated into the porous structure of wood. Nanofillers based WPC as *in situ* nano reinforcement offers new opportunities with enhanced physical, thermal, and mechanical properties.

In this work, WPNC were prepared by impregnating different types of monomer/copolymer like methyl methacylate, melamine formaldehyde-furfuryl alcohol and melamine formaldehyde-acrylamide copolymer along with crosslinker into a softwood *Ficus hispida*. A comparative study of the properties of the WPNC was done using different crosslinking agent. Flame retardant obtained from renewable resource i.e from a local plant *Moringa oleifera* was incorporated into the composites. Different nanoparticles were used for the preparation of WPNC which included nanoclay, ZnO, SiO_2, TiO_2, multiwalled carbon nanotubes (MWCNT). The effect of monomer/copolymer and nanoparticles on the final properties of WPNC was also studied.

Chapter I: This chapter includes introduction part. Here the structure, composition and properties of wood have been discussed. The modification of wood by impregnation of various polymers/monomers, crosslinking agents, flame retarding agents are included. The perception of polymer nanocomposites and the properties of different nanofillers are discussed. The techniques for preparation of composites have been included. The insight of wood polymer nanocomposites has been discussed. Its merits, demerits and applications have been elaborated.

Chapter II: This chapter includes the literature review part. A comprehensive literature survey associated with wood polymer composite has been done and reported in this chapter. Various technical processes used for modification of wood and preparation of WPNC through different curing methods have been discussed. The effect of impregnation of monomer/polymer, crosslinker, nanofillers into wood has been elaborated. The techniques

for the characterization of wood polymer nanocomposites have been included. All the properties of wood polymer nanocomposites have been discussed. Besides, the objective and plan of work of the present investigation has also been focused in this chapter.

Chapter III: This chapter includes the raw materials, chemicals and methods used in the preparation of wood polymer nanocomposites. It also includes the methods of characterization and the procedure for measurement of the various properties of the composites.

Chapter IV: This chapter covers the results and discussion part. This chapter has been subdivided into six sections.

***Section A*: Studies on properties of softwood (*Ficus hispida*)/PMMA nanocomposites reinforced with polymerizable surfactant-modified MMT.**

In this part, chemical modification of softwood was done by impregnation of methyl methacrylate (MMA) monomer in presence of glycidyl methacrylate (GMA), a cross linking agent and montmorillonite (MMT) using catalyst heat treatment. The surface modification of MMT was done by using polymerizable surfactant 2-acryloloxy ethyl trimethyl ammonium chloride (ATAC) and a mixture of surfactants 2-acryloloxy ethyl trimethyl ammonium chloride (ATAC) and cetyl trimethyl ammonium bromide (CTAB) in a molar ratio of (1:1). Comparison between the different properties of the ATAC-MMT treated wood polymer nanocomposite (WPNC) and (ATAC+CTAB)-MMT treated WPNC were studied.

The impregnation condition at which maximum improvement in properties was found by varying monomer concentration, initiator concentration, vacuum, time of impregnation, amount of crosslinking agent and modified MMT. Organophillic clay was dispersed initially in tetrahydrofuran (THF) and finally in MMA prepolymer. The minimum ratio (v/v) of MMA and THF used for the dispersion of clay was 5:1. The final optimized conditions, at which maximum improvement of properties were observed as follows: MMA (mL): 100, THF (mL): 20, 2,2'-Azoisobisbutyronitrile (AIBN): 0.5 %, vacuum: 508 mm of Hg, time of impregnation: 4 h, GMA (mL): 3, (ATAC+CTAB)-MMT: 0.5-1.5 phr and ATAC-MMT: 0.5-1.5phr.

The performance characteristic of the WPNC were evaluated in terms of weight percent gain (WPG %), volume increase (%) and hardness. Fourier transform infrared spectroscopy (FTIR) and X-ray diffractometry (XRD) studies were used to characterize the surface modification of MMT and the formation of WPNC. An increase in interlayer spacing of clay was observed after modification as detected by XRD. However, the increase was more prominent when MMT was modified with combined surfactant. X-ray studies also showed that the crystallinity in WPNC decreased and some silicate nanolaminae were inserted into the amorphous region of wood cellulose. FTIR study indicated that there was some interaction between wood, MMA, GMA and clay. Scanning electron microscope (SEM) study showed the existence of polymer, clay within the cell wall or lumen of wood. Transmission electron microscopy (TEM) study revealed the impregnation of MMT into the composites. WPNC prepared by using combined surfactant modified clay along with MMA/GMA exhibited improved dimensional stability, reduced water uptake capacity, higher water repellency, antiswelling efficiency and chemical resistance than that of WPNC prepared by using single surfactant modified clay and MMA/GMA system. The thermal stability and mechanical properties improved significantly for the treated wood samples with combined surfactant modified clay.

***Section B*: Study on the properties of wood polymer nanocomposites based on melamine formaldehyde-furfuryl alcohol copolymer and modified clay.**

In this part of work, wood polymer nano composite was prepared by impregnating melamine formaldehyde-furfuryl alcohol (MFFA) copolymer, n-methylol acrylamide, (NMA), a crosslinking agent and MMT into wood (*Ficus hispida*) and using catalyst heat treatment. MMT was modified by using a polymerizable surfactant ATAC and a mixture of surfactants ATAC and CTAB in a molar ratio of 1:1. A comparative study was done on the effect of impregnation of unmodified MMT, MMT modified with ATAC and a mixture of surfactants ATAC and CTAB on the various properties of WPNC.

The optimized condition to obtain maximum improvement in properties was found by varying time of impregnation, vacuum, monomer concentration, catalyst concentration and amount of crosslinking agent. The conditions were: 6 h time of impregnation, 500 mm Hg vacuum, 5:1 [MFFA:FA (furfuryl alcohol)-water] prepolymer concentration, 1% (w/w) maleic anhydride, 3 mL NMA, 2 phr MMT.

Nuclear magnetic resonance (NMR) and FTIR studies confirmed the formation of MFFA copolymer, NMA. FTIR studies also confirmed the modification of MMT. It also indicated an interaction between wood, polymer, crosslinker and MMT as observed from the reduction of the intensity of hydroxyl peak of wood cellulose and shifting of the peak to lower wavenumber. XRD studies revealed an increase in gallery distance of MMT after organic modification. The decrease in crystallinity of wood cellulose in the composites was more efficient when wood was impregnated with combined surfactant modified clay. SEM study revealed the presence of polymer, crosslinker and clay in the void spaces of wood. TEM study indicated the dispersion of clay in the MFFA polymer. Wood treated with modified MMT exhibited lower water uptake, higher dimensional stability, enhanced chemical resistance, themostability, flame retardancy, and better mechanical properties than wood samples treated with unmodified clay. Samples treated with combined surfactant (ATAC+CTAB) modified clay exhibited better property compared to those of samples treated with single surfactant (ATAC) modified clay.

***Section C*: Effect of different crosslinkers on properties of melamine formaldehyde-furfuryl alcohol copolymer/montmorillonite impregnated softwood (*Ficus hispida*).**

The aim of the present work is to compare the effect of different crosslinkers on the various properties of WPC. MFFA copolymer is synthesized and impregnated into wood in combination with crosslinking agent and MMT under vacuum condition. Different crosslinkers namely n-methylol acrylamide, (NMA), 2-hydroxyethyl methacrylate (HEMA) and 1,3-dimethylol-4,5-dihydroxyethyleneurea (DMDHEU) and mixture of all the three crosslinkers were used for evaluation of properties of the prepared composites. The effect of MMT on the properties of the composites was also studied.

NMR studies confirmed the formation of DMDHEU. FTIR studies also confirmed the formation of MFFA copolymer, NMA and DMDHEU crosslinkers and showed that maximum interaction was found in samples treated with mixed crosslinkers and MMT. XRD study showed that the incorporation of MMT decreased the crystallinity of wood composites. SEM revealed the existence of polymer and MMT in cell wall and cell lumen of wood. TEM study indicated that MMT was incorporated in the composites. Thermal stability and flammability were checked by thermogravimetric analyser (TGA) and limiting oxygen index (LOI) instrument. It was observed that maximum thermal stability and flame

retardancy were shown by the samples treated with mixture of crosslinkers and MMT followed by the samples treated with mixed crosslinker NMA, HEMA and DMDHEU. Wood treated with MFFA, blended crosslinker and MMT exhibited higher dimensional stability, lower water uptake (%), enhanced chemical resistance and better mechanical properties (flexural, tensile and hardness).

***Section D*: Studies on the properties of wood polymer nanocomposites impregnated with melamine formaldehyde-furfuryl alcohol copolymer and nanoclay.**

The present investigation has been carried out to prepare WPNC using MFFA copolymer, DMDHEU as crosslinker and nanoclay. Attempts have also been made to study the various properties like water repellency, dimensional stability, chemical resistance, flammability, mechanical properties, and ultraviolet (UV) resistance properties.

MFFA, DMDHEU and WPNC were characterized by FTIR. XRD study showed a decrease in crystallinity in WPNC samples. A decrease in the crystallinity index value was obtained as determined from FTIR and XRD studies. The presence of clay in cell lumen and cell wall was detected by SEM study. Energy dispersive X-ray spectroscopy (EDS) and TEM study supported the impregnation of nanoclay into the composites. Addition of nanoclay improved properties like water resistance, dimensional stability, chemical resistance, flame retardancy and mechanical properties. The UV resistance property of WPNC increased considerably as judged by the rate of weight loss, carbonyl index, lignin index, crystallinity index values, SEM and mechanical properties. Treated samples showed an improvement in elastic modulus, loss modulus and damping index as indicated by dynamic mechanical analysis (DMA). The improvement in storage modulus, loss modulus and mechanical loss factor indicated better interfacial interaction between wood, polymer, crosslinker and clay. The incorporation of nanoclay improved the thermal stability of the composites. The apparent activation energy for the relaxation process in the glass transition region increased with the increase in the amount of nanoclay. Untreated wood exhibited maximum biodegradability whereas polymer treated wood showed minimum biodegradability. Addition of nanoclay improved the biodegradability of the polymer treated wood samples. Loss in mechanical properties, weight loss, hardness and SEM analysis showed that untreated wood had higher biodegradability followed by the samples treated with MFFA/DMDHEU/nanoclay and MFFA/DMDHEU.

***Section E*: Thermal decomposition kinetics, flammability and mechanical property study of wood polymer nanocomposite.**

This part of work embodies the results of incorporation of a renewable polymer, collected as gum from a local plant (*Moringa oleifera*) as flame retardant along with MFFA copolymer, DMDHEU, a crosslinking agent and nanoclay under vacuum condition and polymerized by catalyst heat treatment.

FTIR study confirmed the formation of MFFA, DMDHEU and indicated an interaction between the impregnates suggesting the impregnation of polymers and nanoclay into wood. XRD study showed the decrease of crystallinity of WPNC. The morphological structures of the nanocomposites were studied by SEM. TEM showed the uniform distribution of nanoclay in the composites. A notable enhancement in properties such as weight percent gain (%), hardness, dimensional stability, mechanical properties and reduced water uptake (%) were observed for the treated wood samples. The plant polymer had a marked influence on the flammability and thermal stability of the prepared composites. The apparent activation energy was determined by Ozawa-Flynn-Wall's (OFW) and Vyazovkin methods. Both the methods showed similar trends in respect of activation energy but the results of apparent activation energy differ significantly because of the presence of systematic error in OFW method. The activation energy of the composites decreased upto a certain decomposed fraction thereafter it remained constant. With the increase in the amount of plant polymer, there was an increase in the interfacial interaction between the polymer, crosslinker, nanoclay and plant polymer through its abundant hydroxyl groups. The better dispersion and enhanced interaction resulted in higher activation energy of the prepared composites.

***Section F*: Melamine formaldehyde-acrylamide copolymer and plant polymer impregnated softwood polymer composite.**

The objective of the work is to prepare melamine formaldehyde-acrylamide (MFA) copolymer and to vacuum impregnate it into wood in presence of DMDHEU as crosslinker, vinyl trichloro silane (VTCS) modified MMT and plant polymer (PP) derived from *Moringa oleifera* as a flame retarding agent under catalyst heat treatment.

Nuclear magnetic resonance (NMR) study was used to confirm the formation of MFA and DMDHEU. FTIR study was used to confirm the surface modification of MMT and characterization of the wood polymer nanocomposites. The crystallinity of the composites was studied by XRD. SEM and TEM study revealed the presence of polymer and MMT in the composites. Flame retardancy and thermal stability improved remarkably after incorporation of plant polymer in the composites. The other properties of WPNC like hardness, water uptake, chemical resistance, mechanical properties enhanced to a great extent for the treated wood samples.

Chapter V: This chapter deals with the results of the incorporation of multiple nanoparticles like ZnO, SiO_2, TiO_2, and multiwalled carbon nanotubes (MWCNT) into wood. This chapter has been subdivided into four sections.

***Section A*: Effect of ZnO and nanoclay on the properties of softwood chemically modified with melamine formaldehyde-furfuryl alcohol/plant polymer.**

This part of work reports the effect of N-Cetyl-N,N,N-trimethyl ammonium bromide (CTAB) modified ZnO and nanoclay on the performance characteristics of WPNC impregnated with MFFA copolymer, DMDHEU, a crosslinking agent and plant polymer derived from *Moringa oleifera* as a flame retarding agent under vacuum condition.

FTIR and XRD studies were employed for the characterization of modified ZnO and WPNC. XRD revealed no transformation of cellulose I to cellulose II for the treated wood samples. The change in crystallinity index value of the cellulose in wood and the distribution of ZnO nanoparticles in composites were determined by using FTIR and XRD. SEM and TEM study showed the presence of nanoparticles and nanoclay in the cell lumen or cell wall of wood. The UV resistance of the composites increased significantly after incorporation of ZnO and plant polymer into the composites as evidenced by weight loss, carbonyl index, lignin index, crystallinity index values, SEM and lower mechanical properties loss. The treated wood samples showed an improvement in mechanical, flame retarding properties, thermal stability and lower water uptake capacity. Maximum properties improvement was found in WPC loaded with 3 phr each of nanoclay, ZnO and plant polymer.

***Section B*: Properties of softwood polymer composites impregnated with nanoparticles and melamine formaldehyde furfuryl alcohol copolymer.**

SiO_2 is known to increase mechanical properties and thermal stability in polymer composites. In this work, synergistic effect of CTAB modified SiO_2 nanoparticles and nanoclay on the various properties of WPNC impregnated with MFFA copolymer, DMDHEU and plant polymer have been focused.

Surface modification of SiO_2 was verified by FTIR and XRD study. A decrease in crystallinity of wood cellulose was observed as determined from FTIR and XRD studies. The crystallinity index value of wood cellulose decreased from 63.8 to 30.8. The presence of traces of the nanofillers SiO_2, nanoclay and polymer in the wood cell wall and cell lumen was detected by SEM. TEM analysis confirmed the impregnation of nanoclay and SiO_2 into the composites. Remarkable reduction in water uptake capacity was observed for the treated wood samples. Both tensile and flexural properties of WPC were found to improve. An improvement in chemical resistance, flame retardancy and thermal stability were observed in the composites due to treatment.

***Section C*: Synergistic effect of nano TiO_2 and nanoclay on the properties of softwood composites modified with melamine formaldehyde-furfuryl alcohol copolymer and plant polymer.**

This part of work deals with the effect of incorporation of TiO_2 and nanoclay on the various properties of WPNC. MFFA copolymer, DMDHEU and plant polymer were also impregnated into softwood under vacuum condition.

The surface of TiO_2 was modified by using cationic surfactant CTAB. FTIR and XRD were used to confirm the surface modification of TiO_2 and interfacial interaction between wood, polymer, crosslinker and nanoparticles. The crystallinity index value obtained from FTIR and XRD indicated a decrease in crystallinity of wood cellulose for the treated wood samples. Energy dispersive X-ray spectroscopy (EDS) indicated the modification of TiO_2 nanoparticles and the presence of phosphorus in the plant polymer. The uniform distribution of nanoclay and TiO_2 was evidenced by TEM and SEM study. UV resistance of the composites improved significantly as judged by the measurement of weight loss, carbonyl index, lignin index, crystallinity index values, SEM and mechanical properties. The rate of decrease in crystallinity index value was more pronounced in case of

untreated wood than the treated wood samples after UV degradation. The treated wood samples showed reduced water uptake. A considerable improvement in thermal stability, mechanical properties and flame retardant properties of the composites were observed. WPNC loaded with nanoclay, TiO_2 and plant polymer showed an overall improvement in properties.

***Section D*: Strain sensing behavior and dynamic mechanical properties of carbon nanotubes/nanoclay reinforced wood polymer composite.**

Carbon nanotubes (CNT) are considered to be new emergent multifunctional materials that have outstanding mechanical and thermal properties. In this part of work, the synergistic effect of multiwalled carbon nanotubes (MWCNT) and nanoclay on the dynamic mechanical properties, strain sensing behavior and water repellency of the WPNC has been highlighted.

XRD indicated a decrease in crystallinity of wood cellulose in the composites after incorporation of MWCNT. The surface modification of MWCNT and formation of the composites were confirmed from Micro Raman spectroscopy by the increased ratio of D band to G band. Strain dependent Raman spectroscopy showed efficient load transfer from the wood/polymer to the nanotubes. With the increase in the MWCNT content, the shifting of Raman 'G'-band occurred. This indicated an efficient load transfer as well as a good interfacial interaction between wood, polymer, nanoclay and MWCNT in the composite. Surface morphology and the uniform distribution of nanoclay and MWCNT in the cell wall and cell lumen were studied by SEM. An improvement in elastic modulus, loss modulus and damping index was observed in WPNC as indicated by dynamic mechanical analysis (DMA) test. Mechanical loss factor shifted to higher temperature for the treated wood samples. At a fixed nanoclay loading, with the increase in the content of MWCNT in the composites the apparent activation energy for the relaxation process in the glass transition region increased. Tensile, flexural and water repellency properties enhanced considerably for the wood samples treated with 3 phr nanoclay and 1.5 phr MWCNT.

Chapter VI: This last chapter includes summary, conclusion, highlights of the findings and the future scope of the present investigation. The features of the present study have been summarized as follows:

Abstract

In the present investigation, wood polymer nanocomposites were prepared by impregnation of water insoluble monomer MMA, GMA a crosslinking agent, MMT modified by polymerizable surfactant ATAC and a mixture of surfactants ATAC and CTAB in a molar ratio of (1:1). The final optimized conditions were as follows: MMA (mL): 100, THF (mL): 20, AIBN: 0.5 %, vacuum: 508 mm of Hg, time of impregnation: 4 h, GMA (mL): 3. The composites were characterized by conventional spectroscopic techniques. WPNC prepared by using combined surfactant modified clay along with MMA/GMA exhibited improved dimensional stability, chemical resistance, thermal stability, mechanical properties and lower water uptake than that of WPNC prepared by using single surfactant modified clay.

Water soluble MFFA and MFA copolymers were also used for the preparation of WPNC in presence of crosslinking agents namely NMA, HEMA and DMDHEU with different nanofillers. The optimized conditions for getting maximum improvement in properties were 500 mm Hg vacuum, 6 h time of impregnation, 5:1 (MFFA:FA-water)/(MFA:water) prepolymer concentration, 1% (w/w) maleic anhydride/0.75% (w/w) $K_2S_2O_8$, 3 mL DMDHEU/NMA/HEMA. Among the three crosslinker, DMDHEU was found to be the most efficient crosslinker. An improvement in properties of the composites was observed on addition of MMT. MMT was modified by combined surfactant CTAB+ATAC and by single surfactant ATAC alone. Among the unmodified MMT, ATAC-MMT, (CTAB+ATAC)-MMT treated WPC, superior properties was shown by the samples treated with the combined surfactant modified MMT, followed by the single surfactant modified MMT. Least improvement in property was shown by WPC treated with unmodified MMT. Highest improvement in properties was obtained at 2 phr of (ATAC+CTAB) modified MMT. The addition of nanoclay (clay modified by 15–35 wt.% octadecylamine and 0.5–5 wt.% aminopropyltriethoxy silane) to MFFA and DMDHEU improved the overall properties of the composites. Maximum property enhancement was obtained at 3 phr of nanoclay. The use of flame retarding agent obtained from the plant *Moringa oleifera* had a significant influence on thermal stability and flame retardancy of the composites. The thermal decomposition kinetic studies of the composites were performed and the apparent activation energy was determined by Ozawa-Flynn-Wall's and Vyazovkin methods. WPNC prepared by impregnation of MFA copolymer, DMDHEU, vinyl trichloro silane modified MMT and plant polymer showed a maximum improvement in properties loaded with 3 phr plant polymer. The incorporation of CTAB modified ZnO/nanoclay along with MFFA/DMDHEU

and plant polymer showed an improvement in UV resistance, mechanical, flame retarding properties, thermal stability and lower water uptake capacity of the composites. The properties also improved by using CTAB modified SiO_2 nanoparticles along with nanoclay and plant polymer. CTAB modified TiO_2 and nanoclay based WPNC in combination with plant polymer enhanced UV resistance, mechanical, flame retarding properties, thermal stability and lower water uptake capacity of the composites. Incorporation of MWCNT along with nanoclay into WPC leads to enhanced dynamic mechanical properties. The apparent activation energy for the relaxation process in the glass transition region increased. Strain dependent Raman spectroscopy showed efficient load transfer from the wood/polymer to the nanotubes indicating better interfacial interaction. Tensile, flexural, hardness and water repellency properties improved significantly for the composites.

***Future scope*:**

Wood polymer nanocomposites were prepared by impregnation of different monomer/copolymer, crosslinker, plant polymer and multiple nanofillers under vacuum condition. A thorough investigation is essential for large scale commercial consumption of the product, although laboratory study shows improvement in numerous properties. Modification of the lower grade soft wood can be a substitute for the high quality timber as there is a shortage of these higher grade woods. The use of biopolymer and additives obtained from renewable resources is another panorama of wood modification through green route. Nanotechnology with different nanofillers as an *in situ* reinforcement offers prospective for value added materials. The ratio of these nanofillers used can be fine tuned for achieving further better properties of the composites. It is proper to attempt nano technology for wood modification to eradicate the environmental hazards in terms of low emission of volatile organic compounds.

CONTENTS PAGE NO.

LIST OF ABBREVIATIONS & SYMBOLS

Chapter I:

WPC	: Wood polymer composites
WPNC	: Wood polymer nanocomposite
MAA	: Methacrylic acid
PMMA	: Poly(methyl methacrylate)
MF	: Melamine–formaldehyde
FA	: Furfuryl alcohol
%	: Percentage
nm	: Nanometre
LCC	: Lignin-carbohydrate complex
kg	: Kilogram
m	: Metre
lb	: Pound
ft	: Feet
g	: Gram
cm	: Centimetre
μm	: Micrometre
PEG	: Poly(ethylene glycol)
°F	: Degree Fahrenheit
°C	: Degree centigrade
MOE	: Modulus of elasticity
AM	: Acrylamide
GMA	: Glycidyl methacrylate
DMDHEU	: 1,3-dimethylol 4,5-dihydroxyethylene urea
NMA	: N-methylol acrylamide
HEMA	: 2-Hydroxyethyl methacrylate
FR	: Flame retardant
SWCNT	: Single-walled carbon nanotubes
MWCNT	: Multi-walled carbon nanotube
CNT	: Carbon nanotubes
MMT	: Montmorillonite
ZnO	: Zinc oxide

meV	:Megaelectron volts
eV	: Electron volt
SiO_2	: Silicon dioxide
Ccp	: Cubic close-packed
TiO_2	: Titanium dioxide

Chapter II:

min	: Minute
AIBN	: 2,2'-azobis isobutyronitrile
WRE	: Water repellent effectiveness
MMA	: Methyl methacrylate
HEMA	: 2-Hydroxyethyl methacrylate
EGDMA	: Ethylene glycol dimethacrylate
WPG	: Weight percent gain
MUF	: Melamine-urea-formaldehyde resin
PF	: Phenol formaldehyde
OMMT	:Organophilic MMT
XRD	: X-ray diffraction
SEM	: Scanning electron microscopy
FTIR	: Fourier transform infrared spectroscopy
DMTA	: Dynamic mechanical thermal analysis
E_d	: Dynamic Young's modulus
DTG-TG-DTA	: Differential thermogravimetry-thermogravimetric-differential thermal analysis
TGA	: Thermogravimetric analysis
OFW	: Ozawa-Flynn-Wall
APP	: Ammonium polyphosphate
UV	: *Ultraviolet*
MFFA	: Melamine formaldehyde-furfuryl alcohol

Chapter III:

PP	: Plant polymer
CTAB	: N-Cetyl –N, N, N-trimethyl ammonium bromide

ATAC	: 2-Acryloloxy ethyl trimethyl ammonium chloride
mL	: Millilitre
lb_f	: Pound force
h	: Hour
rpm	: Revolution per minute
CEC	: Cation exchange capacity
Meq	: Milli equivalent
THF	: Tetrahydrofuran
pH	: Potential of hydrogen
DHEU	: 4,5-dihydroxyethylene urea
ASTM	: American standard testing machine
NMR	: Nuclear magnetic resonance
FTNMR	: Fourier transform nuclear magnetic resonance
MHz	: Megahertz
DMSO	: Dimethyl sulphoxide
TMS	: Trimethyl silane
CrI	: Crystallinity index
kV	: Kilovolts
WPG	: Weight percent gain
RH	: Relative humidity
ASE	: Antiswelling efficiency
MOR	: Modulus of rupture
kN	: Kilonewton
DMA	: Dynamic mechanical analysis
Hz	: Hertz
LOI	: Limiting oxygen index
cc	: Cubic centimeter
s	: Second
α	: Degree of conversion of decomposed fraction
A	: Pre-exponential factor
E_a	: Activation energy of thermal decomposition
R	: Gas constant
β	: Heating rate

T	: Absolute temperature
n	: Reaction order
LI	: Lignin index

Chapter IV:

mm	: Millimetre
Phr	: Parts per 100 parts of materials
Clay I	: Clay modified with ATAC/CTAB (1:1 mole)
Clay II	: Clay modified with ATAC
Clay III	: Unmodified MMT
w/w	: Weight by weight
T_i	: Initial decomposition temperature
T_m	: Maximum pyrolysis temperature
T_D	: Decomposition temperature at different weight loss
RW	: Residual weight
ppm	: Parts per million
θ	: Scattering angle
λ	: Wavelength
MFA	: Melamine formaldehyde-acrylamide
VTCS	: Vinyl trichloro silane
v/v	: Volume by volume
w/v	: Weight by volume
MWCNT-OH	: Hydroxyl modified MWCNT
I_D	: Intensity of D-band
I_G	: Intensity of G-band
T_g	: Glass transition temperature
E'	: Storage modulus
E''	: Loss modulus
tan δ	: Damping parameter

LIST OF TABLES

LIST OF FIGURES

CHAPTER I

INTRODUCTION

CHAPTER I
INTRODUCTION

1.1. Overview and history

In the past decades, governments have made more strict legislation due to increase in the environmental awareness. This promotes the preservation and protection of the quality of the chemical industry and they must develop cleaner chemical processes or materials by the design of innovative for future generations. Therefore, the cleaner chemical processes or the products formed by the pioneering design should produce minimum environmental impact. Wood is an important natural resource, one of the few that are renewable. The extensive variety of products confirms the versatility of wood [1]. Carbon dioxide in the atmosphere can be minimized by the use of wood and wood products because they are also a store for carbon. Many wood products can be recovered for reuse or recycling, thus extending our wood supply into the future. The high cost of the tropical hardwood species and rise in demand for high quality timber led researchers to investigate new technologies to modify the lower grade wood. These lower grade woods have inferior properties and are not suitable for various engineering and structural applications. There are various manufacturing processes, and a number of ways to apply preservative treatments to these materials [2]. As the needs to replace the less eco-friendly materials with more sustainable ones are growing, attempts have been made to utilize raw materials, increase production efficiencies and develop more sustainable industrial practices. Chemical modification offers opportunities not found in the solid wood preserving industry so as to enhance its service life.

1.2. Wood

The importance of wood for the development of mankind from prehistoric to present time cannot be emphasized enough. A great variety of products including paper products, construction timber and sports equipments are manufactured by utilizing wood as the raw material. The wood species selected for a specific purpose depends on its structural variations. The heavier woods generally have stronger mechanical properties, such as bending strength, crushing strength, hardness, and such properties depend on its density. The

relative thickness of the cell wall and the proportion of thick walled to thin-walled cells determines the density of wood.

1.3. Wood structure

1.3.1. Macro structure of wood

Figure 1.1. shows well defined concentric subdivisions in the three dimensional section of a tree trunk and represents the outside of the tree to the center: periderm, bark, vascular cambium, sapwood, heartwood and the pith. All the tissue in a tree trunk inside the cambium layer to the center of the tree is xylem or wood. Generally, dead xylem tissue is found in a tree trunk. The younger region closer to the cambium has a lighter color and is called sapwood while the darker, central region is called heartwood. The most species of wood is evidently distinguished into sapwood and heartwood. There is a distinct anatomical difference between the gymnosperms (softwoods) and angiosperms (hardwoods) [3]. The term softwood and hardwood do not refer to the hardness or softness of the wood itself; it specifies the water-conducting cells in a living tree from which timber comes. The water-conducting cells are known as xylem tracheids in soft wood whereas these cells are tubular-shaped and are known as xylem vessels in hard wood.

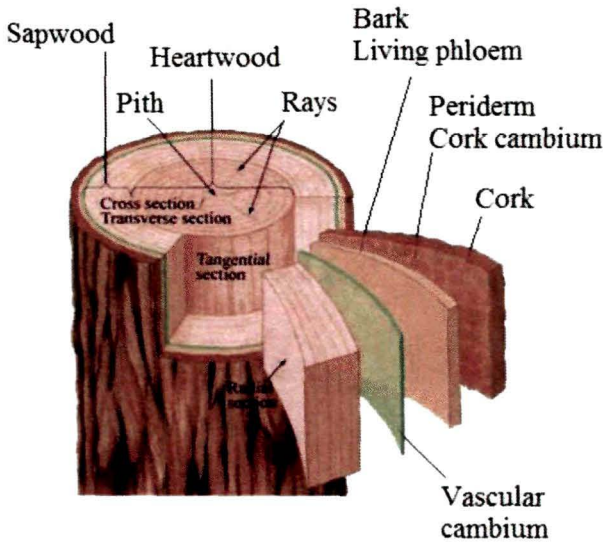

Figure 1.1. The three dimensional section of a tree trunk.

The different cells that comprise xylem are alive when they are initially produced by the meristematic cambium. They lose their cell contents and become hollow, microscopic tubes with lignified walls when they actually become functioning water-conducting cells (tracheids and vessels).

1.3.1.1. Soft wood

The wood of gymnosperms is commonly referred to as softwood, and sometimes as non-pored wood. The bulk of softwood is made up of long narrow cells, or tracheids, that fit closely together (Figure 1.2.). The centres of the cell walls of tracheids are hollow and are made of cellulose. The tracheids lay side by side each other and another substance, lignin, is accumulated between the touching cell walls. The tracheids are firmly held together by these lignins. Because softwoods do not contain vessel cells, conifer tracheids can be up to four millimetres long, and serve both to transport sap and to strengthen the stem of the tree. As the tracheids moves up the stem, the pits in the cell walls enable sap to pass from cell to cell.

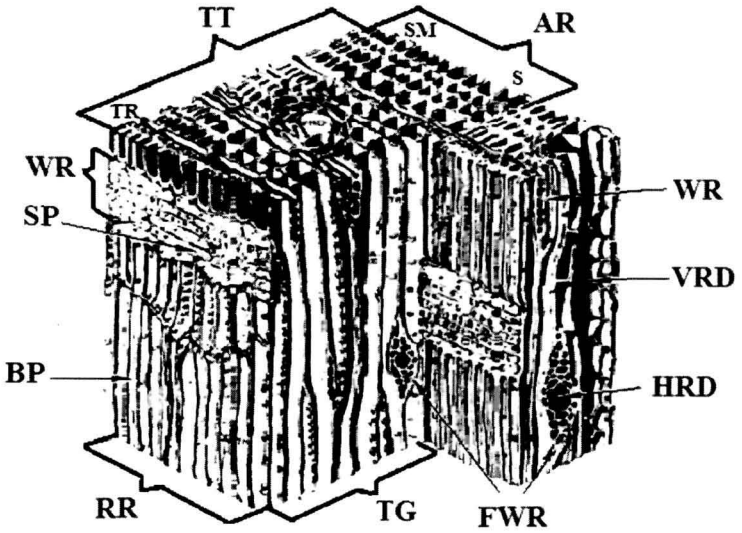

Figure 1.2. Cellular structure of softwood (white pine), enlargement of a block of 1 mm high. AR, annual rings; BP, border pit; FWR, fusiform wood rays; HRD, horizontal resin duct; RR, edge grain; S, earlywood; SM, latewood; SP, simple pits; TG, flat grain; TR, tracheid; TT, end grain; VRD, vertical resin duct; WR, wood rays.

1.3.1.2. Hard wood

Vessels and fibre cells are two main constituent cell types of the hard wood trees. Sap is carried upwards in large ducts known as vessels or pores (Figure 1.3.). These vessels or pores are arranged one above the other and start as wide cells with large cavities. Long pipes are created in some cells where the end walls break down and they run considerable distances. Visualization of the vessels can be done with the naked eye. The hard woods are the timbers with vessels and are sometimes called pored timbers. The arrangement of the vessels in a cross-section is a useful aid to identify different timbers. The fibre cells found in hard wood, are similar to conifer tracheids but are shorter in length (commonly about one millimetre long) and usually thicker-walled. These fibre cells impart strength to the broad-leaved trees. These fibers constitute the bulk of the wood in broad-leaved trees and, like tracheids, the walls of these cells are made of cellulose and neighbouring cells are held together by lignin.

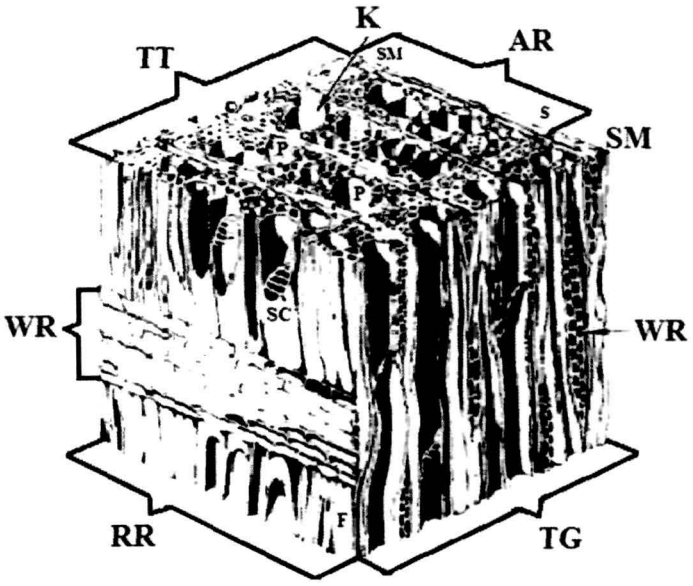

Figure 1.3. Cellular structure of hardwood (yellow poplar), enlargement of a block of 1 mm high. AR, annual rings; F, fiber; K, pits; P, pores; RR, edge grain; S, earlywood; SC, grating separating vessels; SM, latewood; TG, flat grain; TT, end grain; WR, wood rays.

1.3.2. Micro structure of wood

Millions of individual units comprise wood called cells. The shape and size cells depend upon the tree's physiological function [4]. The cells of the dicotyledons have complex structures than the cells that are contained in the xylem of conifers. The cells that are contained in the conifers are mainly of elongated, pointed, tubular and closed at the ends, known as tracheids whereas the cells that consist of the dicotyledon are of different sizes and shapes. The cells of most dicotyledon are composed of long and narrow, with pointed and closed ends called the fibers. Most of the physical and chemical properties of wood are attributed to the tracheids in conifers and the fibers in dicotyledons as they comprise the maximum part of the wood cell wall [5].

Parenchyma is another important constituent and comparatively small quantities, of vessels known as pores are present [6]. Different size and shape of these cells are available and have open ends. They are generally shorter than fiber.

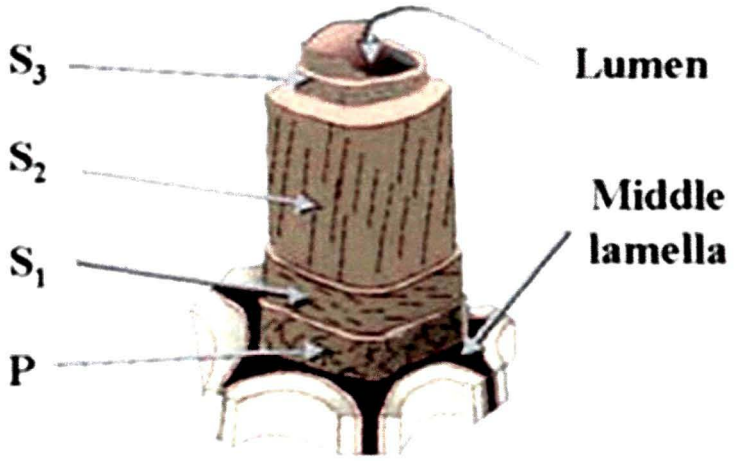

Figure 1.4. Ultra structure of wood cell wall.

The cells of wood are connected by a cemented substance called medium lamella or intercellular layer. A thin external layer called the primary wall (P), and a thicker internal layer called the secondary wall (S)– are the two layers that consists of a mature cell. The secondary wall (S) is again composed of three other layers. The primary layer is the first to be laid down when the cell is formed (Figure 1.4.). It has random orientation that allows

expansion as cell growths and is composed of microfibrils. Afterwards, the secondary layer is formed and each of the sub-layers has different patterns in the microfibrils orientation. Thus, the maximum volume of the cell wall is occupied by the S layer and hence can influence the properties of wood to a great extent. The S layer consists of many lamellae and has a definite microfibrillar orientation. The lamellae are composed of numerous closely associated microfibrils that remain in a helical winding pattern. The middle lamella occupies the space between the cell fibers. But the accessibility to the cell wall under certain conditions is allowed by the micropores. In most of the mature cells, the cellular lumen, which is the interior of the cell is found to be completely empty [4]. The empty cells consist of about 70% of the total volume of wood and the remaining 30% is its constituents. Thus, wood is a very porous material, but it is not always highly permeable. Its permeability varies both within and between species.

1.4. Chemical components of wood

The chemical composition of wood includes carbohydrates (70–80%), lignin (20–30%), and extraneous materials (5–10%). The carbohydrate part of wood consists of cellulose and the hemicelluloses. Cellulose microfibrils in wood serve as a structural framework, hemicellulose is present between the microfibrils, and lignin as the encrusting substance binding the wood cells together, thus providing the rigidity to the cell wall [7]. Each of the layers of the cell wall has their own specific arrangement of cellulose microfibrils that determine the physical and mechanical properties of the wood in that cell [8]. Lignins are complex phenolic polymers of irregular structure. The basic structure unit is a mono- or dimethoxy -substituted propylphenol unit. The molecular weights of lignin have been measured up to 16,000. The extraneous materials can be removed from the wood with organic or aqueous solvents and are of much lower molecular weight (< 1000).

1.4.1. Carbohydrates

It is impossible to identify absolute compositions of wood because the chemical composition varies between and among species. Generally, the amount of cellulose ranges from 40 to 50% of the dry wood weight, and hemicelluloses range from 25 to 35%. The carbohydrate consists primarily of cellulose, a linear polymer of β-D-glucopyranose units

($C_6H_{12}O_6$) linked together by β-(1-4)-glycosidic bonds [9,10]. The hemicelluloses are branch-chained polymers of several different compositions that comprise of five or six anhydro-sugars in addition to uronic anhydride and acetyl substituents. The chain length of wood cellulose polymers is between 7,000 and 10,000 glucose units, whereas the hemicelluloses have chain lengths of 200 or less sugar units.

1.4.1.1. Cellulose

Cellulose molecules combine together into bundles called elementary fibrils, and these in turn aggregated into larger units called microfibrils [9,10]. The diameter of elementary fibrils ranges from 2 to 4 nm, while microfibrils have a diameter ranging from 10 - 30 nm. The adjacent cellulose molecules are interlinked through hydrogen bonding between hydroxyl (-OH) groups leading to the formation of the supramolecular structures. There are also intramolecular linkages by hydrogen bonding between OH-groups in adjacent glucose units that belong to the same cellulose molecule. The stiffness in the molecular chains of the cellulose is imparted by these intramolecular hydrogen bonds. Depending on the degree of array of the elementary fibrils, cellulose microfibrils have both amorphous and crystalline regions. The fibrils have no definite arrangement in the amorphous regions while they are highly ordered and regularly arranged in crystalline regions. The crystallinity of cellulose has been reported to be 52 ± 3% in Norway spruce [11]. The physical and mechanical properties of wood are influenced by the orientation of the microfibrils within the cell wall, measured as the angular displacement from the fibre axis [12,13].

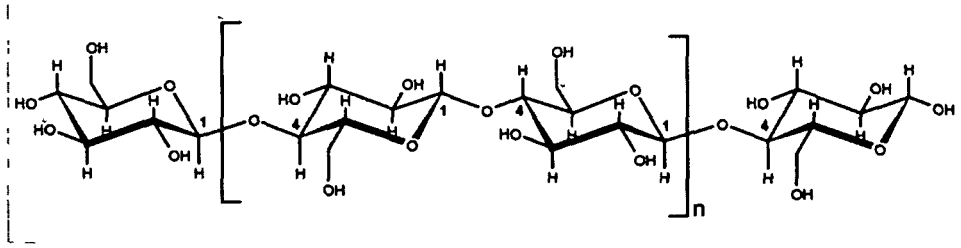

Figure 1.5. Structure of cellulose showing the repeating cellobiose unit.

1.4.1.2. Hemicelluloses

Hemicelluloses are composed of various sugar units that are amorphous and branched polymers. Its main building units are pentoses such as xylose and arabinose, and

hexoses such as glucose, mannose and galactose. The degree of polymerization in hemicelluloses does not usually go beyond 200 sugar units [14]. Both softwoods and hardwoods have a difference in the chemical composition of hemicelluloses. The dry wood mass of soft and hard wood contains approximately 20-25 % and 25-30 % of hemicelluloses [10]. The most abundant hemicellulose found in softwoods are galactoglucomannan (glucomannan), composed of glucose, galactose and mannose units. The principal hemicellulose found in hardwood is glucuronoxylan (xylan), composed of xylose units and 4-O-methylglucuronic acid groups. The acetyl groups partly substitute the glucomannan in softwoods and xylan in hardwoods. Hemicelluloses are held to be closely related to cellulose microfibrils, as they are entrenched in a random network of hemicelluloses and lignin [15,16]. Some authors propose that hemicelluloses are regularly disposed between microfibrils, linking them together, and the gaps are filled up by the lignin [17]. The amorphous regions of cellulose microfibrils might also contain hemicelluloses [18].

1.4.2. Lignin

Lignins, the third major component in wood, are high-molecular-mass amorphous polymer, and are difficult to isolate from wood. Lignin is not a carbohydrate composed of carbon, hydrogen and oxygen, but a complex polyphenolic compound built upon phenylpropane units. The building units of lignin are arranged in irregular pattern. Lignin is difficult to isolate from wood without inducing changes in its native state [14]. The rigidity

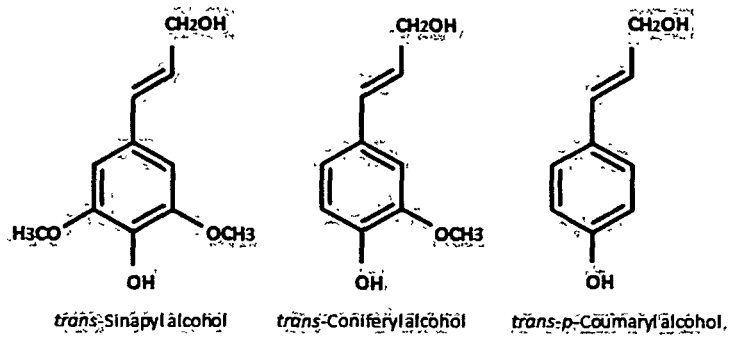

Figure 1.6. Main building units of lignin in wood.

in the cell wall of wood is provided by lignin. It also binds the adjacent cell and thus acts as a gluing agent. Generally, in softwoods lignin accounts for about 25 - 30 % and in hard wood 20 - 25 % of the dry wood mass. Lignin in softwoods is usually referred to as guaiacyl lignin, because more than 90 % of the building units are derived from transconiferyl alcohol, with the remainder being mostly derived from trans-p-coumaryl alcohol. Lignin in hardwoods is referred to as guaicyl-syringyl lignin, because it contains about 50 % of trans-coniferyl and 50 % of trans-sinapyl alcohol-derived building units. Lignin and carbohydrates are bonded by covalent bonding in case of "lignin-carbohydrate complex" (LCC). Though chemical bonding has been reported to be formed between lignin and carbohydrates [19,20], the specific type and amount of bonds has not yet been clarified.

1.4.3. Extraneous materials

Extraneous materials are low molecular weight substances, non-polymeric that can be removed by a solvent without being chemically modified. Organic materials such as mucilages, gums, tannins, sugars, waxes, fats, terpenes, pectins, resin acids, lignins, flavonoids, phenolics, stilbenes, steroids, alcohols, and inorganic salts are included in extraneous materials. The extraneous materials are present in varying amounts, depending on location, tree part, species, and time of year. They comprise 5–10% of most wood in temperate climates; they are usually soluble in neutral or slightly polar solvents, such as diethyl ether or a 2:1 mixture of ethanol–toluene.

1.5. Properties of wood

The versatility of wood is demonstrated by a wide variety of products. These varieties are a result of a spectrum of desirable physical characteristics or properties among the many species of wood. The performance and strength of wood are significantly influenced by the properties of wood used for diverse applications. The properties relevant to performance and structural design are discussed in this section.

1.5.1. Density and specific gravity

The variation of density of wood occurs both within and between species. The range of density generally falls between 160 kg/m^3 (10 lb/ft^3) to 1,040 kg/m^3 (65 lb/ft^3). For some other imported woods, the density of most species even falls between 320 to 720 kg/m^3 (20 and 45 lb/ft^3) [21]. As there is natural variation in moisture content, anatomy and ratio of heartwood to sapwood, the value of density is always used as an approximation. However, this determination of density is adequately precise to allow appropriate use of wood products where weight is important. Specific gravity is used as a standard reference basis, rather than density for standardization of comparisons of species or products and estimations of product weight. Specific gravity is the ratio of the density of the wood to the density of water at a specified reference temperature [often 4.4°C (40°F)] where the density of water is 1.0000 g/cm^3).

1.5.2. Moisture content

The properties of wood like strength, weight, shrinkage and other properties are related to the moisture content of wood. It is defined as the weight of water in wood expressed as a fraction, usually a percentage, of the weight of oven dry wood. The moisture content of trees generally extends from about 30% to more than 200% of the weight of wood. Heartwoods have generally lower moisture content than softwoods. The difference in moisture content between sapwood and heartwood depends on the species in the case of hardwood. There exists considerable variation in the values both within and between trees. Variability of moisture content exists even within individual boards cut from the same tree.

1.5.3. Green wood and fiber saturation point

Water can be bound to the cell wall of wood through hydrogen bonding. It can remain in wood as water vapor in cell lumens and as liquid water in cavities (free water). The maximum possible moisture content is the condition at which the moisture content of both the cell lumens and cell walls are completely saturated with water. The freshly sawn wood in which the cell walls are completely saturated with water is known as green wood. However, additional water is present in the cell lumen of wood in the case of green wood.

Maximum moisture content is determined by the specific gravity of wood. With the increase in the specific gravity of wood, the maximum moisture content decreases since the volume of decreased lumens diminish the free available sites for accommodation of moisture. The fiber saturation point is defined as the moisture content below which the physical and mechanical properties of wood begin to change as a function of moisture content. The fiber saturation point of wood averages about 30% moisture content, but it differs in individual pieces of wood species by several percentages.

1.5.4. Shrinkage

Wood swells on gaining moisture in the cell walls and shrinks when losing moisture from the cell walls. Loss or gain in moisture below the fiber saturation point leads to change in dimension of wood. When the moisture content is greater than the fiber saturation point, wood is dimensionally stable. Splitting, warping, checking, and loosening of tool handles, gaps in strip flooring, or performance problems occurs upon shrinking and swelling of wood that ultimately affect the usefulness of the wood product. Wood is an anisotropic material, therefore, it shrinks most in the direction of the annual growth rings (tangentially), about half as much across the rings (radially), and only slightly along the grain (longitudinally).The shapes of wood pieces are distorted because of the combined effects of radial and tangential shrinkage that can result in the difference in shrinkage and the curvature of annual rings.

1.5.5. Chemical resistance

Wood is resistant to mild acids (pH more than 2.0), acidic salt solutions, and corrosive agents and therefore considered a superior to alternative materials, such as concrete and steel. To enhance its performance in this respect, wood can be treated, with many of the common wood preservatives. Heartwood is more durable to chemical attack than sapwood because heartwood is more resistant to penetration by liquids. Chemical solutions may impart two general types of action: irreversible chemical degradation and normal reversible swelling by a liquid. Irreversible chemical degradation leads to permanent changes within the wood structure from hydrolysis, oxidation, or delignification. The normal

reversible swelling by a liquid will return wood to its original condition on removal of the liquid.

1.5.6. Thermal degradation

Many undesirable properties such as odor, discoloration and the loss of mechanical strength appear in wood when it is exposed to high temperatures due to degradation [22]. The major chemical components of wood viz. cellulose, hemicelluloses, lignin and extractives degrade at different temperatures. Depending on composition of the wood, they are known to present different degradation profiles. Cellulose is thermally stable due to its highly crystalline nature, but hemicelluloses and lignin start degradation before cellulose, as they are amorphous [23]. The presence of acetyl groups in hemicellulose makes it least thermally stable wood components [24]. Lignin starts degradation at relatively low temperatures and covers a wide temperature range [25].

1.5.7. Mechanical properties

Wood is an orthotropic material; i.e., it has unique and independent mechanical properties in the directions of three mutually perpendicular axes: longitudinal, radial, and tangential. Property values in the longitudinal axis are generally significantly higher than those in the tangential or radial axis. The fitness and ability to oppose applied or external forces of wood is its mechanical properties. The mechanical properties of wood include: (1) stiffness and elasticity, (2) tensile strength, (3) compressive or crushing strength, (4) shearing strength, (5) transverse or bending strength, (6) toughness, (7) hardness, (8) cleavability, (9) resilience. Mechanical properties are given in terms of stress (force per unit area) and strain (deformation resulting from the applied stress).

1.5.8. Photodegradation

All the components of wood are susceptible to degradation by UV radiation, but lignin is primarily responsible for UV absorption. Lignin absorbs 80-95% of the total amount of UV light absorbed by wood [26]. Photo-degradation of wood begins with an attack on the lignin-rich middle lamella. Degradation of secondary walls occurs on pro-

longed exposure of wood to UV irradiation. Lignin is converted into water-soluble compounds on UV degradation which are washed from the wood with rain. A fibrous appearance with a cellulose-rich surface remains on the wood surface. Though UV light cannot go through deeper than 75 μm into wood, yet the depth of degradation occurs deeper than the above distance. The components of wood present at the surface initially absorb UV light, and then an energy transfer process occurs from molecule to molecule which dissipates excess energy to create new free radicals. Long times exposure leads to change in the lignin content through the thickness of wood beyond the discolored surface layer, with less lignin at the surface and more in the center portion [27]. Thus, a discoloration reaction occurs due to migration of free radicals deeper into wood. Photodegradation leads to change in wood's appearance such as discoloration, roughening and checking of surfaces, and reduction of mechanical and physical properties.

1.5.9. Biological degradation

Wood is conducive to decay and insect damage in moist, warm conditions. Even in the early stages of decay, decay within a structure cannot be tolerated as strength is rapidly reduced. The heartwood of some species is resistant to decay; on the other hand sapwood is readily decayed by fungi. The use of chemically treated wood or naturally decay resistant wood species is necessary to hinder the decay process, if the warm, moist conditions required for decay cannot be controlled [28]. There are several biological degradations that wood is exposed to in different environments. Biological organisms such as bacteria, mold, stain, decay fungi, insects, and marine borers depend heavily on temperature and moisture conditions to grow.

a) Bacteria: Bacteria are the early colonizers of wood. They are single-celled organisms which can gradually degrade wood that is saturated with water over a long period of time. The properties of wood are little affected when exposed to bacterial environment except over a long time period. The wood becomes more absorptive when bacterial growth occurs on it causing it more susceptible to decay.

b) Mold and stain: Mold and stain fungi differ only on their depth of penetration and discoloration of wood and cause damage to the surface of wood. They are of various colors and grow mainly on sapwood. They are typically fuzzy or powdery development on the surface of wood. The main types of fungus stains are called sapstain or blue stain. They

cannot be removed by planning because they penetrate deeply into the wood. They usually cause blue, black, or brown darkening of the wood, but some can also produce red, purple, or yellow colors. The molds and stains generally do not influence the strength of the wood except for toughness or shock resistance. Nevertheless they make the wood more absorptive rendering it more susceptible to moisture and then decay fungi.

c) Decay fungi: The decay fungi are single-celled or multicellular filamentous organisms and use wood as food. The fungal spores are spread by wind, insects, or animals. They grow on damp, vulnerable wood, and the hyphae extend right through the wood. These hyphae produce enzymes that attack the wood cells thereby deteriorating the wood properties. Toughness or impact bending is most sensitive to decay. The wood may become discolored on unseasoned in the initial stage of decay wood, but becomes harder to detect on dry wood.

d) Insects: Another biological cause of wood deterioration is the insects. They are often not present when the wood is inspected. Both the immature insect and the adult form may cause damage to wood. The types of insect that cause damage to wood are: (i) termites, (ii) powder-post beetles, (iii) carpenter ants, and (iv) beetles.

e) Marine borers: Marine-boring organisms can cause extensive damage to wood and they remain in salt or brackish waters. The marine borers that cause the most damage are shipworms, pholads, crustaceans, and pillbugs.

1.6. Chemical Modification of wood

Chemical modification is one of the techniques for enhancing the durability and performance of wood. The essence of chemical modification is a reaction that takes place between some reactive part of the wood cell wall component and a simple single chemical reagent, with or without catalyst that forms a stable covalent bond [29]. The abundant hydroxyl groups in the wood's polysaccharide molecules are the reactive parts of the wood cell wall. Chemical modification of wood results in a change in molecular conformation and chemical configuration. Therefore, the modified wood can neither absorb water nor can biodegrade and the organisms cannot recognize it as a food source. It is an effective method to improve various properties of wood like dimensional stability, resistance to biological attack, resistance to weathering and acoustic properties. The hydrophilic nature of wood is due to the presence of hydroxyl groups that occur commonly in the wood's organic polymers (cellulose, hemicelluloses and lignin) which are the most reactive functional groups in wood.

They readily combine with water through their hydroxyl groups by hydrogen bonding. The hydrophilicity of wood is removed on chemical modification as these hydroxyl groups participate in bond formation with the reactants. Thus, the wood no longer has the capacity to bind to water molecules. Improvement in properties under weathering trials can be observed both visually and at the microscopic structural level [30]. Plackett et al. has reported an improvement in dimensional stability and resistance to accelerated weathering trials for acetylated Radiata pine [31]. It is also reported that the chemical modification of wood improves photostabilisation [32]. Chemically modified aspen composites of veneers and sawdust prepared by hot pressing stage of production significantly improve its biological resistance [33]. To facilitate the penetration of the reagent into the cell wall, it is necessary for the chemicals to swell the wood. It must react with the cell wall hydroxyl groups, preferably under mild conditions. Ideally the chemical modification of wood should produce no by-products, form stable covalent bonds and maintain the desirable structural properties of the wood [34-36]. Often through impregnation or diffusion, the reactants are allowed to penetrate into the porous structure and then bond formation occurs within the cell wall of wood. The objective may be to produce a reaction throughout the cross-section of a solid component, or to provide a protective envelope treatment. The key to optimize the reaction conditions is to understand the nature of the process and the constraints on the degree of substitution.

1.6.1. Various monomers and polymers for impregnation into wood

The dimensional stability and mechanical properties of wood can be improved on impregnation with suitable chemicals that can react with the cell wall component. The process of impregnation of wood can be carried out via *in-situ* polymerization either by using catalyst-heat treatment or irradiation technique and the resultant product is called wood polymer composite (WPC) [37]. The use of liquid vinyl monomers as impregnation solution for wood under vacuum condition does not swell the cell wall of wood. They are located almost exclusively in the lumens of the wood and are polymerized *in-situ* either by chemical catalyst-heat treatment or gamma radiation. The impregnation technique consists of application of vacuum to the wood samples for evacuating the air and moisture from wood vessels and lumens using a vacuum pump and then introduction of the monomer from a reservoir maintained at atmospheric pressure. The monomers remain in the cell lumens if

the chemical introduced into dry wood does not cause swelling. The various vinyl monomers for treatment of wood include styrene, methyl methacrylate etc [38]. They produce essentially cell-lumen WPC as they have little swelling effect on the cell wall over normal treating times [39]. When the non-swelling monomers are polymerized, the polymer will occupy the cell cavities but not the cell walls. The moisture uptake of wood is reduced since the cell cavities are a major path for moisture movement [40]. The wood becomes more resistant to moisture uptake; especially along the grain as the polymer plug the cavities. Thus, over the short term greater dimensional stability effect can be observed [39]. The selection of a chemical is an important aspect for achieving improved properties of wood and it should be compatible with the lignocellulosic substances. Most attempts to stabilize wood with monomers have failed because the monomers do not penetrate the cell walls or do not react with the wood components. For example, poly (ethylene glycol) (PEG) is water soluble and does not react with wood components; in addition, it is easily leached since it is highly hygroscopic. It has been observed that when wood is impregnated with thermosetting resins such as water-soluble phenolic resins, urea-formaldehyde and melamine-formaldehyde prepolymers, the resultant treated wood leads to an improvement in its moisture-related shrinking and swelling behaviors ; compressive strength. The thermosetting resins swells the wood cell walls which helps in penetrating the resins and thus bulk the cell wall. The wood cell wall is kept in a swollen state like PEG. But, unlike PEG, the resin is bulked in the cell wall because it is polymerized or cured by heat to form a water-insoluble resin. The treated wood samples prevent shrinkage of the wood upon drying as they react with the hydroxyl groups of the wood components.

1.6.1.1. Methyl methacylate

Methyl methacylate, a colourless liquid and the methyl ester of methacrylic acid (MAA), is a monomer produced on a large scale for the production of poly(methyl methacrylate) (PMMA). PMMA is a strong and lightweight material. It has a density of 1.17–1.20 g/cm^3 also has good impact strength, higher than both glass and polystyrene; however, PMMA's impact strength is still significantly lower than polycarbonate and some engineered polymers. It is often preferred because of its moderate properties, easy handling and processing, and low cost. PMMA/clay nanocomposites have shown improved thermal stability and mechanical properties in comparison to pure polymer [41]. Wood impregnated

with PMMA has showed lower moisture absorption, higher water repellent efficiency and mechanical properties compared to raw wood [42].

1.6.1.2. Melamine formaldehyde resin

Melamine–formaldehyde (MF) is widely used for preparation and bonding of both low- and high-pressure paper laminates and overlays. It is extensively used as adhesives for exterior and semiexterior wood panels. It is essential for the resin to swell the wood cell wall for a successful modification of wood cell walls with polymer resins. Mantanis et al. [43,44] has reported in a review of the swelling of wood in different organic and inorganic solvents, that low molecular volume swelling prepolymers capable of forming hydrogen bonds has the ability to swell the cellwall. The structure of methylol melamine is shown in Figure 1.7. MF resins can display a number of beneficial properties e.g., high hardness and stiffness and low flammability as it has the ability to form hydrogen bonds [45] and can enhance the mechanical properties of softwood significantly. It has been documented in the literature that MF resin may penetrate the amorphous region of cellulose [46,47]. Rapp et al. [48] has observed the penetration of MF into secondary cell wall layers and into the middle lamella by using electron energy loss spectroscopy for spruce wood samples impregnated with a water soluble MF resin over seven days. Gindl et al. has made estimated quantitatively the melamine that are glued with the cell wall by using UV-microscopy and reported an improvement in a number of wood properties, such as surface hardness and weathering resistance.

1.6.1.3. Furfuryl alcohol

The utilization of water soluble monomers will provide a potential advantage from environmental concern. Since water act as a solvent and dispersing medium, it can greatly reduce the harmful effect of using hazardous solvents. The applicability of furfuryl alcohol (FA) in wood modification has been known for a long time [49,50]. The structure of FA monomer is shown in Figure 1.7. Petroleum-based chemicals can be widely replaced by some sustainable solution of vegetable biomass. In particular, hemicellulose constitutes an important source of monomers such as FA. FA is usually converted into furanic resin prepolymers and these represent excellent eco-friendly precursors for wood impregnation [51]. It has been found that dimensional stability of wood treated with bio-derived FA has increased with the increase in weight percent gain [52]. Furfurylated wood is an

environmentally acceptable product and its degradation does not release any volatile organic compounds [53]. Though furfurylated wood shows a decrease in equilibrium moisture content and increase in dimensional stability but it cannot enhance the thermal stability and mechanical properties of wood efficiently. The furfurylation does not improve the bending strength and the modulus of elasticity (MOE) is same as that of untreated wood [54].

1.6.1.4. Acrylamide

The structure of acrylamide (AM) is shown in Figure 1.7. AM is a white odourless crystalline solid having density 1.13 g/cm^3. It is a water soluble bi-functional monomer, can substantially improve the polymer loading and mechanical strength of the prepared wood composites [55]. Higher polymer loading can be achieved at lower monomer concentration when wood is impregnated with AM. This results in improved physical and mechanical properties of the treated wood samples [56]. But the main disadvantage associated with AM is its swelling behavior hence it cannot provide dimensional stability to the composites.

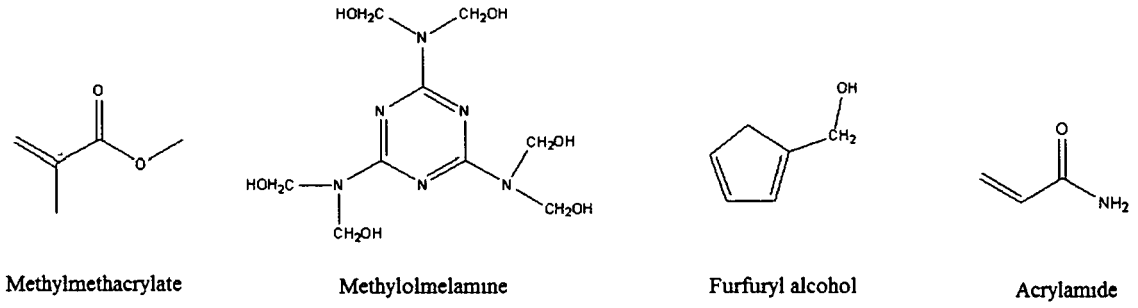

Figure 1.7. The structure of methyl methacrylate, methylol melamine, furfuryl alcohol and acrylamide monomer.

1.6.2. Crosslinking agent

Crosslinking is the formation of physico-chemical bond between molecular chains to form a three-dimensional network of connected molecules. Coupling agents are substances that are used in small quantities to get the best advantages of two semi compatible or incompatible substances. They are generally bifunctional compounds used to treat a surface so that one functionality forms bond with one component (say wood) and other functionality with the other (say polymer). They form bond chemically with hydrophilic fiber and the

polymer chain [57]. They facilitate interaction between the polymers and wood and the resultant polymer can exist in the form of a three dimensional network structure inside the wood pores improving dimensional stability, weather resistance, mechanical properties etc. of the treated wood samples. The organic coupling agents, used in wood polymer composites (WPC) which have bi- or multifunctional groups in their molecular structure include (-N=C=O) of isocyanates, [-$(CO)_2$ O-] of maleic anhydrides, and (-Cl-) of dichlorotriazine derivatives. They can interact with the polar groups [mainly hydroxyl groups (-OH)] of cellulose and lignin to form covalent or hydrogen bond [58-60].

1.6.2.1. Glycidyl methacrylate (GMA)

Glycidyl methacrylate (GMA) is one of the commonly used compatibilizer in wood polymer composite. They are bifunctional having both double bond and epoxy group. The glycidyl group is capable of reacting with groups containing active hydrogen such as amino, hydroxyl, and carbonyl group [61]. The glycidyl group and terminal double bond in GMA can be exploited for reaction with hydroxyl group of cellulose present in wood and for co-polymerization with vinyl or acrylic type monomers, respectively. Its molar mass and density is 142.2 g/mol and 1.07 g/cm^3 with boiling point 189.0 °C.

1.6.2.2. 1,3-dimethylol 4,5-dihydroxyethylene urea (DMDHEU)

N-methylol compounds, such as 1,3-dimethylol 4,5-dihydroxyethylene urea (DMDHEU), are the most commonly used durable press finishing agents for cotton fabrics by the industry. It is water soluble, light yellow colored having molecular formula $C_5H_{10}O_5N_2$. They are expected to enhance the resistance of wood to weathering because they can cross-link the cell wall and dimensionally stabilize wood. The WPC has resulted in significant improvement in mechanical properties and reduced water uptake [62]. It is a multifunctional crosslinker i.e. it contains four hydroxyl groups which can effectively form a three dimensional crosslinked structure with the polymer and wood.

1.6.2.3. N-methylol acrylamide (NMA)

N-methylol acrylamide (NMA) is a bifunctional crosslinking agent where both hydroxyl group and vinyl groups are present. It is water soluble, transparent having molecular formula $C_4H_7O_2N$. The presence of double bond in NMA could undergo self polymerization and the hydroxyl group interacts with the hydroxyl group of wood

components. NMA can serve as an effective coupling agent and improves strength and water resistance of the resulting composites [63].

1.6.2.4. 2-Hydroxyethyl methacrylate (HEMA)

2-Hydroxyethyl methacrylate (HEMA) is a multifunctional monomer that can swell the cell wall of wood and thus improves the penetration of monomers into cell walls. This monomer is water soluble, transparent having molecular formula $C_6H_{10}O_3$ and has four functional groups i.e. an alcohol, ether, an ester, and a polymerizable double bond. The presence of hydroxyl group increases the monomer hydrophilicity and hence the ability to form hydrogen-bond with various wood components. A strong three dimensional network is formed as intermolecular transetherization takes place through reaction of the hydroxyl groups of the HEMA units with wood components thereby providing a good dimensional stability to the resulting WPC.

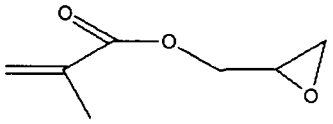

Glycidyl methacrylate (GMA)

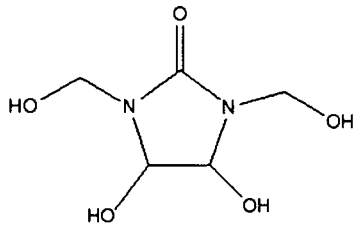

1,3-dimethylol 4,5-dihydroxyethylene urea (DMDHEU)

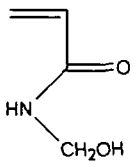

N-methylol acrylamide (NMA)

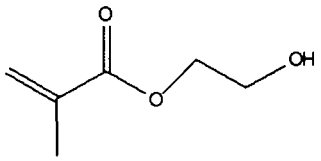

2-Hydroxyethylmethacrylate (HEMA)

Figure 1.8. Structure of Glycidyl methacrylate (GMA), 1,3-dimethylol 4,5-dihydroxyethylene urea (DMDHEU), N-methylol acrylamide (NMA) and 2-Hydroxyethylmethacrylate (HEMA).

1.6.3. Flame retarding agent

There is a continuous effort to enhance thermal stability and flame retardancy of wood to expand its utility. Fire retardants (thermal stabilizer) are additives which are added

to improve fire resistance (or thermal stability) of wood-polymer composites. They are normally applied to pretreat wood or mixed into monomers before impregnating wood. Flame retardancy is a desirable property of wood polymer composites and therefore various flame retardants are incorporated into the composites to meet its specific requirements. Flame retardancy can be achieved by the use of organohalogen, organophosphorus, organoantimony compounds and various silicates and borates compounds [64-66]. While burning, most of them emit toxic fumes which are highly health hazardous and pollutant to the environment. The polymeric flame retarding agent can reduce the leaching problem due to its high molecular weight and thus, may improve the service life of the polymer product. The use of flame retardant (FR) polymer of renewable origin is beneficial from environmental point of view. Jana et al. has studied the flammability and biodegradability of starch based biodegradable film modified with gum derived from *Moringa oleifera* and found an improvement in flame retardancy [67]. Ghosh et al. has studied the adhesive performance, flammability and biodegradation study of various rubber/plant polymer blend and reported an improvement in properties of the prepared blends [68].

1.7. Polymer nanocomposites

Nano science and technology is an attractive and demanding field to develop high-value-added and multifunctional product. Polymeric systems containing organic or inorganic filler have become universal. Numerous commercial applications of polymer composites include aerospace components, automobiles, sporting goods etc. Polymer nanocomposites were developed in the last few years, where at least one of the dimensions of the filler is in the nanometer region (10^{-9}). Nanoscale fillers have a large surface area for a specified volume [69]. High aspect ratios of the nanomaterials are one of its remarkable features that render it to become an effective reinforcing agent [69]. Nanocomposites possess significantly different properties from conventional polymer composites of the same composition because many important chemical and physical interactions are guided by surface related properties [70]. The degree of mixing between the different component phases and its size scale influence the properties of nanocomposites to a great extent. The properties of nanocomposites differ depending on the method of preparation and on the nature of the different types of nanofillers used viz. layered silicate, metal nano particles, nanofiber [71]. Substantial improvements in specific properties of polymers are obtained on

incorporation of fillers to the polymers [72]. Polymer/layered silicate nanocomposites have attracted great interest due to their ability to improve thermal [73], fire retardant [74,75], barrier [76] and mechanical properties [77-79] of composites. The titanium and silver-based nanoparticles possess antibacterial properties and hence nanocomposites based on these nanofillers are widely used in hygiene and hospital disposables applications, filtration, or in consumer products. Physical entanglement or secondary force exists for their interconnection in the composite [80]. Nanocomposites have a wide spectrum of applications ranging from moisture barrier properties [81] to providing photo-catalyst activation [82], electrical conductivity [83] and improving melt processability [84]. In order to achieve the desired properties, a uniform filler distribution in the polymer matrix is required. It is a challenging task to prevent agglomeration of the nanoparticles by creating a good interaction between the polymer and the nanofiller. Tube shaped, spherical, whisker, and plate-like shapes are the different shapes of nanoparticles where at least one of the three dimensions is required to be on a nanometric scale. The combination of inorganic material (metals like Zn, Fe, Ag, Au, Cu, Cd etc. and their oxides, sulphides etc.) with the polymer components may offer improved mechanical, electronic or chemical behavior of the resulting product [85,86]. Single-walled carbon nanotube (SWCNT) and multi-walled carbon nanotube (MWCNT) are the two nanostructures exhibited by carbon nanotubes (CNT). MWNT is composed of several tubes within each other. A good distribution of CNT in the polymer matrix and efficient load transfer at the interface is reflected in the improved properties of nanocomposites.

In case of polymer-clay nanocomposites, three different types of nanocomposites are obtained depending on the strength of interfacial interactions between the polymer matrix and layered silicate (modified or not) [87,88].

a) Intercalated nanocomposites: In intercalated nanocomposites, the interlayer spaces of clay are expanded as few molecular chains of polymer are inserted in between its layers. The insertion of a polymer matrix into the basal spacing of clay occurs in a crystallographic regular fashion, regardless of the clay to polymer ratio. But the shape of layered stack of clay remains unaffected.

b) Exfoliated nanocomposites: The individual layers of clay are separated in a continuous polymer matrix by an average distances that depends on clay loading. Generally, exfoliated nanocomposite has lower clay content than that of an intercalated nanocomposite. Maximum improvement in properties is obtained in an exfoliated structure of clay based

nanocomposite. The maximum interfacial interaction of clay layers with polymer and highest dispersity of clay can be achieved in an exfoliated structure.

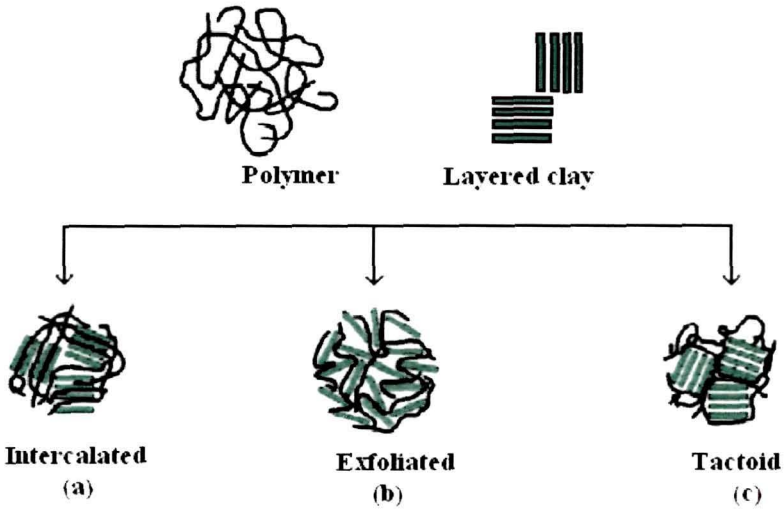

Figure 1.9. Different types of polymer/clay nanocomposite.

c) Tactoid structures: In tactoid structure there is weak affinity between clay layers with the polymer as the interlayer space of the clay does not expand. As a result, a little role is played by the clay in property enhancement and is used only for cost reduction.

1.8. Different types of reinforcing agents

Fillers and reinforcing agents are used for a wide range of applications: to strengthen, stiffen, lighten, matting, reinforce, radio-opacify and extend thermoplastic materials. They are incorporated into the virgin polymers to obtain the desired level of properties for their different applications. They should be efficient in their function, i.e. the purpose for which they are being incorporated into the polymer, should efficiently work for that. They should be stable under processing as well as service conditions. The additive should not degrade or decompose or alter its nature during processing and under service conditions. They should not bleed or bloom. They should be non-toxic and should not impart any taste, odor or color to the polymer matrix. The additives should be inert other than their own functions. The physical state of additive may be solid, liquid or even gaseous.

1.8.1. Clay

The commonly used layered silicates are montmorillonite (MMT), hectorite, and saponite. The two types of structure possessed by layered silicates are tetrahedral-substituted and octahedral substituted. The negative charge is found on the surface of silicate layers in the case of tetrahedrally substituted layered silicates. Therefore, they can more readily react with the polymer matrices than the octahedrally-substituted material. The most commonly used clay montmorillonite is from the group of smectites and a representative of the 2:1 type layered silicates. It consists of two tetrahedral silicate layers and an octahedral layer with adjacent margins. As a result of isomorphous replacement of clay from the octahedral layer by cations of lower valence, an excessive negative charge appears on the packet surface. Figure 1.13. shows the structure of layered silicate.

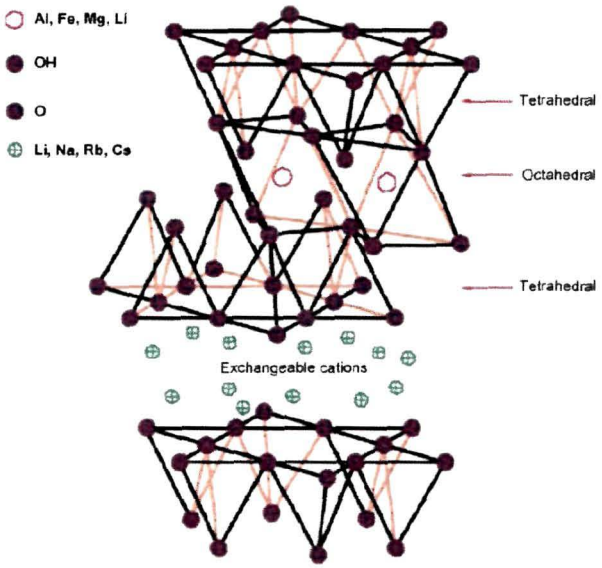

Figure 1.10. Structure of 2:1 phyllosilicates.

Improvement in properties of polymer nanocomposites depends on two particular characteristics of layered silicates. The first one is the capability of the polymer to disperse into the gallery spacing of clay. The second one is the capability to modify their surface chemistry through ion exchange reactions with organic and inorganic cations. These two characteristics are inter-related to each other and the degree of dispersion of layered silicate in a particular polymer matrix depends on the interlayer cation.

1.8.2. Zinc oxide (ZnO)

ZnO is a white powder, insoluble in water, commonly used as an additive in numerous products including plastics, glass, cement, ceramics, foods (source of Zn nutrient), fire retardants, pigments, batteries, first aid tapes and ferrites. It has a large excitation binding energy (60 meV) and a wide band gap (3.37 eV), therefore it can absorb light that lies in the UV range of the solar spectrum and which matches or exceeds their band gap energy [89]. Because of these properties, ZnO is a promising candidate for electronic and optoelectronic applications such as solar cells (anti-reflecting coating and transparent conducting materials), surface acoustic wave devices, liquid crystal displays, heat mirrors, gas sensors etc [90]. ZnO nanoparticles are extensively used in fundamental research as well as potential applications, such as photo catalysts [91], piezoelectric devices, field emitters, hydrogen-storage, ultraviolet lasers and diodes, fluorescence labels in medicine and biology, as high-flame detectors [92] in cosmetic industry and as a component of sun screens [93], controlling units as UV photo detectors etc. In polymer composite, nano ZnO is widely employed as anti-photodegradant. A significant improvement in resistance against UV degradation is observed by Zhao et al. on incorporation of nano ZnO while studying the UV degradation of ZnO filled polypropylene nanocomposites [94].

1.8.3. Silicon dioxide (SiO_2)

Pure silica exists in two forms: quartz and cristobalite. In the case of cristobalite, the silicon atoms are positioned as the carbon atoms in diamond [cubic close-packed (ccp) with half of the tetrahedral holes occupied], with the oxygen atoms situated centrally between each pair of silicon atoms. The empirical formula of quartz is SiO_2 because it is built up of SiO_4 tetrahedra as in silicates with each oxygen atom shared by two silicon atoms.

Silica nanoparticles occupy an important position in scientific research, due to their simple preparation and their extensive applications in various industrial uses, such as pharmacy, humidity sensors, catalysis, electronic and thin film substrates, pigments, electronic and thermal insulators [95]. The size and size distribution of these particles greatly affect the quality of some of these products. Silica-filled polypropylene composites have resulted in an enhancement in mechanical properties, water absorption and thermal properties [96].

1.8.4. Titanium dioxide (TiO_2)

Titanium dioxide, also known as titanium(IV) oxide or titania commonly has four known polymorphs found in nature: anatase (tetragonal), brookite (orthorhombic), rutile (tetragonal), and TiO_2 (B) (monoclinic) [97]. In addition to these polymorphs, two additional high-pressure forms have been synthesized from the rutile phase. These are TiO_2 (II) with a PbO_2 structure and TiO_2 (H) with a hollandite structure [98]. TiO_2 nanoparticles have strong antibacterial functional and anti-aging properties. Adding TiO_2 into polypropylene/polyamide blend can produce excellent mechanical nanocomposites with high antimicrobial and anti-aging properties [99]. Titanium dioxide (TiO_2) has low cost, high stability and safety toward both human and the environment. Due to these properties, it is considered very close to an ideal semiconductor for photocatalysis. Various investigations have established that the photocatalyst property of TiO_2 is much more effective in the form of nanoparticles rather than in bulk powder [100]. When the diameter of the crystallites of a semiconductor particle falls below a critical radius of about 10 nm, each charge carrier appears to behave quantum mechanically as a simple particle [101]. TiO_2 is close to being an ideal photocatalyst and the benchmark for photocatalysis performance. It is cheap, photostable in solution and nontoxic. Its holes are strongly oxidizing and redox selective, therefore several novel heterogeneous photocatalytic reactions have been reported at the interface of illuminated TiO_2 photocatalyst, and TiO_2-based photocatalysis has been investigated exhaustively for environmental cleanup applications. The only drawback is that it does not absorb visible light [97]. Several approaches including dye sensitization, doping, coupling and capping of TiO_2 have been studied extensively to overcome this problem.

1.8.5. Carbon nanotubes (CNT)

Significant improvements in the technology of carbon nanotube-based composites have enabled tremendous research advances made in the scientific base for carbon nanotubes in the last few years. CNT are allotropes of carbon with a cylindrical nanostructure having nanometer radius and length ranging from hundreds of nanometers to micron and even millimeters [102]. The length-to-diameter ratio of the CNT is up to 132,000,000:1, considerably larger than for any other material [103]. This makes them quasi-ideal one

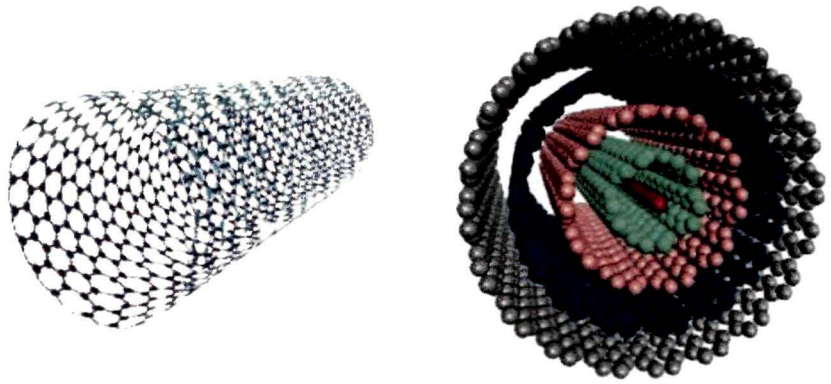

Singlewalled CNT Multiwalled CNT

Figure 1.11. Structure of carbon nanotubes.

dimensional (1D) structures with highly anisotropic properties. The various forms of CNT includes, single-wall and multi-wall, networks or isolated, semiconducting and metallic, bundles, and in a broad distribution of chiralities. The electron delocalization is supported by the carbon atoms on the tube surface that are in sp^2 hybridization, as in most conjugated systems. This happens because even in small diameter tubes, the pyramidalization angle is sufficient for allowing partial overlap of near atomic orbitals. The superb mechanical and physical properties of individual CNTs have driven researchers in developing high-performance continuous fibers based upon carbon nanotubes.

1.9. Techniques for composite preparation

Different synthetic approaches have been used for the preparation of polymer nanocomposites. In general, there are three preparation methods which include solution blending, melt blending and *in-situ* polymerization.

1.9.1. Solution blending

In this method the polymer or prepolymer is dissolved in a solvent and the nanofillers (viz. nanoclay, nano metal oxides, CNT) are dispersed in the same solution. The nanofillers are swollen in the solvent and the polymer chains are intercalated in between the

layers of nanofillers. The solvent is removed through vaporization or precipitation and thus the intercalated nanocomposite is obtained. The polymer chains are diffused into the spaces among nanoparticles depending on the interactions between the nanoparticles and the solvent. Based on the interactions between polymer and the nanofillers, intercalated or exfoliated structures may be obtained in this method. However due to the use of solvent, this technique cannot be applied in industry. However, this method is especially attractive in preparing water soluble polymer-clay nanocomposites [104,105].

1.9.2. Melt blending

In this process, nanofillers are mixed within the polymer matrix in molten condition. Extrusion and injection molding are used for dispersion of nanoparticles within the polymer matrix. Thermoplastic nanocomposites are effectively prepared by this technique [106]. The polymer chains are intercalated or exfoliated in between the spaces of nanofillers. Melt intercalation method has many advantages for the preparation of nanocomposites since no solvent is required and is a popular method for industry [87]. But disadvantage of melt blending process is that it suffers from stress development and generates high temperature [107].

1.9.3. *In situ* polymerization

In this method the nanoparticles are first swollen in monomer liquid or monomer solution. The monomers along with initiators are diffused in between the spacing of nanofillers and are polymerized by the heat or radiation [108]. Due to the lower viscosity of the monomer (as compared to that of polymer melt or polymer solution), it is much easier to break the aggregated particles using either sonication or high shear mixing. The polymerization is carried out within the layer spaces of the nanoparticles. The growth of polymer chains results in the exfoliation and formation of disordered structure. This method is ideal for the preparation of thermoset/clay nanocomposites and has been broadly employed for the epoxies and styrene polymer nanocomposites [109]. The exfoliation and dispersion of nanoparticles can be tailored by the nanofillers and monomer chemistry [110]. Polyaniline/MMT nanocomposites have been prepared by the *in-situ* polymerization of aniline in the presence of MMT [111]. *In-situ* polymerization can be employed to produce

polymer nanocomposites with molecular-level particle dispersion. To conclude, the functionalized nanoparticles become an integral, chemically bonded part of the polymer matrix, leading to an important improvement in both mechanical and physical properties.

1.10. Wood polymer nanocomposites (WPNC)

In the last few decades, research and development has been focused in the field of nanotechnology as it is one of the most popular areas for current research. This obviously comprises of polymer science and technology; and a broad range of topics of investigation can be covered in this field. Polymer nanocomposites can be made with enhanced physical, thermal and other unique properties. They can be synthesized using simple techniques and have properties that are superior to conventional microscale composites. The products are desired to meet a wide range of applications with light weight, high mechanical strength, unique color, stiffness, barrier properties, tunable biodegradability, electrical properties and high reliability in extreme environments. Nanoscience and technology extended an entirely new technique to develop WPC [112]. It is a challenging and attractive field to develop high-value-added and multifunctional wood polymer nanocomposites (WPNC) via nano technique using layered silicate, metal oxide nanoparticles, and carbon nanotubes. Nanomodified WPCs is a potentially new approach to attain better products. Many efforts have been made in the formation of WPNC to obtain superior properties compared to conventional composites so as to meet specific end-use requirements.

Polymer impregnated wood has higher mechanical properties, thermal stability, abrasion resistance, dimensional stability compared to those of natural wood. WPC obtained from impregnation of monomer/polymer in cell wall provides better dimensional stability than that of WPC obtained from impregnation of monomer/polymer in cell lumen. Treatment of wood with thermoplastic like polystyrene, PMMA results in large increase in density as well as thermal conductivity. Wood treated with PMMA in combination with hexamethylene diisocyanate crosslinker resulted in lower moisture absorption and higher water repellent efficiency compared to raw wood. The mechanical property of treated samples in terms of dynamics Young's modulus (E_d) has been found to improve [42] Some polymers increase the moisture content and volumetric swelling of the WPC at 90% relative humidity due to their hygroscopic nature [113]. WPC treated with styrene in combination

with maleic anhydride and glycidyl methacrylate has resulted in enhanced dimensional stability, mechanical properties over the untreated wood [114].

WPNC impregnated with polymer and heterogeneous reinforcing nanofillers dispersed homogenously in the polymer matrix within the wood and thus may overcome all the disàdvantageous properties associated with raw wood. Wood impregnated with water soluble phenol formaldehyde, melamine formaldehyde and alumino silicate as nanofillers shows remarkable improvement in dimensional stability, water repellency, mechanical properties etc. [115,116]. Thus, the properties, which cannot be achieved by raw wood itself, can be achieved by WPNC as it brings a consistency in its quality.

1.11. Merits and demerits of wood polymer nanocomposites

WPNCs offer a number of potential benefits having the advantages of wood, polymer and nanofillers. The properties of wood may vary both between and within species; even wood pieces cut from the same tree. So, in the processing of WPNC, the properties of fragments and reconstituted wood can be better controlled than those of raw wood. Lower-cost maintenance, aesthetic appearance (as it retains its structural integrity) and easy processibility are the primary advantages of WPNC that makes it a potential candidate for construction purposes. WPNCs have superior compression properties (resistance to crushing) compared to that of wood loaded perpendicular to the grain. WPNC require lower maintenance requirements than solid wood because the plastic in the product is not subject to water absorption or biological attack. They put forward great flexibility in the shapes and colors of the materials produced.

Most of the organic treatments lead to some deleterious environmental impact. The use of organic diluents emits volatile organic compounds which are harmful to human health as well as environment. Petroleum based chemical that are used for wood modification are non-renewable, therefore, its use can be substituted by some renewable feedstock biomass.

1.12. Applications of wood polymer nanocomposites

WPNCs can be used in those areas where WPCs are already being used. As mentioned earlier, because of its several advantageous properties compared to natural wood, it is employed in wide range applications. The most common use of WPCs is in outdoor

deck floors, but it is also used for fences, railings, cladding and siding, landscaping timbers, molding and trim, window and door frames, park benches and indoor furniture. Wood-plastic composites were first introduced into the decking market in the early 1990s. Current applications for WPCs include interior auto parts, decking, railing and cladding, railway, wagons, bridges, etc. The major purchasers are of automotive industry, aircraft industry, and construction industry: for the pre-built constructions, door, window and other components used in buildings such as knobs, switches and sockets, and so on. Its applications also include in sports equipment, goods industries and companies manufacturing plastic pipes and fittings, cabinet construction, decoration industries, plate products, office furniture and appliances industries. It is a cheaper alternative to the plastic, wooden and other sheets. Additional potential applications for WPCs include freight containers, the ocean engineering industry, chemical plants, and thermo-acoustic insulation purposes.

REFERENCES

1. Solpan, D. & Guven, O. Preparation and properties of some wood/(co)polymer composites, *Angew. Makromol. Chem.* **269** (1), 30-35, 1999.

2. Gardner, D.J., et al. Wood composite protection, in *Wood deterioration and preservation: advances in our changing world*, B. Goodell et al., eds., American Chemical Society, Washington D.C., 2003, 399-419.

3. Peydecastaing, J. *Chemical modification of wood by mixed anhydrides,* Ph. D. Thesis, Université de Toulouse, Romania, 2008.

4. Young, R. & Rowell, R. (eds.) *Cellulose: Structure, modification and hydrolysis,* Wiley Interscience, New York, 1986.

5. Hon, D.N.S. *Chemical modification of lignocellulosic materials,* Marcel Dekker Inc, New York, Basel, Hong Kong, 1995.

6. Plackett, D. & Dunningham, E. Chemical modification of lignocellulosics, in *Forest Res Inst Bull*, Rotorua, New Zealand, 1992.

7. Saka, S. Chemical composition and distribution, in *Wood and cellulosic chemistry,* D.N.S. Hon & N. Shiraishi eds., Marcel Dekker Inc, New York, USA, 2001, 51-82.

8. Plomion, C., et al. Wood formation in trees, *Plant Physiol.* **127** (4), 1513–1523, 2001.

9. Fengel, D. & Wegener, G. *Wood: Chemistry, ultrastructure, reactions*, Walter de Gruyter, Germany, 1989.

10. Sjöström, E. *Wood chemistry: Fundamentals and applications*, Academic Press, London, 1981.

11. Andersson, S., et al. Studies of crystallinity of scots pine and norway spruce cellulose, *Trees* **18** (3), 346-353, 2004.

12. Cave, I.D. Modelling the structure of the softwood cell wall for computation of mechanical properties, *Wood Sci. Technol.* **10** (1), 19-28, 1976.

13. Salmen, L. & Burgert, I. Cell wall features with regard to mechanical performance: A review, *Holzforschung* **63** (2), 121-129, 2009.

14. Alén, R. Structure and chemical composition of wood, in *Forest Products Chemistry*, P. Stenius, ed., Fapet Oy, Helsinki, 2000, 12-57.

15. Timell, T.E. Recent progress in the chemistry of wood hemicelluloses, *Wood Sci. Technol.* **1** (1), 45-70, 1967.

16. Salmén, L. Micromechanical understanding of the cell-wall structure, *Comptes Rendus-Biologies* **327** (9-10), 873-880, 2004.

17. Yan, L. & Zhu, Q. Direct observation of the main cell wall components of straw by atomic force microscopy, *J. Appl. Polym. Sci.* **88** (8), 2055-2059, 2003.

18. O'Sullivan, A.C. Cellulose: The structure slowly unravels, *Cellulose* **4** (3), 173-207, 1997.

19. Lawoko, M., et al. Changes in the lignin-carbohydrate complex in softwood kraft pulp during kraft and oxygen delignification, Holzforschung **58** (6), 603-610, 2004.

20. Lawoko, M., et al. Structural differences between the lignincarbohydrate complexes present in wood and in chemical pulps, *Biomacromolecules,* **6** (6), 3467-3473, 2005.

21. Kleuters, W. Determining local density of wood by beta ray method, *Forest Prod. J.* **14** (9), 414-420, 1964.

22. Nunez, A.J., et al. Thermal and dynamic mechanical characterization of polypropylene-woodflour composites, *Polym. Eng. Sci.* **42** (4), 733-742, 2002.

23. Hill, A.C. *Wood modification*, 1st ed., John Wiley & Sons, USA, 2006.

24. Bourgois, J., et al. Thermal treatment of wood: analysis of the obtained product, *Wood Sci. Technol.* **23** (4), 303-310, 1989.

25. Nassar, M.M. & Mackay, G.D. Mechanism of thermal decomposition of lignin, *Wood Fiber Sci.* **16** (3), 441-453, 1984.

26. Fengel, D. & Wegener, G. *Wood: Chemistry, ultrastructure, reactions*, Walter de Gruyter, Berlin, 1983.

27. Hon, D.N.S. Weathering and photochemistry of wood, in *Wood and Cellulose Chemistry,* D.N.S. Hon & N. Shiraishi eds., Marcel Dekker, New York, 2001, 512-546.

28. Eaton, R. A. & Hale, M. D. *Wood: Decay, pests and protection,* Chapman & Hall, New York, 1993.

29. Rowell R.M., et al. Chemical modification: adding value through new FPL composite processing technology, *Forest Prod. J.* **38** (7/8), 67-70, 1988.

30. Dunningham E.A., et al. Weathering of chemically modified wood. natural weathering of acetylated radiata pine: preliminary results, *Holz als Roh- und Werkstoff* **50** (11), 429-432, 1992.

31. Plackett D.V., et al. Weathering of chemically modified wood. accelerated weathering of acetylated radiata pine, *Holz als Rohund Werkstoff* **50** (4), 135-140, 1992.

32. Evans, P.D. Review of the weathering and photostability of modified wood, *Wood Mater. Sci. Eng.* **4** (1-2), 2-13, 2009.

33. Timar, M.C., et al. Biological resistance of chemically modified aspen composites, *Int. Biodeter. Biodegr.* **43** (4), 181-187, 1999.

34. Baechler, R.H. Improving wood's durability through chemical modification, *Forest Prod. J.* **9** (5), 166-171, 1959.

35. Rowell, R.M. Chemical modification of wood: Advantages and disadvantages, in *Proceedings of the 71st Annual Meeting of the AWPA,* San Francisco, 1975, 41-51.

36. Rowell, R.M. Chemical modification of wood (Review article), *Forest Prod. Abstracts* **6** (12), 363-382, 1983.

37. Feist, W.C., et al. Moisture sorption and accelerated weathering of acetylated and methacrylated aspen, *Wood Fiber Sci.* **23** (1), 128-136, 1991.

38. Devi, R.R. & Maji, T.K. Chemical modification of rubber wood with styrene in combination with a crosslinker: Effect on dimensional stability and strength property, *Bioresour. Technol.* **88** (3), 185-188, 2003.

39. Schneider, M. Wood polymer composites, *Wood Fiber Sci.* **26** (1), 142-151, 1994.

40. Li, Y., et al. Theory of fluids penetrating wood and its researching method, *Sci. Silvae Sin.* **47** (2), 134-144, 2011.

41. Zhao, Q. & Samulski E.T. A comparative study of poly (methyl methacrylate) and polystyrene/clay nanocomposites prepared in supercritical carbon dioxide, *Polymer* **47** (2), 663–671, 2006.

42. Islam, M.S., et al. Dimensional stability and dynamic young's modulus of tropical light hardwood chemically treated with methyl methacrylate in combination with hexamethylene diisocyanate cross-linker, *Ind. Eng. Chem. Res.* **50** (7), 3900–3906, 2011.

43. Mantanis, G. I., et al. Swelling of wood, *Wood Sci. Technol.* **28** (2), 119-134, 1994.

44. Mantanis, G. I., et al. Swelling of wood, part II. Swelling in organic liquids, *Holzforschung* **48** (6), 480-490, 1994.

45. Hagstrand, P. O. *Mechanical analysis of melamine-formaldehyde composites,* Ph.D. thesis, Chalmers University of Technology, Goteborg, Sweden,1999.

46. Hua, L., et al. Cellulose fiber-polyester composites with reduced water sensitivity (1)—Chemical treatment and mechanical properties, *Polym. Comp.* **8** (3), 199–202, 1987.

47. Hua, L., et al. Cellulose fiber-polyester composites with reduced water sensitivity (2)—Surface analysis, *Polym. Comp.* **8** (3), 203–207, 1987.

48. Rapp, A.O., et al. Electron loss spectroscopy (EELS) for quantification of cell-wall penetration of a melamine resin, *Holzforschung* **53** (2), 111–117, 1999.

49. Baysal, E., et al. Dimensional stabilization of wood treated with furfuryl alcohol catalysed by borates, *Wood Sci. Technol.* **38** (6), 405-415, 2004.

50. Lande, S., et al. Variation in treatability of scots pine (*Pinus sylvestris*) by the chemical modification agent furfuryl alcohol dissolved in water, *Wood Sci. Technol.* **44** (1), 105-118, 2010.

51. Lande, S., et al. Development of modified wood products based on furan chemistry, *Mol. Cryst. Liq. Cryst.* **484** (1), 367-378, 2008.

52. Lande, S., et al. Properties of furfurylated wood, *Scand. J. For. Res.* **19** (5), 22-30, 2004.

53. Lande, S., et al. Chemistry and ecotoxicology of furfurylated wood, *Scand. J. For. Res.* **19** (5), 14-21, 2004.

54. Esteves, B., et al. Properties of furfurylated wood (*Pinus pinaster*), *Eur. J. Wood Prod.* **69** (4), 521-525, 2011.

55. Khan, M.A. & Ali, K.M.I. Wood-plastic composite using water soluble monomer, *Radiat. Phy. Chem.* **40** (6), 433-436, 1992.

56. Bakraji, E. & Salman, N. Properties of wood-plastic composites: effect of inorganic additives, *Radiat. Phy. Chem.* **66** (1), 49-53, 2003.

57. Yang, H.S., et al. Effect of compatibilizing agents on rice-husk flour reinforced polypropylene composites, *Compos. Struct.* **77** (1), 45-55, 2007.

58. Maldas, D. & Kokta, B.V. Improving adhesion of wood fiber with polystyrene by the chemical treatment of fiber with a coupling agent and the influence on the mechanical properties of composites, *J. Adhes. Sci. Technol.* **3** (7), 529-539, 1989.

59. Raj, R. G., et al. Use of wood fibers in thermoplastic composites: VI. isocyanate as a bonding agent for polyethylene-wood fiber composites, *Polym. Comp.* **9** (6), 404-411, 1988.

60. Chtourou, H., et al. Reinforcement of recycled polyolefins with wood fibers, *J. Reinf. Plast. Comp.* **11** (4), 372-394, 1992.

61. Kakiuchi, H. *Manufacture and application of epoxy resins*, Macromolecule Chemistry Publication Society, Kyoto, 1964.

62. Xie, Y., et al. Effects of chemical modification of wood particles with glutaraldehyde and 1,3-dimethylol-4,5-dihydroxyethyleneurea on properties of the resulting polypropylene composites, *Compos. Sci. Technol.* **70** (13), 2003–2011, 2010.

63. Ren, X., et al. Modifications of kenaf fibers with n-methylol acrylamide for production of kenaf-unsaturated polyester composites, *J. Appl. Polym. Sci.* **125** (4), 2846–2853, 2012.

64. Watanabe, M., et al. Preparation of ammonium polyphosphate and its application to flame retardant, *Phosphorus Res. Bull.* **23** (1), 35-44, 2009.

65. Li, B. & He, J. Investigation of mechanical property, flame retardancy and thermal degradation of LLDPE–wood-fibre composites, *Polym. Degrad. Stab.* **83** (2), 241-246, 2004.

66. Baysal, E. Determination of oxygen index levels and thermal analysis of scots pine (*Pinus sylvestris L.*) impregnated with melamine formaldehyde-boron combinations, *J. Fire Sci.* **20** (5), 373-389, 2002.

67. Jana, T., et al. Biodegradable film Modification of the biodegradable film for fire retardancy, *Polym. Degrad. Stab.* **69** (1), 79-82, 2000.

68. Ghosh, S.N. & Maiti, S. Adhesive performance, flammability evaluation and biodegradation study of plant polymer blends, *Eur. Polym. J.* **34** (5-6), 849-854, 1998.

69. Luo, J.J. & Daniel, I.M. Characterization and modeling of mechanical behavior of polymer/clay nanocomposites, *Compos. Sci. Technol.* **63** (11), 1607–1616, 2003.

70. Rozenberg, B.A. & Tenne, R. Polymer-assisted fabrication of nanoparticles and nanocomposites, *Prog. Polym. Sci.* **33** (1), 40–112, 2008.

71. Park, C., et al. The fabrication of syndiotactic polystyrene/organophilic clay nanocomposites and their properties, *Polymer* **42** (17), 7465–7475, 2001.

72. Wypych, G. *Handbook of fillers*, 2nd ed., ChemTec Publishing, Toronto, 1999.

73. Modesti, M., et al. Thermal behavior of compatibilized polypropylene nanocomposite: effect on processing conditions, *Polym. Degrad. Stab.* **91** (4), 672-680, 2006.

74. Hull, T.R., et al. An investigation onto the decomposition and burning behavior of ethylene-vinyl acetate copolymer nanocomposite materials, *Polym. Degrad. Stab.* **82** (2), 365-371, 2003.

75. Tang, Y., et al. Polypropylene/montmorillonite nanocomposites and intumescent, flame-retardant monmorillonite synenergism in polypropylene nanocomposites, *J. Polym. Sci. Part A:Polym. Chem.* **42** (23), 6163-6173, 2004.

76. Gorrasi, G., et al. Transport properties of organic vapors in nanocomposites of organophilic layered silicate and syndiotactic polypropylene, *Polymer* **44** (13), 3679-3685, 2003.

77. Kawasumi, M., et al. Preparation and mechanical properties of polypropylene-clay hybrids, *Macromol.* **30** (20), 6333-6338, 1997.

78. Hasegawa, N., et al. Preparation and mechanical properties of polypropylene-clay hybrids using a maleic anhydride-modified polypropylene oligomer, *J. Appl. Polym. Sci.* **67** (1), 87-92, 1998.

79. Svoboda, P., et al. Morphology and mechanical properties of polypropylene/organoclay nanocomposites, *J. Appl. Polym. Sci.* **85** (7), 1562-1570, 2002.

80. Jancar, J. & Kucera, J. Yield behavior of PP/$CaCO_3$ and PP($Mg(OH)_2$ composites, II: Enhanced interfacial adhesion, *Polym. Eng. Sci.* **30** (12), 714-720, 1990.

81. Lu, C. & Mai, Y.W. Influence of aspect ratio on barrier properties of polymer–clay nanocomposites, *PRL* **95** (8), 088303-1-4, 2005.

82. Xia, H., et al. Visible-light-activated nanocomposite photocatalyst of Fe_2O_3/SnO_2, *Mater. Lett.* **62** (6-7), 1126-1128, 2008.

83. Grossiord, N., et al. High-conductivity polymer nanocomposites obtained by tailoring the characteristics of carbon nanotube fillers, *Adv. Funct. Mater.* **18** (20), 3226–3234, 2008.

84. Okamoto, K., et al. New poly(butylene succinate)/layered silicate nanocomposites. II. Effect of organically modified layered silicates on structure, properties, melt rheology, and biodegradability, *J. Polym. Sci. Part B: Polym. Phy.* **41** (24), 3160–3172, 2003.

85. Zhu, J. & Zhu, Y. Microwave-assisted one-step synthesis of polyacrylamide-metal (M = Ag, Pt, Cu) nanocomposites in ethylene glycol, *J. Phys. Chem. B* **110** (17), 8593-8597, 2006.

86. Corbierre, M.K., et al. Gold nanoparticle/polymer nanocomposites: dispersion of nanoparticles as a function of capping agent molecular weight and grafting density, *Langmuir* **21** (13), 6063-6072, 2005.

87. Ray, S.S. & Okamoto, M. Polymer/layered silicate nanocomposites: a review from preparation to processing, *Prog. Polym. Sci.* **28** (11), 1539–1641, 2003.

88. Giannelis, E.P. Polymer layered silicate nanocomposites, *Adv. Mater.* **8** (1), 29–35, 1996.

89. Nasuaad, A. & Otsego, Y. Rheology and UV protection properties of suspensions of fine titanium dioxides in a silicone oil, *J. Colloid Interface Sci.* **296** (2), 558–564, 2006.

90. Chopra, K.L., et al. Transparent conductors-A status review, *Thin Solid Films* **102** (1), 1-46, 1983.

91. Kim, H., et al. Transparent conducting aluminum -doped zinc oxide thin films for organic light emitting devices, *Appl. Phys. Lett.* **76** (3), 259-261, 2000.

92. Chen, Y., et al. ZnO as a novel photonic material for the UV region, *Mater. Sci. Eng. B* **75** (2-3), 190-198, 2000.

93. Zhang, D.H., et al. The mechanism of blue emission from ZnO films deposited on glass substrate by r.f magneteron sputtering, *J. Phys. D Appl. Phys.* **35** (21), 2837- 2840, 2002.

94. Zhao, H. & Li, R.K.Y. A study on the photo-degradation of zinc oxide (ZnO) filled polypropylene nanocomposites, *Polymer* **47** (9), 3207–3217, 2006.

95. Herbert, G. Synthesis of monodispersed silica powders II. Controlled growth reaction and continuous production process, *J. Eur. Ceram. Soc.* **14** (3), 205-214, 1994.

96. Suryadiansyah, et al. Silica-filled polypropylene composites: the effect of ethylene diamine dilaurate and maleic anhydride grafted polypropylene on mechanical properties, water absorption, morphology, and thermal properties, *Polym. Compos.* **29** (10), 1169-1176, 2008.

97. Carp, O., et al. Photoinduced reactivity of titanium dioxide, *Prog. Solid State Chem.* **32** (1-2), 33–117, 2004.

98. Latroche, M., et al. New hollandite oxides: $TiO_2(H)$ and $K_{0.06}TiO_2$, *J. Solid State Chem.* **81** (1), 78–82, 1989.

99. Baoli, O., et al. Compatibilizing effect of maleated polypropylene on the mechanical properties of injection molded polypropylene/polyamide 6/functionalized-TiO_2 nanocomposites, *Compos. Sci. Technol.* **69** (3-4), 421–426, 2009.

100. Han, H. & Bai. R. Buoyant photocatalyst with greatly enhanced visible-light activity prepared through a low temperature hydrothermal method, *Ind. Eng. Chem. Res.* **48** (6), 2891–2898, 2009.

101. O'Regan, B. & Grätzel, M. A low-cost, high-efficiency solar cell based on dye-sensitized colloidal TiO_2 film, *Nature* **353** (6346), 737–740, 1991.

102. Saito, R., et al. *Physical properties of carbon nanotubes*, Imperial College Press, London, 1998.

103. Wang, X., et al. Fabrication of ultralong and electrically uniform single-walled carbon nanotubes on clean substrates, *Nano Letters* **9** (9), 3137–3141, 2009.

104. Ogata, N., et al. Poly (vinyl alcohol)-clay and poly(ethylene oxide)-clay blends prepared using water as solvent, *J. Appl. Polym. Sci.* **66** (3), 573-581, 1997.

105. Hyun, Y.H., et al. Rheology of poly (ethylene oxide)/organoclay nanocomposites, *Macromolecules* **34** (23), 8084-8093, 2001.

106. Kornmann, X., et al. Synthesis of epoxy–clay nanocomposites: influence of the nature of the curing agent on structure, *Polymer* **42** (10), 4493–4499, 2001.

107. Filippi, S., et al. Structure and morphology of HDPE-g-MA/organoclays nanocomposites: effects of the preparation procedures, *Eur. Polym. J.* **44** (4), 987-1002, 2008.

108. Hussain, F., et al. Review article: Polymer-matrix nanocomposites, processing, manufacturing, and application: an overview, *J. Compos. Mater.* **40** (17), 1511-1565, 2006.

109. Lan, T., et al. Mechanism of clay tactoid exfoliation in epoxy–clay nanocomposites, *Chem. Mater.* **7** (11), 2144–2150, 1995.

110. Pavlidou, S. & Papaspyrides, C.D. A review on polymer-layered silicate nanocomposites, *Prog. Polym. Sci.* **33** (12), 1119-1198, 2008.

111. Olad, A. & Rashidzadeh, A. Preparation and anticorrosive properties of PANI/Na-MMT and PANI/O-MMT nanocomposites, *Prog. Org. Coat.* **62** (3), 293-298, 2008.

112. Zhao, G.J. & Lü, W.H. Nanoscale in wood, nanowood and wood-inorganic nanocomposites. *Forest Stud. China* **5** (1), 44–48, 2003.

113. Ellis, W.D. Moisture sorption and swelling of wood polymer composites, *Wood Fibre Sci.* **26** (3), 333-341, 1994.

114. Li, Y.F., et al. Wood-polymer composites prepared by the in situ polymerization of monomers within wood, *J. Appl. Polym. Sci.* **119** (6), 3207-3216, 2011.

115. Mai, C. & Militz, H. Modification of wood with silicon compounds, inorganic silicon compounds and sol-gel systems: a review, *Wood Sci. Technol.* **37** (5), 339-348, 2004.

116. Sebe, G., et al. Chemical reaction of maritime pine sapwood (*Pinus pinaster Soland*) with alkoxysilane molecules: A study of chemical pathways, *Holzforchung* **58** (5), 511-518, 2005.

CHAPTER II

LITERATURE REVIEW

CHAPTER II

LITERATURE REVIEW

The unique characteristics and comparative abundance of wood have made it a natural material for homes and other structures. Over the years, shortage of high quality hardwood, specialized application of wood coupled with improved technology has driven the attention of researchers in the part to improve quality of the lower grade wood and studies in this area are still being pushed with great interest. The disadvantageous properties associated with wood can be overcome through the formation of wood polymer composites (WPC). The literature relevant to different approaches are discussed in this chapter.

2.1. Various technical processes used for wood modification

The basic technical processes for improvement of quality of wood can be classified into the following types:

a) Impregnation of wood with reactive chemicals: Wood hardening through the impregnation process has been developed since the mid-1960's [1]. The impregnation of the gas or liquid into the wood depends greatly upon diffusion and permeability of the chemicals. Before impregnation the water or air present inside the capillaries of wood must be removed to provide space for the treating fluid. The fluid used must be of low or medium viscosity. The vacuum or pressure is applied by means of which the fluid can be forced into wood. Vinyl monomers such as styrene and methyl methacrylate (MMA), are examples of low viscosity fluids largely used in wood polymer composites preparation through impregnation technique [2,3].

b) Compression of wood: The mechanical properties of wood such as stiffness, strength, surface hardness, and abrasion resistance can be improved by compression perpendicular to the grain direction, resulting in higher wood density [4,5]. Under the influence of moisture, most of the compressed wood can swell almost to its initial uncompressed state. Thus, permanent fixation of deformation after compression is the key to the success of this approach.

c) Chemical impregnation and compression of wood: The resin used for impregnation into the dry wood is compressed in a hot press, and is cured during the process at certain temperature. Without the use of additional adhesive, the impregnated resin can be used to crosslink the veneers. High-density wood-polymer composites were obtained by this approach [6].

2.2. Preparation of wood polymer composites (WPC) through different curing methods

The monomer/polymer impregnated into solid wood can be cured through different approaches. The techniques are discussed below:

a) Radiation curing method: The use of the radiation process for commercial production of wood-polymer materials began in the mid-1960s. The various radiation used are atomic particles, neutrons, photons, gamma rays, X-rays and electrons [7,8]. The cheapest and most practical means of getting a uniform distribution of the polymer into large sections of wood is the gamma radiation treatments. The main drawback of the radiation method is the safety and environment concerns. The cost of transportation of the various wood products to and from the irradiation site would be prohibitive [9].

b) Micro-wave heating curing: The heating rate of a wood material is limited as the heat transfer from the surface into the material is very low for wood. The microwave radiation is efficient for curing treatment of an impregnated wood because bulk heating is observed to be independent from the thermal conductivity of material. It is reported that microwave treatment of birch samples impregnated with urea and formaldehyde resin solutions take 2.5 min to heat the wood up to 100 °C, while it take 32 min in the case of conventional heating process [10].

c) Radio-frequency heating: Radio-frequency heating is used to raise the temperature of the resin impregnated wood quickly, which then polymerizes while exposed to room temperature. Generally a 30-mega watts generator, using a parallel-platen configuration provides the radio-frequency heating [11].

d) Catalyst-heat curing: Out of all the above methods, catalyst heat curing emerges out to be the most efficient route for preparation of WPC. Its main advantages are the simplicity of this technique and the low initial cost to begin production that are attractive for the small companies who make high cost, small volume items [12]. WPC prepared through the catalyst heat treatment is initiated by Meyer [9]. A notable improvement in physical, mechanical and thermal properties is observed by Maji and coworkers while studying the properties of WPC prepared by impregnation of styrene in presence of glycidyl methacrylate (GMA) as crosslinker and 2,2'-azobis isobutyronitrile (AIBN) as catalyst [3,13,14].

2.3. Formation of wood polymer composites by impregnation of monomer/polymer

Property enhancement, uniform finish, aesthetic superiority and reduced maintenance have made modified wood attractive for large-scale use in many industrial applications as a substituent for costly metals and alloys [15]. Fabrication of WPC is one of the promising techniques used to improve the properties of wood by impregnating monomer/prepolymer through catalyst heat treatment followed by *in-situ* polymerization [16-18]. Various types of vinyl monomers and low molecular weight resins are used for impregnating into wood in order to achieve superior properties. Wood impregnated with styrene and MMA can remarkably improve the decay resistance, water repellent effectiveness (WRE) and dimensional stability of wood [19,20]. Vinyl ester monomer can influence the physical and mechanical properties of wood as reported by Garratt et al. [21] When acrylamide is used as impregnating monomer, the WPC results in high polymer loading and improved mechanical properties [22]. Acrylonitrile is used in the production of WPCs mostly in combination with other monomers because the polymer does not improve properties by itself [23,24]. Vinyl chloride is an important vinyl monomer mainly used to produce WPC because of its high reactivity [25]. Recently, the use of this monomer has been restricted in the production of WPC because of its highly toxic and carcinogenic characteristics. The vinyl polymers are clear, colorless and hard thermoplastic materials unlike deep colored phenol formaldehyde (PF) based thermosetting polymers. The vinyl monomer that is polymerized inside the void spaces of wood does not discolor the wood or alter its eye appealing nature [26]. Zhang et al. has impregnated wood with MMA, 2-Hydroxyethyl methacrylate (HEMA), and ethylene glycol dimethacrylate (EGDMA) through vacuum-pressure method which is another useful technique for polymer impregnation into wood and found dimensionally stabilized composites [27].

The harmful effect of using solvent can be removed by using water as a solvent. Impregnating wood with furfuryl alcohol (FA), a renewable chemical obtained from bagasse, residue of sugarcane, using heat and catalyst has been known for decades to improve wood properties [28,29]. The zinc chloride system which is used as a catalyst in the process of furfurylation of wood has a destructive effect on cellulose degradation of wood. This can affect the long-term strength properties of the modified wood. It has been found that among the cyclic carboxylic anhydride system, maleic anhydride is a suitable catalyst for the furfurylation process [30]. Furfurylated wood has been found to improve a number of

wood properties like dimensional stability, weight percent gain (WPG), equilibrium moisture content, hardness, density and durability [31-33]. Other water soluble resin includes urea, melamine and PF resin, polyurethane and polyethylene glycol resins etc. Gao and Li have reported that Poplar wood can be chemically modified with foaming polyurethane resins for the improvement of dimensional stability and mechanical properties [34]. Impregnating wood with melamine formaldehyde (MF) resin can improve surface hardness, weathering, mechanical, thermal and flame retardant properties of wood based composite [35,36]. PF resin treated wood has been reported to improve weight percent gain, surface mechanical properties, flame retardancy, dimensional stability and thermo-mechanical properties [37-39]. Urea formaldehyde resin is widely used to improve antiswelling efficiency, resistance to water absorption, oxygen index, dimensional stability, mechanical properties and hardness of the wood composites [40,41]. Dynamic mechanical properties of wood impregnated with polyethylene glycol are found to improve compared to the pure wood [42].

2.4. Effect of crosslinker on the properties of wood polymer composites

Poor chemical and physical interaction between wood and the polymer lead to failure of the properties of WPC. Though the impregnated polymers impart desirable properties to the final composite, but they are unable to react with the wood cell wall. The monomers are simply bulked the wood cell wall by filling the empty spaces of wood like capillaries and vessels. Various crosslinkers are used to improve the adhesion and interaction between polymer and wood which include EGDMA, trimethylolpropane triacrylate, hexamethylene diisocyanate etc. [43-45]. GMA is another bifunctional crosslinker which can enhance the interaction between wood and styrene resulting in improved dimensional stability and mechanical properties as reported by Devi et al. [13]. Xie et al. has reported that 1,3-dimethylol-4,5-dihydroxyethyleneurea (DMDHEU) can crosslink the cell wall of wood with the polymers and the resulting wood particle/polypropylene composites are thus expected to enhance the properties like dimensional stability, dynamic mechanical properties, tensile properties [46]. N-methylol acrylamide (NMA) crossliker is reported to increase tensile strength, flexural modulus of rupture and flexural modulus of elasticity, and water resistance of fiber reinforced polyester composites [47,48]. The multifunctional monomer HEMA is chosen to improve the penetration of monomers into cell walls resulting in enhanced dimensional stability of wood polymer composites [27].

2.5. Nanofiller based wood polymer composites

The combined effect of inorganic nanofillers and organic polymer has altered the properties of wood and such materials fall under the category of advanced multifunctional nanocomposites. Cai et al. has impregnated melamine-urea-formaldehyde resin (MUF) along with different layered aluminosilicate nanofillers, both hydrophobic and hydrophilic, into solid aspen wood. Significant improvements in wood properties, such as surface hardness, modulus of elasticity and water repellency, are obtained with the addition of hydrophobic nanofillers into the wood [49]. Similar improvement in antiswelling efficiency and dimensional stability is reported when aspen wood is impregnated with MUF resin and three different types of nanoparticles, Cloisite® 30B, Claytone® APA, and Cloisite® Na^+ [50,51]. Nanoclay can also influence the flame retarding characteristic of wood fiber plastic composites [52]. Lu et al. has prepared wood polymer nanocomposites (WPNC) with water soluble PF resin and organophilic MMT (OMMT) and characterized by using X-ray diffractometry (XRD), Scanning electron microscopy (SEM) and Fourier transform infrared spectroscopy (FTIR) [53]. Xue and Zhao has impregnated wood with PF resin and Ca-MMT by vacuum and pressure technique and reported a great enhancement in weight percent gain [37]. Islam and coworker have impregnated five species of Malaysian tropical wood species with PF resin and montmorillonite (MMT) nanoclay using vacuum-impregnation technique. Properties like weight percent gain and density of wood polymer nanocomposites are dependent on wood species. Thermo-mechanical properties of wood samples as investigated by dynamic mechanical thermal analysis (DMTA) are found to improve. The intrinsic properties of the components, morphology of the system and the nature of interface between the phases are also determined through DMTA test. Dynamic Young's modulus (E_d) of wood is also calculated using free vibration testing. A significant increment in properties obtained for the PF-nanoclay impregnated WPNC [39].

The shielding of ultraviolet (UV) irradiation is provided by the nanolayers of clay in polymer nanocomposite but zinc oxide (ZnO) is a promising candidate for providing an efficient photostability [54]. ZnO polymer composites are of technical importance due to their potential applications in optical device, gas sensing, solar cells, electrochromic windows, photonic applications and in antimicrobial application of food preservation [55]. ZnO nanoparticles can efficiently improve the mechanical properties as revealed by dynamic mechanical analysis for carboxylated nitrile rubber [56]. The weatherability and leach resistance of ZnO impregnated wood is studied by Clausen et al. [57,58].

Silicon dioxide (SiO_2) is widely used in polymer composites as nanofillers. SiO_2 based polymer composites are used in electrochemical sensing fuel cells, chemical separation and water treatment [59]. SiO_2 is known to increase the tensile and impact strength of epoxy nanocomposite [60]. Shi et al. has reported an improvement in dimensional stability, flame resistance and hardness after incorporation of nano SiO_2 into the urea formaldehyde modified wood [40]. The application of silica and other inorganic nanosols for restoring and preserving wood products is reported in the literature [61].

Among the different nanofillers, Titanium dioxide (TiO_2) nanopowder is increasingly being investigated to improve UV stability and durability of the composites. TiO_2 reinforcement can improve physiochemical, mechanical and abrasion resistance properties making the nanocomposites a promising category of products [62]. Most of the reports have addressed the enhancement in properties of wood such as weather resistance and antimicrobial activity of wood by the use of TiO_2 sols through sol-gel methods [63,64]. It can enhance flame resistance [65], UV resistance [66] and durability [67] of composites.

Carbon nanotubes (CNT) are considered to be new emergent multifunctional materials that have outstanding mechanical and thermal properties which makes it potential contender for a wide variety of applications [68]. Recent studies show that the functionalized CNT that are homogenously distributed in the polymer matrix leads to a remarkable enhancement in strength, stiffness and fatigue durability [69,70] and fracture toughness [71] of the epoxy nanocomposites. Jin et al. has reported a significant improvement in mechanical properties and reduced moisture uptake of wood plastic composites co-extruded with multiwalled CNT [72].

Reports regarding the development of WPNC reinforced by nanoclay or metal oxide nanoparticles are well addressed as cited in the above literature. Impregnation of wood with combination of metal oxide and nanoclay, CNT has not been reported so far.

2.6. Characterization techniques

2.6.1. Nuclear magnetic resonance (NMR) spectroscopy

Nuclear magnetic resonance (NMR) spectroscopy is a commonly used modern analytical technique that has the potential to determine the influence of the synthesis parameters on the resin structure. The chemical shift in a ^{13}C-NMR experiment is a sensitive probe of chemical structure. The ^{13}C-NMR is an attractive tool for the analysis of complex

materials such as synthetic polymers and resins because of the relatively large chemical-shift range. Both solid and liquid samples can be analyzed *in situ* by NMR spectroscopy without the necessity for prior modification which is one of the best advantages of NMR. Angelatos et al. has studied the structural elucidation of the amino resins viz. urea formaldehyde, melamine formaldehyde and MUF resins by ^{13}C-NMR, ^{1}H-NMR and ^{15}N NMR [73]. Chuang et al. has investigated the structures of urea formaldehyde resin prepared from different formaldehyde-to-urea molar ratios and at different pH by ^{13}C NMR spectroscopy [74].

2.6.2. Fourier transform infrared (FTIR) spectroscopy

Fourier transform infrared (FTIR) spectroscopy is a widely used technique to confirm the formation of compounds and to characterize wood polymer nanocomposites. Islam et al. has impregnated polyvinyl alcohol into Batai tropical wood species and characterized the formation of WPC through FTIR spectroscopy [75]. Devi et al. has prepared styrene-acrylonitile copolymer and impregnated it along with GMA and nanoclay into simul wood. The prepared copolymer and the formation of WPNC have been characterized by FTIR [76]. It has been observed that in the case of WPNC, the intensity of the hydroxyl peak of wood always has decreased and shifted to lower wave number. A decrease in peak intensity of hydroxyl group and shifting to lower wave number in wood polymer composite has been reported by Dikobe and Luyt [77]. The increase in the intensity of –CH peak also indicates the presence of polymer in the composites. An increase in the –CH peak intensity has been observed by Awal et al. for the polypropylene/wood composite [78].

2.6.3. X-ray diffraction (XRD)

X-ray diffraction (XRD) technique is extensively used for characterization of WPNC. XRD can determine conveniently the interlayer spacing of the silicate layers in the original layered silicates and in the intercalated nanocomposites. The degree of intercalation of MMT in high density polyethylene based WPC is detected by XRD [79]. Lu et al. has prepared WPNC by impregnation of PF resin and nanoclay. The XRD characterization of the nanocomposites reveals that some exfoliated MMT enters the non-crystallized region of microfibrils in wood cell walls resulting in decreased crystallinity of wood in WPNC [53]. The appearance of crystalline peak of metal nanoparticles in the case of polymer metal oxide

composite can be confirmed by XRD. Mina et al. has studied the XRD pattern of crystalline peaks of TiO_2 nanoparticles in polypropylene matrix [80].

2.6.4. Scanning electron microscopy (SEM)

Scanning electron microscopy (SEM) is an electron microscopy technique for analyzing surface morphology of wood polymer composites. The void spaces of untreated wood gets filled up by polymer on impregnation as analyzed by SEM [81]. Islam et al. has impregnated several types of tropical wood species with acrylonitrile monomer solution by vacuum-pressure method. The deposition of polymer into the wood has been evidenced by SEM [82]. Xie et al. has impregnated aqueous solution of (3-glycidyloxypropyl) trimethoxysilane, vinyl trimethoxysilane, and (3-aminopropyl) trimethoxysilane into Eurpean spruce wood. Scanning electron microscopy-energy dispersive X-ray spectroscopy (SEM-EDS) analysis has revealed that there is reduced amount of silane in the cell walls with increased aging time [83]. Moreover, SEM analysis also helps in evaluating the existence of microbes in polymer composite after the degradation study. Li et al. has studied the decay resistance of wood and WPC prepared by *in-situ* polymerization of monomers. The SEM observations for the decayed poplar wood, Micheliamacclurel wood and their corresponding treated wood have shown a remarkable improvement in decay resistance of wood after treatment [84].

2.6.5. Transmission electron microscopy (TEM)

Transmission electron microscopy (TEM) is an important microscopy technique and extensively employed in its simplest bright field mode for direct visualization of the nanocomposite structure of polymer nanocomposites. Cai et al. has reported uniform distribution of nanoclay in the cell wall of wood when impregnated along with MUF resin. The presence of nanoclay can be seen as some dark lines [49]. Devi and Maji have reported homogeneous dispersion of ZnO nanopartcles in the cell wall of wood with the SAN polymer matrix while investigating wood polymer nanocomposites [85]. Similarly, Deka and Maji have also reported the presence of dark lines in the TEM micrograph correspond to the layers of nanoclay and the dark spots are for SiO_2 and ZnO nanoparticles while studying the TEM analysis of wood polymer/clay/SiO_2/ZnO nanocomposites [86]. Now-a-days, high resolution TEM (HRTEM) is used to obtain a much closer look at the samples. The information on the composition of polymer surface can be obtained by electron energy loss

spectroscopy imaging techniques to TEM (ESI-TEM) and it proved to be an influential technique for the characterization of colloidal nanocomposites.

2.7. Properties of wood polymer nanocomposites

2.7.1. Dimensional stability and water absorption properties

The dimensional stability and water repellency are the most essential properties of WPCs. Impregnation of wood with FA results in high dimensional stability as reported in literature [87,28]. The PF resin contributes to a remarkable increase in dimensional stability as they penetrate into the cell wall of bamboo [88,89]. Crosslinking agent plays a crucial role in enhancing dimensional stability of the composites by forming a crosslinked structure with the hydroxyl group of wood cellulose. Xie et al. has used both glutaraldehyde and DMDHEU as crosslinker in wood particle/polypropylene composites. The composites have shown a great reduction in water uptake and dimensional swelling of the resulting composites up to 39% and 46%, respectively [46]. The water-uptake rate of the kenaf-unsaturated polyester composites has reduced significantly when kenaf fiber mats is modified with NMA solution with either sulfuric acid or p-toluenesulfonic acid [48]. HEMA is another functional monomer which can reduce the water uptake capacity of WPC when impregnated into wood [27]. GMA can enhance the dimensional stability and reduce water uptake capacity of wood when impregnated into the pinewood with styrene as the impregnating monomer [90]. The process of water accessibility into the composites is further restricted by the incorporation of nanoparticles into the composites. The dimensional stability and water repellency of wood impregnated with MUF resin and nanoclay have been reported to improve due to better interphase between MUF and nanoparticles, and their co-reinforcement on the wood [39]. Initially, water saturates the cell wall (via porous tubular and lumens) of the fiber, and next water occupies void spaces [91]. As the polymer and nanoclay fills the voids and the lumens of wood fiber in composites, the penetration of water by the capillary action into the deeper parts of composite is prevented.

2.7.2. Thermal properties

Improvement of thermal stability is an important research area of the WPC. An increase in thermal stability of WPC is observed in comparison to untreated wood when

mercerized wood species is impregnated with N,N-dimethylacetamide [92]. Modification of the thermal properties of wood impregnated with polyacrylonitrite over untreated wood has been evaluated in terms of differential thermogravimetry-thermogravimetric-differential thermal analysis (DTG-TG-DTA) in air. Resistance of wood against thermo-oxidation has improved for the treated wood samples [93]. An increase in thermostability of the composites has been reported by Awal et al. after addition of compatibilizer into the WPC [78]. Incorporation of clay can enhance the thermal stability of the composites due to the presence of silicate layers which can barricade and defer the diffusion of decomposed volatile products throughout the composites [94]. Laachachi et al. has found an improvement in thermal stability of poly(methyl methacrylate) (PMMA) composite after addition of organo-MMT and ZnO into PMMA [95]. Improvement in thermal properties of PMMA silica nanocomposite is also observed by Katsikis et al. [96]. Laachachi et al. has studied the thermal stability of PMMA by using organoclay and TiO_2 and found a significant increase in thermal stability of PMMA [97].

Thermogravimetric analysis (TGA) is one of the main thermal analysis technique used to study the thermal stability, mass change and degradation behavior of the samples. The determination of kinetic parameters such as activation energy from TGA associated with thermal degradation is an important tool in estimating the thermal decomposition kinetics of composites and polymers [98-100]. Many expressions are used for the evaluation of the non-isothermal kinetic parameters of the thermal degradation of the samples. The activation energy of the composites in terms of the Ozawa-Flynn-Wall (OFW) expression is preferred as it requires less experimental time. It is one of the intergral methods for determination of activation energy from thermal degradation reaction without knowing the order of a reaction and is a relatively simple method [101]. Zhao et al. has studied the influence of fullerene on the kinetics of thermal and thermo-oxidative degradation of high-density polyethylene by the OFW method [102]. The Vyazovkin (V) method represents an advanced non linear isoconversional method that removes the disadvantages associated with OFW method and provides an accurate measurement of activation energy [103,104]. This method has been utilized to determine the effective activation energy of non-isothermal crystallization of the polymer melts [105].

2.7.3. Flame retardant properties

Wood is combustible in nature and there is unremitting attempt to improve fire resistant properties of WPC. Baysal et al. has impregnated wood with styrene and PMMA;

boric acid and borax mixture treatment has been done to the wood prior to the monomer impregnation. The resultant composites have shown improvement in fire resistance properties [106]. Addition of nanoclay into the composite enhances the fire resistance of the composites. Camino et al. has reported the fire resistance of epoxy clay nanocomposites when the silicate char of the clay present on the surface of WPC decreases the flame propagation property of the composite [107]. Li et al. has reported that treatment of low density polyethylene-wood-fibre composites with Ammonium polyphosphate (APP) and the mixtures of APP, melamine phosphate or pentaerythritol can significantly improve the flame resistance of the composites [108]. Other flame retardants that can impart fire resistance to the composites include silica, boron, etc., type of compounds [109,110]. Most of the fire retardants can easily leach to the surface and on burning produce harmful fumes and gases which are highly perilous to the environment as well as to human health. The use of polymeric flame retardant can reduce the leaching problem and enhance the service life of the product [111]. But these are not biodegradable and cause serious threat to the environment. Polymeric flame retardant obtained from renewable resources i.e. from a local plant *Moringa oleifera* will be eco-friendly, cheaper and can minimize the leaching problem [112]. Ghosh et al. has studied the flame resistance properties of natural rubber blended with plant polymer [113].

2.7.4. Mechanical properties

WPCs should display super mechanical properties. Ali et al. has evaluated mechanical properties of WPC from neem, mango and cork wood in terms of compressive test, hardness and reported an improvement in properties in comparison to untreated wood [114]. MF resin impregnation has shown considerable potential to improve a number of wood properties, such as surface hardness and weathering resistance [115]. Wood treated with PF resins shows an improvement in modulus of elasticity (MOE) and hardness as investigated by Huang et al. [116]. Crosslinking agents can further impart an improvement in mechanical properties. Incorporation of DMDHEU and glutaraldehyde as crosslinker into wood particle/polypropylene composite can enhance the mechanical properties of the composites as it can form a crosslinked structure with the cell of wood and stiffen the polymer chains [46].

Polymer/clay nanocomposites exhibit dramatic increment in modulus and strength compared to the conventional composites [117]. WPC treated with nanoclay can provide substantial improvement in flexural and tensile strength [118]. The mechanical properties of

WPC further can be enhanced by the addition of different additives like nano SiO_2, nano ZnO etc. [40,119]. Islam et al. has reported a considerable improvement in dynamic mechanical properties and dynamic young's modulus when wood is impregnated with PF resin and nanoclay [39]. The dynamic mechanical behavior of WPC based on impregnation of maleic anhydride and styrene into wood is also studied [120].

2.7.5. UV resistance

The photodegradation of wood results primarily from the ultraviolet aspect of sunlight and leads to surface roughness, discoloration, loss in strength properties etc. UV resistance is one of the most desirable properties of WPC for outdoor applications. Acetylation has also been used as a potential method for altering the chemical nature of the substrate, so that it is more effectively protected against exposure to solar radiation. Wood on acetylation and subsequently exposed to accelerate weathering has developed less cracks than the untreated ones, however, graying of the surface is not reduced [121]. Patachia et al. has treated wood with ionic liquid and observed an improvement in UV resistance as demonstrated by the low lignin, carbonyl index and cellulose crystallinity index variation, as well as very small color modification of the surface with the increase of the UV exposure period, by comparing to non-treated wood [122]. Xie et al. has prepared WPCs by impregnating scots pine veneers with DMDHEU. SEM has revealed that DMDHEU treatment is highly effective to prevent the degradation of the wood cell wall during weathering as they can cross-link the cell wall of wood and dimensionally stabilize wood [123]. Current approaches of adding photostabilizers and pigments into the composites provide protection against discoloration caused by UV radiation. Du et al. has observed an increase in UV stability of wood flour/high density polyethylene composite after the incorporation of TiO_2 [124]. UV resistance of rubberwood (*Hevea brasiliensis*) coated with zinc oxide (ZnO) nanoparticles dispersed in maleic anhydride modified polypropylene (MAPP) has been evaluated by Salla et al. Dispersion of ZnO nanoparticles in MAPP and polyurethane coatings has restricted the color changes and improved the photodegradation of wood polymer composites [125].

2.7.6. Decay resistance

Wood is vulnerable to degradation when exposed to microorganisms. The conditions essential for fungal growth in wood are food, sufficient oxygen, suitable temperature, and

adequate moisture. Modification of wood with suitable chemicals is the effective way to improve decay resistance of wood. Yalinkilic et al. has prepared WPCs using boric acid and phenylboronic acid which are added into aqueous solutions of non- or low-formaldehyde reagents; DMDHEU, glutaraldehyde and glyoxal. Boron addition to these reagents has improved considerably the decay resistance against *Tyromyces palustris* and *Coriolus versicolor*, which are the representative test fungi of brown- and white-rot [126]. Wood modification by impregnation of polymer is able to provide protection against fungal attack, termite attack and decay resistance [127]. The impregnated polymer can improve both the mechanical properties of wood and defer or stop wood matrix from being attacked by water or microorganisms [128]. Yildiz et al. has used three different monomers; styrene, MMA and styrene/MMA mixture for impregnating into maritime pine (*Pinus pinaster Ait.*) and poplar (*Populus x. euramericana cv. I-214*) wood. Weight losses due to fungal attack for pine and poplar–polymer composites have been determined. Although polymers at full and half loading levels has helped decreasing weight losses due to both fungi for each wood species, but little weight losses has been found for the treated wood samples [129]. Some examples of suitable monomer combinations for *in-situ* copolymerization include tri-n-butyl tin methacrylate maleic anhydride and tri-n-butyl tin methacrylate-glycidyl methacrylate. Comonomers that carry anhydride or epoxy functional groups can be grafted to wood through esterification or etherification of wood hydroxyls. Pentachlorophenol acrylate and Fyrol 6 acrylate polymers provide no protection against decay, whereas tributyltin acrylate, 8- hydroxyquinolyl acrylate, and 5,7-dibromo-8-hydroxyquinolyl acrylate have been found to be resistant to the brown-rot fungus, *Gloeophyllum trabeum,* at low polymer loading of 2–5% retention [130,131]. Treatment of wood with FA also leads to substantial resistance against decay [132].

With the incorporation of nanoclay, the rate of bacterial growth in the composites has also increased due to the catalytic effect of the nanoclay in the degradation process [133]. The hydrophilic nature of nanoclay promotes the growth of micro organisms.

2.8. Objectives and plan of work

Various species of wood are available in the forest of North-eastern part of India. The lower grade softwoods that are widely available in the forest of the region are not suitable for structural components due to their poor mechanical, dimensional and other properties. They are mainly used for fuel applications. These softwoods can be made value

added products by modification. Modification of softwood can be done through treatment with polymers.

Increased awareness of wood preservatives on environmental effect has rendered special importance to FA as an eco-friendly agent for wood modification. FA causes wood cell wall to swell and sufficiently polar so that they enter easily into wood cell walls [28]. Impregnation of wood with FA will lead to considerable improvement in properties such as hardness, density, equilibrium moisture content, dimensional stability and durability [87,30]. Nevertheless, furfurylation does not have marked influence on the bending strength and the modulus of elasticity (MOE) of wood [33]. Modification of wood with MF resin can significantly improve the mechanical properties of wood [115]. Besides, it contains nitrogen and as a result it can influence thermal properties and flammability of the prepared composites. Therefore, a copolymer of melamine formaldehyde and furfuryl alcohol (MFFA) could improve the overall properties of the composites.

Acrylamide modified wood results in improved polymer loading and mechanical properties of the composites [22]. But the composites lack in dimensional stability due to the swelling behavior of acrylamide. Therefore overall properties of wood could be enhanced on treatment with melamine formaldehyde-acrylamide (MFA) copolymer.

Wood is a complex natural biomaterial that is subjected to variation in quality and properties like dimensional stability, strength, durability which restrict its end use applications. The deposition of polymer into the empty spaces of wood can be enhanced by the use of suitable crosslinking agent. The crosslinking agent provides interfacial interaction by forming bond between hydrophilic wood and hydrophobic polymer. It can crosslink with the cell wall of wood forming a networked structure.

Flame retarding agents restrain ignition by acting either through the vapor phase or the condensed phase via chemical and/or physical mechanisms. Phosphorus acts in the condensed phase to support char formation. It can barricade to inhibit gaseous products from diffusing to the flame and shielding the composites from heat. Polymeric flame retardant obtained from renewable resource i.e. from *Moringa oleifera* plant can be effectively used as flame retardant as it contains phosphorus. Moreover it is eco-friendly.

The study of sub micron structure of wood is crucial to facilitate better utilization and preservation of wood resources in future. Nanotechnology deals with the material in sub micron level. It has been applied in many fields of polymer successfully. Nanoscale materials have high aspect ratio and large surface area for a given volume. The properties of nano particles reinforced composites differ significantly from conventional filler reinforced composites of same composition as many physical and chemical properties are governed by

surface and surface properties. The properties greatly depend on the surface area of the nanoparticles and the degree of dispersion of nanoparticles in the polymer matrix. It is not possible to achieve the desirable properties of the nanocomposites without having homogenous dispersion of the nanoparticles.

MMT is commonly employed nanofillers, among all potential nanocomposite precursors. The crystal structure of nanoclay consists of layers of two tetrahedrally coordinated silicon atoms fused to an edge-shared octahedral sheet of either aluminum or magnesium hydroxide. The ability of silicate particles to fine-tune their surface chemistry through ion exchange reactions with organic and inorganic cations is a unique characteristic of the nanoclay. The surface energy of clay particles can be lowered by organic ammonium ion. This facilitates the polymers with different polarities to get intercalated between the silicate layers and proper dispersion of silicate layers.

In addition to clay, other nanoparticles which contribute to improved properties such as thermal stability, flame retardancy, mechanical properties of the nanocomposites include ZnO, SiO_2, TiO_2, carbon nanotubes etc.

Ficus hispida is a lower grade softwood widely available in the north-eastern part of India. The objective of this work is to modify the properties of this wood for making them value added material. Modification is done through vacuum impregnation of different monomer/prepolymer viz. MMA, MFFA and MFA. Various crosslinking agent namely GMA, NMA, DMDHEU and HEMA are used while gum obtained from the plant *Moringa oleifera* is used as flame retardant. Different nanofillers are impregnated along with the monomer/copolymer and polymerized by using catalyst heat treatment. The different nanofillers include organically modified nanoclay, surface modified ZnO, SiO_2, TiO_2, CNT etc. The effect of clay, metal oxide nanoparticles, CNT on the different properties of WPCs has been explained.

Keeping these above in view, WPNC have been prepared by impregnating monomer/prepolymer, crosslinker, flame retarding agent and nanoparticles into wood. Attempts have been made to see the effect of these agents on the properties like dimensional stability, mechanical properties, thermal stability, and fire resistance. Wide literatures are available on WPC, however far less are reported concerning WPNC.

The plan of work has been opted as follows:

i) Preparation of prepolymer/copolymer, DMDHEU, NMA.

ii) Development of a suitable crosslinker that has improved compatibility towards the polymer and wood.

iii) Preparation of WPNCs by vacuum impregnation of polymer/copolymer, crosslinker, flame retardant, nanoparticles into wood.

iv) Optimization of different ingredients to obtain the maximum improvement in properties of the nanocomposites.

v) Study the effect of various parameters like amount of crosslinking agent, amount of flame retardant, percentage of nanoclay, percentage of different nanofillers viz ZnO, TiO_2, SiO_2, CNT used either alone or in combination with other nanofiller on the various properties of the composites.

vi) Characterization of the copolymer and WPNC by nuclear magnetic resonance (NMR), FTIR, XRD, SEM and TEM.

vii) Study of water uptake resistance, dimensional stability, chemical resistance, thermal stability, flame retardancy and mechanical properties like tensile, flexural and dynamic mechanical properties as analyzed by Universal Testing Machine, dynamic mechanical analyzer (DMA).

viii) Study the biodegradability of the nanocomposites.

REFERENCES

1. Siau, J. F., et al. Wood-polymer combinations using radiation techniques, *Forest Prod. J.* **15** (10), 426-434, 1965.

2. Ibach, R. & Ellis, W. Lumen modifications, in *Handbook of Wood Chemistry and Wood Composites,* R.M. Rowell, eds., CRC Press, Washington, D.C., 2005, 421-446.

3. Devi, R.R., et al. Studies on dimensional stability and thermal properties of rubber wood chemically modified with styrene and glycidyl methacrylate, *J. Appl. Polym. Sci.* **93** (4), 1938–1945, 2004.

4. Bekhta, P., et al. Properties of plywood manufactured from compressed veneer as building material, *Mater. Des.* **30** (4), 947-953, 2009.

5. Ito, Y., et al. Compressive-molding of wood by high pressure steam-treatment: part 1. Development of compressively molded squares from thinning, *Holzforschung* **52** (2), 211–216, 1998.

6. Fry, H. J. *Compression impregnation of wood veneers,* **US Patent No. 3950577 A,** April 13, 1976.

7. Cleland, M.R., et al. X-rayinitiated polymerization of wood impregnants, *Radiat. Phys. Chem.* **78** (7-8), 535–538, 2009.

8. Betty, W.R. *Dimensional stabilization of lignocellulosic materials,* **US Patent No. 3968318**, July 06, 1976.

9. Meyer, J. A. Treatment of wood-polymer systems using catalyst-heat techniques, *Forest Prod. J.* **15** (9), 362-364, 1965.

10. Galperin, A. S., et al. Manufacturing and properties of modified wood: A review of 25 years work, *Holzforschung* **49** (1), 45-50, 1995.

11. Beall, F. C., et al. Direct and RF heat curing of wood-plastic composites, *Forest Prod. J.* **16** (9), 99-106, 1966.

12. Meyer, J. A. Industrial use of wood-polymer materials: state of the art, *Forest Prod. J.* **32** (1), 24-29, 1982.

13. Devi, R.R., et al. Chemical modification of rubber wood with styrene in combination with a crosslinker: effect on dimensional stability and strength property, *Bioresour. Technol.* **88** (3), 185–188, 2003.

14. Devi, R.R., et al. Modification of rubber wood with styrene in combination with diethyl allyl phosphate as the flame-retardant agent, *J. Appl. Polym. Sci.* **105** (5), 2461–2467, 2007.

15. Deka, M. & Saikia, C.N. Chemical modification of wood with thermosetting resin: effect on dimensional stability and strength property, *Bioresour. Technol.* **73** (2), 179-181, 2000.

16. Elvy, S.B., et al. Effects of coupling agent on the physical properties of wood-polymer composites, *J. Mater. Process. Technol.* **48** (1–4), 365–371, 1995.

17. Baysal, E., et al. Some physical, biological, mechanical, and fire properties of wood polymer composite (WPC) pretreated with boric acid and borax mixture, *Constr. Build. Mater.* **21** (9), 1879–1885, 2007.

18. Yap, M.G.S., et al. Thermal properties of tropical wood–polymer composites, *J. Appl. Polym. Sci.* **43** (11), 2057–2065, 1991.

19. Dong, X., et al. Characterization and durability of wood-polymer composite prepared by *in-situ* polymerization of methyl methacrylate and styrene, *Sci. Res. Essays* **7** (24), 2143-2149, 2012.

20. Alma, M.H., et al. Water repellency of several wood species impregnated with vinyl monomers, *Int. J. Polym. Mater. Polym. Biomater.* **30** (3-4), 1995.

21. Garratt, P.G., et al. Preparation of wood-plastic composites by impregnation with vinyl ester monomer combinations and polymerization with gamma radiation, *Holzforchung* **26** (3), 96-102, 2009.

22. Khan, M.A. & Ali, K.M.I. Wood-plastic composite using water soluble monomer, *Radiat. Phys. Chem.* **40** (6), 433-436, 1992.

23. Persenaire, O., et al. End-grained wood polyurethane composites, 2a: dimensional stability and mechanical properties, *Macromol. Mater. Eng.* **289** (10), 903-909, 2004.

24. Şolpan D. & Güven, O. Preservation of beech and spruce wood by allyl alcohol based copolymers, *Radiat. Phys. Chem.* **54** (6), 583-591, 1999.

25. Calleton, R., et al. Treatments of southern pine with vinyl chloride and methyl methacrylate (MMA) for radiation-produced wood-plastic combinations, *Wood Sci. Technol.* **4** (3), 216-225, 1970.

26. Haque, N. *A literature review of research into wood-plastic composites,* M.Sc. Thesis, University of Wales, Bangor, UK, 1997.

27. Zhang, Y., et al. Dimensional stability of wood–polymer composites, *J. Appl. Polym. Sci.* **102** (6), 5085–5094, 2006.

28. Baysal, E., et al. Dimensional stabilization of wood treated with furfuryl alcohol catalysed by borates, *Wood Sci. Technol.* **38** (6), 405-415, 2004.

29. Lande, S., et al. Chemistry and ecotoxicology of furfurylated wood, *Scand. J. For. Res.* **19** (5), 14-21, 2004.

30. Schneider, M.H. New cell wall and cell lumen wood polymer composites, *J. Wood Sci. Technol.* **29** (2), 121-127, 1995.

31. Venas, T.M. & Rinnan, A. Determination of weight percent gain in solid wood modified with in situ cured furfuryl alcohol by near-infrared reflectance spectroscopy, *Chemometr. Intell. Lab.* **92** (2), 125-130, 2008.

32. Lande, S., et al. Variation in treatability of Scots pine (*Pinus sylvestris*) by the chemical modification agent furfuryl alcohol dissolved in water, *Wood Sci. Technol.* **44** (1), 105–118, 2010.

33. Esteves, B., et al. Properties of furfurylated wood (*Pinus pinaster*), *Eur. J. Wood Prod.* **69** (4), 521-525, 2011.

34. Gao, Z. & Li, D. Chemical modification of poplar wood with foaming polyurethane resins, *J. Appl. Polym. Sci.* **104** (5), 2980-2985, 2007.

35. Gindl, W., et al. Using a water-soluble melamine-formaldehyde resin to improve the hardness of Norway spruce wood, *J. Appl. Polym. Sci.* **93** (4), 1900-1907, 2004.

36. Bajia, S., et al. Solid-state microwave synthesis of melamine-formaldehyde resin, *E-J. Chem.* **6** (1), 120-124, 2009.

37. Xue, F. & Zhao, G.J. Optimum preparation technology for Chinese fir wood/Ca-montmorillonite (Ca-MMT) composite board, *Forest Stud. China* **10** (3), 199–204, 2008.

38. Lü W.H. & Zhao, G.J. Preparation of chinese fir wood/MMT nanocomposites and the factors affecting it, *Forest Stud. China* **9** (1), 45–50, 2007.

39. Islam, M.S., et al. Tropical wood polymer nanocomposite (WPNC): The impact of nanoclay on dynamic mechanical thermal properties, *Compos. Sci. Technol.* **72** (16), 1995-2001, 2012.

40. Shi, J., et al. Improvement of wood properties by urea-formaldehyde resin and nano-SiO_2, *Front. For. China* **2** (1), 104–109, 2007.

41. Yu, X., et al. Preparation and characterization of urea-formaldehyde resin–sodium montmorillonite intercalation-modified poplar, *J. Wood Sci.* **57** (6), 501–506, 2011.

42. Wallström, L. & Lindberg, K.A.H. Wood surface stabilization with polyethyleneglycol, PEG, *Wood Sci. Technol.* **29** (2), 109-119, 1995.

43. He, S., et al. Injectable biodegradable polymer composites based on poly(propylene fumarate) crosslinked with poly(ethylene glycol)-dimethacrylate, *Biomater.* **21** (23), 2389-2394, 2000.

44. Khalid, M., et al. Effect of trimethylolpropane triacrylate (TMPTA) on the mechanical properties of palm fiber empty fruit bunch and cellulose fiber biocomposite, *J. Eng. Sci. Technol.* **3** (2), 153 – 162, 2008.

45. Islam, M.S., et al. Dimensional stability and dynamic young's modulus of tropical light hardwood chemically treated with methyl methacrylate in combination with hexamethylene diisocyanate cross-linker, *Ind. Eng. Chem. Res.* **50** (7), 3900–3906, 2011.

46. Xie, Y., et al. Effects of chemical modification of wood particles with glutaraldehyde and 1,3-dimethylol-4,5-dihydroxyethyleneurea on properties of the resulting polypropylene composites, *Compos. Sci. Technol.* **70** (13), 2003–2011, 2010.

47. Qui, R., et al. Effect of fiber modification with a novel compatibilizer on the mechanical properties and water absorption of hemp-fiber-reinforced unsaturated polyester composites, *Polym. Eng. Sci.* **52** (6), 1342-1347, 2012.

48. Ren, X., et al. Modifications of kenaf fibers with n-methylol acrylamide for production of kenaf-unsaturated polyester composites, *J. Appl. Polym. Sci.* **125** (4), 2846–2853, 2012.

49. Cai, X., et al. The impact of the nature of nanofillers on the performance of wood polymer nanocomposites, *Compos. Part A* **39** (5), 727–737, 2008.

50. Cai, X., et al. Effects of nanofillers on water resistance and dimensional stability of solid wood modified by melamine-urea-formaldehyde resin, *Wood Fiber Sci.* **39** (2), 307–318, 2007.

51. Cai, X., et al. Formation and properties of nanocomposites made up form solid aspen wood, melamine-ureaformaldehyde, and clay, *Holzforchung* **61** (2), 148–154, 2007.

52. Guo, G., et al. Flame retarding effect of nanoclay on wood-fiber composites, *Polym. Eng. Sci.* **47** (3), 330-336, 2007.

53. Lu, W.H., et al. Preparation and characterization of wood/montmorillonite nanocomposites, *Forest Stud. China* **8** (1), 35–40, 2006.

54. Yu, Y., et al. Growth of ZnO nanofilms on wood with improved photostability, *Holzforchung* **64** (3), 385-390, 2010.

55. Ji, L.W., et al. Preparation and characteristics of hybrid ZnO-polymer solar cells, *J. Mater. Sci.* **45** (12), 3266-3269, 2010.

56. Sahoo, S. & Bhowmick, A.K. Influence of ZnO nanoparticles on the cure characteristics and mechanical properties of carboxylated nitrile rubber, *J. Appl. Polym. Sci.* **106** (5), 3077–3083, 2007.

57. Clausen, C.A., et al. The role of particle size of particulate nano-zinc oxide wood preservatives on termite mortality and leach resistance, *Nanoscale Res. Lett.* **6** (1), 427-431, 2011.

58. Clausen, C.A., et al. Weatherability and leach resistance of wood impregnated with nano-zinc oxide, *Nanoscale Res. Lett.* **5** (9), 1464-1467, 2010.

59. Wu, C., et al. Synthesis and characterizations of novel, positively charged poly(methyl acrylate)–SiO_2 nanocomposites, *Eur. Polym. J.* **41** (8), 1901-1908, 2005.

60. Zheng, Y., et al. Effects of nanoparticles SiO_2 on the performance of nanocomposites, *Mater. Lett.* **57** (19), 2940-2944, 2003.

61. Mahltig, B., et al. Functionalizing wood by nanosol application, *J. Mater. Chem.* **18** (27), 3180-3192, 2008.

62. Mirabedini, S.M., et al. Effect of TiO_2 on the mechanical and adhesion properties of RTV silicone elastomer coatings, *Colloids Surf. A: Physicochem. Eng. Aspects* **317** (1–3), 80–86, 2008.

63. Tshabalala, M.A., et al. Photostability and moisture uptake properties of wood veneers coated with a combination of thin sol-gel films and light stabilizers, *Holzforschung* **65** (2), 215–220, 2011.

64. Tanno, F., et al. Antimicrobial TMSAH-added wood inorganic composite prepared by the sol–gel process, *Holzforschung* **52** (4), 365–370, 1998.

65. Miyafuji, H. & Saka S. Fire-resisting properties in several TiO_2 wood-inorganic composites and their topochemistry, *Wood Sci. Technol.* **31** (6), 449-455, 1997.

66. Han, K. & Yu, M. Study of the preparation and properties of UV-blocking fabrics of a PET/TiO_2 nanocomposite prepared by in situ polycondensation, *J. Appl. Polym. Sci.* **100** (2), 1588-1593, 2006.

67. Schmalzl, K.J. & Evans, P.D. Wood surface protection with some titanium, zirconium and manganese compounds, *Polym. Degrad. Stab.* **82** (3), 409-419, 2003.

68. Gao, Y., et al. An in situ Raman spectroscopy study of stress transfer between carbon nanotubes and polymer, *Nanotechnology* **20** (33), 335703–335711, 2009.

69. Liu, L. & Wagner, H.D. Rubbery and glassy epoxy resins reinforced with carbon nanotubes, *Compos. Sci. Technol.* **65** (11-12), 1861–1868, 2005.

70. Davis, D.C., et al. A strategy for improving mechanical properties of a fiber reinforced epoxy composite using functionalized carbon nanotubes, *Compos. Sci. Technol.* **71** (8), 1089–1097, 2011.

71. Gojny, F.H., et al. Carbon nanotubes reinforced epoxy-composites: enhanced stiffness and fracture toughness at low nanotube content, *Compos. Sci. Technol.* **64** (15), 2363–2371, 2004.

72. Jin, S. & Matuana L.M. Wood/plastic composites co-extruded with multi-walled carbon nanotube-filled rigid poly(vinyl chloride) cap layer, *Polym. Int.* **59** (5), 648–657, 2010.

73. Angelatos, A.S., et al. NMR structural elucidation of amino resins, *J. Appl. Polym. Sci.* **91** (6), 3504-3512, 2004.

74. Chuang, I.S. & Maciel, G.E. ^{13}C CP/MAS NMR study of the structural dependence of urea-formaldehyde resins on formaldehyde-to-urea molar ratios at different urea concentrations and pH values, *Macromolecules* **25** (12), 3204-3226, 1992.

75. Islam, M.S., et al. Dynamic young's modulus and dimensional stability of batai tropical wood impregnated with polyvinyl alcohol, *J. Sci. Res.* **2** (2), 227-236, 2010.

76. Devi R.R. & Maji T.K. Preparation and characterization of wood/styrene-acrylonitrile copolymer/MMT nanocomposite, *J. Appl. Polym. Sci.* **122** (3), 2099-2109, 2011.

77. Dikobe, D.G. & Luyt, A.S. Effect of poly(ethylene-co-glycidyl methacrylate) compatibilizer content on the morphology and physical properties of ethylene vinyl acetate–wood fiber composites, *J. Appl. Polym. Sci.* **104** (5), 3206-3213, 2007.

78. Awal, A., et al. Thermal properties and spectral characterization of wood pulp reinforced bio-composite fibers, *J. Them. Anal. Calorim.* **99** (2), 695–701, 2010.

79. Faruk, O. & Matuana, L.M. Nanoclay reinforced HDPE as a matrix for wood-plastic composites, *Compos. Sci. Technol.* **68** (9), 2073-2077, 2008.

80. Mina, F., et al. Improved performance of isotactic polypropylene/titanium dioxide composites: effect of processing conditions and filler content, *Polym. Degrad. Stab.* **94** (2), 183–188, 2009.

81. Hamdan, S., et al. Wear of wood polymer composite for journal bearing materials, *Wood Res. J.* **1** (1), 22-26, 2010.

82. Islam, M.S., et al. The chemical modification of tropical wood polymer composites, *J. Compos. Mater.* doi:10.1177/0021998313477894, 1-7, 2013.

83. Xie, Y., et al. Effect of dynamic aging (hydrolysis and condensation) behavior of organofunctional silanes in the aqueous solution on their penetrability into the cell walls of wood, *Bioresour.* **6** (3), 2323-2339, 2011.

84. Li, Y., et al. Comparison of decay resistance of wood and wood-polymer composite prepared by in-situ polymerization of monomers, *Int. Biodeterior. Biodegrad.* **84**, 401-406, 2013.

85. Devi, R.R. & Maji, T.K. Effect of nano-ZnO on thermal, mechanical, UV stability, and other physical properties of wood polymer composites, *Ind. Eng. Chem. Res.* **51** (10), 3870–3880, 2012.

86. Deka, B.K. & Maji, T.K. Effect of nanoparticles on flammability, UV resistance, biodegradability, and chemical Resistance of Wood Polymer Nanocomposite, *Ind. Eng. Chem. Res.* **51** (37), 11881-11891, 2012.

87. Lande, S., et al. Properties of furfurylated wood, *Scand. J. Forest Res.* **19** (5), 22-30, 2004.

88. Deka, M., et al. Studies on dimensional stability, thermal degradation and terrible resistant properties of bamboo (Bambusa tulda Roxb.) treated with thermosetting resins, *J. Bamboo Rattan* **1** (1), 29-41, 2003.

89. Anwar, U.K.M., et al. Effect of curing time on physical and mechanical properties of phenolic-treated bamboo strips, *Ind. Crop Prod.* **29** (1), 214-219, 2009.

90. Devi R.R. & Maji T.K. Effect of glycidyl methacrylate on the physical properties of wood–polymer composites, *Polym. Compos.* **28** (1), 1-5, 2007.

91. Das, S., et al. Effect of steam pretreatment of jute fiber on dimensional stability of jute composite, *J. Appl. Polym. Sci.* **76** (11), 1652-1661, 2000.

92. Rahman, M.R., et al. Thermogravimetric analysis and dynamic young's modulus measurement of n,n-dimethylacetamide-impregnated wood polymer composites, *J. Vinyl Addit. Techn.* **17** (3), 177-183, 2011.

93. Pathak, S.K., et al. Study of thermal properties of eucalyptus wood and its polyacrylonitrite composites, *Pacific J. Sci. Technol.* **10** (1), 406-412, 2009.

94. Qin, H., et al. Thermal stability and flammability of polypropylene/montmorillonite composites, *Polym. Degrad. Stab.* **85** (2), 807-813, 2004.

95. Laachachi, A., et al. Effect of ZnO and organo-modified montmorillonite on thermal degradation of poly (methyl methacrylate) nanocomposites, *Polym. Degrad. Stab.* **94** (4), 670-678, 2009.

96. Katsikis, N., et al. Thermal stability of poly(methyl methacrylate)/silica nano- and microcomposites as investigated by dynamic-mechanical experiments, *Polym. Degrad. Stab.* **92** (11), 1966-1976, 2007.

97. Laachachi, A., et al. Use of oxide nanoparticles and organoclays to improve thermal stability and fire retardancy of poly (methyl methacrylate), *Polym. Degrad. Stab.* **89** (2), 344-352, 2005.

98. Arora, S., et al. Catalytic effect of bases in impregnation of guanidine nitrate on poplar (Populus) wood flammability and multiple heating rate kinetic study, *J. Therm. Anal. Calorim.* **107** (3), 1277–1286, 2012.

99. Yan, Q.L., et al. Thermal behavior and decomposition kinetics of formex-bonded explosives containing different cyclic nitramines, *J. Therm. Anal. Calorim.* **111** (2), 1419–1430, 2013.

100. Ak, M., et al. Thermal decomposition kinetics of polypyrrole and its star shaped copolymer, *J. Therm. Anal. Calorim.* **111** (2), 1627–1632, 2013.

101. Zhou, Q. & Xanthos, M. Nanosize and microsize clay effects on the kinetics of the thermal degradation of polylactides, *Polym. Degrad. Stab.* **94** (3), 327–338, 2009.

102. Zhao, L., et al. Influence of fullerene on the kinetics of thermal and thermo-oxidative degradation of high-density polyethylene by capturing free radicals, *J. Therm. Anal. Calorim.* DOI 10.1007/s10973-013-3158-4, 2013.

103. Vyazovkin, S. Evaluation of activation energy of thermally stimulated solid state reactions under arbitrary variation of temperature, *J. Comput. Chem.* **18** (3), 393–402, 1997.

104.Vyazovkin, S. Modification of the integral isoconversional method to account for variation in the activation energy, *J. Comput. Chem.* **22** (2), 178– 183, 2001.

105. Vyazovkin, S. & Sbirrazzuoli, N. Estimating the activation energy for non-isothermal crystallization of polymer melts, *J. Therm. Anal. Calorim.* **72** (2), 681-686, 2003.

106. Baysal, E., et al. Some physical, biological, mechanical, and fire properties of wood polymer composite (WPC) pretreated with boric acid and borax mixture, *Constr. Build. Mater.* **21** (9), 1879-1885, 2007.

107.. Camino, G., et al. Thermal and combustion behaviour of layered silicate epoxy nanocomposites, *Polym. Degrad. Stab.* **90** (2), 354-362, 2005.

108. Li, B. & He, J. Investigation of mechanical property, flame retardancy and thermal degradation of LLDPE–wood-fibre composites, *Polym. Degrad. Stab.* **83** (2), 241–246, 2004.

109. Baysal, E. Determination of oxygen index levels and thermal analysis of scots pine (*Pinus sylvestris L.*) impregnated with melamine formaldehyde-boron combinations, *J. Fire Sci.* **20** (5), 373-389, 2002.

110. Simkovic, I., et al. Flame retardance of insolubilized silica inside of wood material, *J. Appl. Polym. Sci.* **97** (5), 1948-1952, 2005.

111. Devi, R.R., et al. Modification of rubber wood with styrene in combination with diethyl allyl phosphate as the flame-retardant agent, *J. Appl. Polym. Sci.* **105** (5), 2461-2467, 2007.

112. Jana, T., et al. Biodegradable film: 7. Modification of the biodegradable film for fire retardancy, *Polym. Degrad. Stab.* **69** (1), 79-82, 2000.

113. Ghosh, S.N. & Maiti, S. Adhesive performance, flammability evaluation and biodegradation study of plant polymer blends, *Eur. Polym. J.* **34** (5/6), 849-854, 1998.

114. Ali, M.A., et al. Study of mechanical properties of wood polyacrylonitrile composites, *Int. J. Eng. Sci. Technol.* **3** (10), 7265-7269, 2011.

115. Gindl, W., et al. Impregnation of softwood cell walls with melamine-formaldehyde resin, *Bioresour. Technol.* **87** (3), 325–330, 2003.

116. Huang, Y., et al. Effect of modification with phenol formaldehyde resin on the mechanical properties of wood from Chinese fir, *Bioresour.* **8** (1), 272-282, 2013.

117. Messersmith, P.B. & Giannelis, E.P. Synthesis and barrier properties of poly(ε-caprolactone)-layered silicate nanocomposites, *J. Polym. Sci. Part A: Polym. Chem.* **33** (7), 1047-1057, 1995.

118. Lei, Y., et al. Influence of nanoclay on properties of HDPE/Wood composites, *J. Appl. Polym. Sci.* **106** (6), 3958-3966, 2007.

119. Chae, D.W. & Kim, B.C. Effects of zinc oxide nanoparticles on the physical properties of polyacrylonitrile, *J. Appl. Polym. Sci.* **99** (4), 1854-1858, 2006.

120. Li, Y.F., et al. Wood–polymer composites prepared by the *in situ* polymerization of monomers within wood, *J. Appl. Polym. Sci.* **119** (6), 3207-3216, 2011.

121. Plackett, D.V., et al. Weathering of chemically modified wood, *Holz Roh Werkst* **50** (4), 135-140, 1992.

122. Patachiaa, S., et al. Effect of UV exposure on the surface chemistry of wood veneers treated with ionic liquids, *Appl. Surf. Sci.* **258** (18), 6723– 6729, 2012.

123. Xie, Y., et al. Weathering of wood modified with the N-methylol compound 1,3-dimethylol-4,5-dihydroxyethyleneurea, *Polym. Degrad. Stab.* **89** (2), 189-199, 2005.

124. Du, H., et al. Effects of pigments on the UV degradation of wood-flour/HDPE composites, *J. Appl. Polym. Sci.* **118** (2), 1068–1076, 2010.

125. Salla, J., et al. Improvement of UV resistance of wood surfaces by using ZnO nanoparticles, *Polym. Degrad. Stab.* **97** (4), 592-596, 2012.

126. Yalinkilic, M.K., et al. Boron addition to non- or low-formaldehyde cross-linking reagents to enhance biological resistance and dimensional stability of wood, *Eur. J. Wood Prod.* **57** (5), 351-357, 1999.

127. Kartal, S.N., et al. Decay and termite resistance of boron-treated and chemically modified wood by in situ co-polymerization of allyl glycidyl ether (AGE) with methyl methacrylate (MMA), *Int. Biodeterior. Biodegrad.* **53** (2), 111-117, 2004.

128. Hill, C.A.S., et al. An investigation of cell wall micropore blocking as a possible mechanism for the decay resistance of anhydride modified wood, *Int. Biodeterior. Biodegrad.* **55** (1), 69-76, 2005.

129. Yildiz, U.C., et al. Mechanical properties and decay resistance of wood–polymer composites prepared from fast growing species in Turkey, *Bioresour. Technol.* **96** (9), 1003–1011, 2005.

130. Matsuda, H. Preparation and utilization of esterified woods bearing carboxyl groups, *Wood Sci. Technol.* **21** (1), 75-88, 1987.

131. Matsuda, H. Preparation and properties of oligoesterified wood blocks based on anhydride and epoxide, *Wood Sci. Technol.* **27** (1), 23-34, 1993.

132. Lande, S., et al. Eco-efficient wood protection: Furfurylated wood as alternative to traditional wood preservation, *Manage. Environ. Quality: An Int. J.* **15** (5), 529-540, 2004.

133. Karak, N. Polymer (epoxy) clay nanocomposites. *J. Polym. Mater.* **23** (1), 1-20, 2006.

CHAPTER III

EXPERIMENTAL

CHAPTER III

EXPERIMENTAL

This chapter includes the raw materials, methods and techniques used in the preparation of composite. The characterizations of the nanocomposites by different methods are also covered in this chapter.

3.1. Materials used

The chemicals as well as the raw materials used in this study along with the suppliers are listed below:

Materials	Suppliers
(i) Fig wood (*Ficus hispida*)	Local forest, Assam, India
(ii) Plant polymer (PP) (*Moringa oleifera*)	Local forest, Assam, India
(iii) Methyl methacrylate (MMA)	E-Merck (Mumbai, India)
(iv) Furfuryl alcohol (FA)	E-Merck (Mumbai, India)
(v) Melamine	E-Merck (Mumbai, India)
(vi) Formaldehyde	E-Merck (Mumbai, India)
(vii) Maleic anhydride	G.S. Chemical Testing Lab. & Allied Indus. (India)
(viii) 2,3-Epoxy glycidyl methacrylate (GMA)	E-Merck (Mumbai, Germany)
(ix) Glyoxal	E-Merck (Mumbai, India)
(x) Urea	E-Merck (Mumbai, India)
(xi) Acrylamide	E-Merck (Mumbai, India)
(xii) 2-Hydroxyethyl methacrylate (HEMA)	E-Merck (Mumbai, India)
(xiii) N-Cetyl –N, N, N-trimethyl ammonium bromide (CTAB)	Central Drug house (P) Ltd., Delhi India
(xiv) 2-Acryloloxy ethyl trimethyl ammonium chloride (ATAC)	Sigma-Aldrich (USA)
(xv) Montmorillonite K10 (MMT)	Sigma-Aldrich (USA)
(xvi) Nanomer (MMT modified by 15-35 wt.% octadecylamine and 0.5-5 wt.%)	Sigma-Aldrich (USA)
(xvii) Zinc Oxide (ZnO)	Sigma-Aldrich (USA)
(xviii) Silicon Dioxide (SiO_2)	Sigma-Aldrich (USA)
(xix) Titanium Dioxide (TiO_2)	Sigma-Aldrich (USA)
(xx) Multiwalled Carbon nanotubes (MWCNT)	CM-250, Sigma Aldrich, Korea

All other chemicals used were of analytical grade.

3.2. Methods

3.2.1. Preparation of wood samples

Fig wood (*Ficus hispida*) was collected locally. The wood samples obtained from defect-free wood were cut into blocks of 2.5 cm ×1 cm ×2.5 cm (radial× tangential× longitudinal) for hardness test, dimensional stability, water uptake and chemical resistance tests. The wood samples for tensile and flexural test were prepared according to ASTM D-638 and ASTM D-790 whereas for the limiting oxygen index (LOI) study and dynamic mechanical analysis (DMA) test the samples were prepared according to ASTM D-2863 and ASTM-7031.

3.2.2. Preparation of bacterial media

The following composition was taken for the preparation of mineral salt medium for bacterial growth. 2.0 g Na_2HPO_4, 100 mg $CuSO_4$ $7H_2O$, 4.75 g KH_2PO_4, 10 mg H_3BO_3 $5H_2O$, 10 mg MoO_3, 70 mg $ZnSO_4$ $7H_2O$, 2.0 g $(NH_4)_2SO_4$, 0.5 mg $CaCl_2$ $2H_2O$, 100 mg $MnSO_4$ $5H_2O$, 1 mg $FeSO_4$ $7H_2O$ and 1.2 g $MgSO_4$ $7H_2O$ were dissolved in 1000 mL of demineralised water. A 50 mL conical test tube was taken and to it 3 mL of this liquid culture medium was poured. It was then sterilized using autoclave at 121 °C and 15 lb_f pressure for 15 min. The autoclaved media were then allowed to cool down to room temperature and wood polymer composite (WPC) samples were added into the media under sterile condition inside a laminar air flow hood. Media containing only polymer samples were also cultured as negative control.

3.2.3. Preparation of bacterial strains

Bacillus sp. Cd-3 culture was developed by means of nutrient broth at 37 °C for 18 h. 1 mL of bacterial cultures was centrifuged at 6000 rpm for 20 min at room temperature and the pellets were washed with 0.9% NaCl and re-suspended in 1 mL of mineral salt medium. Now 0.5 mL of the culture medium containing 1×10^8/mL microbes was inoculated to the test tube containing 50 mL media for each test. The test tubes were then incubated under sterile condition at 37 °C and 100 rpm for the degradation study.

3.2.4. Biodegradation in soil

The aerobic biodegradation of wood composite exposed to a controlled environment was tested by the degradation test. "Bioreactors" (500 ml glass container) filled with garden soil was used to study the biodegradation studies on wood composites. The soil was sieved to remove all larger particles and was collected from the area where degraded woody biomass is present. A controlled environmental condition in the bioreactor with temperature 30 ± 1 °C, moisture content 40 to 50 % and the pH at 7.0 ± 0.5 was maintained and the tests were carried out for the wood composites for a period of 90 days. The samples were taken out of the soil after 90 days, cleaned carefully, washed with deionized water and finally dried. The samples were then checked for their weight loss, mechanical properties, growth of microorganisms and degradation. Scanning electron microscope was used to study the growth of microorganisms.

3.2.5. Modification of montmorillonite K10

Clay was modified organically by ion exchange reaction [1]. About 20 g of montmorillonite K10 (CEC = 120 meq/100 g) was dispersed in deionised water for 24 h by using mechanical stirrer. It was then subjected to sonication for 30 min. The mixture of surfactants CTAB and ATAC (1:1 mol/mol) was prepared in deionised water separately and added slowly to the dispersed clay. The resultant mixture was stirred for another 24 h. The white precipitate obtained was filtered, washed with (1:9) hot ethanol-water followed by washing with water several times. Finally, it was dried in vacuum oven at 45°C for 24 h and ground into powder. Another set of organophillic clay was prepared in the similar way by using ATAC alone.

3.2.6. Surface modification of ZnO, SiO_2, TiO_2 and MWCNT

Surface modification of nanoparticles is a common approach to prevent agglomeration of nanosized particle in the polymer matrix. Cationic surfactant CTAB was used to modify the surface of ZnO/SiO_2/TiO_2 nanoparticles in order to make a homogenous dispersion of the nanoparticles in the polymer. About 10 g of each of metal oxide nanoparticles was taken in a round bottom flask fitted with spiral condenser containing 1:1 ethanol–water mixture and stirred at 80°C for 24 h. About 12 g of CTAB was taken in

another beaker containing ethanol–water mixture and stirred at 80°C for 6 h. The mixture of $ZnO/SiO_2/TiO_2$ was added to it and finally stirred for another 24 h. It was then filtered and washed with deionized water for several times. Finally it was dried overnight in vacuum oven at 45°C, ground and stored in desiccator to avoid moisture absorption. Thus, the modified nanoparticles would contain the long organic chain cetyl group and the surface hydroxyl groups which can enhance the interaction between $ZnO/SiO_2/TiO_2$, polymers, wood, and clay.

A mixture of potassium hydroxide and ethanol was prepared and 5 g of MWCNT was added to it. The reaction mixture was placed in an ultrasonic bath for 24 h at 80 °C. The resulting mixture was filtered and repeatedly washed with deionized water until the pH value reached 7. Finally it was dried overnight in vacuum oven at 45°C. The product obtained was the MWCNT-OH.

3.2.7. Preparation of methyl methacrylate (MMA) pre-polymer

A pre-polymer of MMA was prepared by bulk technique at 45-50°C in an oil bath in presence of 0.05 phr AIBN for approximately 45 min. It was then poured in a closed flask and placed at ambient temperature to cool down. The viscosity (at 30°C) of different prepared batches of MMA prepolymer was measured and found almost similar as judged by Ubbelohde viscometer. The clay modified by ATAC/CTAB (1:1) (designated as clay I) was dispersed in solvent tetrahydrofuran (THF) and added to the prepolymer. It was then sonicated for about 15 min. Similarly clay modified by ATAC (designated as clay II) was dispersed in THF, added to prepolymer and sonicated for 15 min. These mixtures were used as impregnation solution for subsequent studies.

3.2.8. Preparation of the melamine formaldehyde-furfuryl alcohol (MFFA) copolymer

Melamine and formaldehyde was taken in molar ratio of 1:3 and polymerized by bulk polymerization method at 80-85 °C by maintaining pH at 8.5-9.0 with Na_2CO_3 1 mole FA was added to the prepared aqueous solution of methylol melamine and polymerized for 45 min at the same temperature using maleic anhydride as catalyst. The viscosity (at 30 °C) of different batches of melamine formaldehye-furfuryl alcohol (MFFA) copolymer thus prepared was checked and found almost similar as judged by Ubbelohde viscometer. MMT was dispersed in the prepolymer for 24 h using mechanical stirrer where water and furfuryl

alcohol monomer were used as solvent and co-solvent. It was then sonicated for about 30 min. These mixtures were used as impregnation solution for subsequent studies.

3.2.9. Preparation of N-methylol acrylamide (NMA) crosslinker

4.2 g of formaldehyde and 4.8 g of acrylamide (1:1.3 molar ratio) were added to 100 mL distilled water. The mixture was stirred at 23-25 °C under nitrogen atmosphere. After the dissolution of reagents, the pH was adjusted to 8-9 by adding NaOH. The reaction mixture was stirred for 2 h and the pH was adjusted to 5-6 by adding formic acid. The resin was dried in vacuum oven at 45 °C.

3.2.10. Preparation of 1,3-dimethylol 4,5-dihydroxyethylene urea (DMDHEU) crosslinker

The molar ratio of n(glyoxal), n(urea), n(formaldehyde) were taken as 1 :1.10 : 1.95 for synthesis of DMDHEU. Urea was added slowly to an aqueous solution of glyoxal under nitrogen purge .The pH of the reaction mixture was adjusted to approximately 5.5. The reaction mixture was then heated to 50 °C and allowed to stir for 24 h. The reaction was cooled to room temperature, neutralized and evaporated to near dryness by rotary evaporator to yield crude 4,5-dihydroxyethylene urea (DHEU). DHEU was added to an aqueous formaldehyde solution and pH was adjusted to 8.2-8.5. The reaction mixture was heated to approximately 50 °C and allowed to stir for 24 h. The reaction mixture was then allowed to cool to room temperature, neutralized and kept for subsequent use.

3.2.11. Dispersion of modified MMT in PMMA prepolymer

MMT was swelled in THF for 24 h with mechanical stirring. The mixture can swell the MMT and is a good solvent for the MFFA copolymer. The dispersed MMT was then sonicated for 30 min. Now the PMMA prepolymer was slowly added to the dispersed MMT under stirring condition. This mixture was further sonicated for 15 min and kept ready for use.

3.2.12. Dispersion of nanoclay/ZnO/SiO_2/TiO_2/PP in MFFA copolymer

The nanofillers either alone or in combination with other nanofillers were swelled in FA-water mixture for 24 h with mechanical stirring. FA-water mixture can swell the nanoparticles and is a good solvent for the MFFA copolymer. The dispersed nanofillers were then sonicated for 30 min. Now MFFA was slowly added to the dispersed nanofillers under stirring condition. This mixture was further sonicated for 15 min. To this mixture, plant polymer dissolved in dimethyl formamide (DMF)-water was added and kept ready for use.

3.2.13. Dispersion of nanoclay/multiwalled carbon nanotubes in MFFA copolymer

MWCNT either alone or in combination with nanoclay was swelled for 24 h in FA-water mixture. The mixture was subjected to sonication for 30 min. The prepared MFFA prepolymer was added slowly to the mixture under stirring condition.

3.2.14. Preparation of wood polymer nanocomposites

The samples were placed in an impregnation chamber. Load was applied over each sample to prevent the samples from floatation during addition of the impregnation mixture. Vacuum was applied for a specified time period for removing the air from the pores of the wood before addition of pre-polymer mixture.

Now the respective prepolymeric mixture containing monomer, clay/nanoparticles in different proportion, crosslinker and catalyst was added from a dropping funnel to completely immerse the wood samples. The samples were then kept in the chamber at room temperature (30°C) for specified time period after attaining atmospheric pressure. This is the time (4-6 h) required to get maximum polymer loading. The samples were then taken out of the impregnation chamber and the excess chemicals were wiped out from the surface. Now they were cured in an oven at 90 °C for 24 h by wrapping in aluminum foil. This was followed by drying further at 105 °C in an oven for 24 h. The samples were subjected to solvent extraction for 24 h to remove the homopolymers. Finally, the samples were dried and dimension was measured using a slide caliper and weights were taken.

3.3. Methods of characterization

3.3.1. Nuclear magnetic resonance (NMR) study

NMR spectra of MFFA, DMDHEU, NMA were recorded with 400 MHz Fourier Transform Nuclear Magnetic Resonance (FTNMR) (JEOL, Japan) spectrometer by using dimethyl sulphoxide (DMSO) as solvent and trimethyl silane (TMS) as internal standard.

3.3.2. Fourier transform infrared (FTIR) spectroscopy

The treated and untreated samples were ground and FTIR spectra were recorded by using KBr pellet in a Nicolet (Madison, USA) FTIR Impact 410 spectrophotometer.

3.3.3. X-ray diffraction (XRD) analysis

The crystallographic studies were done by XRD analysis using Rigaku X-ray diffractometer (Miniflax, UK) and employing CuKα radiation (λ = 0.154 nm), at a scanning rate of 2° min^{-1} with an angle ranging from 2° to 60°. The crystallinity index (CrI) was determined from XRD analysis using the following formula

$$CrI = A_{cryst}/A_{total} \times 100 \quad (1)$$

Where 'A_{cryst}' is the area of the peak for 002 plane and 'A_{total}' is the total area of the peak below the whole region.

3.3.4. Morphology of nanocomposites

3.3.4.1. Scanning electron microscopy (SEM) and energy dispersive X-ray spectroscopy (EDS)

The morphologies of untreated and treated wood samples were studied by using (JEOL JSM-6390LV) scanning electron microscope at an accelerated voltage of 5–10 kV. The fractured surface of the samples was used for the study. These were sputtered with platinum and deposited on brass holder.

The impregnated nanoparticles in the composites were identified by energy dispersive X-ray elemental analysis at the same time when the scanning was performed.

3.3.4.2. Transmission electron microscopy (TEM)

TEM was performed to study the dispersion of silicate layers and presence of nanoparticles. An ultramicrotome fitted with a diamond knife was used for ultrathin sectioning (approximately 100 nm thick) of the transverse film surfaces. The samples were embedded with epoxy resin for the preparations of (ultra) thin as well polished sections. The sections were stained with 1 wt. % uranyl acetate for sufficient contrast. The sections were then mounted on grids and examined with a JEOL JEM-2100 transmission electron microscope at an accelerating voltage of 80 kV.

3.3.5. Raman spectroscopy

Raman spectra was collected in the back scattering geometry using a Micro-Raman microscope made by WITec (U.S.A.) using 532 nm excitation laser with polarizer and the analyzer parallel to each other. For the deformation of the composites loaded with MWCNT, the samples were strained under Raman spectrometer by inserting into a four-point bending rig. The strains applied to the samples were increased step wise at intervals of about 0.1% until failure. Three Raman spectra were collected for each strain level from random areas of the samples and the presented results were the average of these three spectra. Since the position of G' band was observed at 2600 cm^{-1} therefore the spectra were centered at that region.

3.4. Measurements

3.4.1. Specific gravity determination of Fig wood

The specific gravity of wood was determined by the pycnometer method. The dried wood flour was covered with the displacement liquid and warmed slightly in a water bath. The specific gravity was measured according to the standard procedure described in literature [2]. Benzene, a nonpolar liquid was used as displacement fluid. It is expressed by using the following relation.

$$\text{Specific gravity} = md/m-[(p+m+w_0) - (p+w_0)] \quad (2)$$

Where 'm' is the weight of oven dried wood sample, 'd' is the density of displacement liquid, 'p' is the weight of the pycnometer, '$(p+w_0)$' is the weight of

pycnometer filled with displacement liquid alone, and '$(p+m+w_0)$' is the weight of pycnometer filled with wood and displacement liquid.

3.4.2. Weight percent gain

Weight percent gain (WPG) after polymer loading was calculated according to the formula

$$WPG\ (\%) = (W_2 - W_1)/W_1 \times 100 \qquad (3)$$

Where W_1 was oven dry weight of wood blocks before polymer treatment and W_2 was oven dry weight of blocks after polymer treatment.

3.4.3. Volume increase (%)

Percentage volume increase after impregnation of wood samples was calculated by the formula:

$$\text{Volume increase}\ (\%) = (V_2 - V_1)/V_1 \times 100 \qquad (4)$$

Where V_1 was oven dry volume of the untreated wood and V_2 was oven dry volume of the treated wood.

3.4.4. Hardness

The hardness of the samples was measured by using a durometer (model RR12) according to ASTM D2240 method and expressed as shore D hardness.

3.4.5. Water uptake test

Both untreated and treated wood samples were immersed in distilled water at room temperature (30°C) and weights were taken after 0.5, 2, 6, 24, 48, 96, 120, 144 and 168 h. It was expressed as

$$\text{Water uptake}\ (\%) = (W_t - W_d)/W_d \times 100 \qquad (5)$$

Where, W_d is the oven dry weight; and W_t is the weight after immersion in distilled water for a specified time period.

3.4.6. Water vapor exclusion test

Oven dried wood samples were conditioned at 30°C and 30% relative humidity (RH) and weighed. Samples were then placed in a chamber where temperature and RH were maintained at 30 °C and 65% respectively. Weights were remeasured after different time period 0.5, 2, 6, 24, 48, 96, 120, 144 and 168 h. It was expressed as a percentage of moisture absorbed based on oven dry weight.

3.4.7. Water repellent effectiveness (WRE) (%)

WRE was measured for different soaking periods. Resistance to water uptake is expressed as WRE and calculated as

$$WRE\ (\%) = (D_o - D_t)/D_o \times 100 \qquad (6)$$

where D_o is the water uptake of untreated samples immersed for 0.5, 2,6, 24, 48, 96, 120, 144, and 168 h; and D_t is the water uptake of treated wood samples immersed for the same periods.

3.4.8. Dimensional stability test

3.4.8.1. Swelling in water vapor

Samples were first dried at 105°C and dimensions were measured. Samples were then placed in chamber where temperature and RH were maintained at 30°C and 65% respectively. The dimensions were remeasured after 0.5, 2, 6, 24, 48, 96, 120, 144, and 168 h.

3.4.8.2. Swelling in water

Dimensions of the oven-dried samples were measured and conditioned at room temperature (30°C) and 30% RH. Final placement of the samples was done in distilled water and then dimensions were remeasured after 0.5, 2, 6, 24, 48, 96, 120, 144, and 168 h. Swelling was considered as a change in volume and expressed as the percentage of volume increase compared to oven-dried samples,

$$\%\ Swelling = (V_{t,u} - V_o)/V_o \times 100 \qquad (7)$$

Where, $V_{t,u}$ is the volume of the untreated or treated wood after water absorption; and V_o is the volume of the untreated or treated wood before water absorption.

The antiswelling efficiency (ASE) index was determined to evaluate dimensional stability of treated wood specimens. The specimens were submerged in distilled water at 30°C for different time periods after conditioning at 30% RH and 30°C. Volumetric swelling coefficients in percentage were calculated according to the formula:

$$S\ (\%) = (V_2-V_1)/V_1 \times 100 \qquad (8)$$

Where, V_2 is the volume of the water saturated blocks and V_1 is the volume of the oven dried blocks. The values were obtained by measuring longitudinal, tangential, and radial dimensions of the oven dried and water saturated blocks using slide caliper.

The percentage of ASE was calculated from the wet and oven dried volumes of treated and untreated wood specimens according to the formula below:

$$ASE\ (\%) = (S_c-S_t)/S_c \times 100 \qquad (9)$$

Where, S_c is the volumetric swelling coefficient of untreated blocks and S_t is the volumetric swelling coefficient of the treated blocks.

3.4.9. Chemical resistance test

The samples were kept immersed in 4% NaOH solution and 4% acetic acid solution for 24 h. The percent swelling was calculated by using the equation as given below:

$$\%\ Swelling = (V_{t,u} - V_o)/V_o \times 100 \qquad (10)$$

where $V_{t,u}$ is the volume of the untreated or treated wood after immersion in chemicals and V_o is the volume of the untreated and treated wood before immersion in chemicals.

3.4.10. Mechanical properties

The flexural strength of the samples was measured by UTM-HOUNSEFIELD, England (model H100K-S) with a cross head speed of 2 mm/min and by calculating the modulus of elasticity (MOE) and modulus of rupture (MOR) according to ASTM D-790 method maintaining span-to-depth ratio 16:1.

MOR was calculated as follows:

$$MOR = 3WL/2bd^2 \qquad (11)$$

Where, W is the ultimate failure load (N), L is the span between centres of support, b is the mean width (tangential direction) of the sample and d is the mean thickness (radial direction) of the sample.

The tensile strength was also performed by using UTM-HOUNSEFIELD, England (model H100K-S) with a 10-kN load cell and crosshead speed of 10 mm/min according to ASTM D-638 method (Type I specimen).

3.4.11. Dynamic mechanical analysis (DMA)

The DMA was performed by using TA instruments Q800. Specimens were scanned over a temperature range of 25–200°C. Frequency of the oscillation was performed at 1, 3, 5 and 10 Hz ramped at 2°C/min to 200°C. Storage modulus, loss modulus and mechanical loss factor (tan δ) were recorded and plotted against temperature.

3.4.12. Limiting oxygen index (LOI) study

The LOI is defined as the minimum concentration of oxygen, expressed in percent volume, in a flowing mixture of oxygen and nitrogen that will support combustion of a material initially at room temperature. It was measured by flammability tester (S.C. Dey Co., Kolkata) according to ASTM D-2863 method. Keeping the total volume of the gas mixture ($N_2 + O_2$) fixed at 18 cc, the volume of nitrogen gas and that of oxygen gas were kept initially at a maximum and minimum level. Now, the volume of nitrogen gas was decreased and that of oxygen gas was increased gradually. The total volume of gas mixture was kept fixed at 18 cc during the experiment. The sample was placed vertically in the sample holder of the LOI apparatus. The ratio of nitrogen and oxygen at which the sample continued to burn for at least 30 s was noted.

$$\text{Limiting oxygen index (LOI)} = \text{Volume of } O_2/\text{Volume of } (O_2 + N_2) \times 100 \qquad (12)$$

3.4.13. Thermal degradation study

Thermogravimetric analyzer (TGA) was used for evaluation of thermal properties of the untreated and treated wood samples. TGA study was carried out using a thermo gravimetric analyzer (model Metler TA 4000) at a heating rate of 20 °C min^{-1} up to 500 °C. The studies were done under nitrogen atmosphere.

The possible kinetic mechanism can be analyzed by finding a correlation of activation energy with conversion in a thermal degradation process. Different isoconversional methods

like the integral method proposed by Ozawa and Flynn Wall [3,4] as well as advanced isoconversional methods [5,6] were available in the literature. The activation energy can be studied from the degree conversion rate. The degree of conversion of decomposed fraction (α) can be calculated using the following equation.

$$\alpha = (M_o - M_t)/(M_o - M_f) \quad (13)$$

where M_o, M_t and M_f are initial mass at time t and final mass of the sample, respectively.

The reaction rate in non-isothermal decomposition kinetics is commonly described by the equation

$$d\alpha/dt = A \exp(-E_a/RT)(1-\alpha)^n \quad (14)$$

Where A = pre-exponential factor, E_a= activation energy of thermal decomposition, R = gas constant (kJ mol^{-1}), β=heating rate, T = absolute temperature (K), n = reaction order.

For a linear heating program with constant heating rate, $\beta = dT/dt$, equation becomes

$$d\alpha/(1-\alpha)^n = A/\beta \exp(-E_a/RT) \quad (15)$$

The method of Flynn-Wall and Ozawa are an integral method [3,4].

Integrating equation (15)

$$\int_0^{\alpha} d\alpha/(1-\alpha)^n = A/\beta \int_{T_0}^{T_1} \exp(-E_a/RT) \quad (16)$$

If, $F(\alpha) = d\alpha/(1-\alpha)^n$, $y = E_a/RT$ then,

$$F(\alpha) = AE_a/\beta R\, P(y) \quad (17)$$

The values of P(y) are calculated for the normal range of experimental values $10 < E_a/RT < 30$.

When $E_a/RT > 20$, a linear approximation is made

$$\log P(y) \approx 2.315 - 0.457y \quad (18)$$

Substituting equation (18) into equation (17)

$$\log \beta = AE/RF(\alpha) - 2.315 - 0.457\, E_a/RT$$

The activation energy (E_a) was evaluated from the slope of the graph between log β and 1/T for a selected fraction of the thermal decomposition. The range of the selected fraction was from 0.1 to 0.7 and the values for the activation energy of each fraction were compared. Using data obtained at several heating rates, a graph of mass loss vs. temperature is plotted for finding the activation energy. The integral isoconversion OFW method led to systematic errors when the value of E_a varies with α [6]. To avoid these errors, Vyazovkin developed an advanced isoconversional method which was applied to the data obtained at arbitrary heating programs, T(t) and was direct numerical integration of equation 10 [5]. In this method, a

possible variation of activation energy was taken into consideration. A set of experiments were carried out at different arbitrary heating programs T(t), and the activation energy was evaluated by finding the value of E_a at any particular value of α which minimizes the function

$$\Phi(E_a) = \sum_{i=1}^{n}\sum_{j\neq i}^{n} J[E_a, T_i(t_\alpha)]/ J[E_a, T_j(t_\alpha)] \quad (19)$$

In the equation (19) the integral $J[E_a, T_i(t_\alpha)] = \int_{i\alpha-\Delta\alpha}^{i\alpha} \exp[-E_a/RT_i(t)]dt$ (20)

was determined numerically by using trapezoid rule. Here i and j, denote thermal measurements with different temperature programs, Δα, an increase of conversion, was varied from Δα to 1−Δα typically set as 0.02 enough to remove accumulative errors in E_a calculation. A set of experiments were carried out according to varied temperature programs to generate sufficient conversion–temperature (α–T(t)) data, and then E_a was calculated at any particular value of α by identifying a suitable E_a value which satisfies Equation 19. The minimization procedure was repeated for each value of α to find the dependence of the activation energy on the extent of conversion.

3.4.14. Ultraviolet (UV) resistance test

The degradation study of the WPC samples was done in UV chamber (Model: S.L.W, voltage: 230 V; Advanced Research Co., India) using a mercury arc lamp system that produces a collimated and highly uniform UV flux in the 200–400 nm range. The exposure period was varied from 0 to 60 days. The weight loss was measured and is expressed as follows:

$$\% \text{ Weight loss} = (W_t - W_o)/W_o \times 100 \quad (21)$$

where, 'W_t' is the specimen weight at time 't' and 'W_o' is the specimen weight before exposure. The UV degradation was studied by FTIR analysis. The intensity of the carbonyl (C=O) stretching peaks at 1715 cm^{-1} in cellulose of untreated wood was measured. The net peak heights were determined by subtracting the height of the baseline directly from the total peak height. The same base line was taken for each peak before and after exposure to UV [7]. The carbonyl index was calculated by using the following equation:

$$\text{Carbonyl index} = I_{1715}/I_{2924}(100) \quad (22)$$

where, I represents the intensity of the peak. The peak intensities were normalized by using -CH stretching peak of alkane at 2924 cm^{-1}. This peak was chosen as reference due to its least change during irradiation. The lignin index (LI) of the wood was calculated for all the

untreated and treated wood samples. It is the ratio of the height of the lignin-characteristic band at 1510 cm^{-1} to that of the band at 2924 cm^{-1}. The band corresponding to C-H stretching of cellulose appeared at 2924 cm^{-1} which is very stable to oxidation and remains constant throughout the UV exposure.

$$LI = I_{1510}/I_{2924}(100) \quad (23)$$

The possibility of change in cellulose crystallinity due to UV irradiation is determined by crystallinity index (CrI). It is defined as the ratio of the areas of the bands at 1437 and 2924 cm^{-1}.

$$CrI = A_{1437}/A_{2924} \quad (24)$$

Surface morphology of UV degraded specimen was characterized by scanning electron microscopy (SEM).

3.4.15. Biodegradation study

The microbial degradation of the untreated and treated wood samples was studied spectrophotometrically by using a UV visible spectrophotometer (CECIL CE7400) at 600 nm against blank culture media under sterile condition.

REFERENCES

1. Vazquez, A., et al. Modification of montmorillonite with cationic surfactants. Thermal and chemical analysis including CEC determination, *Appl. Clay Sci.* **41** (1-2), 24-36, 2008.

2. Browning, B. *Method of wood chemistry*, Interscience Publisher, New York, 1967.

3. Flynn, J.H. & Wall, L.A. General treatment of the thermogravimetry of polymers, *J. Res. Natl. Bur. Stand. A: Phys. Chem.* **70A**, 487–523, 1966.

4. Ozawa, T. A new method of analyzing thermogravimetric data, *Bull. Chem. Soc. Jpn.* **38** (11), 1881–1886, 1965.

5. Vyazovkin, S. Evaluation of activation energy of thermally stimulated solidstate reactions under arbitrary variation of temperature, *J. Comput. Chem.* **18** (3), 393–402, 1997.

6. Vyazovkin, S. Modification of the integral isoconversional method to account for variation in the activation energy, *J. Comput. Chem.* **22** (2), 178– 183, 2001.

7. Stark, N.M. & Matuana, L.M. Surface chemistry changes of weathered HDPE/wood-flour composites studied by XPS and FTIR spectroscopy, *Polym. Degrad. Stab.* **86** (1), 1-9, 2004.

CHAPTER IV

RESULTS & DISCUSSION

CHAPTER IV

RESULTS & DISCUSSION

Section A: Studies on properties of softwood (*Ficus hispida*)/PMMA nanocomposites reinforced with polymerizable surfactant-modified MMT.

Wood is impregnated with polymerizable monomer/prepolymer to enhance its performance characteristics under vacuum condition. In this part of work, modification of Fig wood has been done by vacuum impregnation of poly(methylmethacrylate) (PMMA) prepolymer, glycidyl methacrylate (GMA), a cross linking agent and montmorillonite (MMT) using catalyst heat treatment. MMT was modified by using a mixture of surfactants 2-acryloloxy ethyl trimethyl ammonium chloride (ATAC) and cetyl trimethyl ammonium bromide (CTAB) in a molar ratio of (1:1) (designated as clay I) and a polymerizable surfactant 2-acryloloxy ethyl trimethyl ammonium chloride (ATAC) (designated as clay II). A comparative study on different properties of the prepared wood polymer nanocomposite (WPNC) based on impregnation of intercalating mixture containing MMA/GMA/clay modified by both the surfactants (ATAC and CTAB) and MMA/GMA/clay modified by only surfactant ATAC were done.

4.1. RESULTS AND DISCUSSION

4.1.1. Specific gravity determination of Fig (*Ficus hispida*) wood

Specific gravity of Fig wood was determined and the result was expressed as mean value (Table 4.1.1.). The specific gravity was determined by pycnometer method which is one of the displacement methods for specific gravity determination. The specific gravity was found to be 0.42 which is in accordance of the specific gravity generally found for softwood [1].

Table 4.1.1. Specific gravity determination of Fig wood.

Property	Value
Specific gravity	0.42

4.1.2. Optimization of the system by measuring weight percent gain (WPG %), volume increase (%) and hardness

The maximum improvement in properties was found by varying impregnation conditions like monomer concentration, initiator concentration, vacuum, time of impregnation and amount of cross-linking agent.

Table 4.1.2.1. Effect of variation of monomer concentration (PMMA/tetrahydrofuran (THF) concentration) [AIBN: 0.5%; vacuum: 508 mm Hg; Time: 4 h; GMA: 3 mL].

PMMA/ THF	Weight percent gain (%)	Volume increase (%)	Hardness (Shore D)
1:1	27.46 (±0.87)	2.38 (±0.67)	42 (±0.57)
3:1	30.32 (±0.77)	2.54 (±0.38)	46 (±0.86)
5:1	33.92(±0.42)	2.82(±0.31)	51 (±1.08)

Table 4.1.2.1. shows the result of variation of monomer concentration on weight percent gain (%),volume increase (%) and hardness. When the PMMA: THF concentration was used in the ratio of 5:1 maximum improvement in properties was obtained.

Table 4.1.2.2. Effect of variation of initiator concentration [PMMA/THF: 5:1; vacuum: 508 mm Hg; Time: 4 h; GMA: 3 mL].

PMMA/ THF	AIBN (%)	Weight percent gain (%)	Volume increase (%)	Hardness (Shore D)
5:1	0.25	30.33 (±0.97)	2.42 (±0.76)	48 (±1.02)
5:1	0.5	33.27(±0.56)	2.76 (±0.43)	52 (± 0.48)
5:1	0.75	32.47 (±0.75)	2.63 (±0.47)	51(±0.54)

The result of variation of initiator concentration on weight percent gain (%),volume increase (%) and hardness are shown in Table 4.1.2.2. Highest weight percent gain (%),volume increase (%) and hardness are obtained when 0.5 % AIBN was used.

Table4.1.2.3. Effect of variation of vacuum [PMMA/THF: 5:1; AIBN: 0.5 %; Time: 4 h; GMA: 3 mL].

PMMA/ THF	AIBN (%)	Vacuum (mm/inch Hg)	Weight percent gain (%)	Volume increase (%)	Hardness (Shore D)
5:1	0.5	127 (5)	28.76 (±0.55)	2.27 (±0.62)	48 (±0.89)
5:1	0.5	254 (10)	30.68(±0.39)	2.45(±0.58)	51 (±0.43)
5:1	0.5	508 (20)	33.86 (±0.96)	2.88 (±0.77)	52 (±1.06)

Highest improvement in properties was obtained when 508 mm Hg vacuum was used. The properties varied in the order 127<254<508 mm Hg.

Table 4.1.2.4. Effect of variation of time of impregnation [PMMA/THF: 5:1; AIBN: 0.5%; vacuum: 508 mmHg; GMA: 3 mL].

PMMA/ THF	AIBN (%)	Vacuum (mm/inch Hg)	Time (h)	Weight percent gain (%)	Volume increase (%)	Hardness (Shore D)
5:1	0.5	508 (20)	2	29.87 (±0.64)	2.52 (±0.85)	48 (±0.26)
5:1	0.5	508 (20)	4	32.23 (±0.45)	2.71 (±0.38)	51 (±0.68)
5:1	0.5	508 (20)	6	32.02 (±0.78)	2.68 (±0.97)	50 (±0.83)

Table 4.1.2.5. Effect of variation of glycidyl methacrylate (GMA) concentration (mL) [PMMA/THF: 5:1; AIBN: 0.5 %; vacuum: 508 mmHg; Time: 4 h].

PMMA/ THF	AIBN (%)	Vacuum (mm/inch Hg)	Time (h)	GMA (mL)	Weight percent gain (%)	Volume increase (%)	Hardness (Shore D)
5:1	0.5	508 (20)	4	1	32.15 (±0.74)	2.67 (±0.84)	49 (±1.02)
5:1	0.5	508 (20)	4	3	34.42 (±0.95)	2.92 (±0.64)	53 (±0.83)
5:1	0.5	508 (20)	4	5	34.12 (±0.37)	2.87 (±0.58)	52 (±0.49)

As the time of impregnation was varied from 2 to 6 h, weight percent gain (%), volume increase (%) and hardness were found to increase then it remained constant. Maximum enhancement in all the properties was obtained at 4 h time of impregnation.

The results of variation of glycidyl methacrylate (GMA) on weight percent gain (%), volume increase (%) and hardness are shown in Table4.1.2.5. It was observed that the properties improved initially with the increase in the amount of crosslinking agent then it remained constant. Highest improvement in properties was obtained when 3 mL GMA was used.

Therefore the conditions, at which maximum improvement of properties were obtained, were as follows: PMMA/THF: 5:1, AIBN: 0.5 %, vacuum: 508 mmHg, time of impregnation: 4 h, GMA (mL): 3, clay I: 0.5–1.5 phr, and clay II: 0.5–1.5 phr.

4.1.3. Fourier transform infrared analysis (FTIR)

Figure4.1.1.represents the FTIR spectra of unmodified MMT and MMT modified withcombined surfactant (CTAB and ATAC) and ATAC alone. Unmodified MMT (curvea) showed bands at 3431 cm^{-1} (–OH stretching), 1636 cm^{-1} (–OH bending),1052–532 cm^{-1} (oxide bands of Al, Mg, Si, etc.). In CTAB/ATAC (curve b) modified MMT, two new peaks, appeared at 2927 and 2853 cm^{-1}, were due to–CH_2 asymmetric stretching. Another peak appeared at 1477 cm^{-1} was due to–CH_2 plane scissoring vibration ofmodifying hydrocarbon of the surfactant [2]. Similarpeaks were also observed in the spectrum of MMT modified with ATAC (curve c).

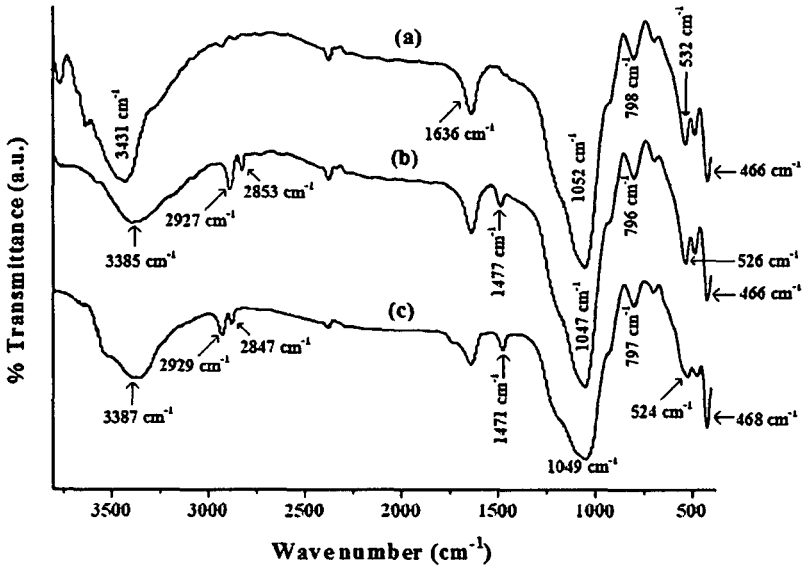

Figure4.1.1. FTIR spectra of (a) unmodified MMT (b) clay I (c) clay II.
Clay I: clay modified with ATAC/CTAB (1:1); Clay II: clay modified with ATAC

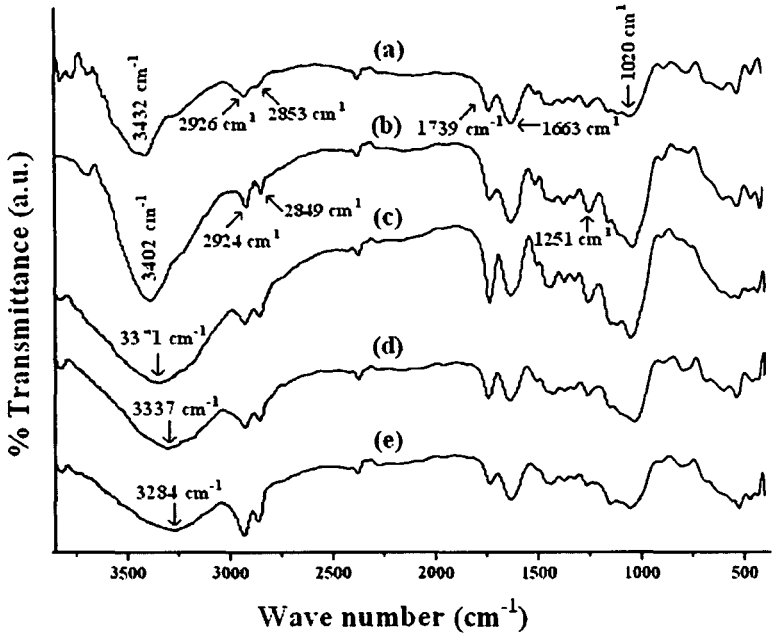

Figure 4.1.2.FTIR spectra of (a) Untreated wood and wood treated with (b) MMA (c) MMA/GMA(d) MMA/GMA/clay II (e) MMA/GMA/clay I.

Figure 4.1.2.shows the FTIR spectra of untreated and treated wood samples. Pure wood (curve a) showed absorption bands at 3432 cm^{-1} (–OH stretching), 2926 cm^{-1}, and 2853 cm^{-1} ($–CH_2$ asymmetric stretching), 1739 cm^{-1} (C=O stretching), 1663 $cm^{-1}$for (–OH bending), 1251 and 1020 cm^{-1} (C–O stretching) and 1000–645 cm^{-1} (out of plane C–H bending vibration). Wood treated with PMMA (curve b) showed characteristic bands at 2924 and 2849 cm^{-1} for $–CH_2$ stretching, 1251 cm^{-1} for C–O stretching of PMMA [3]. Curve 'c' shows the spectrum for wood treated with MMA and GMA. The peak at 1735 cm^{-1} for ester group became prominent and the intensity of bands for –OH stretching decreased as well as shifted to lower wave number. This was due to improvement in interaction between the hydroxyl group of wood and the PMMA polymer by GMA. Curve 'd' and 'e' represent the spectra for wood treated with MMA/GMA/clay II and MMA/GMA/clay I, respectively. It was observed that the intensities of –OH stretching was decreased and shifted to 3371 cm^{-1} (curve c), 3337 cm^{-1} (curve d) and 3284 cm^{-1} (curve e) compared to 3432 cm^{-1} (wood). The decrease in intensity and shifting of peaks to lower wave number might be due to the interaction of hydroxyl group of wood and clay with GMA and polymer. Further, it was observed that $–CH_2$ asymmetric peak intensity at 2926 and 2853 cm^{-1} was more pronounced in treated samples than the untreated ones indicating the interaction between wood, PMMA/GMA, and modified clay. Similar decrease and shifting in intensities of –OH

stretching to lower wave number was reported by Deka and Maji [4] while studying the FTIR analysis of wood/polymer/clay nanocomposite.

4.1.4. X-ray diffraction (XRD) study

Figure 4.1.3.shows the XRD patterns of unmodified and organically modified MMT.The diffraction peak for unmodified MMT (curve a) appeared at $2\theta = 8.37^{\circ}$. Clay I(curve b) and clay II (curve c) showed sharp peak at $2\theta = 5.97^{\circ}$ and 7.09°,respectively. The shifting of peak to lower angle indicated that interlayer spacing ofsilicate layers increased. The shifting was more in the case of clay treated withcombined surfactants. The alkyl group of CTAB was responsible for the expansionof the MMT gallery. The increase of MMT interlayer spacing by the use ofcombined surfactant CTAB and 2-[(acryloyloxy) ethyl](4-benzyl-)dimethyl ammoniumbromide was reported in literature [5].

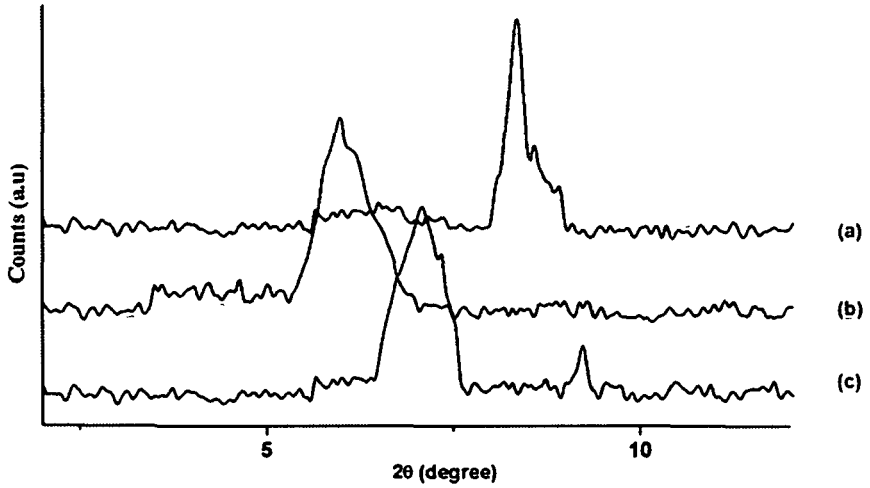

Figure4.1.3. XRD micrographs of (a) unmodified clay (b) clay II (c) clay I.

Figure 4.1.4.shows the XRD spectra of untreated wood and the composites. Woodpowder (curve a) shows a wide diffraction peak near 22.9° of 2θ which was due tothe *maximum diffraction of the (002) crystal plane of cellulose. Cellulose is theprincipal* constituent of wood. Curve b represents the XRD spectra of clay I treatedPMMA composite. A broad band peaking at around $2\theta = 16.27^{\circ}$, which is due tothe presence of PMMA matrix present in the composite [6]. Curves c and d showedthe XRD spectra of wood samples treated with PMMA/GMA/clay II and PMMA/GMA/clay I. In both the cases, the intensity of the diffraction peak of cellulose (002)crystal plane decreased. The crystalline peak of cellulose was also found to shift to22.8° for clay II and $22.5^{\circ}$for clay I from 22.9°.

Furthermore, the characteristic peakfor modified MMT at 5.97° disappeared. It could be said that either the full expansion of clay galleries occurred which was not possible to detect by XRD or the MMT layers became delaminated and no crystal peak appeared [7]. The XRDresults suggested that crystallinity in wood composite decreased and some silicatenanolamina were penetrated into the amorphous region of cellulose wood cell wall.Similar observation was reported by Devi and Maji [2].

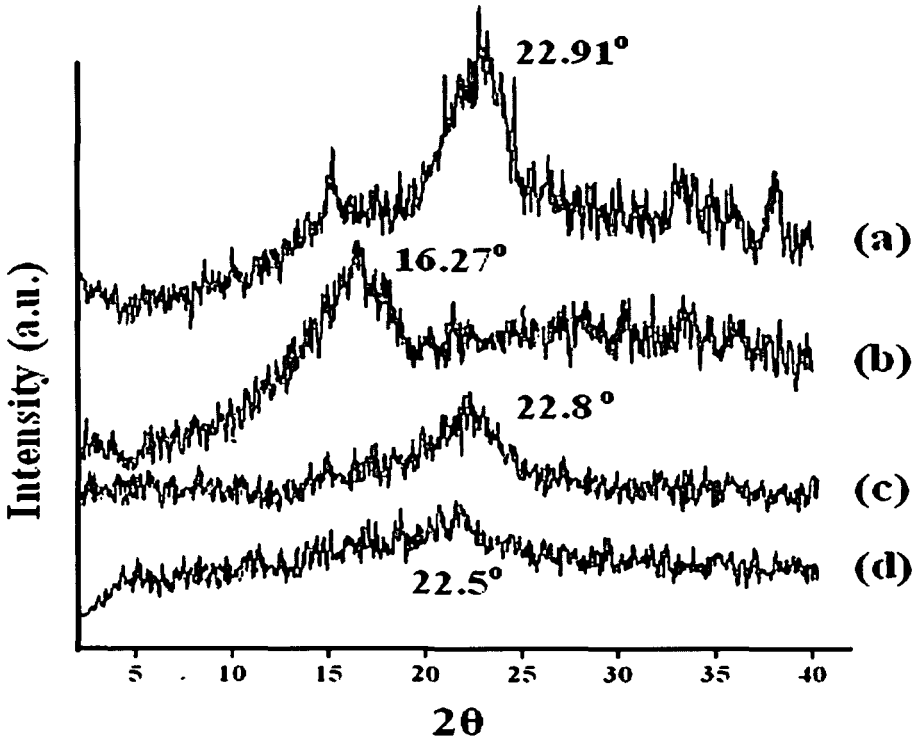

Figure 4.1.4.XRD micrographs of (a) untreated wood, (b) MMA/GMA/clay I composite and wood treated with (c) MMA/GMA/clay II, and (d) MMA/GMA/clay I.

4.1.5. Morphological studies

Figure 4.1.5.shows the scanning electron microscopy (SEM) micrographs of fractured surfaces of unmodified andmodified wood samples. The empty cell wall of wood was seen in untreated woodsample (Figure4.1.5.a). These empty spaces were filled with the MMA polymer, MMA/GMA, MMA/GMA/clay (Figure4.1.5.b–e). The polymeric materials were found to bepresent either in the cell lumen or in the cell wall. The presence of nanoclay wasdetected as white spot in the micrographs. (Figure4.1.5.d, e).

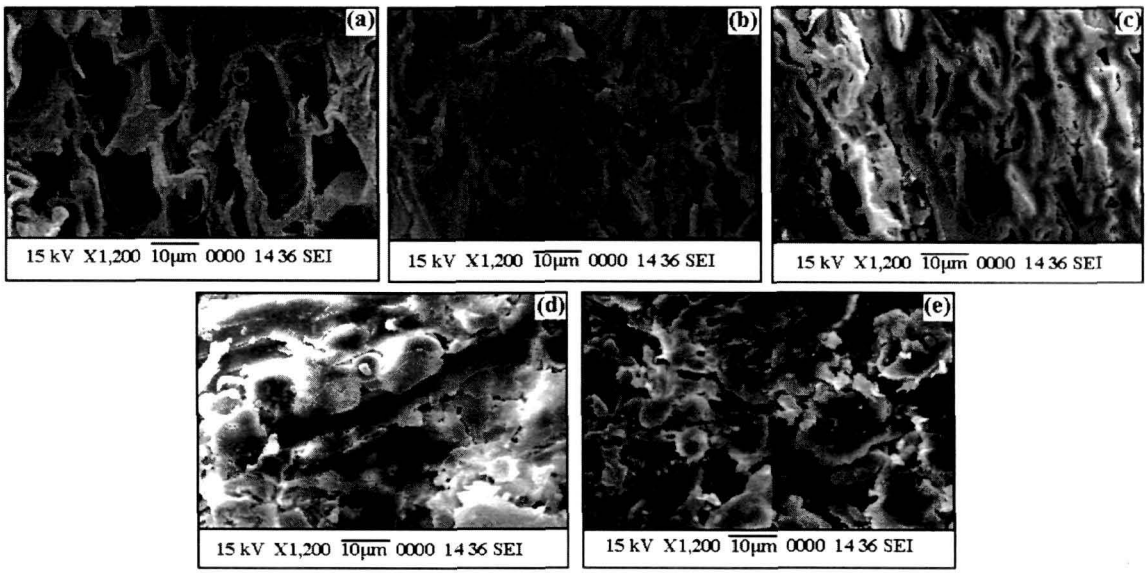

Figure 4.1.5. Scanning electron micrographs of (a) untreated wood and wood treated with (b) MMA (c) MMA/GMA (d) MMA/GMA/clay II (e) MMA/GMA/clay I.

4.1.6. Effect of variation of clay on WPG %, volume increase and hardness

Results are shown in Table 4.1.3. It was observed that wood treated with MMA/THF improved overall properties like weight gain (%), volume increase and hardness. This was due to deposition of polymer in the void spaces and capillaries of wood. The deposition of polymer was improved by the presence of cross-linking agent GMA which could interact with both the polymer and wood through its double bond and glycidyl group. The addition of clay further improved the properties. The improvement in properties was more in clay I treated samples compared to those of clay II treated samples. The enhancements in properties were due to restriction in the mobility of the intercalated polymer chain inside the silicate layers of clay. Further the acrylic group of ATAC in clay I could undergo copolymerization with MMA monomer while the long chain alkyl group of CTAB facilitated the expansion of clay gallery to accommodate the MMA polymer [5]. The ATAC alone in clay II might not able to expand the interlayer spacing of clay like that of clay I.

Table 4.1.3. Effect of variation of clay modified with ATAC/CTAB (1:1) and only ATAC on polymer loading (WPG %), volume increase and hardness.

Samples particulars	Weight % gain	Volume increase %	Hardness (Shore D)
Untreated wood			
Samples treated with MMA/THF/ GMA/clay I/clay II			
100/20/0/0/0	23.59 (±0.83)	2.78 (±0.71)	47 (±1.14)
100/20/3/0/0	33.92 (±0.42)	2.96 (±0.31)	51 (±1.08)
100/20/3/0.5/0	37.43 (±0.57)	3.68 (±0.89)	57 (±1.21)
100/20/3/0/0.5	34.67 (±0.58)	3.13 (±1.37)	54 (±1.25)
100/20/3/1.0/0	39.56(±1.43)	3.97 (±1.06)	58 (±1.06)
100/20/3/0/1.0	36.17 (± 0.94)	3.32 (± 0.63)	56 (±1.32)
100/20/3/1.5/0	40.37(±1.02)	4.11(±0.68)	62(±1.12)
100/20/3/0/1.5	38.87(±1.07)	3.73(±1.24)	57(±0.76)

4.1.7. Water uptake study

Related results are shown in Figure4.1.6. With the increase in time of immersion, it wasfound that water uptake (%) increased for both treated and untreated wood samples. Untreated wood samples showed highest water absorption capacity. Samples treatedwith MMA showed less water uptake since the capillaries of wood were filled up bythe polymer. The water uptake of the samples treated with MMA/GMA decreasedfurther due to the crosslinks formed between double bond and glycidyl group ofGMA with double bond of MMA and hydroxyl group of wood, respectively [8].Samples treated with MMA/GMA/modified MMT showed least water uptake. Thelayers of modified clay provided the tortuous path for water transport and hencerestricted the diffusion of water molecules [9]. Wood samples treated with MMA/GMA/clay I absorbed less water compared to samples treated with MMA/GMA/clay II. CTAB present in clay I increased the interlayer spacing of clay andenhanced the tortuous path for diffusion of water molecules.

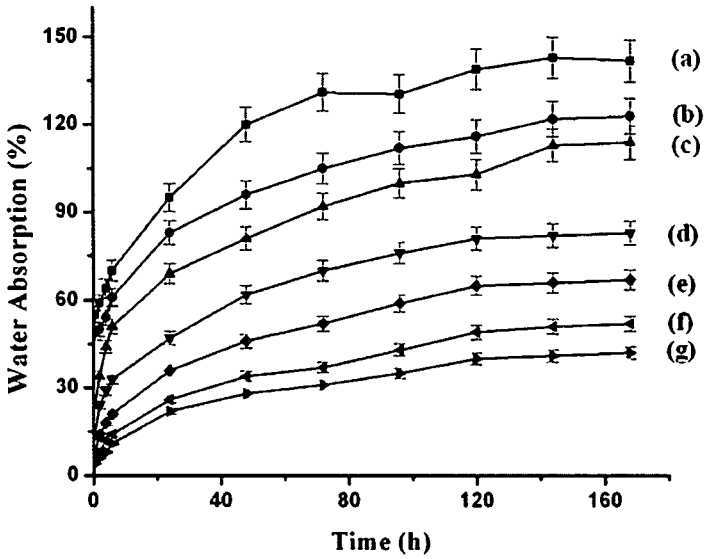

Figure4.1.6. Water absorption test of (a) untreated wood and wood treated with (b) MMA (c) MMA/GMA (d) MMA/GMA/clay I (0.5 phr) (e) MMA/GMA/clay I (1.0 phr) (f) MMA/GMA/clay II (1.5 phr) and (g) MMA/GMA/clay I (1.5 phr).

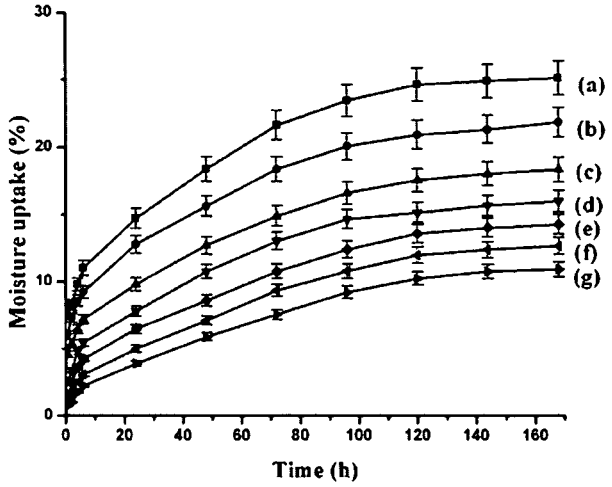

Figure4.1.7. Water vapor exclusion test (a) untreated wood and wood treated with, (b) MMA(c) MMA/GMA (d) MMA/GMA/clay I (0.5 phr) (e) MMA/GMA/clay I (1.0 phr) (f) MMA/GMA/clay II (1.5 phr) (g) MMA/GMA/clay I (1.5 phr).

4.1.8.Water vapor exclusion test

The results showing the water vapor exclusion test are presented in Figure4.1.7. The rate of water vapor absorption followed the order: untreated> MMA treated> MMA/GMA treated>MMA/GMA/clay II (1.5 phr)>MMA/GMA/clay I (1.5 phr). Hydrophilic nature of

untreated wood was responsible for showing highest water uptake. Impregnation of wood with MMA would fill the void spaces and capillaries present in the wood. The addition of GMA would form the cross-linking between wood and polymer due to which it absorbed less water. Water diffusivity further decreased on addition of clay due to increase in tortuous path as explained earlier.

4.1.9.Water repellent efficiency (WRE) study

Results are shown in Table 4.1.4. Maximum improvement in WRE was observed forthe samples treated with MMA/GMA/clay I. The explanation was similar to that ofdescribed earlier.

4.1.10. Dimensional stability test

4.1.10.1. Swelling in water vapor

The results showing the effect of swelling are shown in Figure4.1.8. The samples treated with MMA/GMA/clay I showed least swelling in water. This was due to the increase of silicate layer spacing caused by the presence of alkyl group of CTAB along with the deposition of cross-linked MMA polymer in the void spaces of wood.

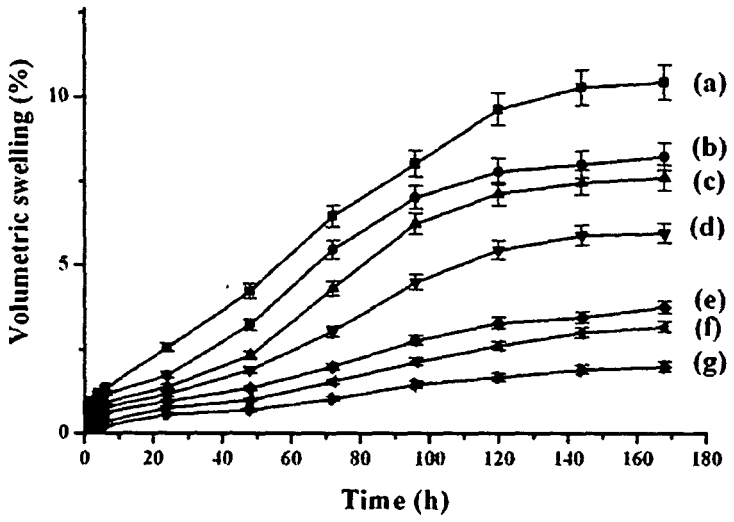

Figure 4.1.8. Volumetric swelling in water vapour at 65 % relative humidity and 30°C of wood samples(a) untreated wood and wood treated with, (b) MMA (c) MMA/GMA (d)MMA/GMA/clay I (0.5 phr) treated (e) MMA/GMA/clay I (1.0 phr) treated (f) MMA/GMA/clay II (1.5 phr) (g) MMA/GMA/clay I (1.5 phr).

Table 4.1.4. Water Repellant Effectiveness (WRE %) of wood polymer composite.

Time (h)	MMA/GMA/ Clay I (1.5 phr) treated	MMA/GMA/ Clay II (1.5 phr) treated	MMA/GMA/Clay I (1 phr) treated	MMA/GMA/Clay I (0.5 phr) treated	MMA/GMA treated	MMA treated
0.5	97.03 (±0.32)	96.52 (±0.88)	96.19 (±0.12)	94.37 (±0.97)	89.43(±0.77)	47.60 (± 0.5)
2	90.37 (±0.03)	88.61 (±0.51)	81.17 (±0.16)	79.26 (±1.09)	76.58 (±0.45)	44.69 (±0.76)
4	86.46 (±0.43)	80.47 (±0.37)	77.91 (±0.24)	75.44 (±0.76)	72.64 (±0.84)	42.53 (±0.47)
6	78.62 (±0.12)	76.77 (±0.43)	75.91 (±0.09)	73.51 (±0.49)	69.98 (±1.74)	38.47 (±0.86)
24	69.53 (±0.37)	66.58 (±0.67)	61.08 (±0.64)	61.73 (±0.54)	59.30 (±1.54)	37.74 (±1.38)
48	62.81 (±0.15)	58.27 (±0.54)	57.33 (±0.73)	56.07 (±0.41)	55.47(±1.68)	33.02 (±1.63)
72	61.27 (±0.56)	57.92 (±0.48)	57.12 (±0.04)	55.68 (±0.72)	55.21 (±0.37)	29.63 (±1.52)
96	60.93 (±0.08)	57.34 (±0.72)	57.11 (±0.57)	55.31 (±0.34)	51.71 (±0.47)	26.74 (±0.74)
120	60.72 (±0.85)	57.17 (±0.57)	57.04 (±0.46)	55.23 (±0.64)	49.96 (±0.29)	26.51 (±0.27)
144	60.48 (±0.63)	58.88 (±0.04)	56.94 (±0.48)	54.81 (±0.53)	49.43 (±0.74)	16.07 (±1.73)
168	60.33 (±0.53)	58.56 (±0.58)	56.83 (±0.71)	54.69(±0.71)	49.27 (±0.52)	16.02 (±0.66)

4.1.10.2. Swelling in water

The results of the effects of swelling in water at room temperature for both treatedand untreated samples are shown in Figure4.1.9. Treated samples showed more reductionin swelling in comparison with the untreated ones. At similar clay loading, clay Itreated wood samples swelled less compared to clay II treated samples. In clay I, theincrease of silicate layer spacing caused by interaction of alkyl group of CTABoffered more resistance to the passage of water molecules and hence showed morereduction in swelling.

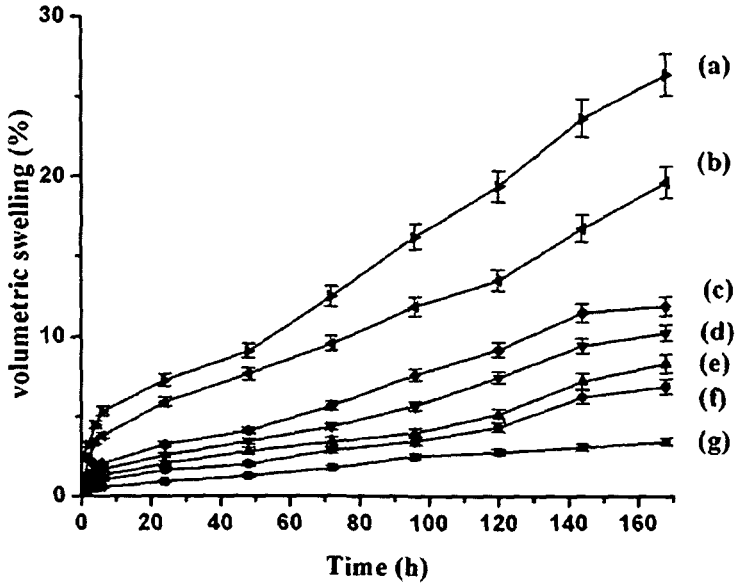

Figure 4.1.9. Volumetric swelling in water at 30°C of wood samples (a) untreated wood and wood treated with (b) MMA (c) MMA/GMA (d)MMA/GMA/clay I (0.5 phr)(e) MMA/GMA/clay I (1.0 phr) (f) MMA/GMA/clay II (1.5 phr)(g) MMA/GMA/clay I (1.5 phr).

4.1.10.3. Antiswelling efficiency (ASE)

The results of the ASE are shown in Table 4.1.5. ASE was highest in case of thesamples treated with MMA/GMA/clay I.The improvement of the dimensional stability was due to the combined effect ofdeposition of polymer inside the void spaces and capillaries of wood and thepresence of clay. The clay layer acted as a barrier for the diffusion of watermolecules.

Table 4.1.5. Antiswelling efficiency (%) of treated wood samples at different time period.

Time (h)	MMA treated	MMA/GMA treated	MMA/GMA/ Clay I (0.5 phr) treated	MMA/GMA/ Clay I (1 phr) treated	MMA/GMA/ Clay I (1.5 phr) treated	MMA/GMA/ Clay II (1.5 phr) treated
0.5	59.12 (±0.07)	65.65 (±0.89)	73.18 (±0.84)	78.45 (±0.56)	90.64 (±0.67)	85.39 (±0.61)
2	57.38 (±0.86)	57.41 (±0.06)	68.52 (±0.42)	72.36 (±0.36)	89.49 (±0.46)	79.31 (±0.93)
4	56.70 (±0.05)	84.71 (±0.72)	87.53 (±1.08)	88.22 (±0.71)	89.05 (±0.68)	88.43 (±1.21)
6	56.20 (±1.42)	84.27 (±0.68)	87.31 (±0.64)	87.69 (±0.29)	88.53 (±0.47)	87.91 (±0.58)
24	55.28 (±0.67)	83.06 (±0.82)	86.77 (±0.28)	87.32 (±0.52)	87.49 (±0.04)	87.48 (±0.17)
48	54.91 (±0.07)	82.14 (±1.63)	86.28 (±0.57)	86.72 (±0.47)	86.75 (±0.32)	86.87 (±0.47)
72	54.64 (±0.23)	81.97 (±1.46)	85.82 (±0.44)	86.02 (±0.63)	85.78 (±0.08)	86.13 (±0.03)
96	53.06 (±0.42)	81.15 (±1.12)	85.37 (±0.75)	85.56 (±0.52)	84.55 (±0.37)	85.73 (±0.34)
120	52.75 (±0.69)	80.89 (±1.45)	84.92 (±1.04)	85.13 (±0.84)	83.49 (±0.46)	85.25 (±0.23)
144	51.34 (±0.57)	80.36 (±0.08)	84.46 (±0.68)	84.63 (±0.12)	83.36 (±0.02)	84.83 (±1.02)
168	51.22 (±0.88)	80.14 (±0.75)	84.03 (±0.42)	84.27 (±0.96)	83.12 (±0.06)	84.62 (±0.73)

Table 4.1.6. Chemical resistance test of the WPC samples.

Medium	Time (h)	Volumetric swelling						
		Untreated	MMA	MMA/ GMA	MMA/GMA /Clay I (0.5 phr)	MMA/GMA /Clay I (1 phr)	MMA/GMA /Clay I (1.5 phr)	MMA/GMA /Clay II (1.5 phr)
NaOH solution (4%)	24	12.33 (±0.33)	7.46 (±0.48)	7.43 (±0.87)	6.31 (±0.03)	5.84 (±0.53)	4.65 (±0.04)	5.38 (±0.06)
	168	14.76 (±0.46)	9.69 (±0.01)	9.58 (±0.52)	7.88 (±0.64)	7.01 (±0.41)	5.89 (±0.32)	6.91 (±0.37)
Acetic acid (4%)	24	7.63 (±0.75)	4.89 (±0.04)	4.87 (±1.01)	4.33 (±0.08)	3.91 (±0.11)	2.12 (±0.47)	3.67 (±0.43)
	168	10.11 (±0.83)	5.88 (±1.13)	5.36 (±1.07)	5.19 (±0.33)	5.03 (±0.09)	3.18 (±0.76)	4.73 (±0.53)

4.1.11. Chemical resistance test

Results are shown in Table 4.1.6. Swelling was least in the case of samples treated with MMA/GMA/clay I. With the increase in the amount of clay swelling decreased. The void spaces and capillaries of the wood were filled up by MMA. GMA enhanced the interaction through the formation of cross-linking between MMA and wood which resulted in decrease of swelling. Clay layers further restricted the path for the diffusion of chemicals and hence swelling decreased. The interaction between sodium hydroxide, wood cellulose, and clay layers might be responsible for the observed higher swelling of samples in sodium hydroxide compared to acetic acid [2].

4.1.12. Mechanical properties

Table 4.1.7.shows the value of flexural and tensile properties of untreated and treated wood samples. Both the flexural and tensile properties were found to enhance for the wood samples after the impregnation of MMA and GMA. The incorporation of GMA with MMA into untreated wood samples facilitated bond formation between wood and polymer through its glycidyl group and double bond, respectively. Devi and Maji studied the impregnation of styrene–acrylonitrile copolymer into wood and observed an increase in mechanical properties due to the incorporation of GMA [10]. The values were further increased after the incorporation of organically modified clay. The higher the amount of clay, the higher was the tensile and flexural values. The observed higher values might be due to the well dispersion of silicate layers of clay and the restriction in the mobility of the polymer chains inside the intercalated layers of clay. At similar clay loading, wood samples treated with clay I exhibited better tensile and flexural values compared to clay II treated wood samples. The long alkyl chain of CTAB could expand the gallery of MMT and thereby could accommodate more MMA polymer. The mobility of the polymer chains were more restricted in clay I treated wood composite compared to clay II treated wood composite. Hence clay I treated wood composite showed higher tensile and flexural values.

4.1.13. Thermogravimetric analysis

Table 4.1.8.represents the initial decomposition temperature (T_i), maximum pyrolysis temperature (T_m), decomposition temperature at different weight loss (%) (T_D) and residual weight (RW%) for the untreated wood samples and treated wood samples. T_i values

Table 4.1.7. Flexural and tensile properties of untreated and treated wood loaded with different percentage of clay.

Sample	Flexural properties		Tensile properties	
	Strength (MPa)	Modulus (MPa)	Strength (MPa)	Modulus (MPa)
Untreated wood	119.3 (± 0.24)	6009 (± 0.78)	40.1(± 0.68)	299.6 (± 16.12)
Wood treated withPMMA	121.3(± 0.87)	6097(± 1.15)	43.6 (± 1.25)	310.7 (± 14.62)
PMMA/GMA	122.1 (± 1.21)	6120 (± 1.12)	46.5 (± 1.16)	324.1 (± 16.37)
PMMA/GMA/ 0.5 phr clay I	123.7 (± 1.18)	6504 (± 0.76)	50.3 (± 1.42)	354.6 (± 17.87)
PMMA/GMA/ 1.0 phr clay I	123.9 (± 1.32)	8812 (± 1.16)	56.2 (± 1.53)	408.5 (± 18.34)
PMMA/GMA/ 1.5 phr clay I	129.6 (± 0.94)	8893 (± 1.42)	74.2 (± 1.23)	469.5 (± 15.38)
PMMA/GMA/ 1.5 phr clay II	127.3 (±1.14)	8836 (± 1.19)	62.1 (± 1.17)	447.6 (± 16.42)

of treated samples were higher than untreated samples. The polymerincreased the thermal resistance and the crosslinker increased the interfacialadhesion between wood and polymer. T_i value increased further after theincorporation of clay. The intercalated silicate layers of clay provided a barrier tothe passage of decomposed volatile products throughout the composite. Better thedistribution of silicate layers, higher is the barrier effect and hence better is theproperty [11]. With the increase in the amount of clay (0.5–1.5 phr), the thermalstability of the wood composite increased. Wood samples treated with doublesurfactant (CTAB + ATAC) modified clay exhibited higher thermal stability thanthose of treated with single surfactant (ATAC) modified clay. This might be due tothe presence of long alkyl chain of CTAB along with the acryloxy group of ATACthat increased the interaction among wood, polymer, and clay.T_m values for both the stages of pyrolysis for composites were more thanuntreated wood samples. T_m values for the first stage of pyrolysis was due to thedepolymerization of hemicellulose, glycosidic linkage of cellulose, and thermaldecomposition of cellulose [12] while the second stage of pyrolysis was due to thedegradation of PMMA [13]. The incorporation of GMA improved T_m values forboth the

stages. The values increased further after the incorporation of clay. $T_D$values of (ATAC + CTAB)-modified clay (clay I) treated WPC samples werehigher than those of ATAC-modified clay (clay II) treated WPC samples.RW values of untreated wood sample were found maximum. RW valuesdecreased after incorporation of polymer. GMA and clay further improved the RWvalues.

Table 4.1.8. Thermal analysis of wood polymer nanocomposite.

Sample	T_i	T_m[a]	T_m[b]	Temperature of decomposition (T_D) in °C at different weight loss (%)				RW% at
				20%	40%	60%	80%	600°C
Untreated wood	165	308	396	265	299	330	---	27.1
Wood treated withPMMA	192	316	404	273	307	339	384	8.1
PMMA/GMA	215	321	411	282	315	347	396	10.6
PMMA/GMA/clay I (0.5)	229	329	418	291	321	353	410	13.5
PMMA/GMA/clay I (1.0)	245	336	425	301	332	364	439	16.4
PMMA/GMA/clay I (1.5)	272	351	439	321	354	384	---	23.1
PMMA/GMA/clay II (1.5)	258	342	432	310	345	375	556	19.8

T_i: value for initial degradation; [a]T_m: value for 1st step; [b]T_m: value for 2nd step.

Section B: Study on the properties of wood polymer nanocomposites based on melamine formaldehyde-furfuryl alcohol copolymer and modified clay.

Wood polymer nano composite was prepared by impregnating melamine formaldehyde-furfuryl alcohol (MFFA) copolymer, n-methylol acrylamide (NMA), a crosslinking agent and MMT into wood (*Ficus hispida*) and using catalyst heat treatment.MMT was modified by using a polymerizable surfactant ATAC and a mixture of surfactants ATAC and CTAB in a molar ratio of 1:1. A comparative study is done on the effect of WPNC impregnated with unmodified MMT (designated as clay III), MMT modified with ATAC (designated as clay II) and a mixture of surfactants ATAC and CTAB (designated as clay I) on its various properties.

4.2. RESULTS AND DISCUSSION

4.2.1. Optimization of the system by measuring weight percent gain (WPG %), volume increase (%) and hardness.

Monomer concentration, initiator concentration, vacuum, time of impregnation and amount of cross-linking agent were varied to get optimized condition at which property enhancement was achieved.

Table 4.2.1.1. Effect of variation of monomer concentration (MFFA/furfuryl alcohol (FA)-H_2O concentration) [maleic anhydride: 1.00%; vacuum: 508 mm Hg; Time: 6 h; NMA: 3 mL].

MFFA/ FA-H_2O	Weight percent gain (%)	Volume increase (%)	Hardness (Shore D)
1:1	29.12 (±0.37)	2.56 (±0.35)	47 (±0.68)
3:1	32.78 (±0.98)	2.71 (±0.83)	50 (±0.47)
5:1	33.72(±0.76)	2.78(±0.64)	54 (±0.93)

Table 4.2.1.1. shows weight percent gain (%), volume increase (%) and hardness when monomer concentration is varied. The optimum properties was observed when the ratio of MFFA:FA-water concentration was 5:1.

Table 4.2.1.2. Effect of variation of initiator concentration [MFFA/FA-H_2O: 5:1; vacuum: 508 mm Hg; Time: 6 h; NMA: 3 mL].

MFFA/ FA-H_2O	Maleic anhydride (%)	Weight percent gain (%)	Volume increase (%)	Hardness (Shore D)
5:1	0.50	29.88 (±0.47)	2.51 (±0.83)	50 (±0.54)
5:1	0.75	32.08(±0.38)	2.68 (±0.65)	53 (± 0.83)
5:1	1.00	33.47 (±0.63)	2.71 (±0.25)	55 (±0.76)

The effect of variation of initiator concentration on weight percent gain (%), volume increase (%) and hardness are shown in Table 4.2.1.2. Maximum improvement in properties was obtained at 1.00 wt. % maleic anhydride.

Table4.2.1.3. Effect of variation of vacuum [MFFA/FA-H_2O: 5:1; maleic anhydride: 1.00%; Time: 6 h; NMA: 3 mL].

MFFA/ FA-H_2O	Maleic anhydride (%)	Vacuum (mm/inch Hg)	Weight percent gain (%)	Volume increase (%)	Hardness (Shore D)
5:1	1.00	127 (5)	30.02 (±0.48)	2.31 (±0.48)	49 (±0.65)
5:1	1.00	254 (10)	31.42 (±0.59)	2.61(±0.76)	52 (±0.46)
5:1	1.00	508 (20)	33.31 (±0.75)	2.82 (±0.82)	54 (±0.57)

Highest improvement in on weight percent gain (%), volume increase (%) and hardness was found when 508 mm Hg was used.

Results of the effect of variation of time on weight percent gain, volume increase and hardness are shown in Table 4.2.1.4. Improvement in properties was maximum when time of impregnation was 6 h.

It was observed from the Table 4.2.1.5.that when amount of NMA was varied from 1 to 5 mL, the properties improved and then it became almost constant. Enhancement in properties was highest when 3 mL of NMA was used.

Thus the conditions, at which enhancement in properties were optimized, were as follows: MFFA/FA-H_2O: 5:1, maleic anhydride: 1% (w/w), vacuum: 508 mmHg, time of impregnation: 6 h, NMA (mL): 3, clay I: 0.5–2.0 phr, clay II: 0.5–2.0 phr, clay III: 0.5–2.0 phr.

4.2.2. Effect of modified and unmodified clay on polymer loading (WPG %), volume increase, and hardness of wood polymer composite

From Table 4.2.2. it was observed that overall properties like weight gain %, volume increase, and hardness were improved in case of samples treated with MFFA or with MFFA/NMA or with MFFA/NMA/clay I or with MFFA/NMA/clay II or with MFFA/NMA/clay III. The observed higher properties were due to filling up the empty cell

Table 4.2.1.4. Effect of variation of time of impregnation [MFFA/ FA-H_2O: 5:1; maleic anhydride: 1.00%; vacuum: 508 mm Hg; NMA: 3 mL].

MFFA/ FA-H_2O	Maleic anhydride (%)	Vacuum (mm/inch Hg)	Time (h)	Weight percent gain (%)	Volume increase (%)	Hardness
5:1	1.00	508 (20)	2	31.21 (±0.53)	2.61 (±0.94)	51 (±1.03)
5:1	1.00	508 (20)	4	32.08 (±0.78)	2.67 (±0.65)	54 (±0.86)
5:1	1.00	508 (20)	6	33.73 (±0.72)	2.73 (±0.58)	56 (±0.41)

Table 4.2.1.5. Effect of variation of n-methylol acrylamide (NMA) concentration (mL) [MFFA/ FA-H_2O: 5:1; maleic anhydride: 1.00%; vacuum: 508 mmHg; Time: 6 h].

MFFA/ FA-H_2O	Maleic anhydride (%)	Vacuum (mm/inch Hg)	Time (h)	NMA (mL)	Weight percent gain (%)	Volume increase (%)	Hardness
5:1	1.00	508 (20)	6	1	31.73 (±0.52)	2.58 (±0.94)	51 (±1.17)
5:1	1.00	508 (20)	6	3	33.97 (±0.25)	2.76 (±0.48)	54 (±0.91)
5:1	1.00	508 (20)	6	5	33.94 (±0.64)	2.75 (±0.71)	54 (±1.12)

wall and void spaces of the capillaries with polymers. NMA thus enhanced the deposition of polymer within the void spaces of wood and could react through its hydroxyl group with the wood and polymer. The addition of clay further reduced the mobility of the polymer chains which were intercalated in between the silicate layers. Maximum improvement in properties was observed for clay I treated samples followed by clay II treated samples and clay III treated samples. In case of clay I treated samples, the long alkyl chain of CTAB facilitated expansion of clay layers and acrylate group of ATAC would undergo polymerization with double bond of NMA resulting in improvement in properties [5].ATAC alone present in clay II might not be able to expand the clay layers. It was reported that the interaction between wood and MMT is weak so MMT is to be made organophillic [7]. Clay III is the unmodified MMT and showed inferior properties compared to the clay I and clay II treated samples.

Table 4.2.2. Effect of variation of unmodified clay, clay modified with ATAC/CTAB (1:1) and ATAC on polymer loading (WPG %), volume increase and hardness.

Samples particulars	Weight % gain	Volume increase (%)	Hardness (Shore D)
Untreated wood		-	46 (±1.07)
Samples treated with MFFA/FA-water/NMA/ clay I/clay II/clayIII			
100/20/0/0/0/0	23.24 (±0.63)	2.08 (±0.81)	57 (±1.02)
100/20/3/0/0/0	25.32 (±0.58)	2.17 (±0.37)	60 (±0.74)
100/20/3/0.5/0/0	33.76 (±0.46)	2.77 (±1.05)	68 (±0.54)
100/20/3/1.0/0/0	35.93 (±0.57)	2.98 (±0.86)	69 (±0.79)
100/20/3/2.0/0/0	40.52 (±0.55)	3.26 (±0.64)	72 (±1.13)
100/20/3/0/2.0/0	37.36 (±0.64)	3.05 (±0.36)	70 (±0.43)
100/20/3/0/0/2.0	32.89 (±1.02)	2.69 (±1.13)	67 (±0.68)

Clay I: MMT modified with ATAC/CTAB (1:1).
Clay II: MMT modified with ATAC.
Clay III: unmodified MMT.

4.2.3. Nuclear magnetic resonance (NMR) study of MFFA copolymer and NMA

Figure 4.2.1. shows the ^{13}C NMR spectra of MFFA and NMA. In the spectrum of the copolymer (Figure 4.2.1.a) appearance of peak at 49.1 ppm was for linear methylene unit (-N-CH_2-Fu-). Appearance of singlet peak at 56.07 ppm was due to (Fu-CH_2OH). Signal at 60.22 ppm was due to –N-CH_2OH and peak at 64.54 ppm was due to –O-CH_2-Fu. Other peaks at 68.68-89.95 ppm were due to the methylene ether linkage (N-CH_2-O-CH_2-N). Peak at 107.41 ppm was assigned to the presence of 3-position of terminal furan ring, and the peaks around 109.65 and 110 ppm were due to 3-position of terminal furan ring which has the substituted –OH group and 4 position of terminal furan rings. Signal arising at 142.59-143.42 ppm was due to the 5-position of terminal furan ring. Appearance of signal at 152.24 ppm and 155.82 ppm were due to 2-position of terminal furan ring which has the substituted –OH group and 2-position of terminal furan ring which has the unsubstituted –OH group respectively. Signals at 166.46 ppm and 167.64 ppm were due to triazine carbon of methylol melamine and unsubstituted triazine nucleus. Figure 4.2.1.b shows the NMR spectrum of NMA; peak observed in 63.94 ppm was due to -$NHCH_2OH$. The peaks appeared at 128.76 ppm and 129.94 ppm were assigned to CH_2=CH-. Another peak appeared at 168.85 ppm was due to the carbonyl carbon. Cho et al. studied ^{13}C NMR spectrum of chito-oligosaccharide side chain containing NMA and reported the presence of its characteristic peaks [14].

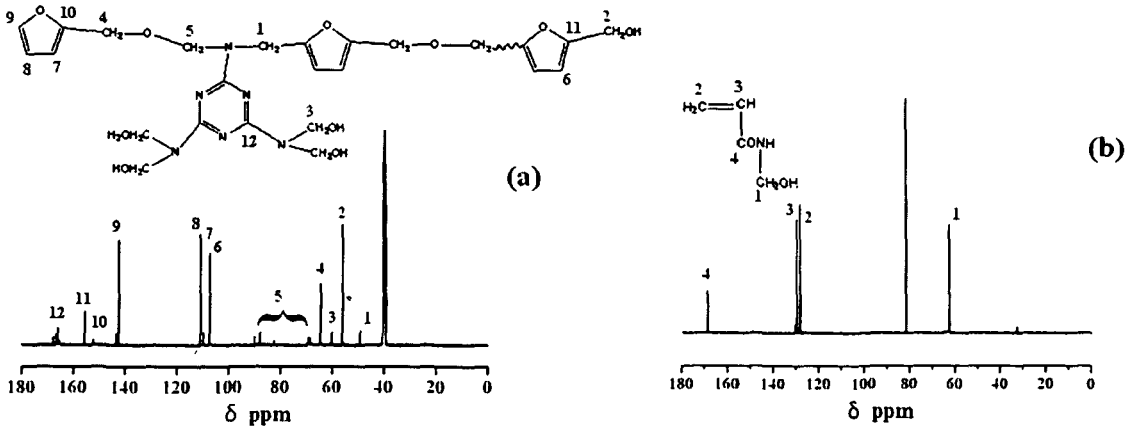

Figure 4.2.1. NMR spectra of (a) MFFA (b) NMA.

4.2.4. FTIR study

Figure 4.2.2. shows the FTIR spectrum of MFFA, NMA, unmodified MMT, and MMT modified by 1:1 ratio of ATAC & CTAB and ATAC. MFFA copolymer (curve a)

showed band at 3402 cm^{-1} (-OH stretching), 1567 cm^{-1} and 1507 cm^{-1} (furan ring vibration), 1189 cm^{-1} (C-N stretching), 813 cm^{-1} (out plane trisubstitution of triazine ring) [15]. NMA (curve b) was characterized by the absorption bands at 3420 cm^{-1} (-OH stretching), 3299 cm^{-1} (NH_2 stretching), 1665 cm^{-1} (C=O stretching), 1544 cm^{-1} (CO-NH stretching), 1237 cm^{-1} (NH-CH_2 stretching), 1027 cm^{-1} (C-H asymmetric stretching) [16].Modification of MMT was justified by the FTIR spectrum. Peaks appeared at 3452 cm^{-1}(–OH stretching), 1632 cm^{-1} (–OH bending), 1053–534 cm^{-1} (oxide bands of Mg, Al, Si, etc.) were for unmodified MMT (curve c). Modification of MMT by (ATAC+CTAB) was confirmed by the appearance of two new peaks at 2932 cm^{-1} and 2860 cm^{-1} which were due to –CH_2 asymmetric stretching of the modifying hydrocarbon of the surfactant for the ATAC+CTAB modified MMT (curve d). Another peak appearing at 1477 $cm^{-1}$was due to the –CH_2 plane scissoring vibration. Similar observation was also made in the ATAC modified MMT (curve e) [17].

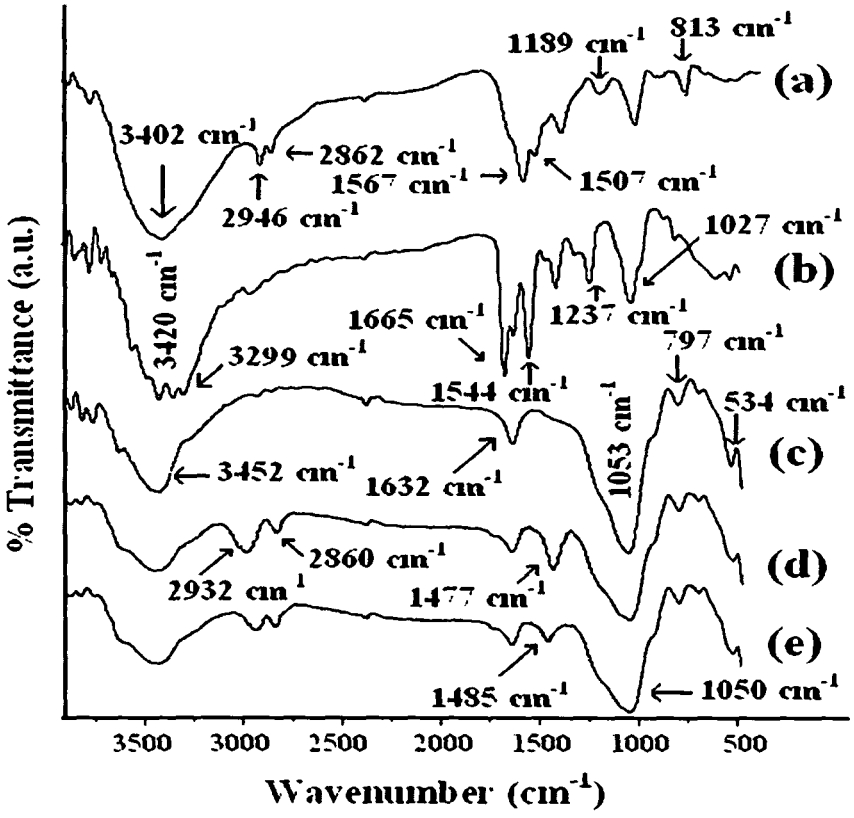

Figure 4.2.2. FTIR spectra of (a) MFFA (b) NMA (c) unmodified MMT and MMT modified by(d) 1:1 ratio of ATAC & CTAB (e) ATAC.

Figure 4.2.3. shows the FTIR spectra of untreated wood and wood polymer composites. For untreated wood (curve a) absorption band was found to appear at 3445 cm^{-1} (–

OH stretching), 2926 cm^{-1}, and 2851 cm^{-1} (–CH_2 asymmetric stretching), 1741 cm^{-1} (C=O stretching), 1664 cm^{-1} for (–OH bending), 1252 and 1023 cm^{-1} (C–O stretching) and 1,000–645 cm^{-1} (out of plane C–H bending vibration). The presence of the characteristic peaks of MFFA and crosslinker in WPC indicated the impregnation of MFFA and NMA into wood (curve b and c). In all the curves (b-f) the intensity of the hydroxyl peak decreased and shifted to 3421 cm^{-1}(curve b), 3373 cm^{-1} (curve c), 3322cm^{-1} (curve d), 3282 cm^{-1}(curve e), 3263 cm^{-1} (curve f) which was due to interaction of hydroxyl group of wood with the polymer and crosslinker. Addition of clay III has an enhanced interaction with the hydroxyl group of wood and polymer.This resulted in further shifting and decrease of intensity of hydroxyl group (curve d). Further it was noticed that the treated samples had pronounced peaks at 2926 $cm^{-1}$and 2851 cm^{-1} due to the –CH_2 asymmetric stretching compared to the untreated samples suggesting an improvement in interaction between wood, MFFA, NMA and clay. Maximum improvement in interaction was observed in clay I treated samples (curve e) followed by clay II treated samples (curve f) [18].

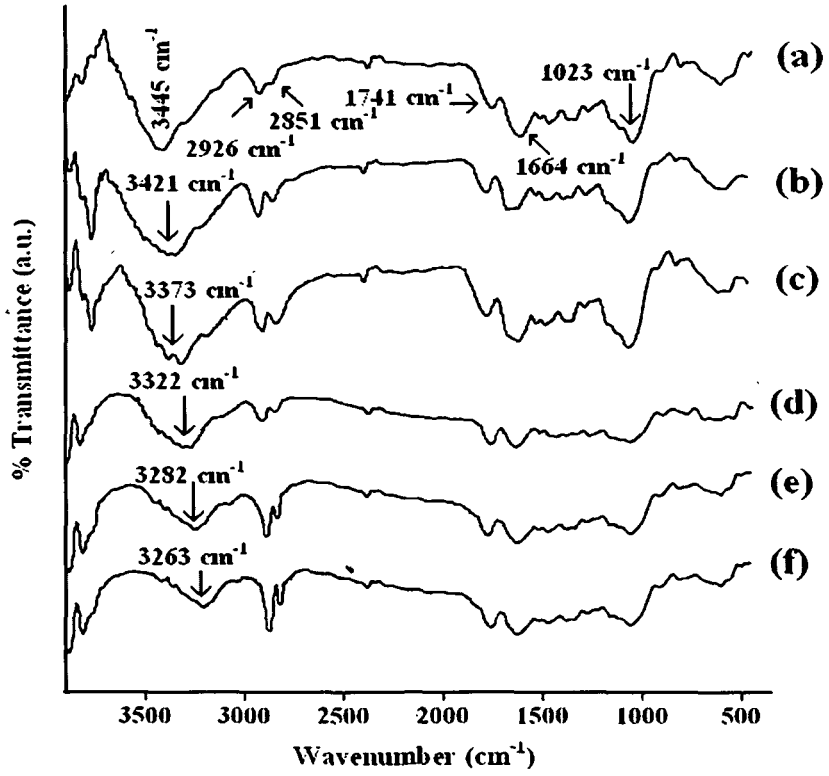

Figure 4.2.3.FTIR spectra of (a) untreated wood and wood treated with (b) MFFA prepolymer (c) MFFA/NMA (d) MFFA/NMA/clay III (2.0 phr) (e) MFFA/NMA/clay II (2 phr) (f) MFFA/NMA/clay I (2.0 phr).

4.2.5. X-ray diffraction studies

The X-ray diffraction patterns of clay III, clay II and clay I are shown in Figure 4.2.4. The diffraction peaks appeared at 8.31°, 7.4°, 6.3° were for clay III, clay II and clay I respectively. The interlayer spacing was calculated according to Bragg's law and was found to be 1.06 nm for the clay III, 1.19 nm for the clay II, 1.41 nm for the clay I. Thus it could be concluded that sodium cations present in between the layers of MMT could be efficiently replaced by the long alkyl chain.

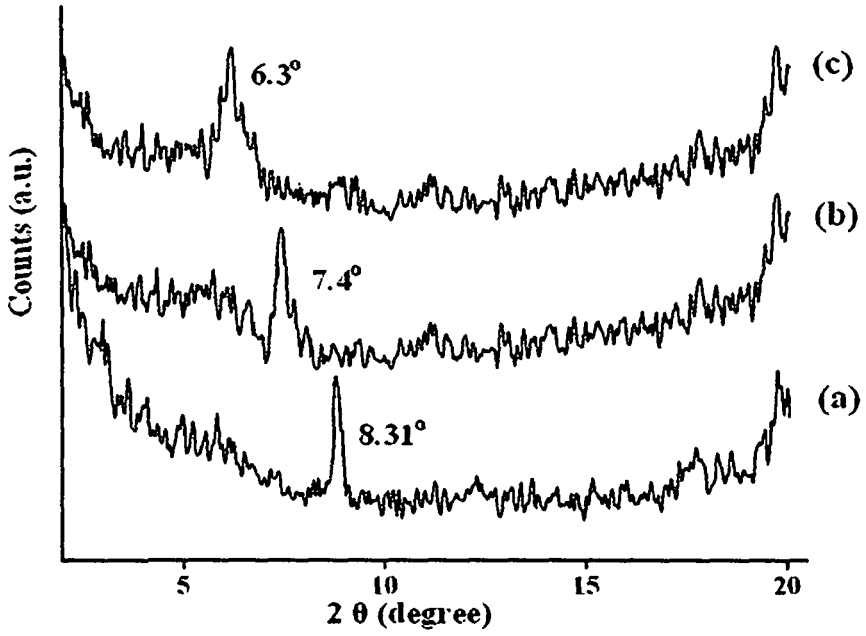

Figure 4.2.4.X-ray diffraction of (a) unmodified MMT (b) modified by ATAC (c) modified by 1:1 ratio of ATAC & CTAB.

Figure 4.2.5. shows the X-ray diffraction pattern of untreated wood, MFFA/NMA/clay I composite, WPNC samples. For the untreated wood a wide diffraction peak occurring at 22.96° was due to the (002) crystal plane of cellulose. A small weaker peak appeared near 37.72°and was due to the 040 crystal plane of cellulose. The peak near 15.05° was due to the amorphous region of cellulose (curve a) [7]. A broad peak (curve b) appeared at 22.56° was due to copolymerization of polyfurfuryl alcohol with melamine formaldehyde resin. The diffraction peak of clay I was found to be disappeared in MFFA/NMA/MMT composite. It might be said that the full expansion of gallery layers of MMT occurred which was not possible to detect by XRD. Both MMT and prepolymer contain hydroxyl groups and

could interact through formation of hydrogen bonding (curve b). The crystalline intensity peak of cellulose present in wood decreased and shifted to lower values in the WPNC indicating the formation of the composite. The peak at 15.05° and 37.72° were alsobecame dull (curve c). With the increase in the amount of clay I, the intensity of crystalline peak of wood decreased further signifying better interaction of wood with polymer, crosslinker and clay (curve d-e). Samples treated with MFFA/NMA/clay I showed a further decrease in the crystallinity (curve g) and shifting of the peak in 22.48° occurred. The crystallinity peak of MFFA/NMA/clay II (2 phr) treated samples showed a peak at 22.72° and the characteristic peak for the modified MMT disappeared. In all the cases of WPNC, the peak at 15.05° and 37.72° became dull and the diffraction peak for the modified MMT disappeared[19].

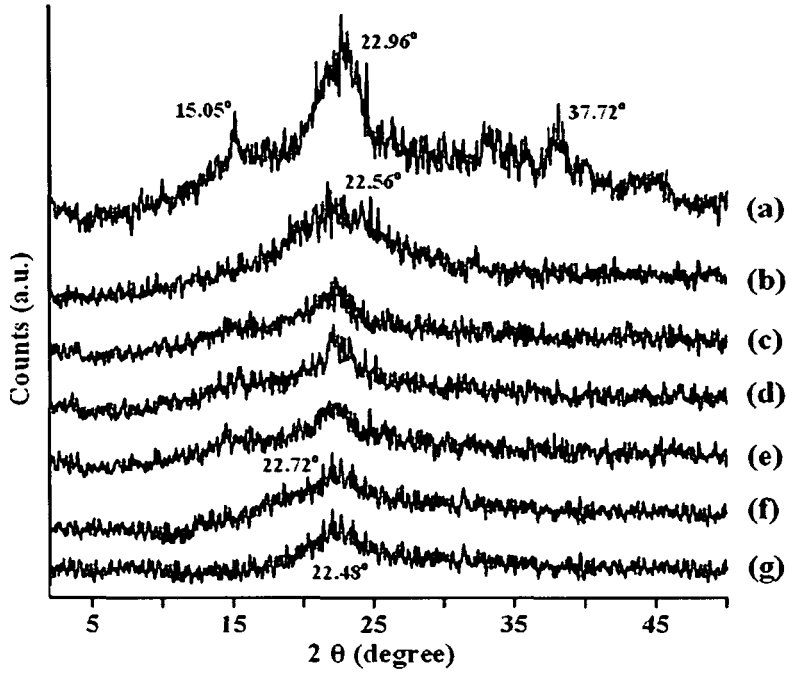

Figure 4.2.5.X-ray diffraction of (a) untreated wood (b) MFFA/NMA/clay I composite and wood treated with (c) MFFA/NMA/clay III (2.0 phr) treated (d) MFFA/NMA/clay I (0.5 phr) treated (e) MFFA/NMA/clay I (1.0 phr) treated (f) MFFA/NMA/clay II (2.0 phr) treated (g) MFFA/NMA/clay I (2.0 phr) treated wood samples.

4.2.6. Water uptake test

Water uptake results for treated and untreated samples are shown in Figure 4.2.6. Untreated wood showed the utmost water absorption capacity (curve a). As the cellular porous structure of wood was filled up by the polymer, its water uptake capacity decreased

(curve b). NMA contained double bond and hydroxyl groups and could provide better interfacial adhesion with the prepolymer and the resultant composites was found to be dimensionally stable(curve c). Incorporating clay III to the composites decreased its water uptake (curve d) since the silicate layers provided a meandering path for diffusion of water molecules. The samples treated with clay I and clay II showed a further decrease in water uptake capacity. It was also observed that with increase in the amount of clay water absorption capacity further decreased (curve e-h). The long alkyl chain of CTAB caused full expansion of the silicate layers and as a result tortuous path for diffusion of water molecules increased. ATAC could polymerize with the double bond of NMA through its acrylate group. The full expansion of clay layers was not possible in the case of clay II treated samples. Therefore, water uptake capacity was least in clay I treated followed by clay II treated and finally by the clay III treated samples [18].

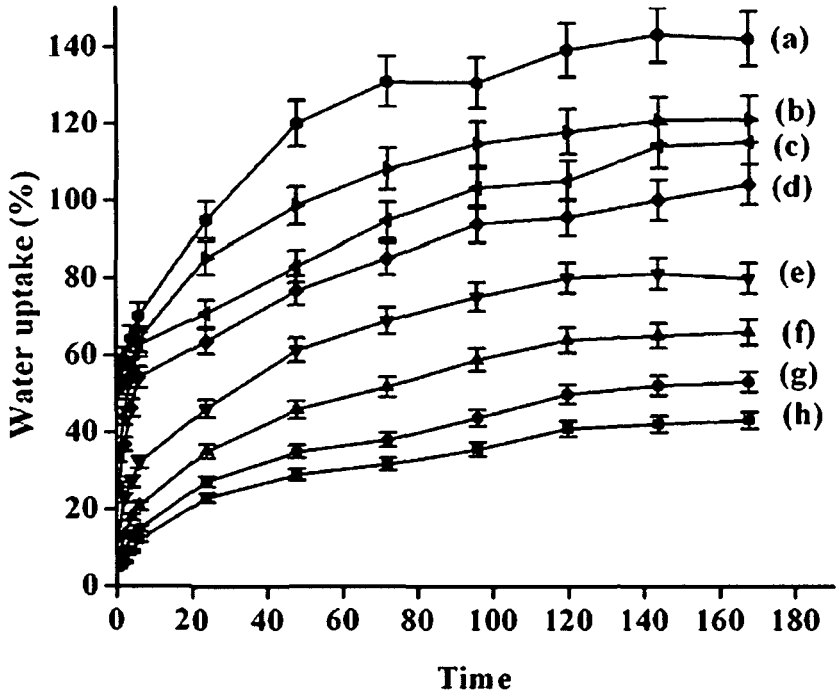

Figure 4.2.6. Water absorption test of (a) untreated wood and wood samples treated with (b) MFFA prepolymer (c) MFFA/NMA (d) MFFA/NMA/clay III (2.0 phr) (e) MFFA/NMA/clay I (0.5 phr) (f) MFFA/NMA/clay I (1.0 phr) (g) MFFA/NMA/clay II (2.0 phr) (h) MFFA/NMA/clay I (2.0 phr).

Table 4.2.3. Water repellant effectiveness (WRE %) of WPC.

Time (h)	MFFA treated	MFFA/ NMA treated	MFFA/ NMA/ Clay I (0.5 phr) treated	MFFA/ NMA/ Clay I (1 phr) treated	MFFA/ NMA/ Clay I (2 phr) treated	MFFA/ NMA/ Clay II (2 phr) treated	MFFA/ NMA/ Clay III (2 phr) treated
0.5	43.37 (±0.39)	62.82 (±0.65)	80.81 (±0.53)	84.35 (±0.68)	90.47 (±0.42)	89.13 (±1.04)	78.42 (±0.28)
2	41.86 (±0.62)	52.27 (±0.43)	73.46 (±0.31)	77.69 (±0.47)	85.74 (±0.73)	80.69 (±0.87)	70.51 (±0.75)
4	38.54 (±0.73)	46.53 (±0.71)	71.65 (±0.78)	74.57 (±0.86)	82.88 (±0.47)	75.49 (±0.55)	68.37 (±0.57)
6	35.46 (±0.47)	40.65 (±0.16)	68.44 (±0.39)	70.92 (±0.19)	77.42 (±1.08)	73.38 (±0.65)	66.85 (±0.58)
24	33.85 (±0.42)	34.32 (±1.13)	65.74 (±0.59)	67.32 (±1.16)	75.49 (±0.74)	72.73 (±0.59)	63.37 (±0.45)
48	29.94 (±0.68)	31.57 (±0.88)	64.12 (±1.09)	66.74 (±0.78)	74.86 (±0.95)	70.33 (±0.36)	61.23 (±0.74)
72	26.74 (±0.76)	27.23 (±0.72)	63.71 (±0.94)	66.17 (±0.35)	74.43 (±0.27)	69.46 (±0.21)	60.92 (±1.07)
96	24.38 (±1.03)	24.47 (±0.83)	63.52 (±0.56)	65.67 (±0.98)	74.27 (±0.66)	69.32 (±0.54)	60.43 (±0.29)
120	23.88 (±0.76)	22.96 (±0.64)	63.24 (±0.66)	65.37 (±0.77)	73.98 (±1.14)	68.76 (±1.03)	60.18 (±0.47)
144	22.56 (±0.21)	21.33 (±0.26)	62.89 (±0.28)	65.42 (±0.67)	73.76 (±0.85)	68.53 (±0.93)	59.89 (±0.52)
168	21.87 (±0.72)	21.12 (±0.92)	62.47 (±0.76)	65.25 (±0.83)	73.58 (±0.46)	68.36 (±0.12)	59.67 (±1.02)

4.2.7. Water repellant efficiency study

Results are shown in Table 4.2.3. An increase in water repellent efficiency was observed for the treated samples compared to untreated ones. The improvement in WRE was due to the combined effect of deposition of polymer and crosslinker. Addition of clay improved WRE more as the clay layers provided more hindrance for the diffusion of water molecules. Samples treated with MFFA/NMA/clay I showed maximum improvement in WRE. CTAB present in clay I increased the interlayer spacing of clay and enhanced the tortuous path for diffusion of water molecules.

4.2.8.Dimensional stability test

4.2.8.1. Swelling in water

Related results are shown in Figure 4.2.7. Both treated and untreated samples were kept in distilled water to observe the effect of swelling in water at room temperature. The

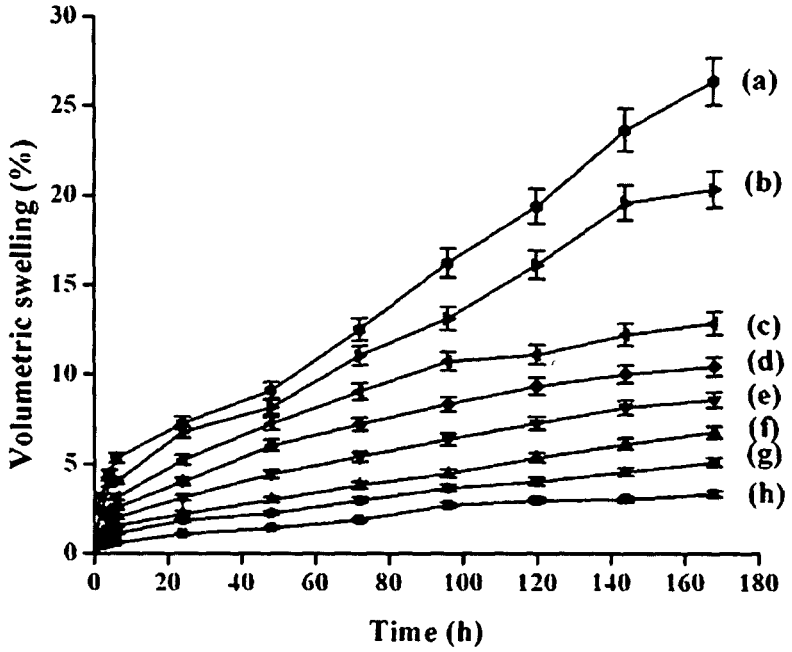

Figure 4.2.7. Volumetric swelling in water at 30°C of wood samples (a) untreated (b) MFFA prepolymer treated (c) MFFA/NMA treated (d) MFFA/NMA/clay III (2.0 phr) treated (e) MFFA/NMA/clay I (0.5 phr) treated (f) MFFA/NMA/clay I (1.0 phr) treated (g) MFFA/NMA/clay II (2.0 phr) treated (h) MFFA/NMA/clay I (2.0 phr) treated wood samples.

swelling of samples followed the trend: untreated > MFFA treated > MFFA/NMA treated > MFFA/NMA/clay III (2 phr) > MFFA/NMA/clay I (0.5 phr) > MFFA/NMA/clay I (1.0 phr) > MFFA/NMA/clay II (2.0 phr) > MFFA/NMA/clay I (2.0 phr). Untreated wood swelled more due to its porous structure. Polymer treated samples swelled less due to deposition of polymer in the capillaries and void spaces of wood. Esteves et al. reported that the dimensional stability of furfuryl alcohol treated wood samples under different relative humidity was improved compared to untreated ones [20]. The deposition of polymers was further enhanced by NMA. Samples treated with MFFA/NMA/modified MMT showed least water uptake compared to the samples treated with unmodified MMT. Higher the amount of modified clay I, the higher was the dimensional stability of the wood polymer composites. The layers of clay constrained the transmission of water molecules through the composites [9]. MFFA/NMA/clay I treated samples absorbed less water than MFFA/NMA/clay II treated samples as CTAB was able to expand interlayer spacing of clay thereby enhancing tortuous path for diffusion of water.

4.2.8.2. Antiswelling efficiency

Related results were shown in Table 4.2.4.ASE was highest for samples treated with MFFA/NMA/clay I. With the increase in time, ASE was found to decrease. Higher antiswelling efficiency of the treated samples was due to the mutual effect of deposition of polymer, crosslinker and clayinto the void spaces.

4.2.9. Chemical resistance test

Samples were kept immersed in 4% acetic acid and 4% NaOH solution and the results are shown in Table 4.2.5. Treated samples swelled less compared to the untreated samples. The capillaries and pores of treated wood samples were occupied by the polymers. The addition of NMA formed a crosslinked structure and as a result there was more decrease in swelling. Incorporating clay would decrease its swelling further since clay layers barricade the diffusion of chemicals. Higher swelling of samples in NaOH compared to the samples in acetic acid might be due to the interaction of clay layers, wood cellulose and sodium hydroxide [2].

Table 4.2.4. ASE (%) of treated wood samples at different time period.

Time (h)	MFFA treated	MFFA/ NMA treated	MFFA/ NMA/ Clay I (0.5 phr) treated	MFFA/ NMA/ Clay I (1 phr) treated	MFFA/ NMA/ Clay I (2 phr) treated	MFFA/ NMA/ Clay II (2 phr) treated	MFFA/ NMA/ Clay III (2 phr) treated
0.5	67.53(±1.07)	69.27 (±0.51)	79.65 (±0.76)	80.98 (±0.85)	83.65 (±0.75)	81.47 (±0.37)	75.88 (±0.21)
2	66.37 (±0.78)	67.84 (±0.27)	79.24 (±0.92)	80.72 (±0.78)	82.16 (±0.68)	80.18 (±0.49)	75.34 (±0.44)
4	65.76 (±0.57)	66.63 (±1.03)	78.79 (±0.51)	80.44 (±0.63)	81.64 (±0.52)	79.41 (±0.73)	74.78 (±0.87)
6	65.42 (±0.68)	66.52 (±0.52)	78.32 (±0.47)	80.28 (±0.18)	81.43 (±0.72)	79.26 (±1.08)	74.43 (±0.59)
24	65.02 (±1.12)	66.11 (±0.34)	78.24 (±1.06)	80.02 (±1.05)	81.24 (±0.65)	78.87 (±0.95)	74.12 (±0.78)
48	64.86 (±0.63)	65.91 (±0.47)	77.92 (±0.78)	79.84 (±0.37)	80.87 (±0.72)	78.67 (±0.47)	73.03 (±0.85)
72	64.39 (±0.52)	65.62 (±0.71)	77.57 (±0.81)	79.53 (±0.45)	80.54 (±0.67)	78.46 (±0.14)	72.84 (±1.06)
96	64.13 (±0.28)	65.26 (±1.12)	77.35 (±0.62)	79.32 (±0.82)	80.36 (±0.83)	78.19 (±0.84)	72.54 (±0.72)
120	63.96 (±0.46)	65.01 (±0.46)	77.17 (±0.77)	78.87 (±0.46)	80.07 (±1.04)	77.72 (±0.69)	72.32 (±0.28)
144	63.76 (±0.67)	64.83 (±0.18)	76.87 (±0.33)	78.63 (±0.58)	79.84 (±0.57)	77.38 (±0.25)	72.09 (±0.61)
168	63.49 (±0.84)	64.52 (±0.38)	76.62 (±1.12)	78.25 (±0.86)	79.66 (±0.29)	77.21 (±0.76)	71.92 (±1.02)

Table 4.2.5. Chemical resistance test of the WPC samples.

Samples	Volumetric swelling			
	Time			
	24 h		168 h	
	NaOH solution (4%)	Acetic acid (4%)	NaOH solution (4%)	Acetic acid (4%)
Untreated wood	12.82 (±0.51)	8.83 (±0.58)	13.26 (±0.73)	11.18 (±0.68)
Wood treated with MFFA	8.64 (±0.74)	5.62(±0.55)	11.54 (±0.62)	6.71 (±0.83)
MFFA/NMA	8.24 (±0.76)	5.45(±0.41)	10.78(±0.82)	6.48(±0.33)
MFFA/NMA/Clay I (0.5 phr)	5.13 (±0.62)	3.19 (±0.64)	6.10 (±0.37)	4.08 (±0.28)
MFFA/NMA/Clay I(1 phr)	4.88 (±0.43)	2.91 (±0.64)	5.98 (±0.78)	3.78 (±0.37)
MFFA/NMA/Clay I(2 phr)	3.96 (±0.66)	2.11 (±0.36)	5.05 (±0.87)	3.14 (±0.57)
MFFA/NMA/Clay II(2 phr)	4.27 (±0.84)	2.48 (±0.28)	5.42 (±0.75)	3.31 (±0.47)
MFFA/NMA/Clay III(2 phr)	5.76 (±0.35)	3.89 (±0.23)	6.93 (±0.75)	4.78 (±0.56)

4.2.10. Mechanical properties

The results of tensile and flexural values of treated and untreated samples are shown in Table 4.2.6. Treatment of wood with MFFA would fill the void spaces of wood and as a result, there would be an improvement in properties. NMA could crosslink the cell wall of wood with the polymer and improved interaction. Therefore samples treated with MFFA/NMA exhibited better properties than the samples treated with MFFA. A significant improvement in mechanical properties of NMA treated hemp fiber/unsaturated polyester composite was reported by Qiu et al. [21]. Both the flexural and tensile properties were further improved due to addition of clay.The observed higher values might be due to combined effect of crosslinking by NMA and the restriction in the mobility of the polymer chains inside the intercalated layers of clay. Lee and Kimprepared wood/polypropylene/clay nanocomposites and reported an improvement in mechanical properties after the inclusion of organoclay [22].Wood samples treated with MFFA/NMA/clay I showed highest tensile and flexural values than MFFA/NMA/clay II treated samples followed by MFFA/NMA/clay III treated ones.The long alkyl chain of CTAB increased the interlayer distance of MMT and thereby could accommodate more polymers whereas ATAC alone could not expand the clay layers to that extent. The mobility of the polymer chains were more restricted in clay I treated wood composite compared to clay II and clay III treated wood composite. Hence clay

I treated wood composite showed higher tensile and flexural values. The flexural properties were found higher than the tensile values as reported by Huda et al. while studying the mechanical properties of wood reinforced poly(lactic acid) composites [23].Similar observation was also made by Lin et al. during study of the mechanical properties of wood flour/continous glass mat/polypropylene composite [24].

Table 4.2.6. Flexural and tensile properties of untreated and treated wood.

Sample	Flexural properties		Tensile properties	
	Strength (MPa)(±SD)	Modulus (MPa)(±SD)	Strength (MPa)(±SD)	Modulus (MPa)(±SD)
Untreated wood	99.81±0.63	5039.76±1.33	28.37±2.86	208.53±2.04
Wood treated with MFFA	106.59±0.90	5379.78±1.68	31.66±0.60	234.65±2.92
MFFA/NMA	110.79±1.21	5584.72±1.22	36.82±1.29	272.69±3.75
MFFA/NMA/0.5 phr clayI	118.63±2.05	5986.78±0.70	45.61±1.22	337.74±5.30
MFFA/NMA/1.0 phr clayI	121.60±1.17	6131.27±1.24	48.56±2.89	358.62±4.55
MFFA/NMA/2.0 phr clayI	123.63±1.26	6233.90±1.24	50.34±0.63	372.26±3.69
MFFA/NMA/2.0 phr clayII	126.51±1.22	6372.11±1.25	48.50±1.21	359.54±5.13
MFFA/NMA/2.0 phr clayIII	115.51±1.15	5824.61±2.74	41.83±1.28	309.65±1.87

4.2.11. Limiting oxygen index (LOI)

Results of LOI values are shown in Table 4.2.7. Samples treated with MFFA showed higher values than the untreated ones. Fire retardancy of MFFA treated samples was due to high nitrogen content of melamine. As the samples were subjected to combustion, release of oxides of nitrogen had taken place displacing oxygen present on the surface of the samples. Incorporation of clay would produce excellent barrier effect prevent dripping, promote char formation and hence improved the thermostability of the prepared composites [25].The char layers of individual clay improved the flame retardant properties. Char protected the bulk of the sample from heat and decreased rate of mass loss during thermal decomposition and thus providing an improved flame resistance [26]. Samples treated with MFFA/NMA/clay I showed the highest LOI values compared to MFFA/NMA/clay II and MFFA/NMA/clay III treated samples. CTAB and ATAC present in clay I expanded the silicate layers more

compared to either clay II or clay III and thus provided better barrier property to the oxygen and heat resulting in delayed burning of WPNC.

Table 4.2.7. Limiting oxygen indices (LOI) and flaming characteristics of treated and untreated samples.

Samples	LOI (%)	Flame description	Smokes and fumes	Char
Untreated	21	Candle-like localized flame	-	Little
Wood treated with MFFA	23	Small localized flame	Small and black smoke	Medium
MFFA/NMA	26	Small localized flame	Small and black smoke	Medium
MFFA/NMA/0.5 phr clay I	30	Small localized flame	Small and black smoke	Medium
MFFA/NMA/1.0 phr clay I	32	Small localized flame	Small and black smoke	Medium
MFFA/NMA/2.0 phr clay I	35	Small localized flame	Small and black smoke	Higher
MFFA/NMA/2.0 phr clay II	33	Small localized flame	Small and black smoke	Higher
MFFA/NMA/2.0 phr clay III	28	Small localized flame	Small and black smoke	Medium

4.2.12. Thermal degradation study

The results of initial degradation temperature (T_i), maximum pyrolysis temperature (T_m), decomposition temperature at different weight loss (%) (T_D) and residual weight (RW %) are shown in Table 4.2.8. For both untreated and treated samples a decrease in weight loss was observed below 100°C which was due to loss of moisture. The treated samples had higher T_i values than the untreated ones. Treatment of wood with polymer and crosslinker would form crosslinked structure and improved interfacial adhesion as well as thermal stability. On addition of clay, there was an improvement in thermal properties. Clay can act as a heat sink and mass transport barrier for the volatile products generated during

decomposition. Higher the amount of clay, the better was the thermal stability [27]. Samples treated with modified MMT had superior properties than the unmodified MMT treated samples. Samples treated with clay I exhibited higher thermal stability than the clay II treated samples because the long alkyl chain of CTAB and acrylic group of ATAC enhanced the interaction between wood, polymer and MMT. Similarly, T_m values increased for the treated samples for both the stages of pyrolysis. T_D values of clay treated samples were higher than MFFA/NMA treated ones. RWvaluewas highest for the untreated wood. Its value decreased upon addition of MFFA. Further addition of NMA and clay increased its value again [4].

Table 4.2.8. Thermal analysis of wood polymer nanocomposite.

Sample	T_i	T_m^a	T_m^b	Temperature of decomposition (T_D) in °C at different weight loss (%)				RW% at 600°C
				20%	40%	60%	80%	
Untreated	166	311	398	267	302	332	--	27.23
Wood treated with MFFA	199	322	413	282	314	345	389	7.9
MFFA/NMA	237	337	431	303	326	365	429	8.7
MFFA/NMA/0.5 phr clay I	241	342	436	321	332	370	433	10.3
MFFA/NMA/1.0 phr clay I	252	350	441	329	339	377	442	12.5
MFFA/NMA/2.0 phr clay I	257	355	446	333	345	382	448	20.5
MFFA/NMA/2.0 phr clay II	254	352	443	331	342	373	445	16.8
MFFA/NMA/2.0 phr clay III	239	339	432	307	329	366	431	9.7

4.2.13. Morphology of nanocomposites

Figure 4.2.8. shows the SEM micrographs of untreated and treated wood samples. The empty pit and parenchyma were seen in untreated wood (Figure 4.2.8.a). These void spaces were occupied by MFFA/NMA/clay in treated wood samples (Figure 4.2.8.b-f). The

presence of impregnated MMT could be seen as some white patches that were adhered in cell wall or filled in the cell lumen (Figure 4.2.8.d-f).

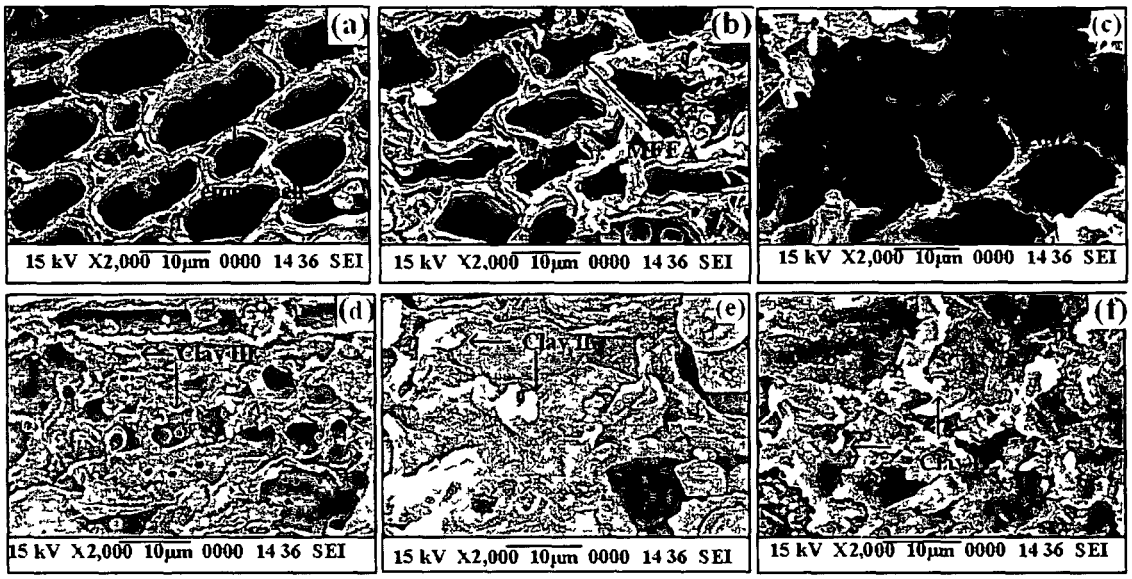

Figure 4.2.8. Scanning electron micrograph of (a) untreated (b) MFFA prepolymer treated (c) MFFA/NMA treated (d) MFFA/NMA/clay III (2.0 phr) treated (e) MFFA/NMA/clay II (2.0 phr) treated (f) MFFA/NMA/clay I (2.0 phr) treated wood samples.

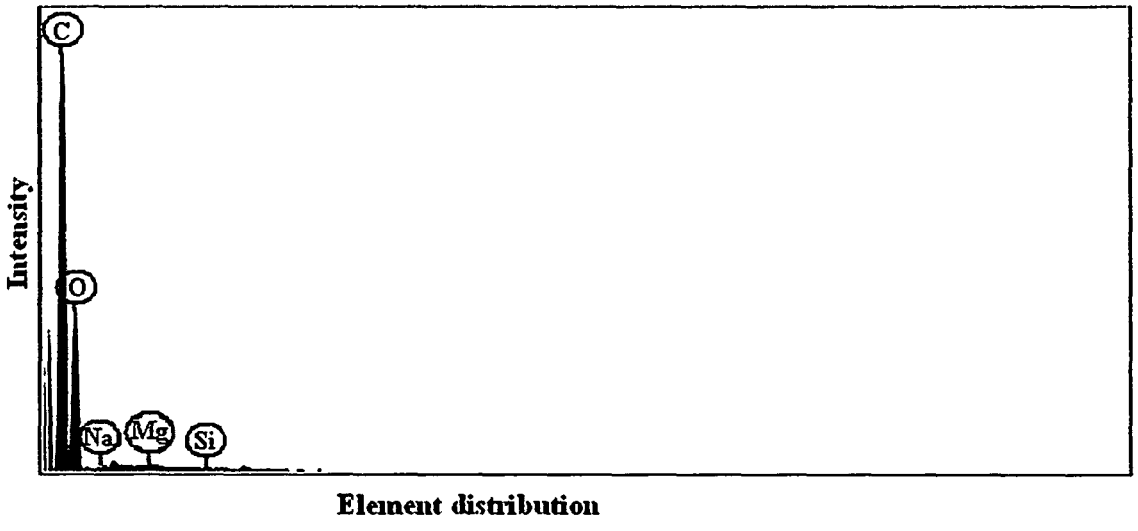

Figure 4.2.9. Energy dispersive X-ray spectroscopy of MFFA/NMA/Clay I (2 phr)

The presence of trace amount of clay observed in the fractured surface of the sample taken for SEM was also investigated by energy dispersive X-ray spectroscopy (EDS). The

EDS analysis of wood polymer composite was shown in Figure 4.2.9. The presence of C, O, Na, Mg, Si in the composites indicated impregnation of clay into wood.

Figure 4.2.10. shows the TEM micrographs of untreated and treated wood samples. For untreated wood (Figure 4.2.10.a), orientation of the cell wall components could not be detected. In the samples treated with MFFA/NMA/clay I (Figure 4.2.10.b), MFFA/NMA/clay II (Figure 4.2.10.c), MFFA/NMA/clay III (Figure 4.2.10.d), the dispersion of clay was observed in the MFFA copolymer and in the cell wall of wood. The dispersion of clay was found better in combined surfactant modified clay based wood composite. This study indicated that clay was impregnated into porous structure of wood. Cai et al. prepared WPNC with melamine urea formaldehyde (MUF) resin and MMT and reported impregnation of clay in the cell wall of wood [9].

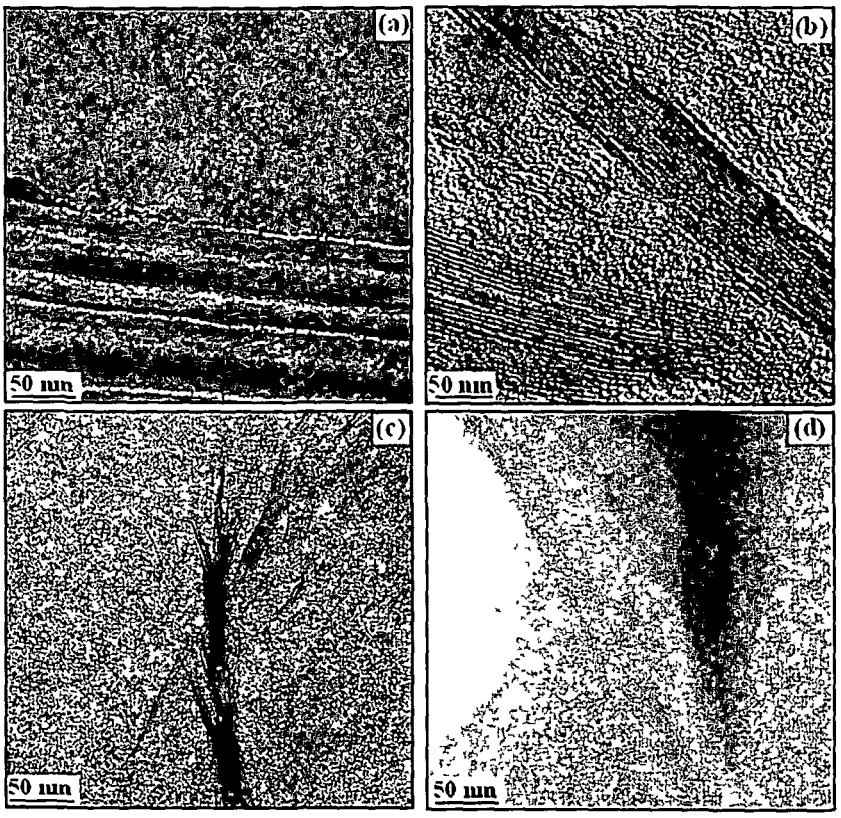

Figure 4.2.10. Transmittance electron micrograph of (a) Untreated wood (b) MFFA/NMA/clayI treated (c) MFFA/NMA/clay II treated (d) MFFA/NMA/clay III treated.

Section C: Effect of different crosslinkers on properties of melamine formaldehyde-furfuryl alcohol copolymer/montmorillonite impregnated softwood (*Ficus hispida*).

The aim of this work isto comparethe effect of different crosslinkers on the various properties of WPC. MFFA copolymer was synthesized and impregnated into woodin combination with crosslinking agent and MMT under vacuum condition. Different crosslinkers namely NMA, 2-Hydroxyethyl methacrylate (HEMA) and 1,3-dimethylol-4,5-dihydroxyethyleneurea (DMDHEU) and mixture of all the three crosslinkers were used for evaluation of properties of the prepared composites. The effect of MMT on the properties of the composites had also been studied. The optimized condition to obtain maximum improvement in properties was found by varying time of impregnation, vacuum, monomer concentration, catalyst concentration and amount of crosslinking agent. The conditions were : 6 h time of impregnation, 500mm Hg vacuum, 5:1 (MFFA:FA-water)prepolymer concentration, 1% (w/w) maleic anhydride, 3 mL NMA, 3mL HEMA, 3 mL DMDHEU, 2 phr MMT.

4.3. RESULTS AND DISCUSSION

4.3.1. Effect of variation of crosslinker on polymer loading (WPG %), volume increase, and hardness

Related results are shown in Table 4.3.1. The wood samples treated with (MFFA+NMA+HEMA+DMDHEU) exhibited improved properties like polymer loading, volume increase and hardness compared to those of properties of the wood samples treated with MFFA/NMA, MFFA/HEMA and MFFA/DMDHEU. The wood samples treated with MFFA showed an enhancement in properties due to fill up of the void spaces and capillaries by the copolymer. Gindl et al. reported that the surface properties of wood were improved due to impregnation with melamine formaldehyde resin [28]. The properties were further improved after the incorporation of NMA, DMDHEU and HEMA as crosslinkers to the MFFA copolymer. The improvement of properties followed the order- : DMDHEU> HEMA> NMA. The presence of double bond and hydroxyl group in both NMA and HEMA could undergo self polymerization and crosslinking reactions with the hydroxyl and methylol group of wood and MFFA copolymer. HEMA has ester linkage which results in

low viscosity and possesses several functional groups [29,30] and can able to penetrate more in the cell wall of the wood compared to NMA. Thus HEMA could provide better crosslinking and hence exhibited better properties compared to NMA. On the other hand DMDHEU has four hydroxyl groups which are capable of reacting with the hydroxyl and methylol groups of wood and MFFA copolymers. As a result it would provide maximum crosslinking and highest improvement in properties. The samples treated with MFFA/(NMA+HEMA+DMDHEU) showed better properties compared to those of samples treated with MFFA/NMA, MFFA/HEMA and MFFA/DMDHEU. The improvement in properties might be due to the synergistic effect caused by different crosslinkers used. The properties were again improved after the incorporation of clay to the mixed crosslinker treated wood/MFFA composite. This was due to the reinforcing effect of silicate layers of clay that bind the polymer chains inside the gallery space and restrict the mobility of the polymer chains. Devi et al. [2] reported that hardness was improved by the addition of nanoclay into wood/styrene-acrylonitile polymer composite.

Table 4.3.1. Effect of variation of crosslinker on polymer loading (WPG %), volume increase and hardness.

Sample	Weight % gain	Volume increase %	Hardness (Shore D)
Untreated wood	–	–	45 (±1.5)
Wood treated with MFFA/FA-H_2O/NMA/HEMA/DMDHEU/MMT			
100/20/0/0/0/0	22.4 (±0.8)	2.0 (±0.5)	56 (±1.2)
100/20/3/0/0/0	25.5 (±0.2)	2.1 (±0.6)	59 (±1.3)
100/20/0/3/0/0	26.8 (±0.6)	2.2 (±1.0)	61 (±1.0)
100/20/0/0/3/0	28.7 (±0.3)	2.4 (±0.8)	63 (±1.0)
100/20/1/1/1/0	33.6 (±0.7)	2.7 (±0.4)	66 (±0.8)
100/20/1/1/1/2	39.3 (±1.0)	3.2 (±0.6)	69 (±0.7)

4.3.2. NMR study of DMDHEU

The peaks appearing in the spectrum of DMDHEU (Figure 4.3.1.), at 159.85, 81.83 and 63.99 ppm were due to carbonyl carbon, -CHOH and –$NHCH_2OH$ respectively [31-

33].Similar observation was reported by Hermanns et al. while studying the ^{13}C NMR spectrum of synthesized DMDHEU[34].

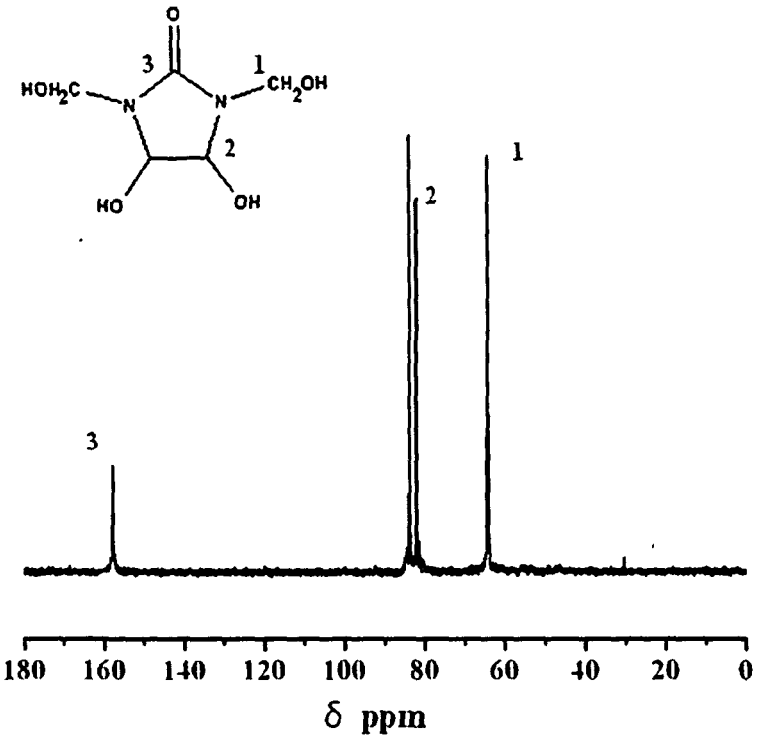

Figure4.3.1. NMR spectra of DMDHEU.

4.3.3. FTIR study

Figure 4.3.2. shows the FTIR spectra of MF, FA polymer, MFFA copolymer, NMA, HEMA and DMDHEU. In the spectrum of MF resin (curve a), appearance of peaks at 3344 cm^{-1} was due to N-H stretching of secondary amineclose to the methylene bridge. Bands at 2926 cm^{-1} and 2853 cm^{-1} were assigned to asymmetric and symmetric stretching of $-CH_2$ group. Peaks at 1549 cm^{-1}, 1173 cm^{-1} were attributed to N-H bending and secondary amine and C-N stretching respectively. In the spectrum of polyfurfuryl alcohol (curve b), assignment of peaks at 3402, 3021, 2928, 1617, 1561, 1152 and 742 cm^{-1} were for -OH stretching, -CH stretching of aromatic rings, aliphatic –CH stretching, C=C aromatic, ring vibrations, C-O stretching and 2,5- disubstitution of furan ring respectively. MFFA copolymer (curve c) showed band at 3401 cm^{-1} (-OH stretching), 1568 cm^{-1} and 1509 cm^{-1} (furan ring vibration), 1342 cm^{-1} (N-CH_2-furan ring), 1188 cm^{-1} (HOH_2C-N stretching), 812 cm^{-1} (out plane trisubstitution of triazine ring) [35,15]. NMA (curve d) had absorption band at 3419 cm^{-1} (-OH stretching), 3297 cm^{-1} (NH_2 stretching), 1664 cm^{-1} (C=O stretching),

1543 cm^{-1} (CO-NH stretching), 1238 cm^{-1} (NH-CH_2 stretching), 1028 cm^{-1} (C-H asymmetric stretching)[16]. The main bands of HEMA (curve e) were at 3430 cm^{-1} (-OH stretching), 2950 cm^{-1}(-CH stretching), 1710 cm^{-1} (C=O stretching), 1634 cm^{-1} (methacrylate C=C vibration), 1174 cm^{-1} (C-O stretching) [36]. In the spectrum of DMDHEU, (curve f) the absorption band appeared at 3416, 1700, 1244, 1019 cm^{-1} were for -OH stretching, C=O stretching, -CHOH stretching, -CH_2OH stretching respectively [37].

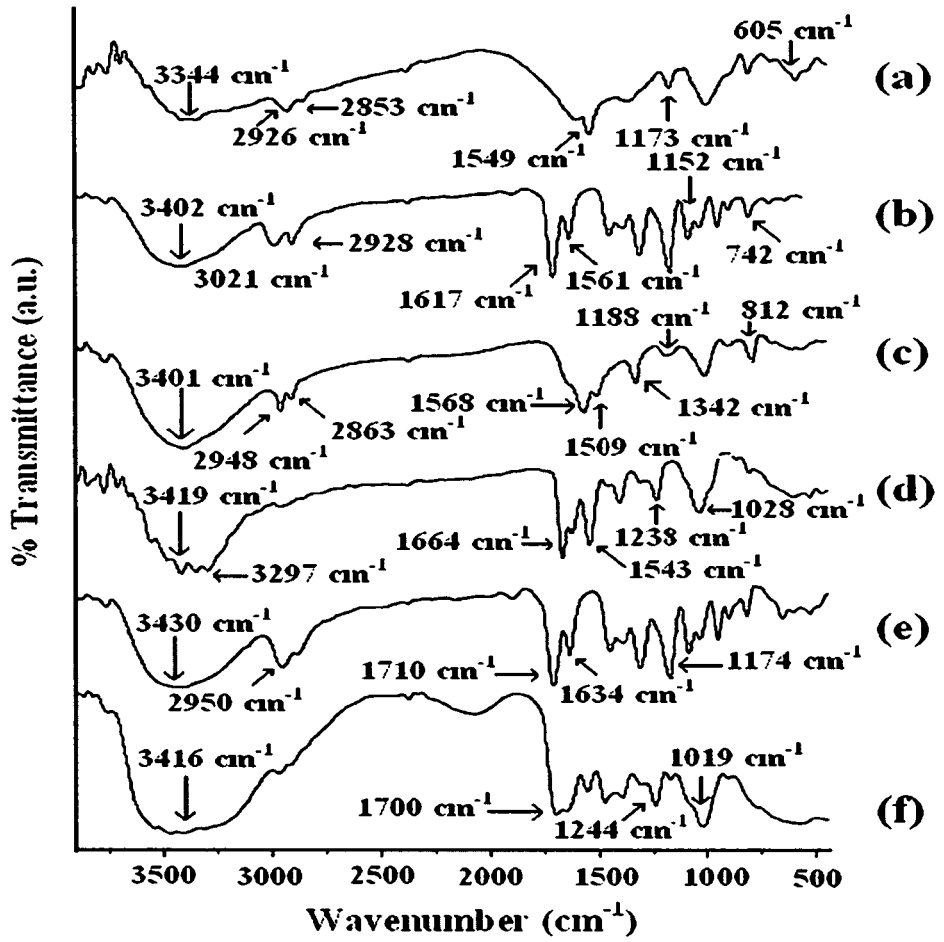

Figure4.3.2. FTIR spectra of (a) MF (b) FA polymer (c) MFFA (d) NMA (d) HEMA (d) DMDHEU.

Figure 4.3.3. shows the FTIR spectra of MMT, wood and wood polymer composites. Unmodified MMT (curve a) exhibits bands at 3434 cm^{-1} (–OH stretching), 1638 cm^{-1} (–OH bending), 1050–535 cm^{-1} (oxide bands of Al, Mg, Si, etc.) [4]. Untreated wood (curve b) was characterized by the absorption band at 3429 cm^{-1} (–OH stretching), 2925 cm^{-1}, and 2848 cm^{-1} (–CH_2 asymmetric stretching), 1732 cm^{-1} (C=O stretching), 1642 $cm^{-1}$for (–OH

bending), 1258 and 1046 cm^{-1} (C–O stretching) and 1000–646 cm^{-1} (out of plane C–H bending vibration).

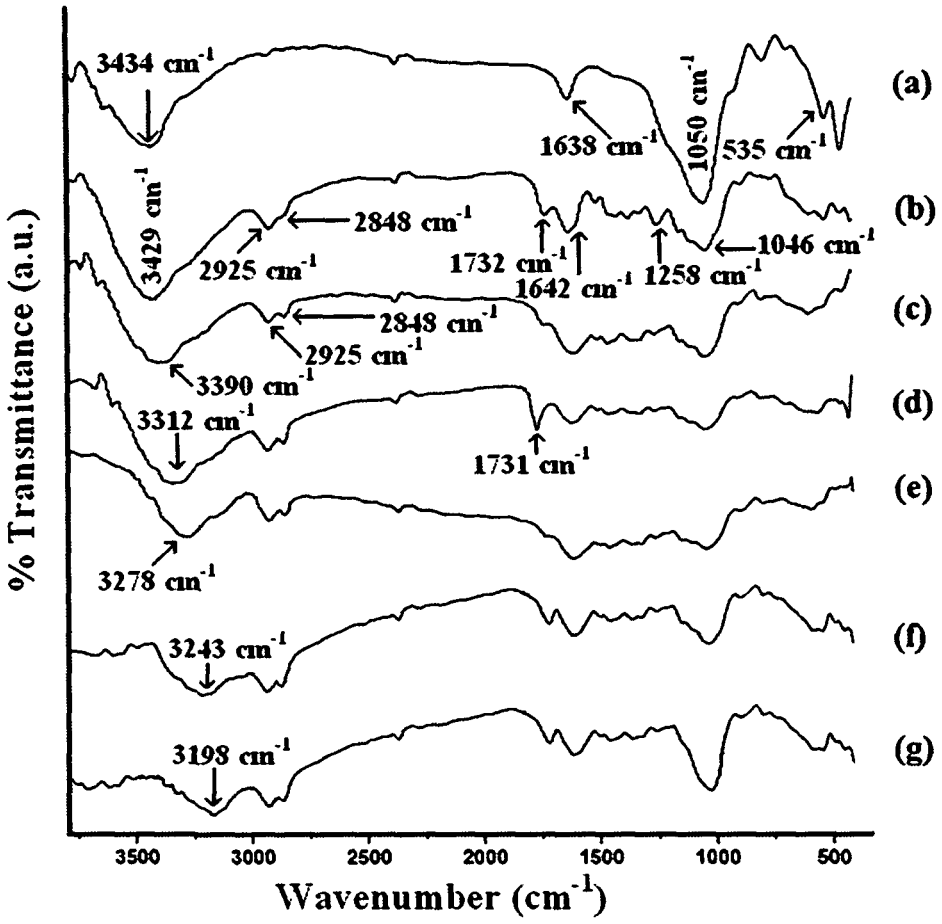

Figure 4.3.3.FTIR spectra of (a) unmodified MMT (b) untreated wood and wood samples treated with(c) MFFA/NMA (d) MFFA/HEMA(e)MFFA/DMDHEU (f) MFFA/(NMA+HEMA+DMDHEU) (g) MFFA/(NMA+HEMA+DMDHEU)/MMT samples.

Figure 4.3.3. (curve c-f) shows the spectra of wood samples treated with MFFA/NMA, MFFA/HEMA, MFFA/DMDHEU and MFFA/(NMA+HEMA+DMDHEU) respectively. In all the cases, the characteristic peaks of wood, MFFA and corresponding crosslinker were found to appear. Figure 4.3.4.g shows the spectrum of wood samples treated with MFFA/(NMA+HEMA+DMDHEU)/MMT. The increase of peak intensity in the range 1050-535 cm^{-1} suggested the incorporation of MMT in the wood/MFFA composite. Moreover, it was observed that the intensity of the hydroxyl group stretching decreased and shifted to 3390 cm^{-1} (curve c), 3312 cm^{-1} (curve d), 3278 cm^{-1} (curve e), 3243 cm^{-1}(curve f) from 3434 cm^{-1} (curve a) of MMT and 3429 cm^{-1} (curve b) of wood. The decrease in

intensity of the hydroxyl group and shifting to lower wavenumber was due to the improvement in interaction between the hydroxyl groups of wood with MFFA and crosslinkers. Similar decrease in hydroxyl peak intensity and shifting to lower wavenumber was reported by Awal et al.[38] while studying the FTIR analysis of wood/polypropylene/maleated polypropylene composite. The presence of MMT in composite further reduced the intensity of hydroxyl peak and shifted it to lower wave number (3198 cm^{-1}). This indicated the participation of hydroxyl group of clay in the crosslinking reaction with wood and MFFA copolymer (curve g). The intensities of peaks at 2926 cm^{-1} and 2848 cm^{-1} assigned for $-CH_2$ stretching of wood (curve a) were also found to increase in WPC (curve b) due to the incorporation of methylene groups of the copolymer and crosslinkers. The improvement in interaction due to addition of MMT to wood polymer composites was investigated and reported by Deka et al. [39].

4.3.4. XRD analysis

Figure 4.3.4.shows the X-ray diffraction pattern of (a) MMT (b) untreated wood (c) MFFA copolymer and wood samples treated with (d) MFFA/(NMA+HEMA+DMDHEU)(e) MFFA/(NMA+HEMA+DMDHEU)/MMT. The diffraction peak of MMT was appeared at $2\theta = 8.2^{\circ}$with a basal spacing of 1.07 nm. This was due to the presence of silicate layers in clay. Since cellulose is the principal component of wood, it shows a wide diffraction peak at $2\theta = 22.9^{\circ}$ due to the crystal plane (002) of cellulose (curve b). A broad peak (curve c) appeared at around $2\theta = 22.4^{\circ}$ (002) was due to polyfurfuryl alcohol present in the MFFA copolymer [40]. A reduction in the intensity of the diffraction peak at $2\theta = 22.9^{\circ}$ was observed in case of the samples treated with MFFA/(NMA+HEMA+DMDHEU) and the peak shifted to 22.7° (curve d). Curve e represents the diffractogram of wood treated with MFFA/(NMA+HEMA+DMDHEU)/MMT samples. With the incorporation of MMT, the intensity of the crystalline peak of cellulose was further found to decrease and shifted to 22.2°. The characteristic diffraction peak of MMT at $2\theta = 8.2^{\circ}$ was also disappeared. Similar results were also reported by Devi et al. [10]. It could be said that either the full expansion of MMT galleries occurred which was not possible to detect by XRD or the MMT layers become delaminated and no crystal diffraction peak appeared. This result indicated that the crystallinity in wood composites decreased and some MMT nano laminae were introduced into the amorphous region of wood cellulose [7].

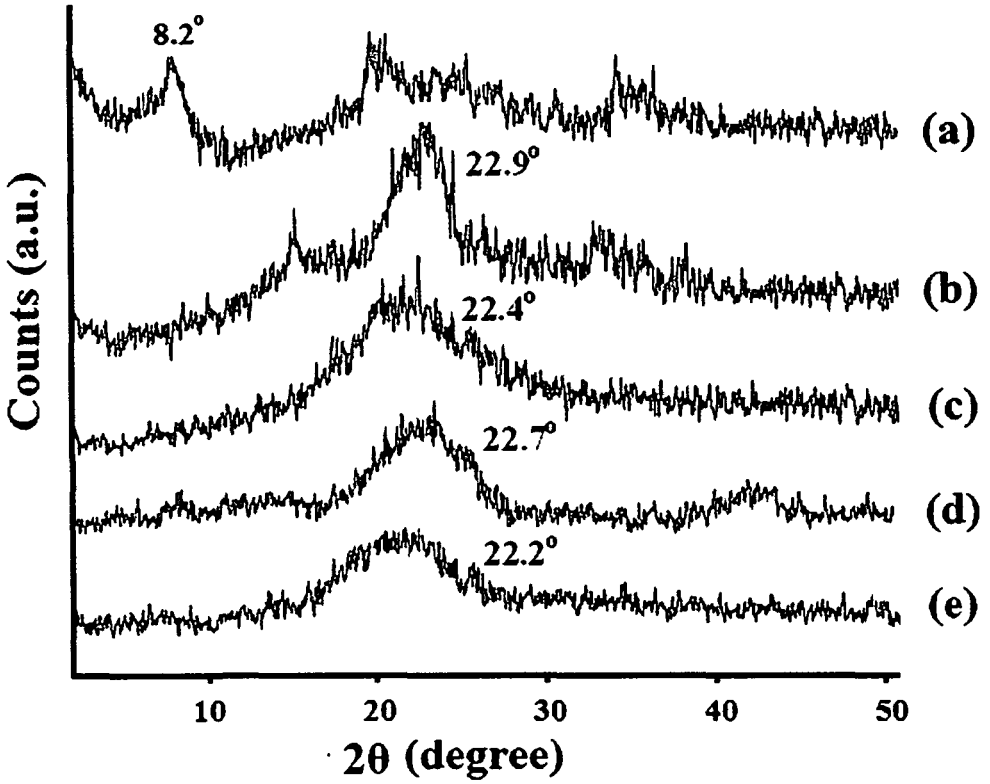

Figure 4.3.4. X-ray diffraction of (a) MMT (b) MFFA (c) untreated wood and wood samples treated with (d) MFFA/(NMA+HEMA+DMDHEU) (e) MFFA/(NMA+HEMA+ DMDHEU)/MMT.

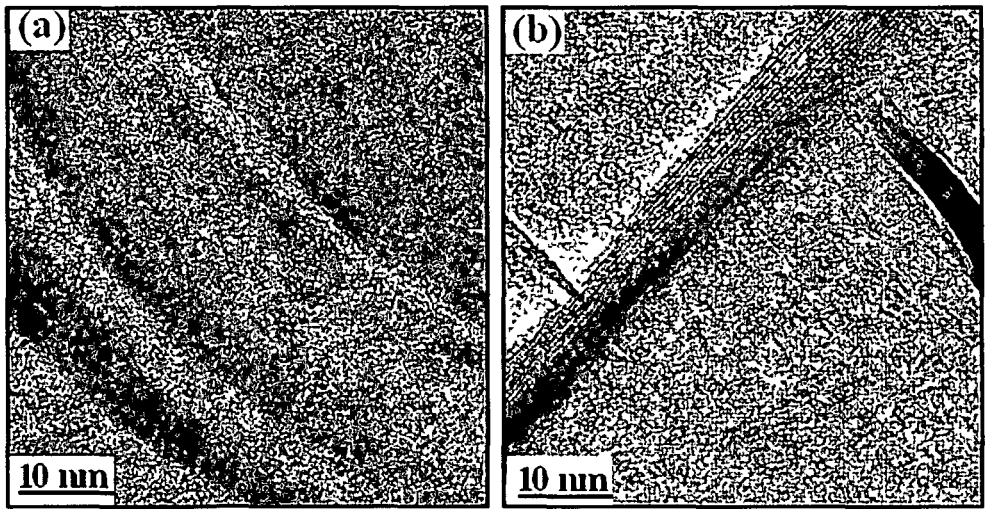

Figure. 4.3.5. Transmission electron micrograph of wood samples treated with (a) MFFA/(NMA+HEMA+DMDHEU)and (b) MFFA/(NMA+HEMA+DMDHEU)/MMT.

4.3.5. Transmission electron microscopy (TEM)

Figure 4.3.5. shows the TEM micrograph of wood samples treated with (a) MFFA/(NMA+HEMA+DMDHEU)and (b) MFFA/(NMA+HEMA+DMDHEU)/MMT. In Figure4.3.5.a, no orientation of the cell wall components could be detected. MMT was dispersed in the MFFA copolymer and in the cell wall of wood indicating the impregnation of MMT into the cell wall (Figure4.3.5.b).

4.3.6. Water uptake and volumetric swelling test

Figure4.3.6. and 4.3.7. shows the water uptake capacity and the effects of swelling in water at room temperature for untreated and treated wood sample.The water uptake capacity was found to increase with the increase in the time of immersion. Untreated wood samples showed highest water absorption capacity (Figure4.3.6.a and4.3.7.a). With the increase in time, the capillaries and void spaces were filled up with water resulting in an increase in water absorption capacity. In treated samples, the void spaces decreased due to deposition of polymers and hence water absorption capacity decreased (Figure4.3.6.b, 4.3.7.b). Further deposition of polymer enhanced due to the presence of crosslinker. The

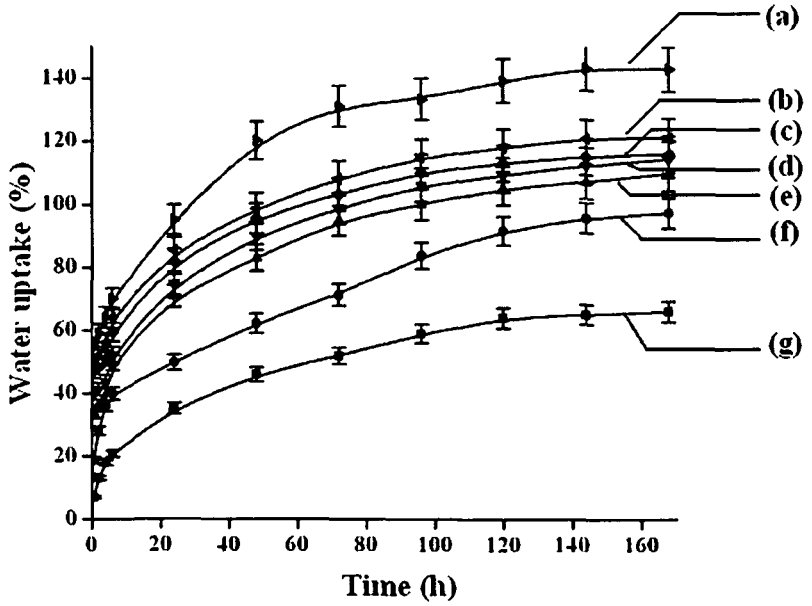

Figure 4.3.6. Water absorption test of (a) untreated wood and wood samples (b) MFFA (c) MFFA/NMA, (d) MFFA/HEMA (e) MFFA/DMDHEU (f) MFFA/(NMA+HEMA+ DMDHEU) (g) MFFA/(NMA+HEMA+DMDHEU)/MMT.

trend of water absorption followed the order: MFFA treated> MFFA/NMA treated>MFFA/HEMA treated> MFFA/DMDHEU treated. DMDHEU would produce maximum crosslinking and NMA would produce minimum crosslinking with wood as explained earlier. Xie et al. [41] prepared wood composites using glutaraldehyde and DMDHEU as crosslinker and reported a higher reduction in water uptake and volumetric swelling. The samples treated with MFFA/(NMA+HEMA+DMDHEU) showed further decrease in water absorption and volumetric swelling due to synergistic effect. A significant decrease in water absorption was noticed after MMT was incorporated into the WPC. The silicate layers of MMT increased the tortuous path for water transport causing a decrease in water absorption [10].

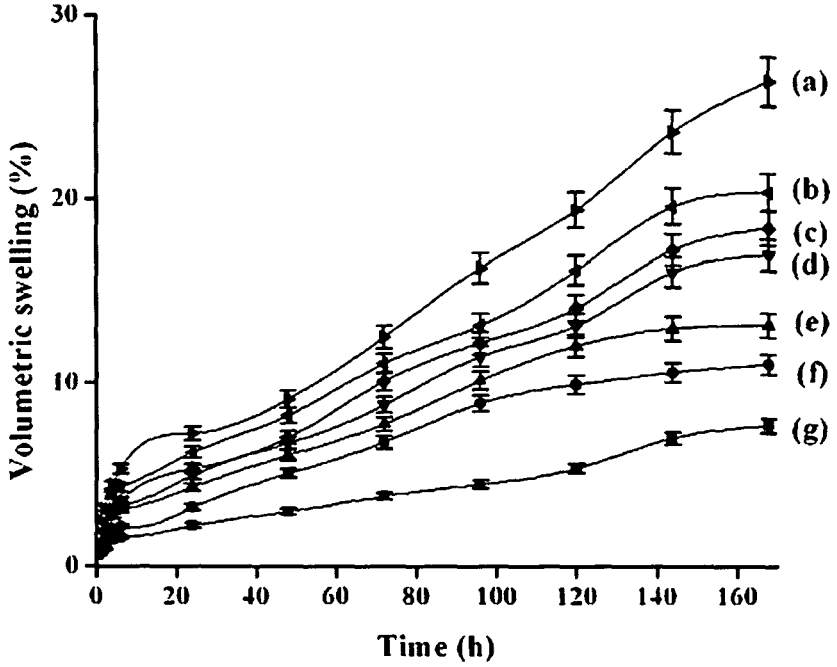

Figure 4.3.7. Volumetric swelling in water at 30°C of wood samples (a) untreated wood and wood samples (b)MFFA(c) MFFA/NMA (d) MFFA/HEMA (e) MFFA/DMDHEU (f) MFFA/(NMA+HEMA+DMDHEU) (g) MFFA/(NMA+HEMA+DMDHEU)/MMT.

4.3.7. Chemical resistance test

Results of the chemical resistance test were shown in Table 4.3.2. Treated samples swelled less in comparison to the untreated samples. The samples treated with MFFA/(NMA+HEMA+DMDHEU)/MMTshowed least swelling. The empty spaces in wood were filled up by the MFFA polymer. The addition of crosslinker formed the network

structure between MFFA copolymer and wood which resulted in a decrease in swelling. Among the single crosslinker treated samples, wood treated with MFFA/DMDHEU samples exhibited maximum improvement in properties followed by the samples treated with MFFA/HEMA and MFFA/NMA samples. Wood samples treated with MFFA/(NMA+HEMA+DMDHEU)showed an enhancement in interfacial adhesion between wood and MFFA copolymer due to synergistic effect. The inclusion of clay enhanced the tortuous path for diffusion of chemicals and as a result swelling decreased. Higher swelling of samples was observed in sodium hydroxide environment compared to acetic acid environment. This might be due to higher interaction of sodium hydroxide with clay layers and wood cellulose [2].

4.3.8. Mechanical properties

The tensile and flexural values of treated and untreated samples were shown in the Table 4.3.3. The samples treated with MFFA/(NMA+HEMA+DMDHEU)produced higher tensile and flexural values compared to those of samples treated with MFFA/NMA, MFFA/HEMA or MFFA/DMDHEU. NMA and HEMA could form bond with the wood and polymer through their hydroxyl groups and double bond. HEMA being a less viscous material and multifunctional monomer would produce more interaction with wood and MFFA polymer compared to NMA. The interaction between wood and MFFA copolymer would be improved due to the presence of four hydroxyl groups in DMDHEU and as a result, MFFA/DMDHEU treated samples exhibited higher tensile and flexural properties than those of either MFFA/NMA or MFFA/HEMA treated samples. Xie et al. [41] found an improvement in mechanical properties of wood samples treated with glutaraldehyde and DMDHEU as crosslinker. Further improvement in mechanical properties was observed after addition of MMT into the combined crosslinker treated MFFA samples. This improvement might be due to the restriction in the mobility of the polymer chains intercalated in between the silicate layers. The improvement in mechanical properties due to the incorporation of nanoclay was reported by Deka and Maji [4].

4.3.9. Limiting oxygen index (LOI)

Limiting oxygen index values of treated and untreated wood are summarized in Table 4.3.4. Treated wood samples show higher LOI values than the untreated ones. The

Table 4.3.2. Chemical resistance test of the WPC samples.

Medium	Time (h)	Volumetric swelling						
		Untreated wood	MFFA treated	MFFA/ NMA treated	MFFA/ HEMA treated	MFFA/ DMDHEU treated	MFFA/ (NMA+ HEMA+ DMDHEU) treated	MFFA/ (NMA+ HEMA+ DMDHEU)/MMT treated
NaOH solution (4%)	24	12.3(±0.3)	8.5 (±0.3)	8.1 (±0.2)	7.6 (±0.5)	6.3 (±0.2)	5.6 (±0.1)	5.2 (±0.9)
	168	14.7 (±0.4)	11.1(±0.7)	10.4 (±0.1)	8.9 (±0.8)	7.8 (±0.4)	6.7 (±0.3)	6.2 (±1.1)
Acetic acid (4%)	24	7.6 (±0.7)	5.7 (±0.8)	5.4 (±0.6)	4.9 (±1.1)	4.3 (±0.8)	3.6 (±0.1)	3.2 (±0.5)
	168	10.1 (±0.8)	6.9 (±0.6)	6.3 (±1.1)	5.8 (±0.3)	5.1 (±1.1)	4.5 (±0.8)	4.1 (±0.3)

Table4.3.3. Flexural and tensile properties of untreated and treated wood.

Sample	Flexural properties		Tensile properties	
	Strength (MPa)	Modulus (MPa)	Strength (MPa)	Modulus (MPa)
Untreated wood	120.4±0.2	6058.1±0.7	41.2±0.62	306.3±15.1
Wood treated with MFFA	124.5±0.7	6123.7±1.1	42.8±1.3	304.3±12.5
MFFA/NMA	125.3±0.4	6365.9±1.1	46.5±1.2	312.1±10.7
MFFA/HEMA	126.8±1.1	6737.2±1.2	48.7±1.1	324.4±13.8
MFFA/DMDHEU	127.9±0.9	7216.3±0.7	51.6±0.5	338.6±11.6
MFFA/NMA+HEMA+DMDHEU	130.7±0.7	7502.6±0.6	57.3±1.4	353.2±14.7
MFFA/(NMA+HEMA+DMDHEU) /MMT	134.2±0.8	7855.8±1.1	59.9±1.2	384.2±15.3

high nitrogen content ofmelamine isresponsible for showinghigher LOI value of MFFA treatedsamples compared to untreated wood samples. The release of oxides of nitrogen on combustion, displacing the oxygen at the surface of the combustible material, appears to be the mechanism of fire control. DMDHEU is also a nitrogen provider and hence it further improved the flame retardancy of MFFA/DMDHEUtreated samples. Wu et al. developed flame retarding systems for cotton consisting of a hydroxy-functional organophosphorus oligomer (FR), carboxylic acid binder, DMDHEU and MF resin .They reported that DMDHEU and MF could act as nitrogen providers and enhance the flame retarding performance of the treated fabric due to phosphorus-nitrogen synergism [42]. It was observed that MFFA/HEMA treated samples showed less LOI value than the MFFA/NMA treated samples. This was due to presence of ester linkage in HEMA which enhanced its flammability. Wood treated with MFFA/(NMA+HEMA+DMDHEU)/MMT showed highest LOI values due to synergistic effect of crosslinkers and presence of silicate layers of MMT. MMT on burning produced an insulating char layer of silicate which provided thermal protection to the virgin polymer and delayed the volatilization of fuel [43]. Further the tortuous path provided by the silicate layer had better barrier property to the oxygen and heat and thus delaying the burning capacity of the composites.

Table 4.3.4. Limiting oxygen indices (LOIs) and flaming characteristics of treated and untreated samples.

Samples	LOI (%)	Flame description	Smokes and fumes	Char
Untreated wood	21	Candle-like localized flame	-	Higher
Wood treated with MFFA	24	Small localized flame	Small and black smoke	Medium
MFFA/NMA	27	Small localized flame	Small and black smoke	Medium
MFFA/HEMA	25	Small localized flame	Small and black smoke	Medium
MFFA/DMDHEU	28	Small localized flame	Small and black smoke	Medium
MFFA/NMA+HEMA+ DMDHEU	30	Small localized flame	Small and black smoke	Medium
MFFA/(NMA+HEMA+ DMDHEU)/MMT	33	Small localized flame	Small and black smoke	Higher

4.3.10. Thermogravimetric analysis

Table 4.3.5.represents the initial decomposition temperature (T_i), maximum pyrolysis temperature (T_m), decomposition temperature at different weight loss (%) (T_D) and residual weight (RW %) for the untreated wood samples and treated wood samples. In all the cases, T_i, T_m, T_D values for treated samples were found to be higher than those of untreated sample. But the thermal stability of MFFA/HEMAtreated samples was found less due to the presence of ester linkage. Higher thermal stability was observed in case of the MFFA/(NMA+HEMA+DMDHEU)treated samples. The thermal stability was further enhanced by the addition of MMT to the MFFA/(NMA+HEMA+DMDHEU)treated samples.

Treatment of wood with polymer and crosslinker will increase its $T_i$value. The increase in T_i value may be attributed to the fact that the crosslinker enhanced the interfacial adhesion between wood and polymer. Among the single crosslinker treated samples, DMDHEU produced maximum improvement in properties due to interaction caused by the

presence of four hydroxyl groups. An enhancement in properties was observed if mixture of crosslinkers was used with wood and MFFAcopolymer. The interfacial adhesion between wood and polymer was more in presence of mixed crosslinkers compared to those of samples treated with single crosslinker alone due to synergistic effect. Awal et al. [38] reported the increase in thermostability of wood after the incorporation of crosslinker. The T_i, T_m and T_D values were found to improve further by the incorporation of MMT and mixture of crosslinkers in MFFA treated system. The silicate layers acted as a barrier and delayed the passage of decomposed volatile products through the composite. The improvement in thermal stability due to the addition of clay in wood/polymer composite was reported by Deka and Maji [4].

The RW(%) value of untreated sample was higher than polymer treated samples. The carbonization of the wood component was responsible for that. RW(%) value decreased on addition of polymer and crosslinker and improved further on addition of MMT due to formation of silicate char by the inorganic clay.

Table 4.3.5. Thermal analysis of wood polymer composite.

Sample	T_i	T_m^a	T_m^b	Temperature of decomposition (T_D) in °C at different weight loss (%)				RW% at 600°C
				20%	40%	60%	80%	
Untreated wood	163	305	393	263	296	328	---	26.7
Wood treated with MFFA	198	320	410	280	312	344	388	7.6
MFFA/NMA	228	330	426	293	324	359	407	8.4
MFFA/HEMA	221	326	418	287	321	356	403	8.0
MFFA/DMDHEU	236	335	429	302	327	364	428	8.5
MFFA/(NMA+HEMA+ DMDHEU)	239	339	431	312	345	372	457	8.9
MFFA/(NMA+HEMA+ DMDHEU)/MMT	242	344	437	318	351	377	563	10.2

T_i: value for initial degradation; ^aT_m: value for 1st step; ^bT_m: value for 2nd step.

4.3.11. Morphological studies

Scanning electron microscope results of untreated and treated wood samples are shown in Figure 4.3.8. Void spaces in untreated wood were seen (Figure 4.3.8.a) and were filled up by the polymer (Figure 4.3.8.b). The polymer and crosslinker adhered to the cell wall could be seen in treated wood samples (Figure 4.3.8.c). The presence of MMT could be detected by some white patches in the micrograph (Figure 4.3.8.d).

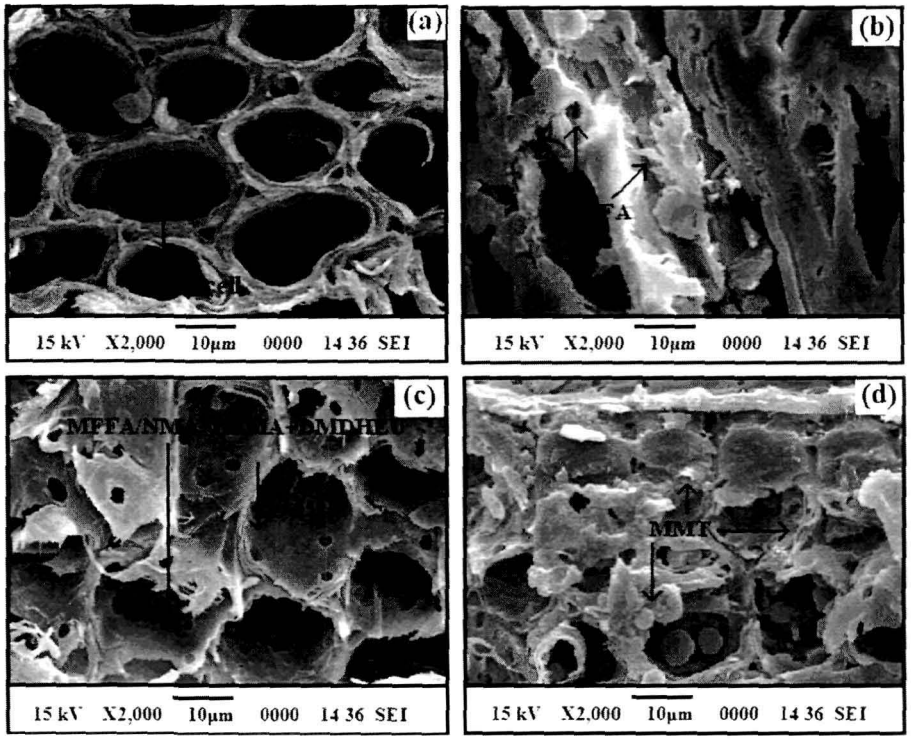

Figure 4.3.8. Scanning electron micrographs of (a) untreated woodand wood treated with (b)MFFA(c) MFFA/(NMA+HEMA+DMDHEU) (d) MFFA/(NMA+HEMA+ DMDHEU)/ MMT.

Section D:Studies on the properties of wood polymer nanocomposites impregnated with melamine formaldehyde-furfuryl alcohol copolymer and nanoclay.

The present investigation has been carried out to prepare WPNC using MFFA copolymer, DMDHEU as crosslinker and nanoclay. Attempts have also been made to study the various properties like water repellency, dimensional stability, chemical resistance,

flammability, mechanical properties, and ultraviolet (UV) resistance of WPNC. The parameters like vacuum, time of impregnation, monomer concentration, initiator concentration, amount of crosslinking agent and nanoclay were varied to get optimum properties. The conditions, at which maximum improvement in properties were obtained, were 500mm Hg vacuum, 6 h time of impregnation, 5:1 (MFFA:FA-water) prepolymer concentration, 1% (w/w) maleic anhydride, 3 mL DMDHEU and 1-3 phr nanoclay.

4.4. RESULTS AND DISCUSSION

4.4.1. Effect of variation of nanoclay concentration on polymer loading (WPG %), volume increase, and hardness

It was observed from Table 4.4.1. that properties like weight percent gain, volume increase, and hardness improved than the untreated samples. Treatment with MFFA copolymer would fill the empty cell lumen, pits and parenchyma present in the wood. The

Table 4.4.1. Effect of variation of nanoclay on polymer loading (WPG %), volume increase and hardness.

Samples particulars	Weight % gain	Volume increase %	Hardness (Shore D)
Untreated		-	46 (±1.07)
Samples treated with MFFA/FA-water/DMDHEU/nanoclay			
100/20/0/0	23.63 (±0.48)	2.11 (±0.37)	57 (±1.08)
100/20/3/0	25.86 (±1.02)	2.15 (±0.54)	60 (±0.82)
100/20/3/1.0	32.88 (±0.96)	2.69 (±0.78)	66 (±0.65)
100/20/3/2.0	38.75 (±1.03)	2.98 (±1.07)	72 (±0.88)
100/20/3/3.0	42.56 (±1.12)	3.31 (±0.97)	74 (±0.38)

hydroxyl and methylol groups present in the prepolymer would interact with the hydroxyl group of wood. DMDHEU is a multifunctional monomer and can interact with both wood and prepolymer through its hydroxyl group. This would lead to an enhancement in

deposition of polymer. Xie et al. prepared wood polypropylene composites by using glutaraldehyde and DMDHEU as crosslinkers and reported that both glutaraldehyde and DMDHEU could crosslink with the cell wall of wood as well as with the polymer [41]. Further improvement in properties was observed on treatment with nanoclay. With the increase in the amount of nanoclay, a remarkable improvement in properties was noticed. This was due to the restriction in mobility of polymer chains in between the silicate layers. Devi and Maji reported an improvement in weight percent gain as well hardness with the increase in amount of nanoclay [10].

4.4.2. Morphological studies

Energy dispersive X-ray spectroscopy (EDS) was employed for investigating the presence of trace amount of clay observed in the fractured surface of the sample. The EDS analysis of composites is shown in Figure 4.4.1. The impregnation of nanoclay into wood was indicated by the presence of C, O, Na, Al, Mg, Si.

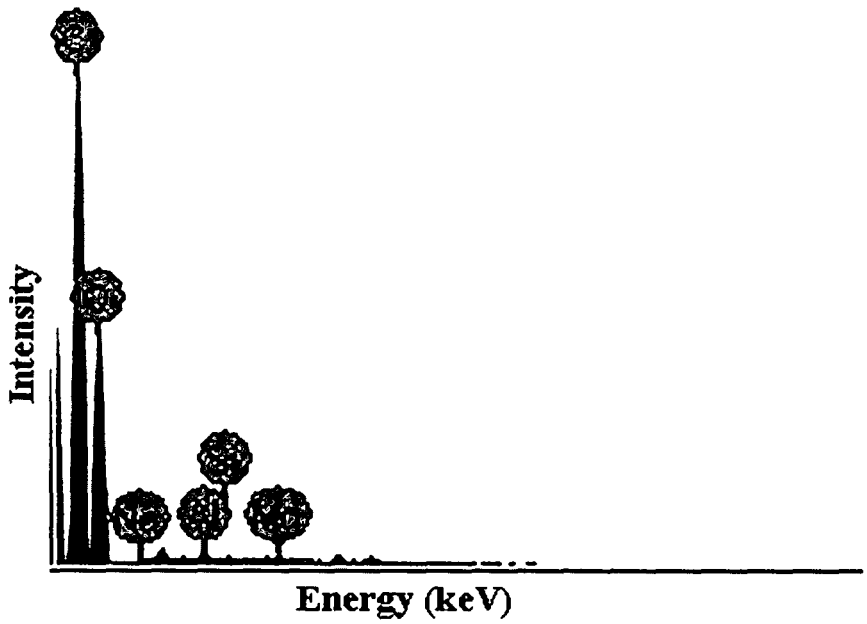

Figure 4.4.1. EDS of MFFA/DMDHEU/nanoclay (3 phr) treated wood samples.

Scanning electron micrographs of the fractured surfaces of the untreated and treated wood samples were shown in Figure 4.4.2. The empty cell lumens observed in untreated wood (Figure 4.4.2.a) were filled by the polymer, crosslinker and nanoclay (Figure 4.4.2.b-d). The presence of nanoclay could be seen from the micrograph as white spots.

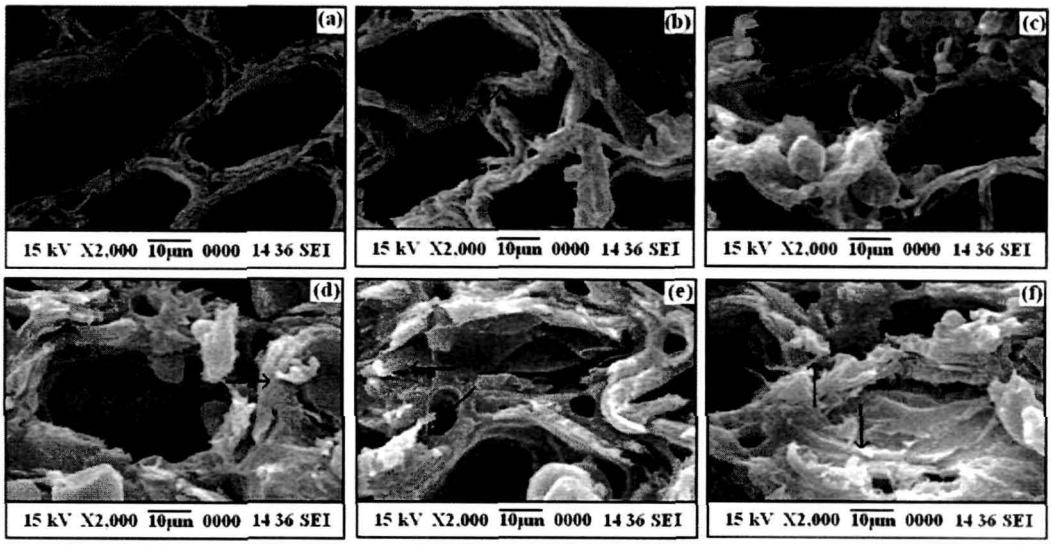

Figure 4.4.2. Scanning electron micrograph of wood samples (a) untreated and treated with (b) MFFA prepolymer (c) MFFA/DMDHEU (d) MFFA/DMDHEU/nanoclay (1.0 phr) (e) MFFA/ DMDHEU /nanoclay (2.0 phr) (f) MFFA/DMDHEU/ nanoclay (3.0 phr).

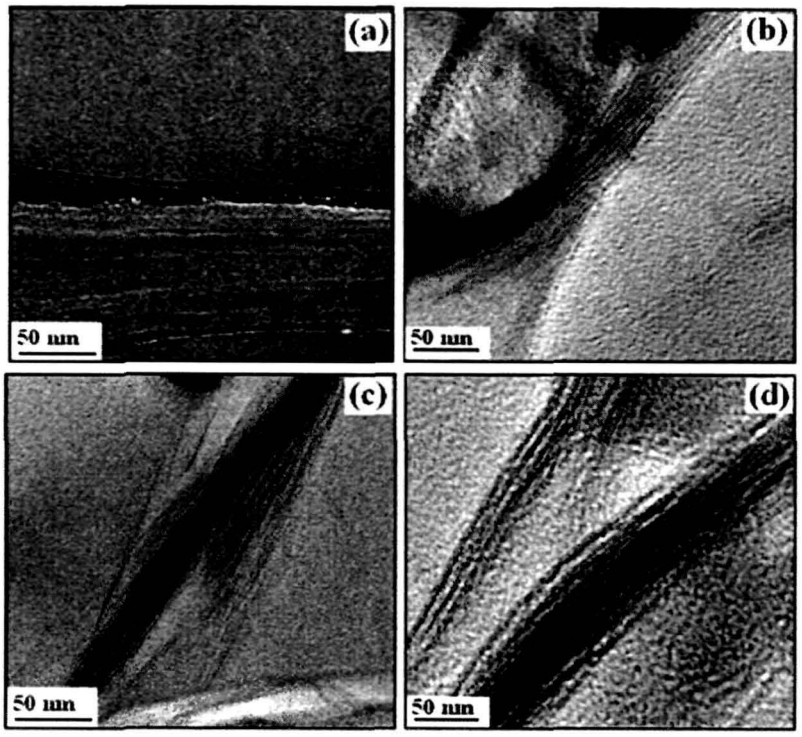

Figure 4.4.3. Transmission electron micrograph of wood samples (a) untreated wood and treated with (b) MFFA/DMDHEU/nanoclay (1.0 phr) (c) MFFA/ DMDHEU/nanoclay (2.0 phr) (d) MFFA/DMDHEU/nanoclay (3.0 phr).

4.4.3. Transmission electron microscopy (TEM)

Figure 4.4.3. represents the TEM micrographs of untreated and treated wood samples. In untreated wood samples, radial fracture patterns perpendicular to the compound middle lamella were observed. No orientation of the cell wall components could be detected. In case of samples treated with MFFA/DMDHEU/nanoclay (1phr), MFFA/DMDHEU/nanoclay (2phr) MFFA/DMDHEU/nanoclay (3phr) (Figure 4.4.9.b-d) treated samples; it was observed that an even dispersion of nanoclay occurred. The dispersion became more homogenous at higher percentage of loaded nanoclay indicating the successful impregnation of nanoclay into wood.

4.4.4. FTIR study

Figure 4.4.4. represents the FTIR spectra of nanoclay, MFFA and DMDHEU. Curve a represents the absorbance spectrum of nanoclay where peaks appeared at 3466 cm^{-1} for –OH stretching, 2929 and 2854 cm^{-1} for –CH stretching of modified hydrocarbon, 1620 cm^{-1} for –OH bending, 1032–459 cm^{-1} for oxide bands of metals like Si, Al, Mg, etc. Peaks at 3404, 2926, 2851, 1566 and 1510, 1186 and 811 cm^{-1} were assigned to -OH stretching, aliphatic –CH asymmetric stretching, -CH symmetric stretching, furan ring vibration, C-N stretching and out plane trisubstitution of triazine ring respectively for MFFA (curve b) [15]. The spectrum of DMDHEU (curve c) showed peaks at 3416, 1700, 1244 and 1019 cm^{-1} which could be assigned for -OH stretching, C=O stretching, -CHOH stretching, $-CH_2OH$ stretching respectively [37].

Figure 4.4.5.represents the FTIR spectra of (a) untreated and treated with (b) MFFA/DMDHEU (c) MFFA/DMDHEU/nanoclay (1 phr) (d) MFFA/DMDHEU/nanoclay (2 phr) (e) MFFA/DMDHEU/nanoclay (3 phr). Absorbance for the untreated wood samples appeared at 3441 cm^{-1}(–OH stretching), 2927cm^{-1} and 2846cm^{-1}(–CH_2 asymmetric stretching), 1736 cm^{-1}(C=O stretching), 1643 cm^{-1}(–OH bending), 1256 cm^{-1} and 1045 cm^{-1}(C–O stretching) and 1002–643 cm^{-1}(out of plane C–H bending vibration). In the curves b-e there was a shifting and decrease in intensity of the hydroxyl peak which was due to interaction of wood, MFFA, DMDHEU and nanoclay. The peak shifted from 3441 cm^{-1} (curve a) to 3403 cm^{-1} (curve b), 3364 cm^{-1} (curve c), 3330 cm^{-1} (curve d), 3288 cm^{-1} (curve e). Furthermore, the peak intensity at 2927cm^{-1} and 2846 cm^{-1} for -CH stretching were more pronounced in the nanoclay treated composites compared to that in the untreated wood. The

presence of characteristic peak of MFFA and nanoclay in wood/MFFA/DMDHEU/nanoclay composite indicated successful impregnation of MFFA and clay into wood.

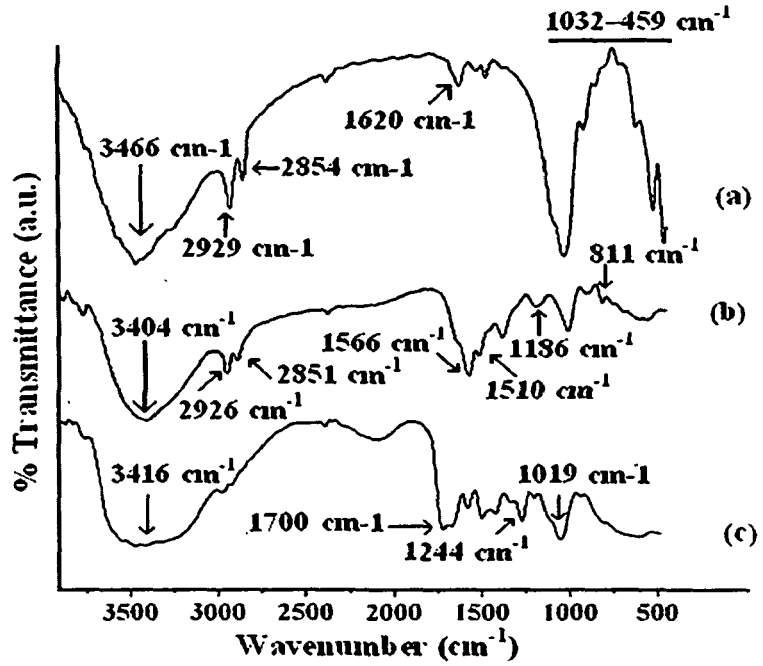

Figure 4.4.4. FTIR spectra of (a) nanoclay (b) MFFA (c) DMDHEU.

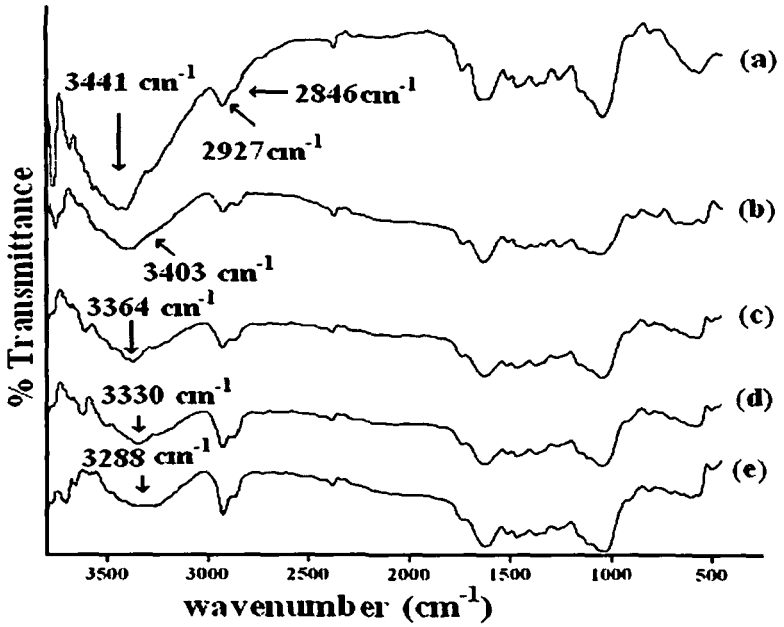

Figure 4.4.5. FTIR spectra of (a) untreated wood and treated with (b) MFFA/DMDHEU (c) MFFA/DMDHEU/nanoclay (1 phr) (d) MFFA/DMDHEU/nanoclay (2 phr) (e) MFFA/DMDHEU/nanoclay (3 phr).

4.4.5. XRD study

Figure 4.4.6. shows the XRD diffractogram of (a) nanoclay (b) MFFA/DMDHEU /nanoclay polymer composite (c) untreated wood and wood treated with (d) MFFA/DMDHEU/nanoclay (1 phr) (e) MFFA/DMDHEU/nanoclay (2 phr) (f) MFFA/DMDHEU/nanoclay (3 phr) respectively. The organically modified nanoclay (curve a) shows a sharp peak at $2\theta = 4.3^{\circ}$. The gallery distance was calculated using Bragg's equation and found to be 2.05 nm. For MFFA/DMDHEU/nanoclay composite (curve b), the sharp peak of the organically modified clay disappeared and a broad peak due to MFFA copolymer was appeared at 22.51° [40]. This suggested that either the full expansion of interlayers of nanoclay occurred which was not possible to detect or the nanoclay layers

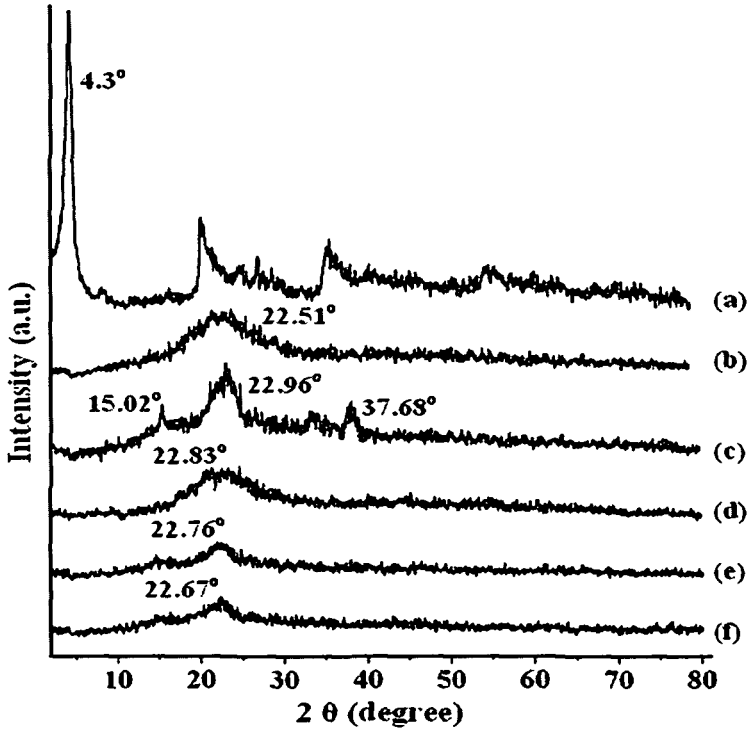

Figure 4.4.6.X-ray diffraction of (a) nanoclay (b) MFFA/DMDHEU /nanoclay polymer composite (c) untreated wood (d)/MFFA/DMDHEU/nanoclay (1 phr) treated (e) MFFA/DMDHEU/nanoclay (2 phr) treated (f) MFFA/DMDHEU/nanoclay (3 phr) treated wood samples.

become delaminated and no crystal diffraction peak appeared [2]. Untreated wood shows a wide diffraction peak at 22.96° due to the (002) crystal plane of cellulose. Other small peaks appearing at 37.68° and 15.02° were assigned to the 040 crystal plane of cellulose

andamorphous region of cellulose respectively. WPNC containing modified nanoclay showed a decrease in the intensity of the peak at 22.96°. A reduction in intensity as well as shifting of the peak corresponding to 002 crystal plane of cellulose (curve d-f) to lower angles was observed in the composites. Further the peaks appearing at 37.68° and 15.02° became dull [19].Therefore, it could be concluded that crystallinity in wood decreased and some delaminated nanoclay was introduced into the amorphous region of wood cellulose.

4.4.6.Crystallinity determination from FTIR and XRD

Table 4.4.2.shows the crystallinity index values of untreated and treated wood samples. Among the different functions used for analysis of the diffraction peaks, fitting the curves with the Voigst functions resulted in the best fit [44]. The treated wood samples with 3 phr nanoclay showed the least value of cellulose crystallinity index while the highest value was shown by the untreated wood. The structures of crystallites of wood cellulose became nebulous as chemical grafting reaction occurred in wood. MFFA, DMDHEU, nanoclay break the intermolecular and intra molecular hydrogen bonds of cellulose as they participated in the bond formation with the wood cellulose thereby lowering the rigidity of cellulose of wood [45]. The chemical grafting reaction occurred in the amorphous region of wood cellulose since the distribution of polymer chains in the crystallites region of cellulose was difficult [46]. Some hydrogen bonds were ruptured and the cellulose chains were opened up as the polymer chains reacted on the surface of the crystallites. With the progress of the reaction, more amorphous cellulose was produced. Both FTIR and XRD were employed to determine the crystallinity index values and the results found were in good agreement with each other. Thus, the treated wood samples showed lower values of crystallinity index than the untreated wood samples.

4.4.7. UV resistance

The crystallinity index values were found to decrease for both the untreated and treated wood samples after UV exposure as shown in Table 4.4.2. The values were calculated from FTIR spectra on exposure to UV rays for different time period. It was observed that the rate of decrease of crystallinity index was less pronounced in treated wood than the untreated wood. MFFA/DMDHEU interacted with the hydroxyl group of cellulose forming a crosslinked structure. Nanoclay prevented photodegradation process by acting as a

screen for the UV rays. Thus the crystallinity of the composite was least affected by the UV irradiation.

Table 4.4.2. Crystallinity index values of cellulose matrix of untreated and treated wood samples calculated by the area method before and after UV exposure.

Samples		Untreated wood	MFFA/ DMDHEU treated	MFFA/ DMDHEU/ nanoclay (1phr) treated	MFFA/ DMDHEU/ nanoclay (2phr) treated	MFFA/ DMDHEU/ nanoclay (3phr) treated
XRD results	Before	62.23	54.35	48.87	46.67	43.45
FTIR results	irradiation	62.97	53.45	48.37	45.97	43.88
	After irradiation					
	10 days	59.33	51.78	46.87	45.11	42.99
	20 days	57.75	49.12	45.93	44.64	42.34
	30 days	55.43	47.48	45.04	43.85	41.86
FTIR	40 days	51.21	46.84	44.32	43.03	41.47
results	50 days	47.24	46.01	43.72	42.67	41.10
	60 days	44.86	45.46	42.89	42.14	40.56

Both untreated and treated wood samples on exposure to UV irradiation for different time periods showed an early increase in weight due to moisture gain and weight loss in the later part as per expectation(Figure 4.4.7.). The material loss induced by the degradation was lower than the early increase in weight loss. Highest weight loss was shown by the untreated wood samples. The rate of weight loss decreased with the increase in the amount of nanoclay.

The change of carbonyl index value with time is shown in Figure 4.4.8. After 60 days of exposure to an UV environment, an increase in carbonyl index value was shown by both the untreated and treated wood samples. Untreated wood samples showed highest value of carbonyl index followed by the treated ones due to higher oxidation of cellulose of wood. Chain scission of the polymer and wood was responsible for the increase in the value for

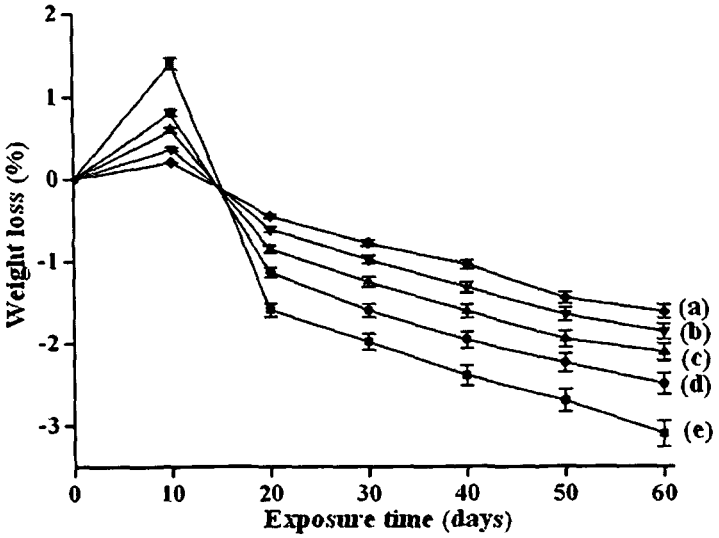

Figure 4.4.7. Weight losses versus exposure time of (a) MFFA/DMDHEU/nanoclay (3 phr) treated (b) MFFA/DMDHEU/nanoclay (2 phr) treated (c) MFFA/DMDHEU/nanoclay (1 phr) treated (d) MFFA/DMDHEU treated (e) untreated wood samples.

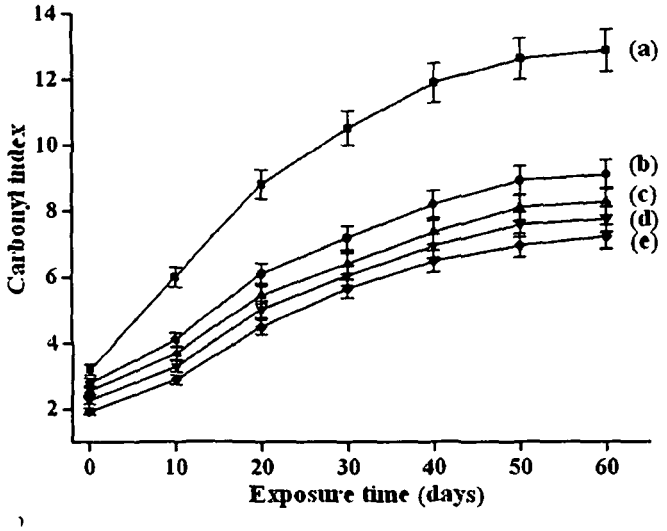

Figure 4.4.8. Carbonyl index values of (a) untreated wood and treated with (b) MFFA/DMDHEU (c) MFFA/DMDHEU/nanoclay (1 phr) (d) MFFA/DMDHEU/ nanoclay (2 phr) (e) MFFA/DMDHEU/nanoclay (3 phr).

carbonyl index. The polymer chain scission lowers the density of entanglements of polymer decreasing the weight of the samples. Wood samples treated with MFFA/DMDHEU delayed the photodegradation process as DMDHEU could form crosslinked structure through its hydroxyl groups with the cellulose thereby lowering the carbonyl index value. Further lowering of carbonyl index values was observed on addition of nanoclay. Nanoclay could stabilize the composites by shielding the composites from UV rays. Higher the amount of

nanoclay lower was the carbonyl index value. Grigoriadou et al. reported an increase in UV stability on addition of montmorillonite clay in high density polyethylene [47].

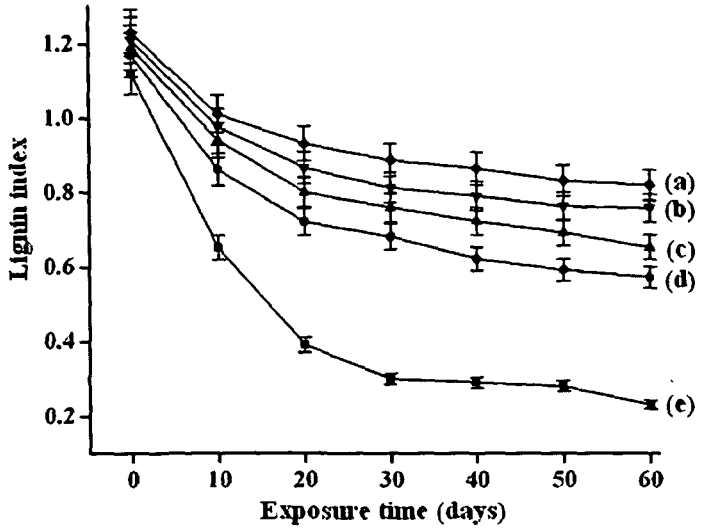

Figure 4.4.9. Lignin index values of wood treated with (a) MFFA/DMDHEU/nanoclay (3 phr) (b) MFFA/DMDHEU/nanoclay (2 phr) (c) MFFA/DMDHEU/nanoclay (1 phr) (d) MFFA/DMDHEU (e) untreated wood samples.

The lignin index values with time for untreated and treated wood samples are shown in Figure 4.4.9. Addition of nanoclay acted as a screen for the composites and it inhibited the photodegradation of lignin from the formation of quinones, carbonyls or peroxides.Untreated wood samples showed lower lignin index values than the treated ones and the values decreased with the increase in UV exposure time.A similar decrease in the lignin index values on exposure to UV radiation was observed for the ionic liquid treated wood [48].

Scanning electron micrographs of UV degraded samples after 60 days of exposure to UV rays are shown in Figure 4.4.10.Photo degradation occurred and the surface morphology of the samples changed due to exposure to UV radiation. Untreated wood samples showed cracks on its surfaces. The treated samples with MFFA/DMDHEU enhanced the interfacial interaction lowering the formation of cracks on the surface. Addition of nanoclay to MFFA/DMDHEU increased its surface smoothness by protecting it from UV rays.

The changes in mechanical properties after 60 days of UV exposure are presented in Table 4.4.3.WPC treated with nanoclay showed less reduction in mechanical properties while highest loss was observed in the case of untreated wood. With the increase in the

amount of nanoclay, the rate of loss of mechanical properties was found to decrease due to UV screening effect provided by nanoclay.

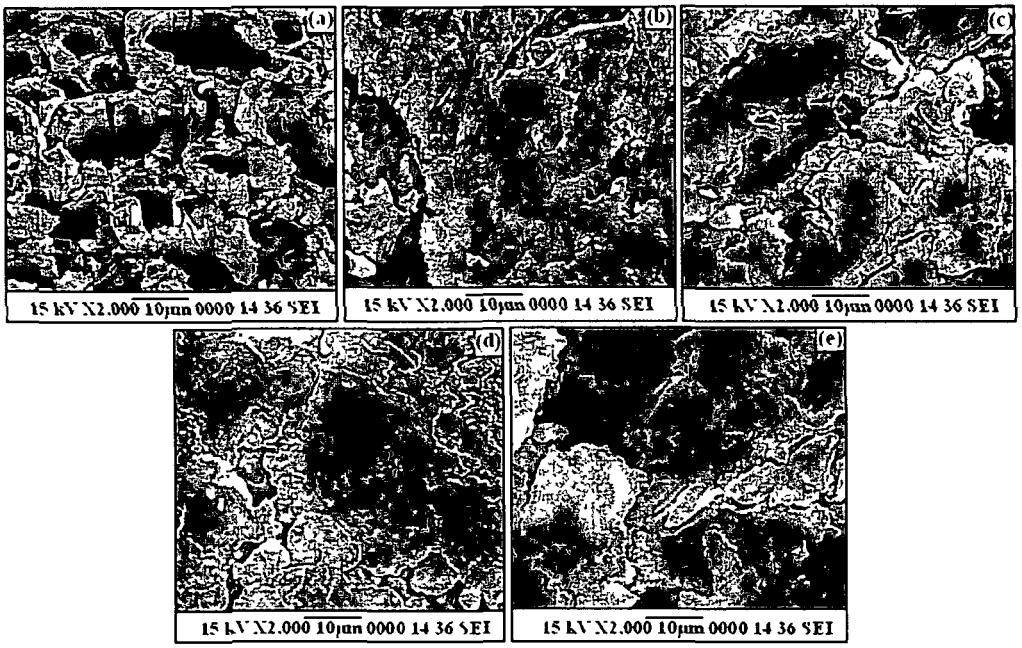

Figure 4.4.10. SEM micrographs of UV treated samples after 60 days (a) untreated wood and treated with(b) MFFA/DMDHEU (c) MFFA/DMDHEU/nanoclay (1 phr) (d) MFFA/DMDHEU/nanoclay (2 phr) (e) MFFA/DMDHEU/nanoclay (3 phr).

4.4.8. Mechanical properties

Table 4.4.3. represents the tensile and flexural properties of untreated and treated wood samples. Treated samples exhibited higher tensile and flexural values than the untreated ones. Melamine formaldehyde resin is one of the stiffest polymeric resins and is known to enhance greatly the mechanical properties [28].Addition of DMDHEU to MFFA copolymer would enhance the mechanical properties of the prepared composites as DMDHEU could crosslink with the wood cellwall and polymer [41].The values were found to increase further when modified nanoclay was added to the wood/MFFA/DMDHEU composite. There was a remarkable improvement in mechanical properties with the increase in the amount of nanoclay. The obtained higher values were due towell dispersed silicate layers that fasten the polymer chains in its gallery and thereby restricted its mobility [4].

Table 4.4.3. Flexural and tensile properties of untreated and treated wood before and after UV degradation.

Sample	Flexural properties				Tensile properties			
	Before degradation		After degradation		Before degradation		After degradation	
	Strength (MPa) (±SD)	Modulus (MPa) (±SD)	Strength (MPa) (±SD)	Modulus (MPa) (±SD)	Strength (MPa) (±SD)	Modulus (MPa) (±SD)	Strength (MPa) (±SD)	Modulus (MPa) (±SD)
Untreated wood	117.69 (±1.49)	5936.76 (±3.47)	100.43 (±0.86)	5017.84 (±0.58)	40.73 (±1.67)	303.76 (±7.33)	30.37 (±0.65)	223.76 (±10.12)
Wood treated with MFFA	125.55 (±1.60)	6337.57 (±2.09)	113.64 (±1.23)	5677.85 (±1.34)	43.63 (±2.18)	322.80 (±7.07)	35.78 (±1.64)	263.61 (±12.13)
MFFA/DMDHEU	128.50 (±0.80)	7237.69 (±1.71)	118.97 (±1.47)	6009.68 (±0.86)	50.62 (±3.13)	376.69 (±8.20)	43.45 (±0.73)	290.98 (±9.54)
MFFA/DMDHEU/nanoclay (1 phr)	135.53 (±1.62)	7642.52 (±1.74)	127.74 (±1.86)	6443.72 (±0.95)	58.58 (±1.70)	439.52 (±7.90)	52.43 (±0.84)	386.29 (±8.32)
MFFA/DMDHEU/nanoclay (2 phr)	138.87 (±1.55)	7831.55 (±3.25)	131.65 (1.43)	6640.95 (±1.53)	62.58 (±2.53)	465.66 (±3.23)	57.67 (±1.56)	424.90 (±11.76)
MFFA/DMDHEU/nanoclay (3 phr)	139.78 (±0.74)	7882.67 (±1.66)	133.87 (1.17)	6752.94 (±2.12)	65.61 (±4.71)	486.43 (±9.00)	61.78 (±0.75)	455.18 (±7.87)

4.4.9. Water uptake study

The water uptake capacities of untreated and treated wood samples are shown in Figure 4.4.11.Untreated wood samples had the highest water absorption capacity (curve a). When the wood samples were impregnated with MFFA copolymer, its water absorption capacity had decreased (curve b). The empty spaces of wood were occupied by the water repellent copolymer MFFA. Water absorption capacity of wood decreased on addition of DMDHEU with MFFA (curve c). The presence of four hydroxyl groups in DMDHEU was responsible for showing the lower water uptake capacity. The hydroxyl groups could form a crosslinked structure with the wood and the polymer through their hydroxyl groups resulting in a decrease in water absorption capacity [49]. Addition of nanoclay would further decrease its water uptake capacity further. Higher the amount of nanoclay, lower was the water uptake capacity of the wood samples (curve d-f). The clay layers acted as a barrier for the diffusion of water molecules and provided a convoluted path for water transportation through the composite [9]. In all the cases, the water uptake of the samples decreased with the increase in the time of immersion.

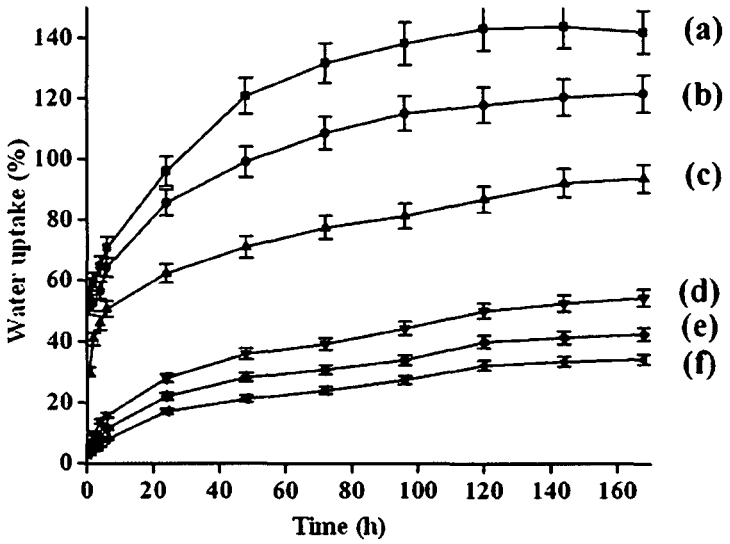

Figure 4.4.11. Water absorption test of wood (a) untreated and treated with (b) MFFA prepolymer (c) MFFA/DMDHEU (d) MFFA/DMDHEU/nanoclay (1.0 phr) (e) MFFA/ DMDHEU /nanoclay (2.0 phr) (f) MFFA/ DMDHEU/ nanoclay (3.0 phr).

4.4.10. Water-repellent effectiveness (WRE) study

Related results are shown in Table 4.4.4.Highest water repellency was exhibited by the samples treated with MFFA/DMDHEU/nanoclay (3 phr). The reason would be same as stated earlier.

Table 4.4.4. Water repellant effectiveness (WRE %) of WPC.

Time (h)	MFFA treated	MFFA/ DMDHEU treated	MFFA/ DMDHEU/ nanoclay (1.0 phr) treated	MFFA/ DMDHEU/ nanoclay (2.0 phr) treated	MFFA/ DMDHEU/ nanoclay (3.0 phr) treated
0.5	43.72 (±0.65)	65.17(±0.45)	81.22 (±1.09)	85.13 (±0.53)	89.11 (±0.68)
2	41.44 (±0.38)	55.64(±0.55)	75.32 (±0.75)	79.89 (±0.75)	84.58 (±0.76)
4	38.77 (±0.45)	48.37(±0.32)	73.64 (±0.87)	76.24 (±0.36)	80.96 (±0.48)
6	35.63 (±0.21)	44.25(±0.83)	71.66 (±0.54)	74.38 (±1.12)	78.62 (±0.74)
24	33.54 (±0.67)	36.58(±0.27)	69.36 (±0.73)	72.13 (±0.71)	77.51 (±1.05)
48	30.13 (±0.49)	30.81(±0.74)	68.63 (±0.95)	71.09 (±0.46)	75.83 (±0.94)
72	26.36 (±0.87)	29.62(±0.19)	68.28 (±0.42)	70.67 (±0.93)	74.67 (±0.54)
96	24.52 (±0.99)	25.46(±0.35)	67.87 (±0.34)	70.25 (±0.43)	74.35 (±0.47)
120	23.74 (±0.42)	24.67(±0.58)	67.41 (±1.14)	69.78 (±0.62)	73.76 (±0.75)
144	22.36 (±0.81)	24.26(±0.61)	66.93 (±0.88)	69.36 (±0.82)	72.95 (±0.41)
168	21.91 (±0.53)	23.64(±0.39)	66.54 (±1.07)	68.69 (±0.33)	72.33 (±0.58)

4.4.11. Dimensional stability test

4.4.11.1. Swelling in water

The effect of swelling in water at room temperature for both treated and untreated samples are shown in Figure 4.4.12. Hydrophilic nature of wood was responsible for more swelling of untreated wood. Deposition of hydrophobic prepolymerin the void space and cell lumen of wood would decrease the swelling of wood. Further DMDHEU could crosslink with the cellwall of wood and the polymer resulting in enhanced dimensional stability [41]. Treatment of the WPC samples with modified nanoclay would decrease its swelling further. The layers of silica restricted the diffusion of water molecules through the composite.

Higher the amount of nanoclay, higher was the restriction in diffusion of water molecules. As a result shrinking and swelling of wood cell wall would be less and an improvement in dimensional stability was observed.

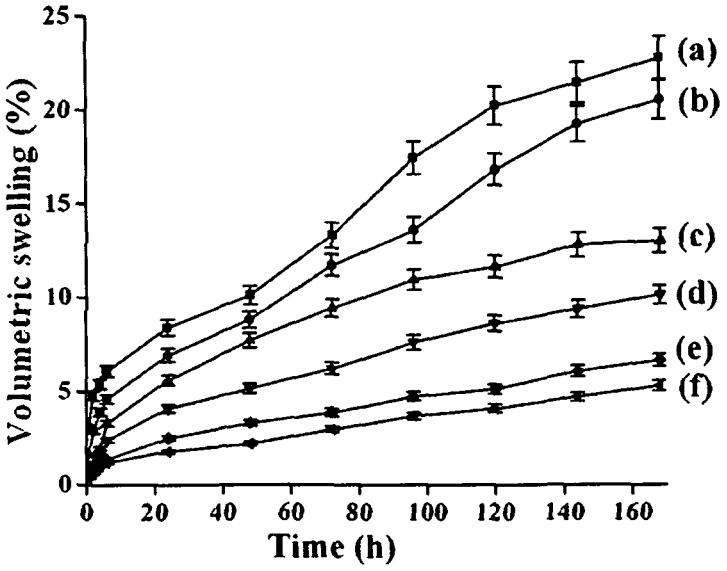

Figure 4.4.12. Volumetric swelling in water at 30°C of wood samples (a) untreated and treated with (b) MFFA prepolymer (c) MFFA/DMDHEU (d) MFFA/DMDHEU/nanoclay (1.0 phr)(e) MFFA/ DMDHEU /nanoclay (2.0 phr) (f) MFFA/ DMDHEU/ nanoclay (3.0 phr).

4.4.11.2. Antiswelling efficiency

Related results are shown in Table 4.4.5.Highest antiswelling efficiency was shown by the samples treated with MFFA/DMDHEU/nanoclay (3 phr). The reason would be similar to that of stated earlier.

4.4.12. Chemical resistance test

The results of the swelling of the samples in 4% acetic acid and 4% NaOH solution are shown in Table 4.4.6. Impregnation of the samples with MFFA and DMDHEU would occupy the empty pits and parenchymas of wood. So treated samples swelled less compared to the untreated ones. It was observed that incorporation of nanoclay into samples treated with MFFA/DMDHEU decreased the swelling. A further decrease in swelling of the composite was noticed with the increase in the amount of clay. Clay layers provided a meandering path for chemicals diffusivity through the composite. In all the cases, the swelling was less in acetic acid compared to sodium hydroxide solution. This may be

possibly due to the increase in interaction by sodium hydroxide with wood cellulose and clay layers [2].

Table 4.4.5.ASE (%) of treated wood samples at different time period.

Time (h)	MFFA treated	MFFA/ DMDHEU treated	MFFA/ DMDHEU/ nanoclay (1.0 phr) treated	MFFA/ DMDHEU/ nanoclay (2.0 phr) treated	MFFA/ DMDHEU/ nanoclay (3.0 phr) treated
0.5	67.38(±0.47)	70.72(±0.42)	78.23 (±0.75)	80.56 (±0.32)	85.23 (±0.46)
2	66.46(±0.65)	69.34(±0.53)	77.54 (±0.43)	79.32 (±0.84)	84.46 (±0.23)
4	65.78 (±1.10)	67.96(±0.72)	76.72 (±1.08)	78.64 (±0.36)	83.82 (±0.68)
6	65.65 (±0.73)	67.67(±0.38)	76.58 (±0.27)	78.35 (±0.54)	83.69 (±0.77)
24	65.23 (±0.82)	67.41(±0.74)	76.38 (±0.51)	78.21 (±0.35)	83.56 (±0.18)
48	64.54 (±0.28)	67.28(±0.68)	76.26 (±0.93)	78.05 (±0.72)	83.32 (±0.47)
72	64.61 (±0.49)	67.08(±0.61)	76.11 (±0.74)	77.67 (±0.47)	83.21 (±1.12)
96	64.34 (±0.66)	66.52(±0.87)	75.88 (±0.65)	77.52 (±0.27)	83.14 (±0.09)
120	63.83 (±0.14)	66.39(±0.69)	75.63 (±0.76)	77.38 (±0.87)	82.92 (±0.51)
144	63.68 (±0.42)	66.26(±0.37)	75.49 (±0.35)	77.23 (±0.34)	82.78 (±0.33)
168	63.37 (±0.63)	66.18(±0.43)	75.32 (±0.86)	77.14 (±0.91)	82.63 (±0.73)

4.4.13. Limiting oxygen index (LOI)study

Table 4.4.6.shows the LOI values of untreated and treated wood samples. Treatment of the samples with MFFA copolymer would lead to higher LOI values compared to the virgin wood. Nitrogen present in MFFA released its oxides on combustion and hence displaced the oxygen present on the surface of the samples. Addition of DMDHEU would further increase its LOI values since it was also another supplier of nitrogen [42]. Samples treated with MFFA/DMDHEU/nanoclay showed substantial improvement in LOI values. It was observed that with the increase in the amount of nanoclay, the LOI values of the samples also increased. The silicate layers would barricade the oxygen and heat thereby delaying the flaming ability of the composites. Further, the silicate layers of nanoclay on burning produced char which would insulate the burning material and thus provided flame resistance to the composites [25].

Table 4.4.6. Chemical resistance and LOI test of the untreated and treated wood samples.

		Volumetric swelling					
Medium	Time (h)	Untreated	MFFA treated	MFFA/ DMDHEU treated	MFFA/ DMDHEU/ nanoclay (1.0 phr) treated	MFFA/ DMDHEU/ nanoclay (2.0 phr) treated	MFFA/ DMDHEU/ nanoclay (3.0 phr) treated
NaOH solution (4%)	24	12.12 (±0.63)	7.96 (±0.68)	5.98 (±0.92)	4.06 (±1.03)	3.78 (±0.45)	3.64 (±0.96)
	168	13.34 (±0.86)	10.57 (±0.73)	8.02 (±0.78)	5.34 (±0.81)	4.87 (±1.01)	4.48 (±0.52)
Acetic acid (4%)	24	8.27 (±0.49)	5.76 (±0.28)	4.68 (±0.54)	2.99 (±0.64)	2.76 (±0.19)	2.44 (±1.12)
	168	11.41 (±0.85)	6.59 (±0.66)	5.47 (±0.39)	3.88 (±0.57)	3.68 (±0.33)	3.32 (±0.67)
LOI (%) (±SD)		20 (±1.12)	23 (±0.87)	27 (±0.95)	31 (±0.67)	34 (±1.05)	36 (±0.58)

4.4.14.Dynamic mechanical analysis

4.4.14.1. Storage modulus and loss modulus

Figure 4.4.13.represents the storage modulus of untreated and treated wood samples. With the increase in temperature, the storage modulus was found to decrease because of increased chain mobility of the wood cell wall polymeric components [50]. The viscoelastic behavior of wood was responsible for steep decrease of E' values near the glass transition temperature (T_g) of wood (50-120°C). It was observed that higher storage modulus was shown by the samples treated with MFFA/DMDHEU. The methylol and hydroxyl group present in the MFFA copolymer interacted with the hydroxyl group of the polymeric constituents of the cell wall of wood. DMDHEU facilitated the deposition of polymer by enhancing the interaction between wood and MFFA through its hydroxyl groups. The better the interfacial interaction, the higher is the stress transfer at the interface [9].Samples treated with MFFA/DMDHEU/nanoclay (3phr) further improved the value of storage modulus. The polymer chains were intercalated in between the silicate layers of nanoclay resulting in stiffening of the composites and improvement in properties.

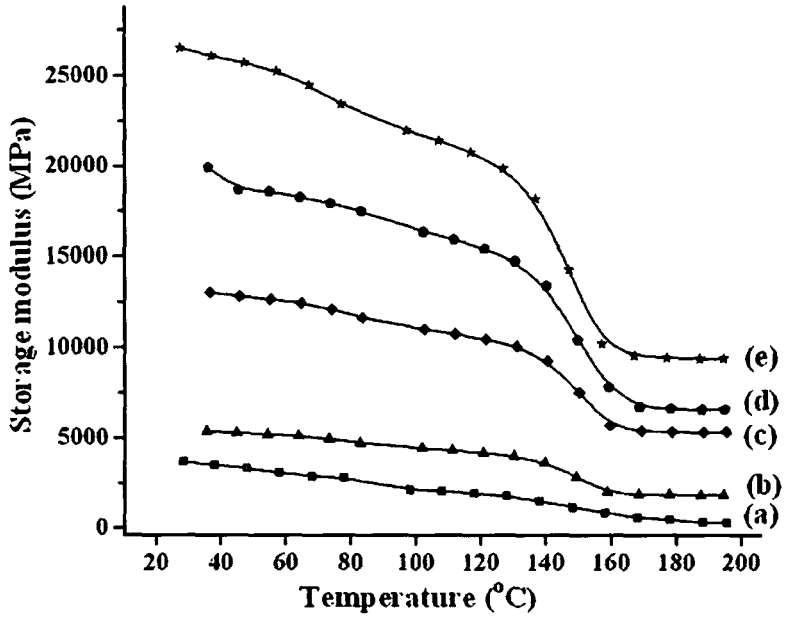

Figure 4.4.13. Storage modulus of (a) untreated and wood treated with (b) MFFA/DMDHEU (c) MFFA/DMDHEU/nanoclay (1.0 phr) (d) MFFA/ DMDHEU/nanoclay (2.0 phr) (e) MFFA/ DMDHEU/nanoclay (3.0 phr).

Figure 4.4.14.represents the loss modulus of untreated and treated wood samples. The loss modulus followed the same trend as that of storage modulus. Samples treated with MFFA/DMDHEU/nanoclay showed higher loss modulus compared to those of wood samples either untreated or treated with MFFA/DMDHEU. The polar and nonpolar groups of nanoclay enhanced the interfacial interaction between the reactants and thus improving its E'' value [10]. With the increase in temperature, the loss modulus curves reached a maximum and thereafter decreased due to the maximum dissipation of energy caused by the free movement of the polymeric chains. With the increase in the amount of nanoclay, the peak height for the loss modulus increased. This might be due to an increase in internal friction, which promoted energy dissipation and inhibited the relaxation process within the composite [51].

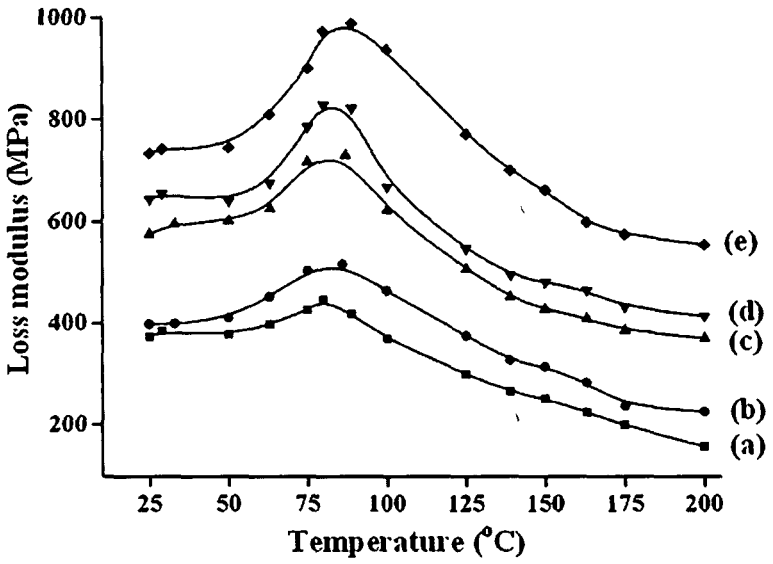

Figure 4.4.14. Loss modulus of (a) untreated and wood treated with (b) MFFA/DMDHEU (c) MFFA/DMDHEU/nanoclay (1.0 phr) (d) MFFA/ DMDHEU /nanoclay (2.0 phr) (e) MFFA/ DMDHEU/ nanoclay (3.0 phr).

4.4.14.2. Damping parameter (tan δ)

Figure 4.4.15. shows variation of tan δ as a function of temperature. The equilibrium between viscous part and elastic part is judged by the damping properties. The magnitude of the peak for the wood treated with MFFA/DMDHEU was found to decrease compared to the untreated wood. Further reduction in peak height was observed when nanoclay was added to the composite. Moreover, tan δ peak was also found to shift to the higher temperature. The crosslinker improved the interaction between wood and MFFA polymer. The shifting of tan

δ peak of polypropylene/wood fiber composite to higher temperature by using compatibilizer was reported in the literature [52]. The higher the percentage of nanoclay, the higher was the shifting of tan δ peak. The movement of polymer chains became restricted due to confinement in between the silicate layers [26]. A greater part of the force was carried out by the nanoclay leaving only a small part to deform at the interface. Energy dissipation took place at the interface and since there was a stronger interfacial interaction, the energy dissipation was less at the interface.

The tan δ peak is not only associated with the glass transition temperature but is also associated with crosslinking density. The tan δ peak became broader in case of the composites than the untreated wood samples. A wider peak indicated a more time for relaxation of molecules due to lower polymeric chains movement resulting from formation of higher crosslinking density in the composites [53].

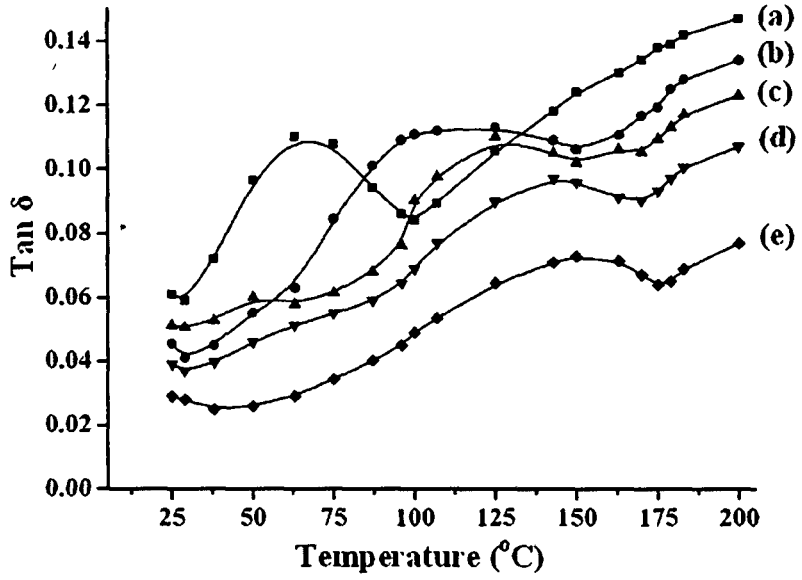

Figure 4.4.15. Tan δ of (a) untreated and wood treated with (b) MFFA/DMDHEU (c) MFFA/DMDHEU/nanoclay (1.0 phr) (d) MFFA/DMDHEU/nanoclay (2.0 phr) (e) MFFA/DMDHEU/ nanoclay (3.0 phr).

4.4.14.3. Effect of frequency

The storage modulus, loss modulus, tan δ of a material depends upon temperature and frequency. Higher values of the modulus are obtained when measurements were performed over a high frequency region [54]. A direct impact of frequency on tan δ values was observed from the Figure 4.4.16. Small chain segments and group movement occur due

to partial loosening of the polymer chain which is associated with the tan δ peak. It was observed that the amplitude of the tan δ peak increased with the increase in the frequency. Therefore T_g of the WPC and WPNC was also shifted to higher temperature with the increase in frequency. The shift in T_g allows calculation of apparent activation energy of the relaxation process of each composites assuming a linear equation.

$$\log f = \log f_o - E_a/2.303RT$$

where 'f', 'f_o', E_a, R and T denote the measured frequency, the frequency when the temperature approaches infinite, activation energy, universal gas constant and tan δ maximum temperature respectively.

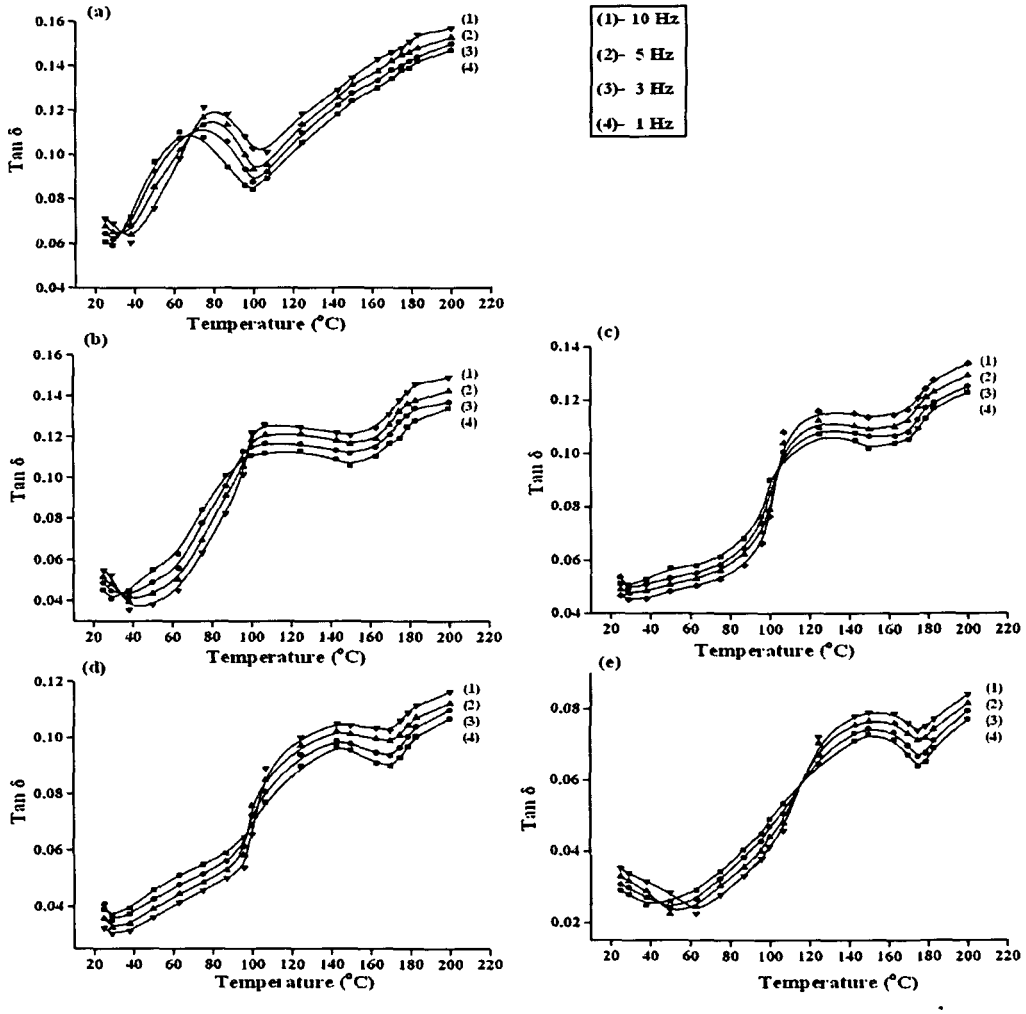

Figure 4.4.16. Tan δ at different frequency range (a) untreated and wood treated with (b) MFFA/DMDHEU (c) MFFA/DMDHEU/nanoclay (1.0 phr) (d) MFFA/DMDHEU/ nanoclay (2.0 phr) (e) MFFA/DMDHEU/nanoclay (3.0 phr).

Activation energy for the relaxation processwas calculated from the slope of the plot of log f vs reciprocal of temperature (Figure 4.4.17.).

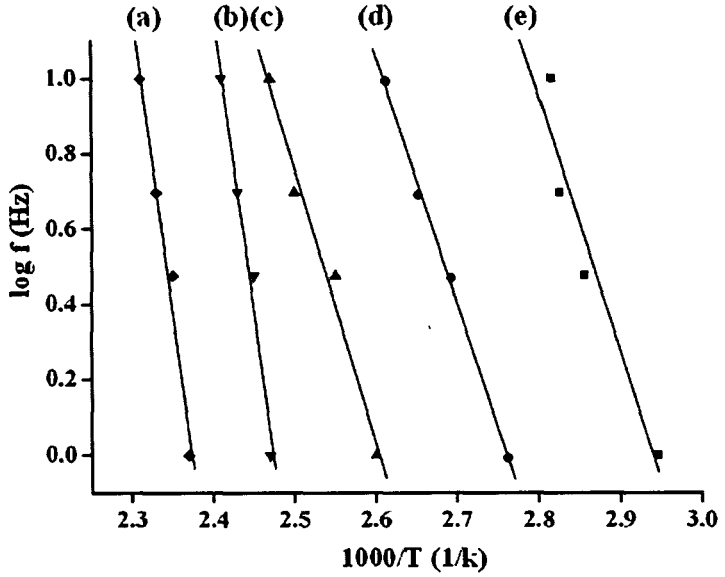

Figure 4.4.17. Calculation of the activation energies of wood treated with (a) MFFA/ DMDHEU/nanoclay (3.0 phr) (b) MFFA/DMDHEU/nanoclay (2.0 phr) (c) MFFA/ DMDHEU/nanoclay (1.0 phr) (d) MFFA/DMDHEU (e) untreated wood samples.

The calculated activation energy is presented in Table 4.4.7. The activation energy in the glass transition region helps to estimate the energy required for promotion of the initial movement of some molecular segments [55]. An increase in the activation energy was observed for the treated wood samples and further the value increased with the increase in the amount of nanoclay. The nanoclay imposed stiffness to the composites by reducing the mobility of the polymer chains. More energy was needed to initiate the movement due to increase in reinforcement to the composites.

4.4.15.Thermal study

The initial decomposition temperature (T_i), maximum pyrolysis temperature (T_m), and residual weight (%) (RW) for both untreated and treated wood samples are shown in Table 4.4.7. Moisture, $CO_2$and non combustible material were produced in the temperature range 100-200°C. T_i, T_m and T_D values were found to improve for the treated wood samples. T_m values for the first stage of pyrolysis was due to the depolymerization of hemicellulose,

glycosidic linkage of cellulose, thermal decomposition of cellulose and disintegration of interunit linkages and condensation of aromatic rings during pyrolytic degradation of lignin [45]. The second stage of pyrolysis was due to the degradation of polymers. The addition of MFFA and DMDHEU enhanced the thermal stability of the composites. DMDHEU could form a crosslinked structure with that of MFFA and cell wall of wood through its hydroxyl groups. Addition of nanoclay into the MFFA/DMDHEU improved its thermal stability. With the increase in the amount of nanoclay, a noticeable improvement in thermal stability was observed. This was attributed to the presence of silicate layers which could barricade and deferred the diffusion of decomposed volatile products throughout the composites [11].

Table 4.4.7. Thermal analysis of wood polymer nanocomposite.

Sample	T_i	T_m^a	T_m^b	Temperature of decomposition (T_D) in °C at different weight loss (%)				RW% at 600°C	E_a (kJ/mol)
				20%	40%	60%	80%		
Untreated wood	168	310	395	269	305	330	--	26.53	118.78
Wood treated with MFFA/DMDHEU	236	339	432	306	324	363	431	8.9	129.65
MFFA/DMDHEU/ 1.0 phr nanoclay	250	352	443	332	342	378	445	12.8	160.54
MFFA/DMDHEU/ 2.0 phr nanoclay	258	354	445	334	346	384	447	18.7	198.25
MFFA/DMDHEU/ 3.0 phr nanoclay	262	358	449	337	351	388	452	21.53	232.42

Untreated wood samples showed highest RW values due to formation of char caused by carbonization of wood samples. The presence of inorganic silicate layers improved the RW value in nanoclay treated composites.

4.4.16.Biodegradation study

4.4.16.1. Decay evaluation and microscopic analysis

The untreated and treated wood samples were exposed to cellulolytic bacterial strain directly in broth culture medium. The samples exposed to the broth culture media were incubated for a period of 1 month. The bacterial growth on the samples was clearly recognized and is plotted versus time as shown in Figure 4.4.18.

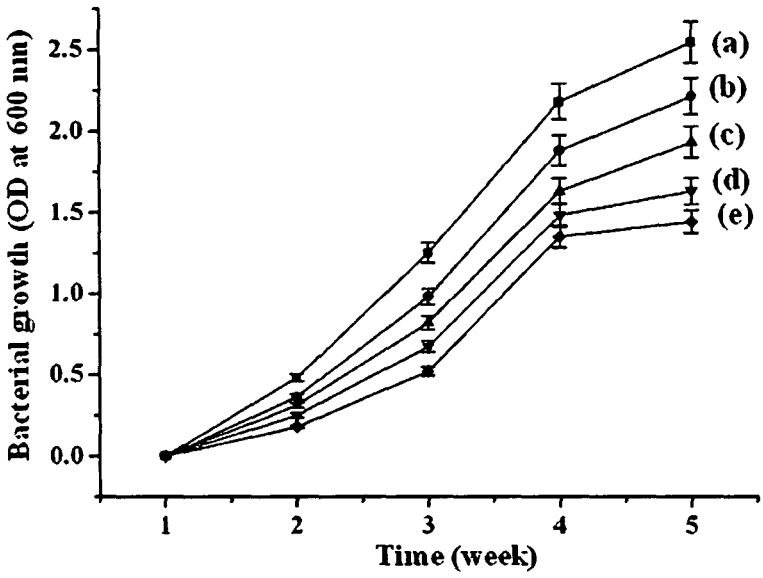

Figure 4.4.18. Growth of Bacillus sp. on (a) untreated and wood treated with (b) MFFA/DMDHEU/nanoclay (3.0 phr) (c) MFFA/DMDHEU/nanoclay (2.0 phr) (d) MFFA/DMDHEU /nanoclay (1.0 phr) (e) MFFA/ DMDHEU.

It was observed that with the increase in time of bacterial exposure, the rate of bacterial growth increased quite progressively. After a period of 4 weeks of incubation, the rate of bacterial growth decreased. The rate of degradation was found highest for the untreated wood samples followed by the samples treated with MFFA/DMDHEU/nanoclay. The polymer treated samples had the least bacterial growth. This was evident by the SEM analysis as shown in Figure 4.4.19.

The bacterial growth was enhanced by the effectual cellulolytic and pectinolytic activity of bacteria and the Bacillus sp. bacteria was responsible for degradation of lignin present in wood [56,57]. The wood was a source of carbon for the bacterial growth. The rate of degradation and growth of bacteria decreased after 4 weeks of incubation because

themicrobes generated some toxic metabolites. With the increase in the amount of nanoclay, the rate of bacterial growth in the composites also increased due to the catalytic effect of the nanoclay in the degradation process [58]. The hydrophilic nature of nanoclay promoted the growth of microorganisms. The loss in mechanical properties of the untreated wood was more than those of treated composites as shown in Table 4.4.8. The bacteria were responsible for breaking down the chemical bond that took place between wood, polymer, crosslinker and nanoclay.

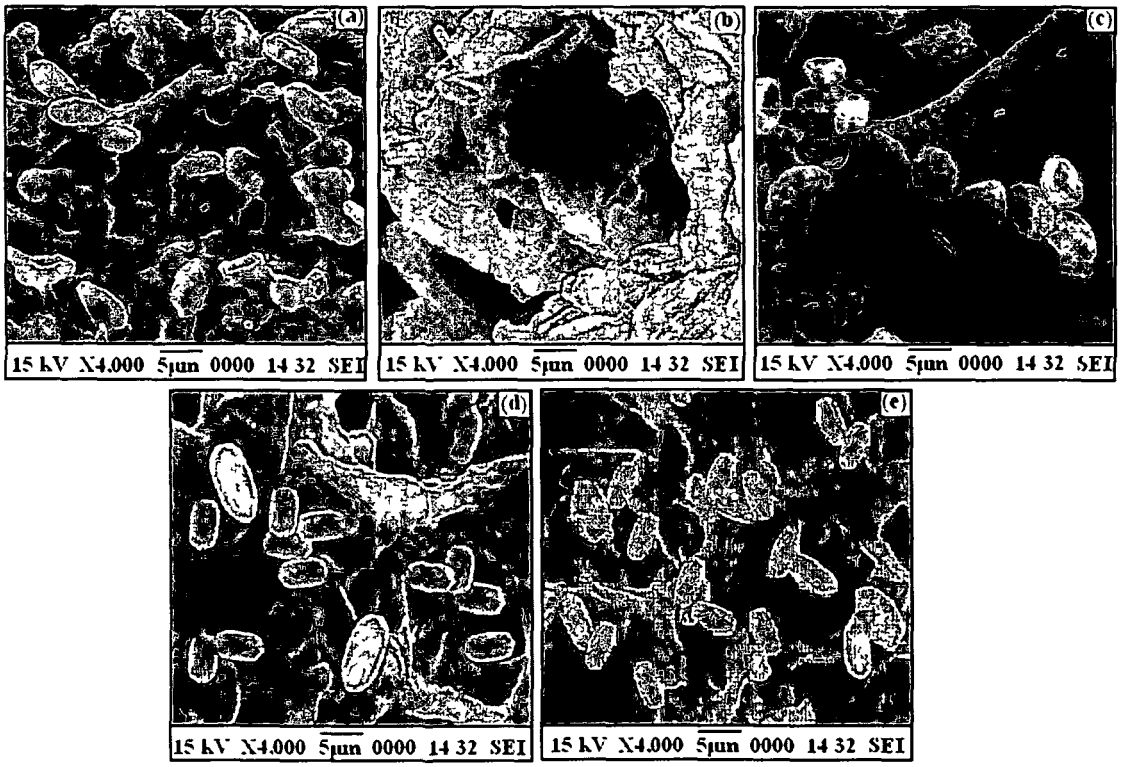

Figure 4.4.19.SEM micrograph after microbial test on (a) untreated wood and wood treated with (b) MFFA/DMDHEU (c) MFFA/DMDHEU/nanoclay (1.0 phr)
(d) MFFA/DMDHEU/nanoclay (2.0 phr) (e) MFFA/ DMDHEU/nanoclay (3.0 phr).

4.4.16.2. Soil burial test

The untreated and treated wood samples were buried in biologically active soil and exposed to natural microbial conglomerate during in vitro soil experiments for 1 month. Soil microflora is composed of a mixed microbial population (including actinomycetes, bacteria and fungi). They could degrade the samples collaboratively and reproduce under naturally occurring conditions [59].

Table 4.4.8. Flexural and tensile properties of WPNC loaded with different percentages of nanoclay after the microbial degradation.

Sample	Flexural properties				Tensile properties			
	Before degradation		After degradation		Before degradation		After degradation	
	Strength (MPa) (±SD)	Modulus (MPa) (±SD)	Strength (MPa) (±SD)	Modulus (MPa) (±SD)	Strength (MPa) (±SD)	Modulus (MPa) (±SD)	Strength (MPa) (±SD)	Modulus (MPa) (±SD)
Untreated wood	117.71 (±1.52)	5936.82 (±3.44)	98.68 (±3.21)	4977.02 (±2.12)	40.69 (±1.62)	303.72 (±7.31)	23.76 (±0.85)	177.35 (±5.25)
Wood treated with MFFA	125.52 (±1.62)	6330.72 (±2.12)	117.12 (±4.21)	5907.06 (±1.23)	43.65 (±2.15)	322.83 (±7.04)	37.87 (±5.32)	282.67 (±4.42)
MFFA/DMDHEU	128.47 (±0.84)	6479.51 (±1.75)	123.23 (±3.28)	6215.22 (±2.23)	50.66 (±3.12)	376.64 (±8.25)	45.21 (±3.96)	337.45 (±3.65)
MFFA/DMDHEU/ nanoclay(1 phr)	135.55 (±1.65)	6836.59 (±1.76)	126.31 (±0.89)	6370.56 (±2.85)	58.53 (±1.74)	439.54 (±7.92)	50.43 (±4.21)	376.42 (±6.89)
MFFA/DMDHEU/ nanoclay(2 phr)	138.84 (±1.53)	7002.53 (±3.28)	128.64 (±1.98)	6488.08 (±4.75)	62.56 (±2.56)	465.64 (±3.21)	52.65 (±2.96)	392.99 (±7.34)
MFFA/ DMDHEU/ nanoclay (3 phr)	140.76 (±0.73)	7099.36 (±1.63)	129.43 (±2.76)	6527.92 (±6.73)	65.64 (±4.74)	486.46 (±9.06)	54.53 (±2.35)	407.02 (±4.68)

SEM study was employed to check the growth of microorganisms after a period of 1 month (Figure 4.4.20.). The growth of fungal species, bacteria and actinomycetes were more on the surface of the untreated wood compared to those of the treated composites.

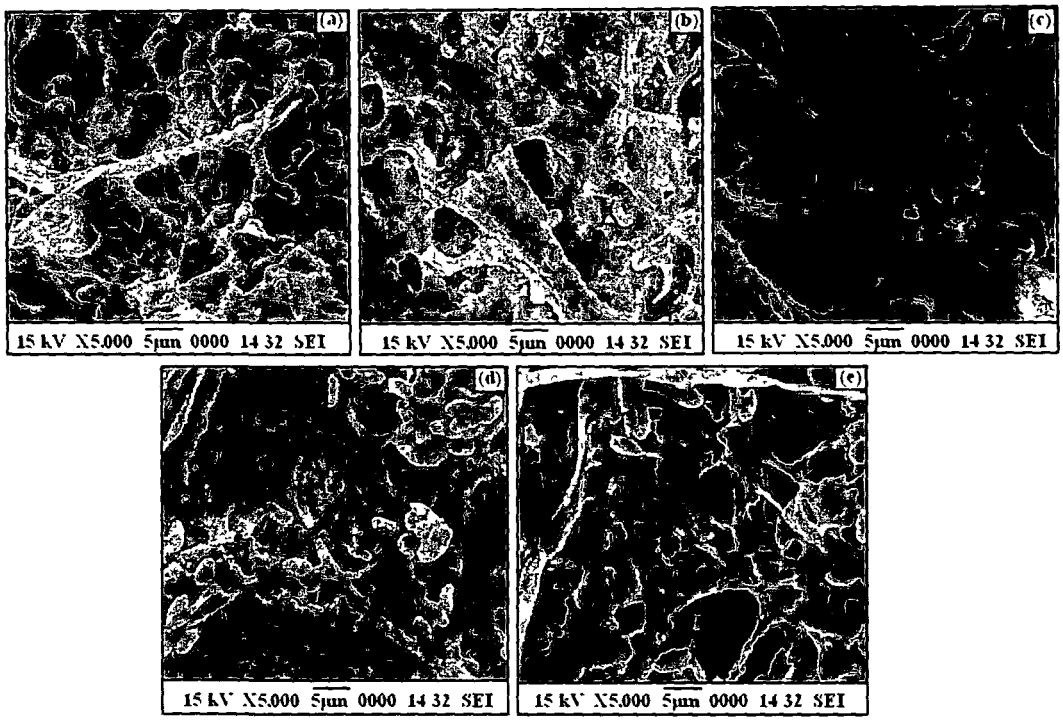

Figure 4.4.20.SEM micrograph after soil burial test on (a) untreated wood and wood treated with (b) MFFA/DMDHEU (c) MFFA/DMDHEU/nanoclay (1.0 phr)
(d) MFFA/DMDHEU/nanoclay (2.0 phr) (e) MFFA/ DMDHEU/nanoclay (3.0 phr).

The mechanical properties and weight of the degraded samples were checked and are presented in Table 4.4.9.and 4.4.10.There was a loss in weight and mechanical properties of the samples. Loss was highest for the untreated samples followed by the samples treated with MFFA/DMDHEU/nanoclay and MFFA/DMDHEU respectively. The various microorganismspresent in the soil were responsible for breaking the chemical bonds that were formed between the wood and polymers.

Table 4.4.9. Flexural and tensile properties of WPNC loaded with different percentages of nanoclay after the soil burial test.

Sample	Flexural properties				Tensile properties			
	Before degradation		After degradation		Before degradation		After degradation	
	Strength (MPa) (±SD)	Modulus (MPa) (±SD)	Strength (MPa) (±SD)	Modulus (MPa) (±SD)	Strength (MPa) (±SD)	Modulus (MPa) (±SD)	Strength (MPa) (±SD)	Modulus (MPa) (±SD)
Untreated wood	116.87 (±1.35)	5894.45 (±2.74)	97.39 (±2.98)	4911.96 (±2.76)	41.72 (±2.12)	311.40 (±8.13)	24.21 (±1.76)	180.70 (±5.32)
MFFA	124.12 (±1.76)	6260.11 (±2.98)	116.32 (±5.12)	5866.71 (±1.57)	42.98 (±3.52)	320.81 (±7.87)	36.37 (±4.76)	271.47 (±8.54)
MFFA/DMDHEU	127.39 (±1.28)	6425.04 (±1.23)	124.03 (±3.13)	6255.57 (±2.67)	51.26 (±2.87)	382.61 (±8.32)	46.43 (±3.16)	346.56 (±4.21)
MFFA/DMDHEU/nanoclay (1 phr)	134.65 (±2.15)	6791.20 (±1.65)	125.45 (±1.45)	6327.19 (±2.21)	57.67 (±3.42)	430.46 (±7.46)	49.87 (±2.86)	372.24 (±3.78)
MFFA/DMDHEU/nanoclay (2 phr)	137.37 (±2.02)	6928.39 (±3.29)	129.37 (±1.34)	6524.90 (±4.59)	63.43 (±1.89)	473.45 (±6.34)	53.25 (±4.26)	397.47 (±6.89)
MFFA/DMDHEU/nanoclay (3 phr)	141.12 (±0.47)	7117.52 (±1.96)	130.23 (±3.21)	6568.27 (±7.32)	66.24 (±3.42)	494.43 (±10.32)	55.63 (±3.86)	415.23 (±9.12)

Table 4.4.10. Weight loss and loss of hardness for untreated and treated wood samples after the soil burial test.

Sample	Weight of specimen (in g)		Hardness (Shore D)	
	Before degradation	After degradation	Before degradation	After degradation
Untreated wood	6.17 (±0.78)	2.46 (±0.76)	45 (±1.02)	31 (±0.87)
Wood treated with MFFA	8.12 (±0.43)	6.98 (±0.54)	56 (±1.12)	48 (±0.58)
MFFA/DMDHEU	8.34 (±0.27)	7.50 (±0.29)	59 (±0.47)	53 (±0.59)
MFFA/DMDHEU/ nanoclay(1 phr)	8.53 (±0.85)	6.39 (±0.72)	65 (±0.73)	54 (±1.03)
MFFA/DMDHEU/ nanoclay(2 phr)	8.89 (±0.42)	6.48 (±0.65)	71 (±0.38)	60 (±0.27)
MFFA/DMDHEU/ nanoclay (3 phr)	9.02 (±1.09)	6.40 (±0.32)	73 (±0.48)	61 (±0.48)

Section E: Thermal decomposition kinetics, flammability and mechanical property study of wood polymer nanocomposite.

This part of work embodies the results of incorporation of a renewable polymer, collected as gum from a local plant (*Moringa oleifera*) as flame retardant along with MFFA copolymer, DMDHEU, a crosslinking agent and nanoclay under vacuum condition and polymerized by catalyst heat treatment. Optimum properties are obtained by varying various parameters like vacuum, time of impregnation, monomer concentration, initiator concentration, amount of crosslinking agent, nanoclay and plant polymer (PP). The conditions to get maximum improvement in properties were 500mm Hg vacuum, 6 h time of impregnation, 5:1 (MFFA:FA-water) prepolymer concentration, 1% (w/w) maleic anhydride, 3 mL DMDHEU, 3 phr nanoclay and 1.0-3.0 % w/v plant polymer (PP).

4.5.RESULTS AND DISCUSSION

4.5.1. Effect of variation of plant polymer (PP)*Moringa oleifera* on polymer loading (WPG), volume increase, and hardness

It was observed from Table 4.5.1., that WPG (%) and volume increase (%) of wood occurred due to impregnation of polymer. MFFA prepolymer and PP filled up the void spaces in wood and hence an improvement in properties was noticed. The properties improved further when DMDHEU and nanoclay were added to the prepolymer. The addition of DMDHEU facilitated the formation of crosslinked structure between wood and polymer through its hydroxyl groups [41]. Further the mobility of polymer chains was restricted due to intercalation of polymer chains between the silicate layers [10]. The higher the PP, the higher was the improvement in properties. This might be due to the increase in interaction between wood, polymer, DMDHEU, nanoclay and PP. PP had hydroxyl groups and could interact with wood/MFFA prepolymer, DMDHEU and nanoclay which resulted in an overall improvement in properties.

Table 4.5.1. Effect of variation of plant polymer on weight % gain (WPG %), volume increase and hardness.

Samples particulars	Weight % gain (WPG %)	Volume increase (%)	Hardness (Shore D)
Untreated wood		---	46 (±1.07)
Samples treated with MFFA/FA-H_2O/PP/DMDHEU/ nanoclay			
100/20/3/0/0	29.43 (±0.38)	2.16 (±0.31)	59 (±1.08)
100/20/3/3/0	32.44 (±0.65)	2.23 (±0.43)	64 (±0.76)
100/20/1/3/3	43.68 (±0.28)	2.87 (±0.41)	73 (±1.04)
100/20/2/3/3	45.92 (±0.56)	2.92 (±1.12)	76 (±0.76)
100/20/3/3/3	47.44 (±0.82)	3.01 (±1.09)	77 (±0.67)

4.5.2. FTIR study

The FTIR spectra of untreated wood, MFFA, plant polymer, DMDHEU, nanoclay are represented in Figure 4.5.1.Untreated wood (curve a) exhibited bands at 3449 cm^{-1} (–OH stretching), 2925 cm^{-1}, and 2848 cm^{-1} (–CH_2 asymmetric stretching), 1732 cm^{-1} (C=O stretching), 1642 for (–OH bending), 1258 and 1046 cm^{-1} (C–O stretching) and 1000–646 cm^{-1} (out of plane C–H bending vibration). MFFA copolymer (curve b) was characterized by the bands at 3408 cm^{-1} (-OH stretching), 1568 cm^{-1} and 1509 cm^{-1} (furan ring vibration), 1346 cm^{-1} (N-CH_2-furan ring), 1188 cm^{-1} (C-N stretching), 812 cm^{-1} (out plane trisubstitution of triazine ring) [15]. All the components of PP (L-arabinose, D-galactose, D-glucuronic acid, L-rhamnose, D-mannose, D-xylose and leucoanthocyanin) has abundant hydroxyl groups. PP (curve c) showed bands at 3430 cm^{-1} (-OH stretching), 2926 cm^{-1}, 2857 cm^{-1} (–CH_2 asymmetric and symmetric stretching), 1618 cm^{-1} (–OH bending), 1440 cm^{-1} and 1375 cm^{-1} (-CH bending). In the spectrum of DMDHEU, (curve d) the appearance of absorption bands at 3422, 1700, 1248, 1021 cm^{-1} were for -OH stretching, C=O stretching, -CHOH stretching, -CH_2OH stretching respectively [37]. Peaks appeared at 3468 cm^{-1} for –OH stretching, 2930 and 2858 cm^{-1} for –CH stretching of modified hydrocarbon, 1622 cm^{-1} for –OH bending, 1033–456 cm^{-1} for oxide bands of metals like Si, Al, Mg, etc. in the absorption spectrum of nanoclay (curve e).

The FTIR spectra of wood samples treated with MFFA/PP (3phr), MFFA/PP (3phr)/DMDHEU, MFFA/PP (1phr)/DMDHEU/nanoclay, MFFA/PP (2phr)/DMDHEU/nanoclay, MFFA/PP (3phr)/DMDHEU/nanoclay are represented in Figure 4.5.2. The presence of the characteristic peaks of MFFA, PP and nanoclay into wood polymer composite indicated the successful impregnation of material into wood (curve a-d). Further a decrease in intensity of hydroxyl peak and shifting of the peaks occurred to 3431 cm^{-1}(curve a), 3372 cm^{-1} (curve b), 3292 cm^{-1} (curve c), 3288 cm^{-1} (curve d), 3254 cm^{-1} (curve e) from 3449 cm^{-1} (for untreated wood) were observed. This indicated the participation of hydroxyl groups of wood in bond formation with MFFA, PP, DMDHEU and nanoclay. Moreover, the peaks at 2925 cm^{-1}, and 2848 cm^{-1} (–CH_2 asymmetric stretching) were more pronounced in treated wood samples than untreated wood suggesting an enhancement in interaction. Similar decrease in hydroxyl peak intensity and shifting to lower wavenumber was reported by Deka and Maji while studying the FTIR analysis wood polymer composites [60].

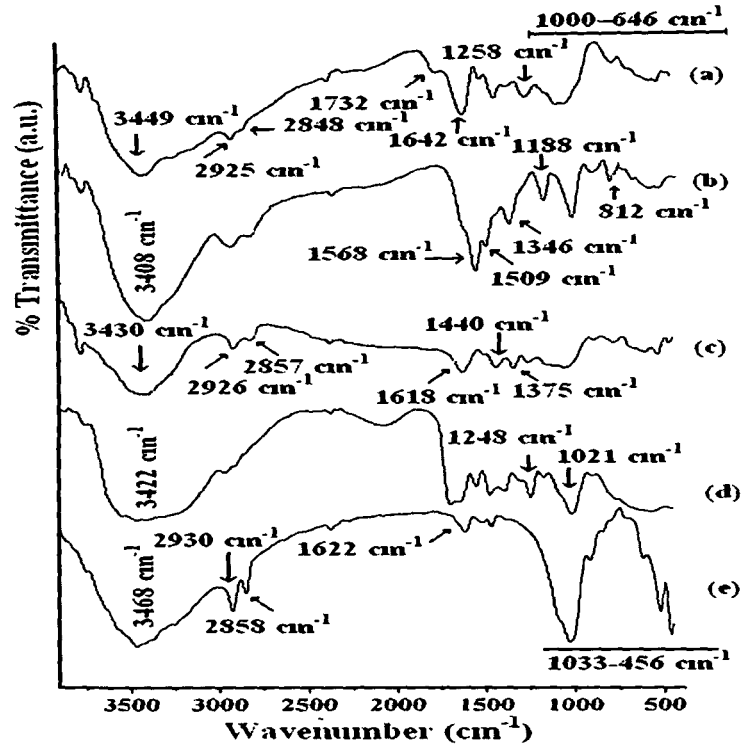

Figure 4.5.1.FTIR spectra of (a)untreated wood (b) MFFA (c) PP (d) DMDHEU (e) nanoclay.

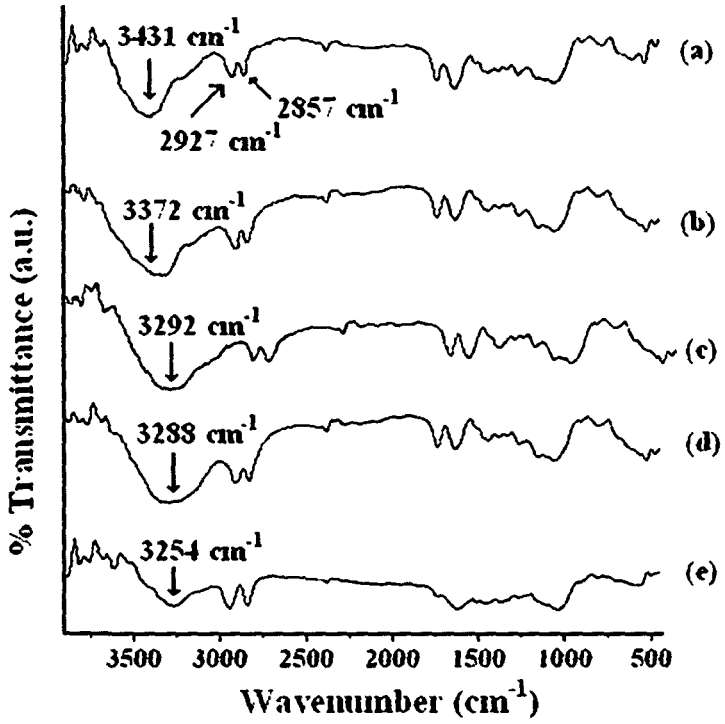

Figure 4.5.2. FTIR spectra of (a) MFFA/PP (3phr) (b) MFFA/PP (3phr)/DMDHEU (c) MFFA/PP (1phr)/DMDHEU/nanoclay (d) MFFA/PP (2phr)/DMDHEU/nanoclay (e) MFFA/PP (3phr)/DMDHEU/nanoclay.

4.5.3. XRD study

The X-ray diffraction patterns of nanoclay, untreated wood and treated wood samples are represented in Figure 4.5.3.The organically modified nanoclay (curve a) showed a diffraction peak at 2θ = 4.30°. The gallery distance was calculated using Bragg's equation and found to be 2.05 nm. Untreated wood samples (curve b) showed a broad diffraction peak near 22.94° of 2θ due to the (002) crystal plane of cellulose present in wood. Appearance of small crests at 37.77° and 15.04° were assigned to (040) crystal plane of

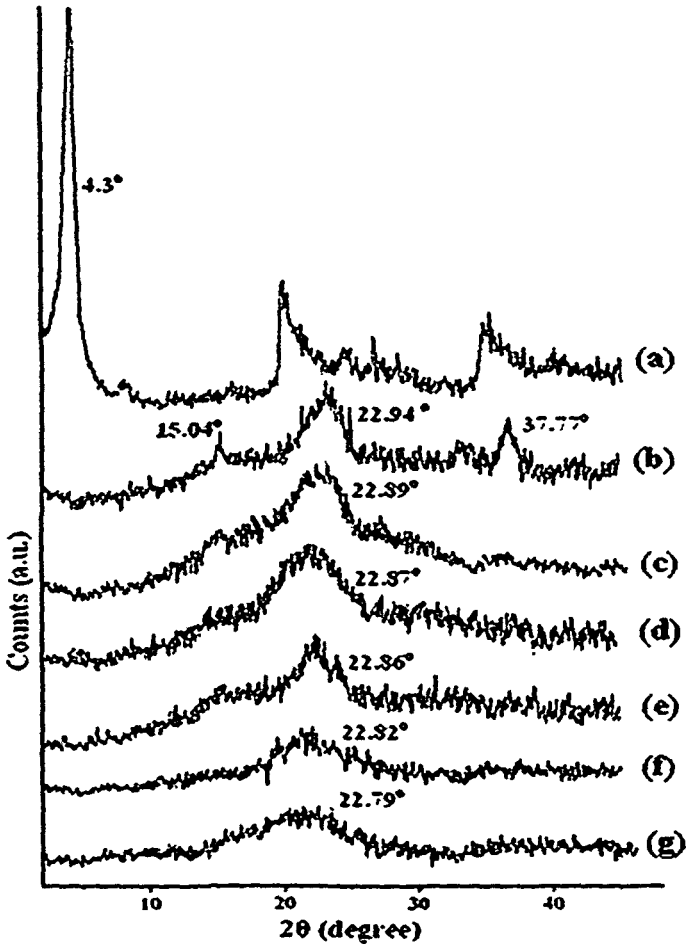

Figure 4.5.3.X-ray diffraction of (a) nanoclay, (b) untreated wood and wood treated with (c) MFFA/PP (3phr) (d) MFFA/PP (3phr)/DMDHEU (e) MFFA/PP (1phr)/DMDHEU/nanoclay (f) MFFA/PP (2phr)/DMDHEU/nanoclay (g) MFFA/PP (3phr)/DMDHEU/nanoclay.

cellulose and amorphous region of cellulose respectively [7]. The crystalline peak of wood appeared at 2θ = 22.94° was found to broadened slightly and shifted to 22.89° (curve c) and 22.87° (curve d) due to treatment with polymer. Wood treated with

MFFA/PP/DMDHEU/nanoclay showed a further decrease in crystallinity peak intensity and shifting to lower angle. With the increase in the amount of PP, the peak intensity decreased and further shifted to 22.86° (curve e), 22.82° (curve f) and 22.79° (curve g). The peak at 15.04° and 37.77° for untreated wood were become dull in the prepared composites (curve c-g). The diffraction peak for the nanoclay also disappeared which might be either due to the delamination of the nanoclay layer or the full expansion of the nanoclay gallery layers which was not possible to detect by XRD [2]. Therefore it could be concluded that the crystallinity in wood decreased and some nanoclay, MFFA polymer and PP were introduced into the amorphous region of wood cellulose (curve c-g).

4.5.4. Transmission electron microscopy (TEM) study

The TEM micrographs of wood treated with (a) MFFA/PP (3phr) (b) MFFA/PP (3phr)/DMDHEU/nanoclayare represented in Figure 4.5.4.A homogenous dispersion of clay (shown as dark slices) was observed in MFFA/PP (3 phr)/DMDHEU/nanoclay treated samples which were not observed in case of MFFA/PP (3phr) treated samples.

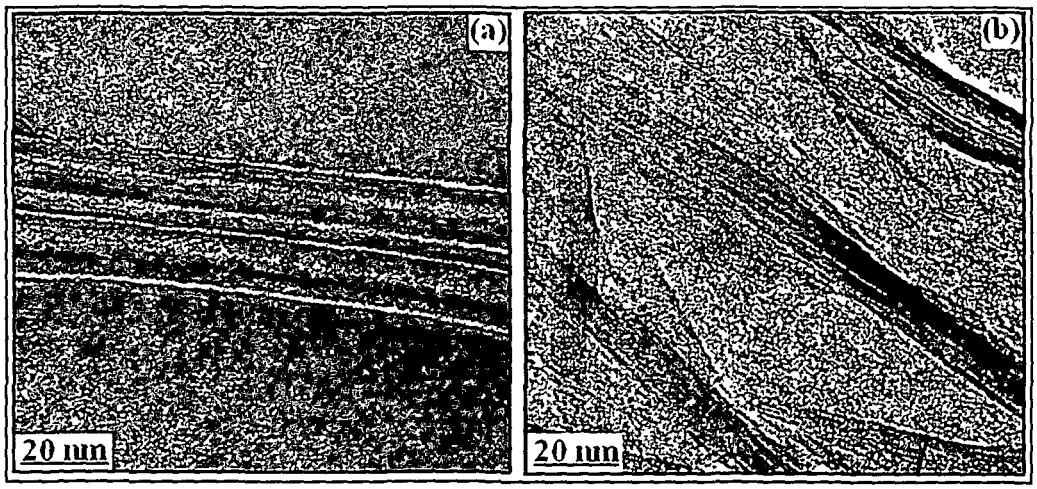

Figure 4.5.4.TEM micrographs of wood treated with (a) MFFA/PP (3phr)(b) MFFA/PP (3phr)/DMDHEU/nanoclay.

4.5.5. Scanning electron microscopy study

Scanning electron micrographs of the fractured surfaces of the untreated wood and treated wood samples were shown in Figure 4.5.5.The empty pits and parenchymas present

in untreated wood (Figure 4.5.5.a) were filled by the MFFA and PP as shown in MFFA/PP (3 phr) treated samples (Figure 4.5.5.b). In the case of wood treated with MFFA/PP/DMDHEU/nanoclay some white patches of nanoclay were seen indicating the successful impregnation of nanoclay into the wood (Figure 4.5.5.c-e).

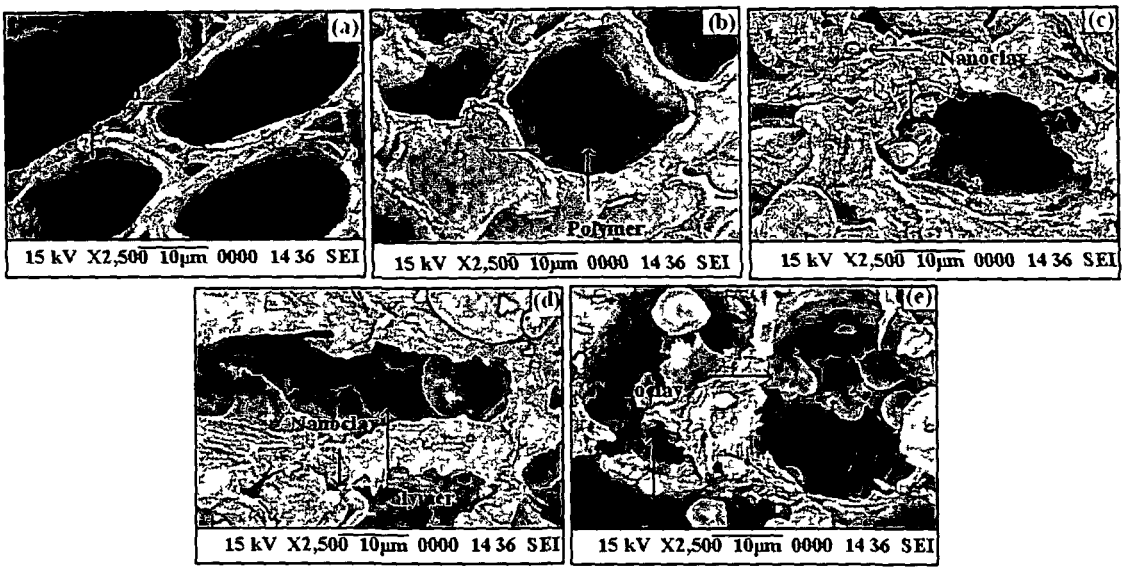

Figure 4.5.5.SEM micrographs of (a) untreated woodand wood treated with
(b) MFFA/PP (3phr) (c) MFFA/PP (1phr)/DMDHEU/nanoclay
(d) MFFA/PP (2phr)/DMDHEU/nanoclay (e) MFFA/PP (3phr)/DMDHEU/nanoclay.

4.5.6. Mechanical properties

Table 4 5.2. shows the tensile and flexural values of untreated and treated wood samples. The porous structure of wood was filled up by the copolymer due to impregnation with MFFA and the PP. Wood treated with MFFA/PP/DMDHEU/nanoclay showed better properties than those of either untreated or MFFA/PP (3phr) or MFFA/PP (3phr)/DMDHEU treated samples. The hydroxyl groups of the PP could interact with the hydroxyl groups of wood and prepolymer resulting in improved tensile and flexural values Samples treated with MFFA/PP/DMDHEU/nanoclay showed better properties than the MFFA/PP (3 phr) treated samples. DMDHEU could further enhance the interaction between wood, prepolymer and PP by forming a crosslinked structure through its hydroxyl groups [41]. In the case of nanoclay treated samples, the mobility of the polymer chains that were intercalated between the silicate layers became restricted. Therefore, crosslinking along with restriction in the mobility of the polymer chains played a role in enhancing both the tensile and flexural

values of the nanoclay treated wood samples. With increase in the amount of PP, further increase in the values was observed due to enhancement in interfacial adhesion between the wood, polymer, crosslinker and nanoclay.

Table 4.5.2. Flexural and tensile properties of untreated and treated wood.

Sample	Flexural properties		Tensile properties	
	Strength (MPa)	Modulus (MPa)	Strength (MPa)	Modulus (MPa)
Untreated wood	120.56 (±2.90)	6047.45 (±3.15)	41.50 (±0.90)	307.83 (±11.60)
Wood treated with MFFA/PP (3phr)	129.57 (±0.83)	6539.57 (±2.98)	50.50 (±0.98)	377.39 (±11.14)
MFFA/PP (3phr)/DMDHEU	131.90 (±1.8)	6674.28 (±2.96)	53.67 (±4.27)	399.57 (±1.45)
MFFA/PP(1phr)/ DMDHEU/nanoclay	140.68 (±3.09)	7097.54 (±3.11)	67.29 (±1.51)	500.69 (±9.60)
MFFA/PP(2phr)/ DMDHEU/nanoclay	143.53 (±0.85)	7209.52 (±3.97)	69.55 (±1.55)	518.60 (±8.76)
MFFA/PP(3phr)/ DMDHEU/nanoclay	145.59 (±1.60)	7315.49 (±3.69)	70.66 (±1.62)	526.55 (±6.88)

4.5.7. Water uptake and volumetric swelling test

The water absorption capacity and volumetric swelling of untreated wood and treated wood samples are represented in Figure 4.5.6.and 4.5.7.The void spaces in untreated wood have rendered it to demonstrate highest water uptake capacity and volumetric swelling (curve 4.5.6.a and 4.5.7.a). With the increase in time of immersion, an increasing trend in water uptake capacity was found. Deposition of MFFA/PP into the capillaries and pores of wood would lessen its water uptake capacity and volumetric swelling (curve 4.5.6.b and 4.5.7.b). DMDHEU would crosslink with the wood and polymer leading to a further reduction in water uptake capacity (curve 4.5.6.c and 4.5.7.c). Wood treated with MFFA/PP/DMDHEU/nanoclay showed the least water uptake capacity (curve 4.5.6.f and 4.5.7.f). The silicate layers provided a tortuous path for the transmission of water molecules (curve 4.5.6.d and 4.5.7.d) [9]. With the increase in the amount of PP, the absorption

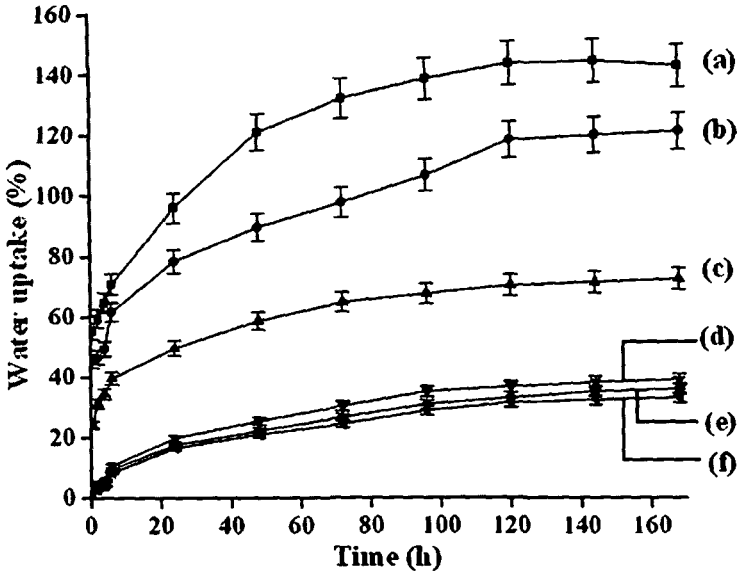

Figure4.5.6. Water absorption test of (a) untreated wood and wood treated with (b) MFFA/PP (3phr) (c) MFFA/PP (3phr)/DMDHEU (d) MFFA/PP (1phr)/DMDHEU/nanoclay (e) MFFA/PP (2phr)/DMDHEU/nanoclay (f) MFFA/PP (3phr)/DMDHEU/nanoclay.

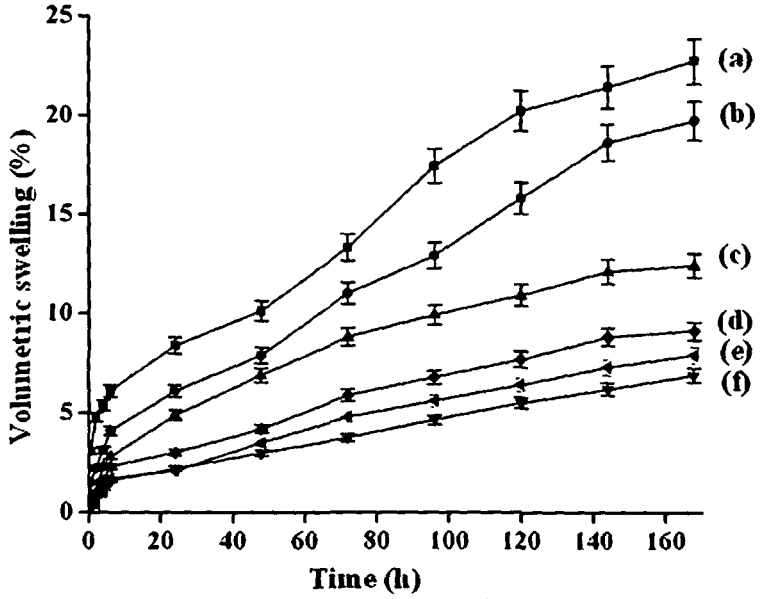

Figure4.5.7. Volumetric swelling test of (a) untreated wood and wood treated with (b) MFFA/PP (3phr) (c) MFFA/PP (3phr)/DMDHEU (d) MFFA/PP (1phr)/DMDHEU/nanoclay (e) MFFA/PP (2phr)/DMDHEU/nanoclay (f) MFFA/PP (3phr)/DMDHEU/nanoclay.

capacity as well as volumetric swelling was found to decrease (curve 4.5.6.d-4.5.6.f and 4.5.7.d-4.5.7.f). The PP contains L-arabinose, D-galactose, D-glucuronic acid, L-rhamnose, D-mannose, D-xylose and leucoanthocyanin. All the constituents have hydroxyl groups capable of interacting with the wood, polymer, crosslinker and nanoclay thereby decreasing its water uptake capacity.

4.5.8. LOI study

Table 4.5.3.shows the limiting oxygen index values of treated and untreated wood. The high LOIvalue of the MFFA/PP (3phr)treated samples was due to the synergistic effect of nitrogen in melamine of the MFFA copolymer and phosphorus present in the PP. The displacement of oxygen present on the surface of the sample by the oxides of nitrogen and phosphorus released during combustion was supposed to be the mechanism of fire control. Addition of DMDHEU and nanoclay further enhanced its flame retardancy. DMDHEU

Table 4.5.3. Limiting oxygen indices (LOI) and flaming characteristics of treated and untreated samples.

Samples	LOI (%)	Flame description	Smokes and fumes	Char
Untreated wood	19	Candle-like localized flame	---	Little
Wood treated with MFFA/PP (3phr)	26	Small localized flame	Small and black smoke	Medium
MFFA/PP(3phr)/ DMDHEU	28	Small localized flame	Small and black smoke	Medium
MFFA/PP(1phr)/ DMDHEU/nanoclay	31	Small localized flame	Small and black smoke	Higher
MFFA/PP(2phr)/ DMDHEU/nanoclay	34	Small localized flame	Small and black smoke	Higher
MFFA/PP(3phr)/ DMDHEU/nanoclay	36	Small localized flame	Small and black smoke	Higher

acted as a crosslinker and could also provide nitrogen. Clay layers also provided a barrier by promoting char formation. Char helps in decreasing the rate of mass loss during thermal

decomposition and it shield the sample from burning thereby improving its flame resistance property [43].LOI value was further improved on addition of PP. The presence of phosphorus in the PP and the enhanced interaction between wood, MFFA and DMDHEU caused by the hydroxyl groups of PP were responsible for exhibiting improved LOIvalue. The fire retardancy of biodegradable film/rubber was found to improve due to treatment with PP [61,62].

4.5.9. Thermal study

The TGA and DTG thermograms of untreated and treated wood samples are represented in Figure4.5.8.and 4.5.9.Initial degradation temperature (T_i), maximum pyrolysis temperature (T_m), decomposition temperature at different weight loss (%) (T_D) and residual weight (RW %) are shown in Table 4.5.4.The weight loss observed below 100 °C in both the untreated and treated wood samples was due to moisture loss. Treated wood samples had higher T_i and T_m values compared to the untreated wood samples. MFFA along with the plant polymer increased the thermal stability of wood. A further increase in T_i values was observed in MFFA/PP (3 phr)/DMDHEU/nanoclay treated samples. This was due to the synergistic effect of crosslinker, nanoclay and PP. DMDHEU improved the interfacial adhesion between wood and polymer and the silicate layers of nanoclay provided an obstruction to the passage of decomposed volatile products throughout the composite [63].PP contains phosphorus (4.34%, w/w) and as a result the thermal stability of the composites enhanced further [62]. With the increase in the amount of the PP, the thermal stability of the prepared composites improved.

$T_m$values for the first stage of untreated and treated wood samples might be due to the depolymerization of hemicellulose, glycosidic linkage of cellulose, thermal decomposition of cellulose [12] while the second stage was due to the degradation of MFFA copolymer. DMDHEU, nanoclay and PP improved the $T_m$values of the composites.

Untreated wood had the highest RW value due to the high ash content. RW value decreased when samples were treated with MFFA and PP. Addition of nanoclay would increase its value again.

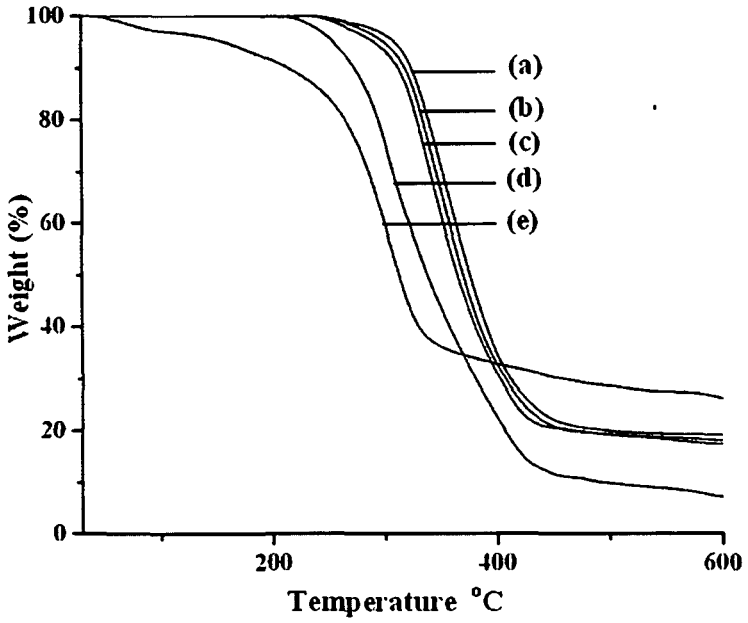

Figure 4.5.8. Thermogravimetric curves of wood samples treated with (a) MFFA/PP (3 phr)/DMDHEU/nanoclay (b) MFFA/PP (2 phr)/DMDHEU/nanoclay(c) MFFA/PP (1phr)/DMDHEU/nanoclay (d) MFFA/PP (3phr) (e) untreated wood samples.

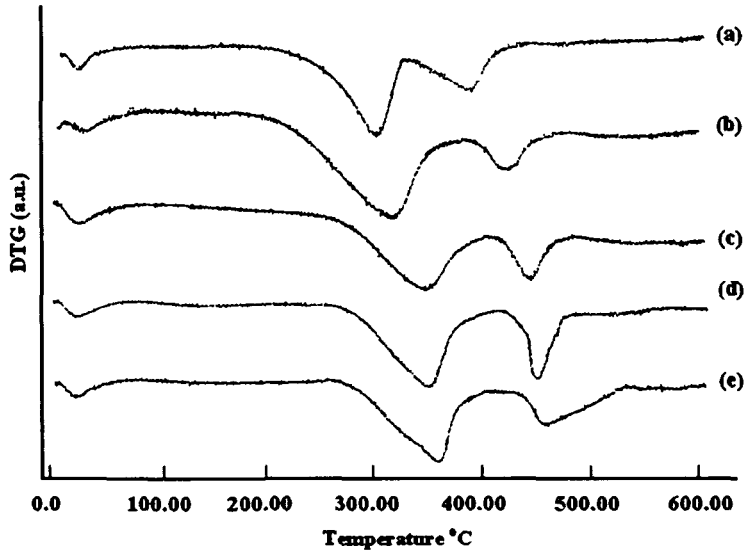

Figure4.5.9. DTG curves of (a) untreated wood and wood treated with (b) MFFA/PP (3phr)(c) MFFA/PP (1phr)/DMDHEU/nanoclay(d) MFFA/PP (2 phr)/DMDHEU/nanoclay (e) MFFA/PP (3 phr)/DMDHEU/nanoclay.

Table 4.5.4. Thermal degradation of untreated and treated wood samples.

Sample	T_i	T_m^a	T_m^b	Temperature of decomposition (T_D) in °C at different weight loss (%)				RW% at 600°C
				20%	40%	60%	80%	
Untreated wood	162	305	392	264	298	329	--	26.12
Wood treated with								
MFFA/PP (3 phr)	232	332	427	294	321	357	406	7.2
MFFA/PP (1 phr)/ DMDHEU/nanoclay	260	352	444	327	351	378	450	17.4
MFFA/PP (2 phr)/ DMDHEU/nanoclay	267	357	449	334	357	383	456	18.0
MFFA/PP (3 phr)/ DMDHEU/nanoclay	273	363	455	340	362	390	461	19.1

4.5.10. Activation energy of thermal decomposition from TGA

TGA was performed at four different heating rates of 3, 5, 10 and 20 °C min^{-1}in a nitrogen atmosphere to find out the kinetic parameters of the composites, such as the activation energy. The higher the heating rate, the higher was the decomposition temperature (T_D). T_D was determined where the mass loss started to raise. This indicated that higher heating rate improved the thermal stability of the prepared composites [64-66].

At 10% of thermal degradation region (α = 0.1), the temperature of decomposition was determined at the four different heating rate. Similarly, the temperatures at various values of α were determined at different heating rate for all samples. The temperatures at α = 0.1, 0.2, 0.3, 0.4, 0.5, 0.6 and 0.7 were obtained for the untreated wood and wood treated withMFFA/PP (3phr),MFFA/PP (1phr)/DMDHEU/nanoclay,MFFA/PP (2 phr)/DMDHEU/nanoclayand MFFA/PP (3 phr)/DMDHEU/nanoclay. The values of α were selected between 0.1 and 0.7 andβ values from 3 °C min^{-1} to 20 °C min^{-1} to obtain the average activation energy. Log β was calculated and were plotted aslog β vs 1/T as shown in Figure4.5.10.a-e. The activation energy was obtained from the slope of this plot. It was observed that linear fittings were more closely spaced in the MFFA/PP/DMDHEU/nanoclay treated samples compared to those of untreated wood and wood treated with MFFA/PP (3phr). Moreover the linear fittings were more closely spaced with the increase in the

amount of PP. This indicated that the thermal stability and the decomposition temperature were controlled by the PP. Kim et al. observed that thermal stability and decomposition temperature decreased on increasing rice husk content in rice husk flour filled thermoplastic composite. They reported that linear fittings were broadly distributed with increase in the rice husk content [67].

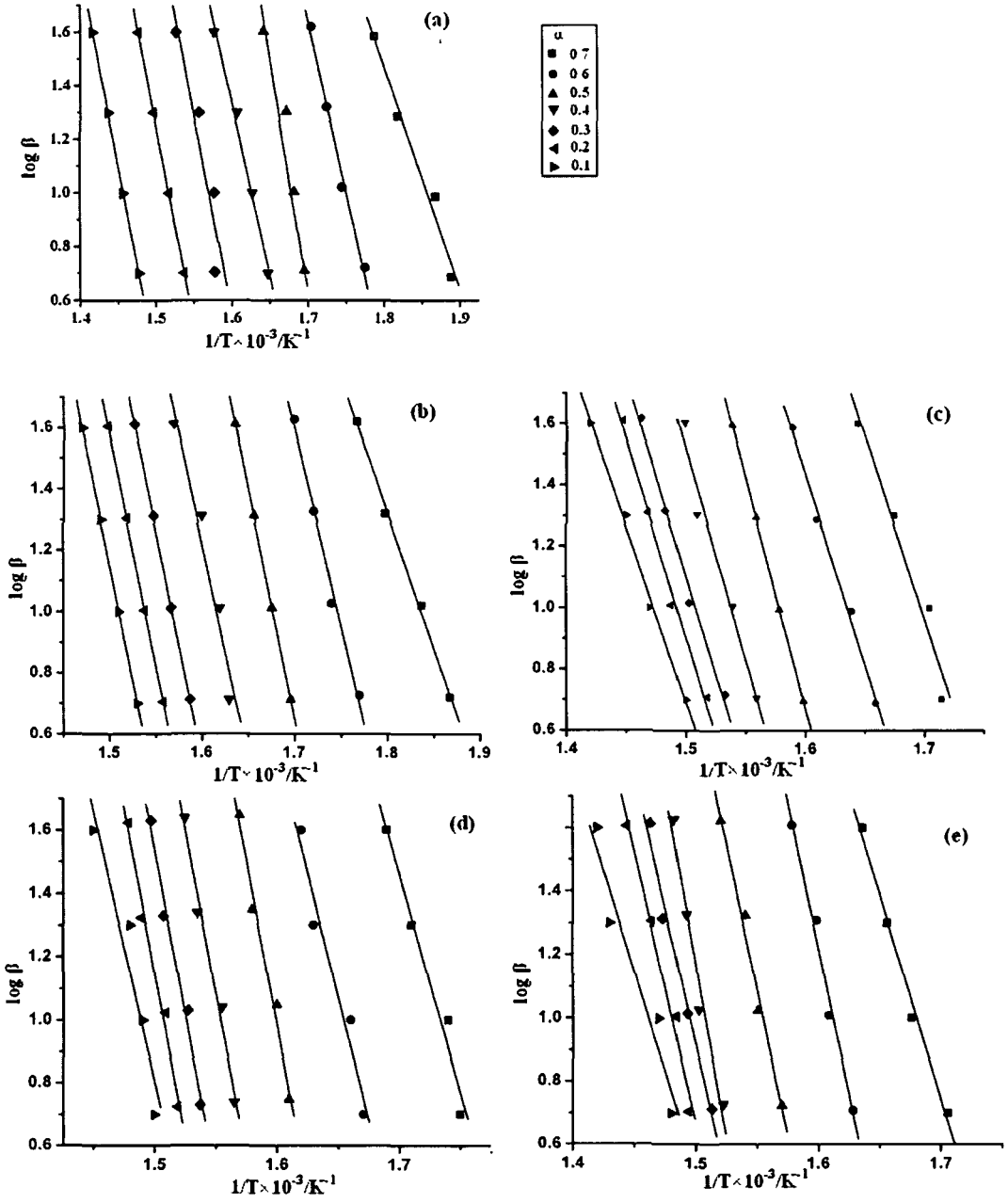

Figure4.5.10. Isoconversion curves of (a) Untreated wood and wood treated with (b) MFFA/PP (3phr) (c) MFFA/PP (1phr)/DMDHEU/nanoclay (d) MFFA/PP (2 phr)/DMDHEU/nanoclay (e) MFFA/PP (3 phr)/DMDHEU/nanoclay.

The activation energies of the prepared composites are represented in Figure 4.5.11. In all the cases, the activation energy decreased steeply upto $\alpha = 0.3$ and then it became constant. MFFA/PP/DMDHEU/nanoclaytreated samples had higher activation energy than the untreated wood and the MFFA/PP (3 phr) treated samples. Higher the amount of PP higher was the activation energy of the composites. The energy barrier, which prevented the polymer chain movement, was associated with the activation energy. The interfacial adhesion determined the interaction between the wood, polymers, crosslinker and nanoclay. The PP had abundant hydroxyl groups which resulted in an increase in the interaction between the wood, MFFA, DMDHEU and nanoclay. Hence it showed higher activation energy.

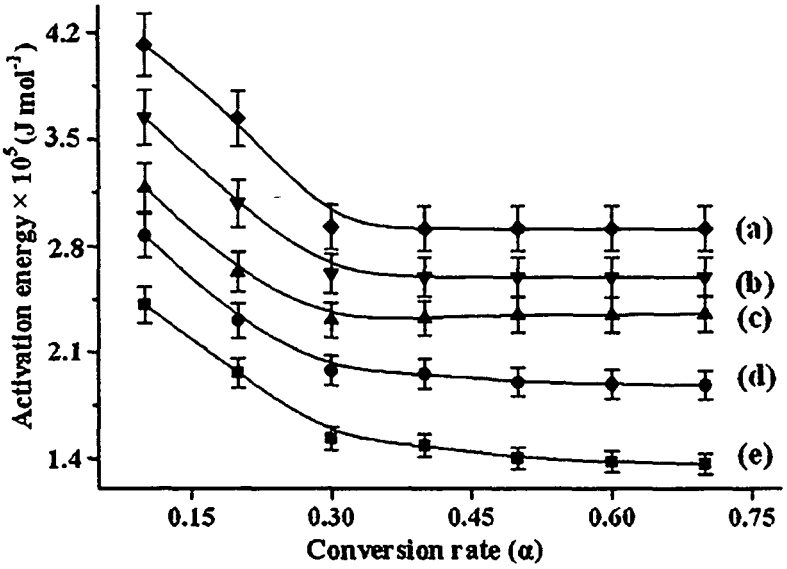

Figure4.5.11. Activation energy of thermal decomposition according to OFW method for wood samples treated with (a) MFFA/PP (3phr)/DMDHEU/nanoclay (b) MFFA/PP (2phr)/DMDHEU/nanoclay(c) MFFA/PP (1phr)/DMDHEU/nanoclay (d) MFFA/PP (3phr) (e) untreated wood.

4.5.10.1. E_α- α dependence

The variation of activation energy $E_a$with conversion α relates to the contributionsof parallel reaction channels to overall reaction kinetics and the change of reaction mechanisms [68]. From the conversion values,α is plotted as a function of T(t) for the different heating rate as shown in Figure 4.5.12.The conversional curves shifted to higher temperature with the increase in the heating rate suggesting that the reaction rate was a rising function of the temperature.

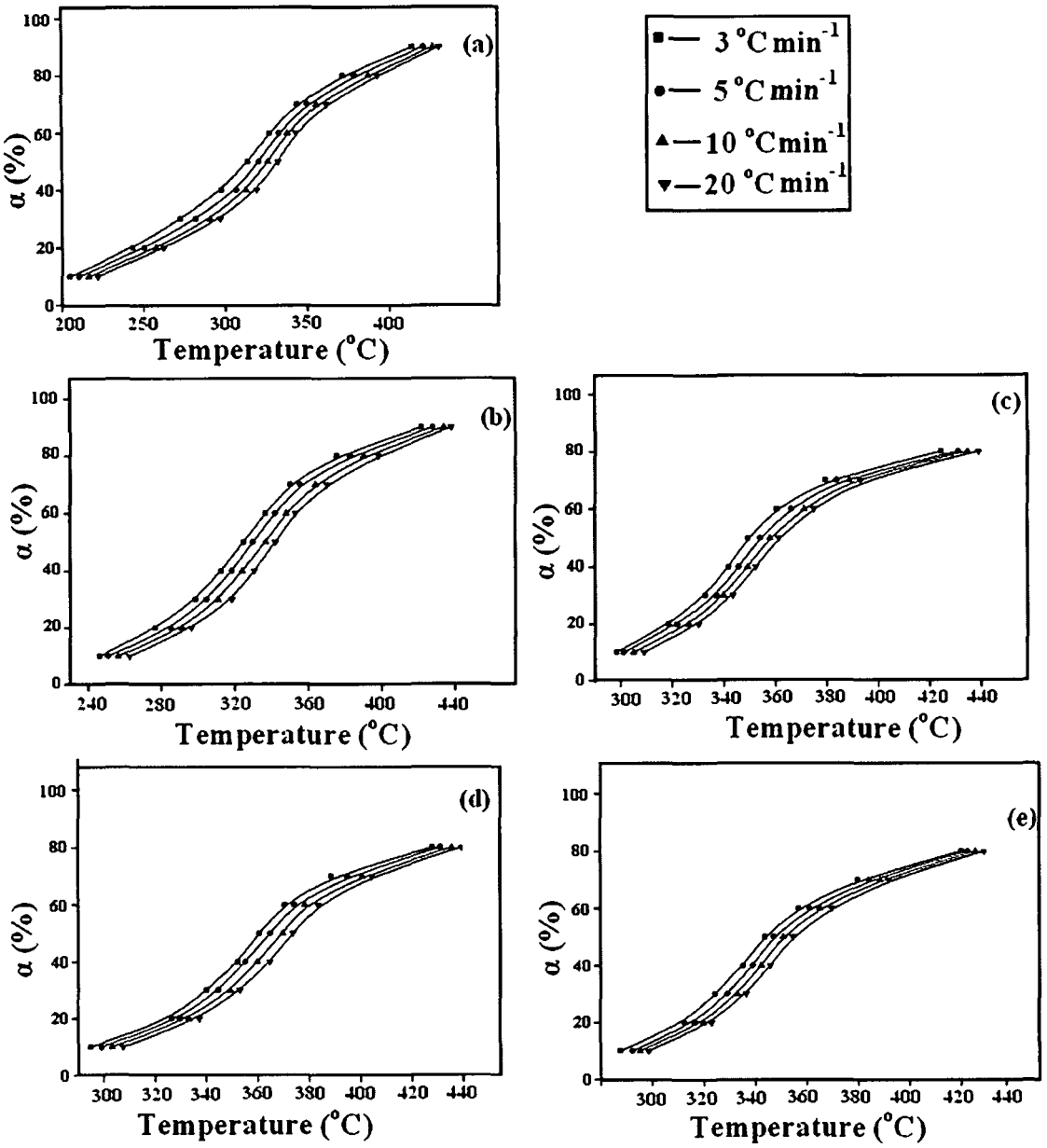

Figure 4.5.12. Variation of conversion (α)with T at heating rates(a) untreated wood and wood treated with (b) MFFA/PP (3phr) (c) MFFA/PP (1phr)/DMDHEU/nanoclay (d) MFFA/PP (2 phr)/DMDHEU/nanoclay (e) MFFA/PP (3 phr)/DMDHEU/nanoclay.

The α -T(t) values obtained from the graph were put in the equation (19) and (20) (Chapter III, Section 2.4.13., page no. 79).E_a was evaluated for each value of αby minimizing equation (19). Figure 4.5.13.shows the plot of E_a vs.α which indicated that the non-isothermal reaction followed multi-step mechanisms as $E_a$varies to a great extent with α [69]. The curves followed a similar trend as that obtained from OFW method but E_a-dependencies obtained evidently showed a systematic difference between OFW and

Vyazovkin methods. The treated samples showed higher E_a values than the untreated ones. The explanation was similar to that of described earlier.

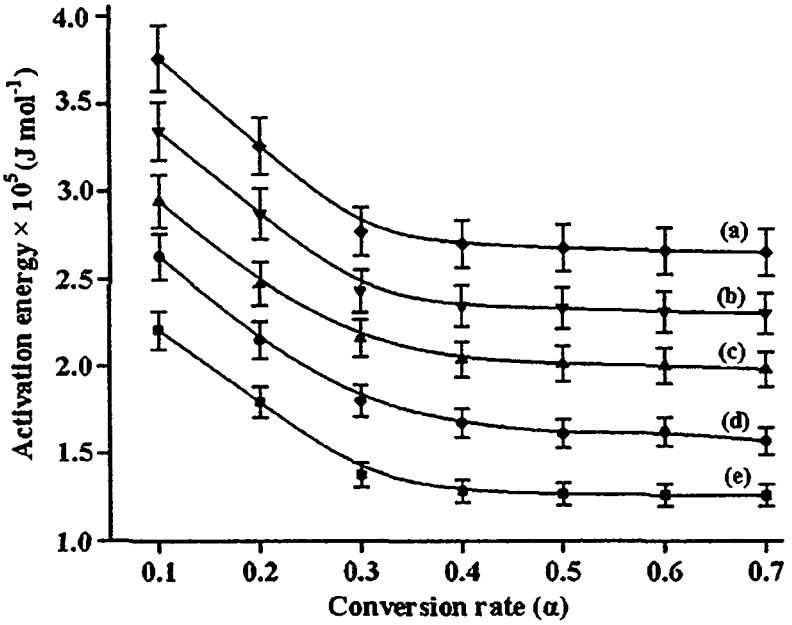

Figure 4.5.13. Activation energy of thermal decomposition according to Vyazovkin method for wood samples treated with (a) MFFA/PP (3phr)/DMDHEU/nanoclay (b) MFFA/PP (2phr)/DMDHEU/nanoclay(c) MFFA/PP (1phr)/DMDHEU/nanoclay (d) MFFA/PP (3phr) (e) untreated wood.

Section F: Melamine formaldehyde-acrylamide copolymer and plant polymer impregnated softwood polymer composite.

The objective of the work is to prepare melamine formaldehyde-acrylamide (MFA) copolymer and vacuum impregnate it into wood in presence of DMDHEU as crosslinker, vinyl trichloro silane (VTCS) modified MMT and plant polymer (PP) derived from *Moringa oleifera* as a flame retarding agent under catalyst heat treatment. The maximum improvement in properties was found by varying impregnation conditions like monomer concentration, initiator concentration, vacuum, time of impregnation, amount of crosslinking agent and modified MMT. The minimum ratio (v/v) of MFA and water used for the dispersion of clay was 5:1. The final optimized conditions, at which maximum improvement of properties were observed were as follows: MFA(mL): 100, water (mL): 20, $K_2S_2O_8$: 0.5 phr, vacuum: 508 mm of Hg, time of impregnation: 4 h, DMDHEU (mL): 3, MMT: 0.5-1.5phr.

4.6.RESULTS AND DISCUSSION

4.6.1. NMR study

Figure 4.6.1. represents the NMR spectrum of MFA and DMDHEU. In the NMR spectrum of MFA peaks appearing at 166.86 and 168.57 ppm were due to triazine carbon of methylol melamine and unsubstituted triazine nucleus. Peaks appearing at 167.63, 129.81, 62.12 and 48.32 ppm were assigned to carbonyl carbon, $-CH_2-CH_2-$, $-CH_2OH$ and $-NH-CH_2-N-$ respectively. The spectrum of DMDHEU showed signals at 159.88 ppm and 81.79 ppm due to the presence of carbonyl carbon and –CHOH respectively. Another peak at 64.02 ppm was appeared due to $-NHCH_2OH$ [70].

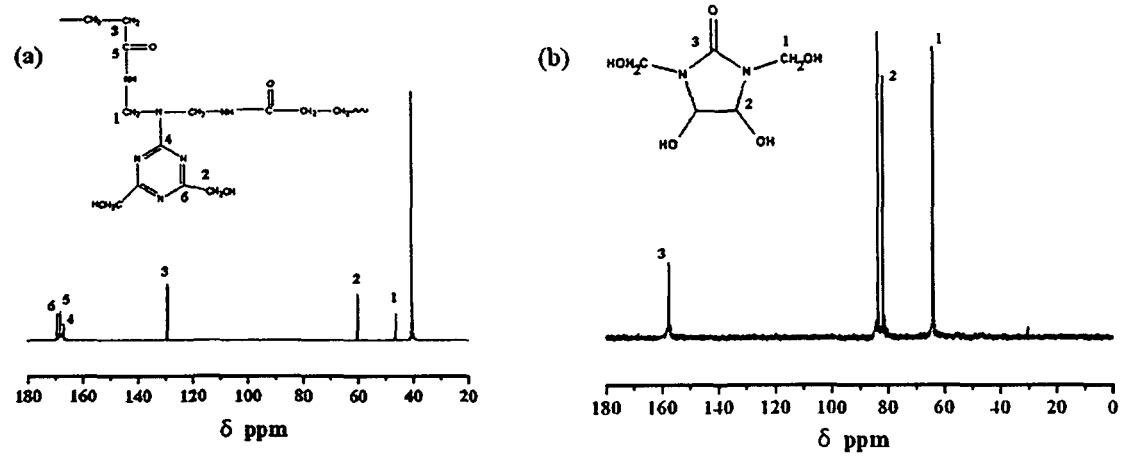

Figure 4.6.1. NMR spectra of (a) MFA copolymer (b) DMDHEU.

4.6.2. FTIR study

Figure 4.6.2 represents the FTIR spectrum of unmodified MMT, VTCS modified MMT, MFA, DMDHEU and PP. Unmodified MMT (curve-a) showed bands at 3431 cm^{-1} (–OH stretching), 1636 cm^{-1} (–OH bending) and 1052–532 cm^{-1} (oxide bands of Al, Mg, Si, etc.). The modified MMT (curve b) showed the presence of bands at 2927cm^{-1} and 2852 cm^{-1} (C-H stretching of modifying hydrocarbon),1477 cm^{-1} (CH_2 deformation) and 1046cm^{-1}, 526cm^{-1},468cm^{-1} (metal oxide bands Al, Mg, Si etc.). The absorption peaks for MFA (curve c) appeared at 3401 cm^{-1} (–OH stretching), 2920 cm^{-1} ($-CH_2$ stretching), 1672 cm^{-1} (-OH bending) and 1559 cm^{-1} (–NH stretching). DMDHEU (curve d) showed absorption bands at 3412 cm^{-1} (-OH stretching), 1702 cm^{-1} (carbonyl group stretching), 1241cm^{-1} ($-CH_2OH$

stretching), 1017cm^{-1} (–CHOH stretching) [37].The peaks for the PP appeared at 3326 cm^{-1} for -OH stretching, 2921 cm^{-1} and 2851 cm^{-1} for -CH_2 stretching, 1642 cm^{-1} for –OH bending and 1011cm^{-1} for R-O-Ar linkage (curve e) [71].

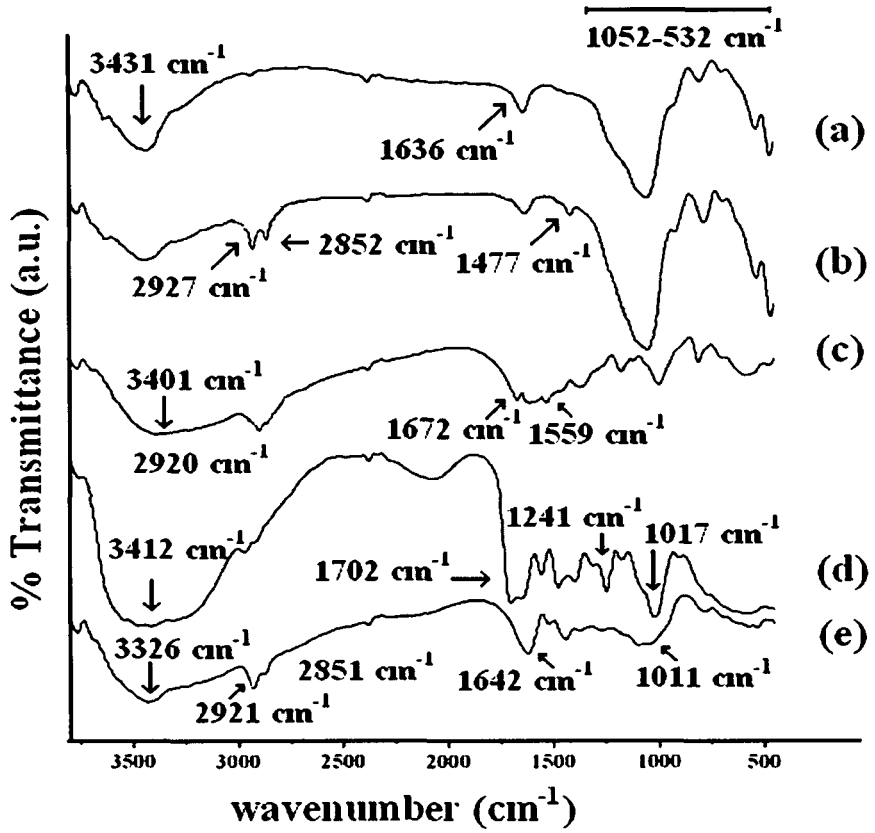

Figure 4.6.2.FTIR spectra of (a)unmodified MMT (b) VTCS modified MMT (c) MFA (d) DMDHEU (e) PP.

Figure 4.6.3. shows the FTIR spectra of untreated and treated wood samples loaded with different percentage of PP. Pure wood (curve a) was characterized by bands at 3439 cm^{-1} (–OH stretching), 2925 cm^{-1}, and 2852 cm^{-1} (–CH_2 asymmetric stretching), 1744 cm^{-1} (C=O stretching), 1662 cm^{-1} for (–OH bending), 1255 and 1026 cm^{-1} (C–O stretching) and 1,000–640 cm^{-1} (out of plane C–H bending vibration). In all the cases (curve b-e), it was observed that the intensity of –OH stretching peak of wood decreased and shifted to 3433 cm^{-1} (curve b), 3364 cm^{-1} (curve c), 3342 cm^{-1} (curve d), 3325 cm^{-1} (curve e). Besides this, the intensity of-CH_2 stretching peak appearing at 2925 cm^{-1}, and 2852 cm^{-1} for pure wood was also found to increase. This study confirmed the incorporation and interaction of hydroxyl peak of wood with the hydroxyl groups of MFA, DMDHEU, PP and MMT.

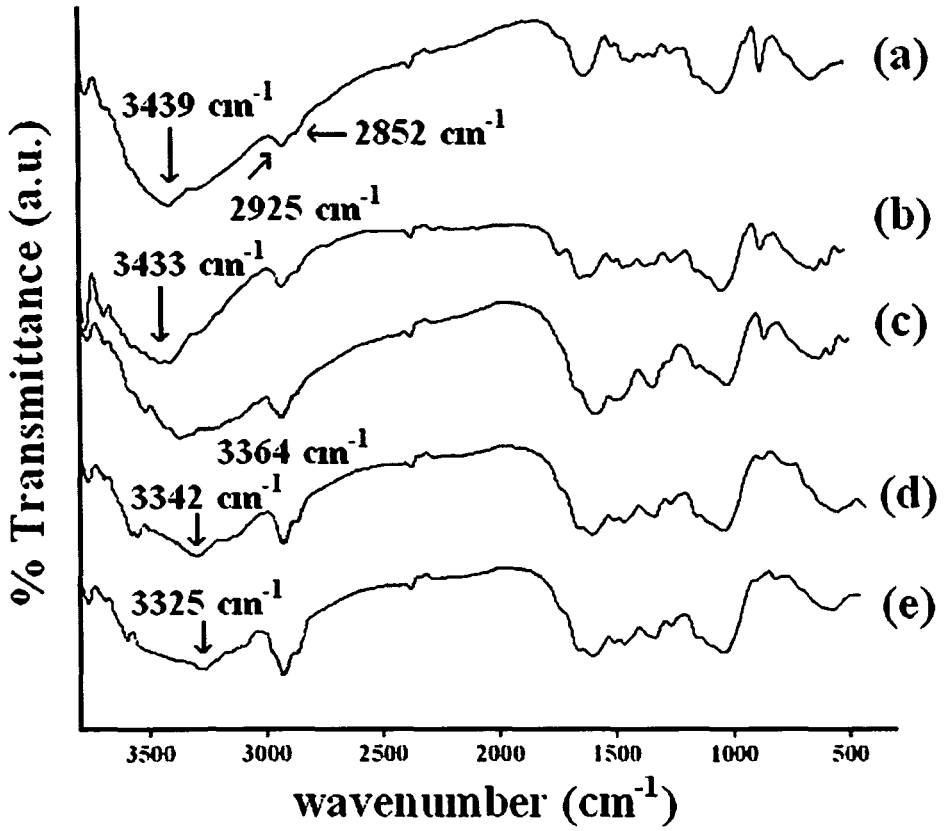

Figure 4.6.3.FTIR spectra of (a) untreated wood (b) MFA/PP (3 phr) treated (c) MFA/ DMDHEU/MMT/PP (1 phr) treated (d) MFA/ DMDHEU/MMT/PP (2 phr) treated (e) MFA/ DMDHEU/MMT/PP (3 phr) treated wood samples.

4.6.3. XRD analysis

Figure 4.6.4.shows the XRD spectra of unmodified and VTCS modified MMT. The diffraction peak for unmodified MMT appeared at $2\theta = 8.2°$ with a basal spacing of 1.07 nm as determined by the Bragg equation $2d\sin\theta = n\lambda$. The peak shifted to $2\theta = 6.7°$ for the VTCS modified MMT with a gallery distance of 1.4 nm. Thus it could be concluded that interlayer grafting of VTCS occurred efficiently to MMT through the silanol groups of VTCS and hydroxyl groups of MMT leading to an increase in basal spacing of the clay layers.

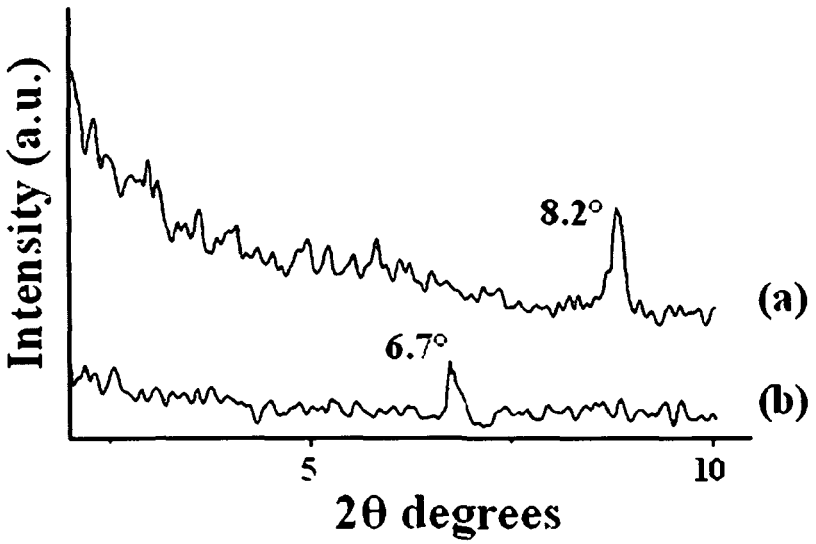

Figure 4.6.4.X-ray diffraction of (a) unmodified MMT (b) VTCS modified MMT.

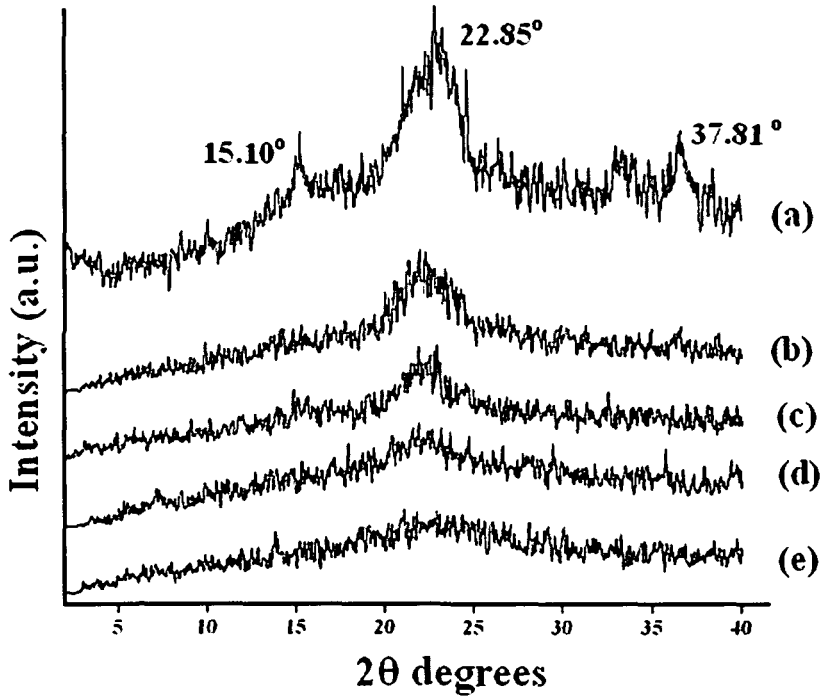

Figure 4.6.5.X-ray diffraction of (a) untreated wood and wood treated with (b) MFA/PP (3 phr) (c) MFA/ DMDHEU/nanoclay/PP (1 phr) (d) MFA/ DMDHEU/nanoclay/PP (2 phr) (e) MFA/DMDHEU/nanoclay/PP (3 phr).

Figure 4.6.5. shows the XRD spectra of untreated and treated wood samples. Untreated wood showed a wide peak at 22.85° (002 crystal plane)due to the abundant cellulose constituent of wood. Other small peaks appeared at 15.10° and37.81° were due to

the amorphous region of cellulose and 040 crystal plane of cellulose respectively (curve a) [7]. In the case of the composites, (curve b-e), it was observed that the intensity of the peak for 002 crystal plane at 22.85° decreased and other peaks at15.10° and37.81° disappeared suggesting a decrease of crystallinity due to impregnation. The diffraction peak of MMT appeared at 6.7° was found to disappear in the composites. It could be due to the full expansion of the gallery layers of MMT or the delamination of MMT layers [2].

4.6.4. Morphological studies

Figure 4.6.6. shows the scanning electron micrograph of untreated and treated wood samples. Untreated wood has empty cell walls and pits (Figure 4.6.6.a) which were filled up on treatment with MFA/PP (Figure 4.6.6.b). The presence of MMT could be detected by some white patches adhered to the cell wall for the samples treated with MFA/DMDHEU/PP/MMT (Figure 4.6.6.d).

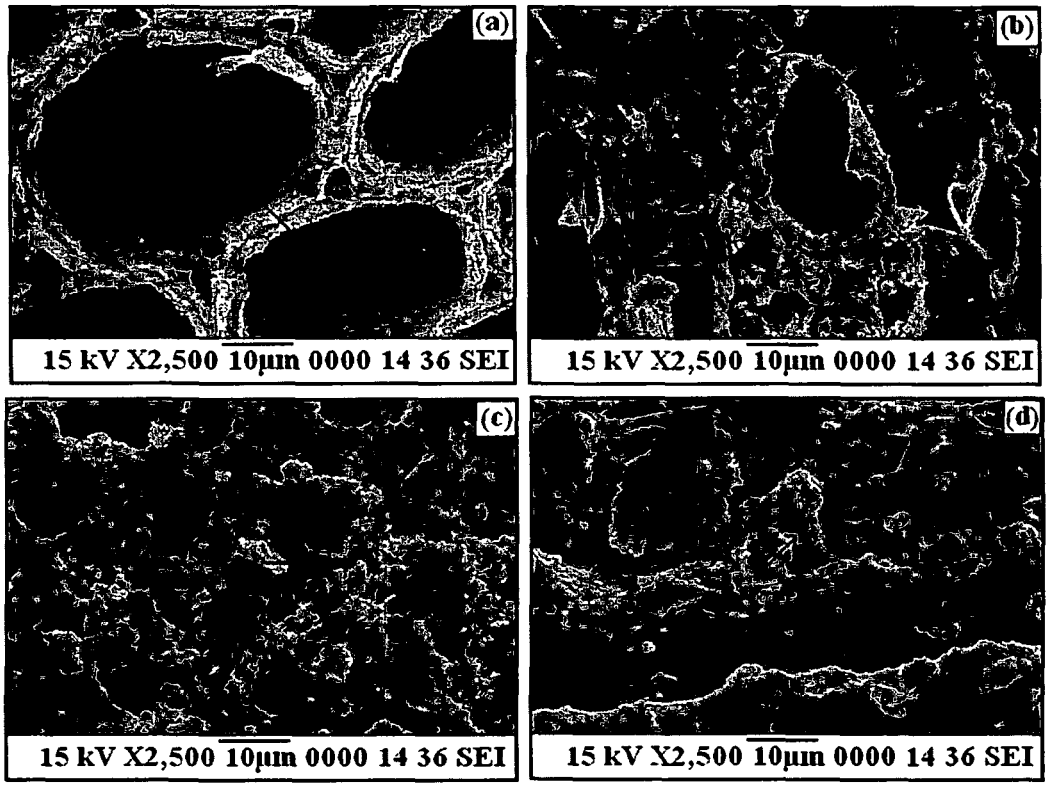

Figure 4.6.6. Scanning electron micrographs of wood (a) untreated wood and wood treated with (b) MFA/PP(c) MFA/ PP/DMDHEU (d) MFA/PP (3 phr)/DMDHEU/nanoclay.

4.6.5. Transmission electron microscopy

Transmission Electron micrograph of wood treated with MFA/PP and MFA/DMDHEU/PP/MMT are shown in Figure 4.6.7. No orientation of cell wall components was observed in case of samples treated with MFA/PP (Figure 4.6.7.a). The dispersion of MMT in the cell wall of wood could be seen as dark slices for the samples treated with MFA/DMDHEU/PP/MMT (Figure 4.6.7.b).

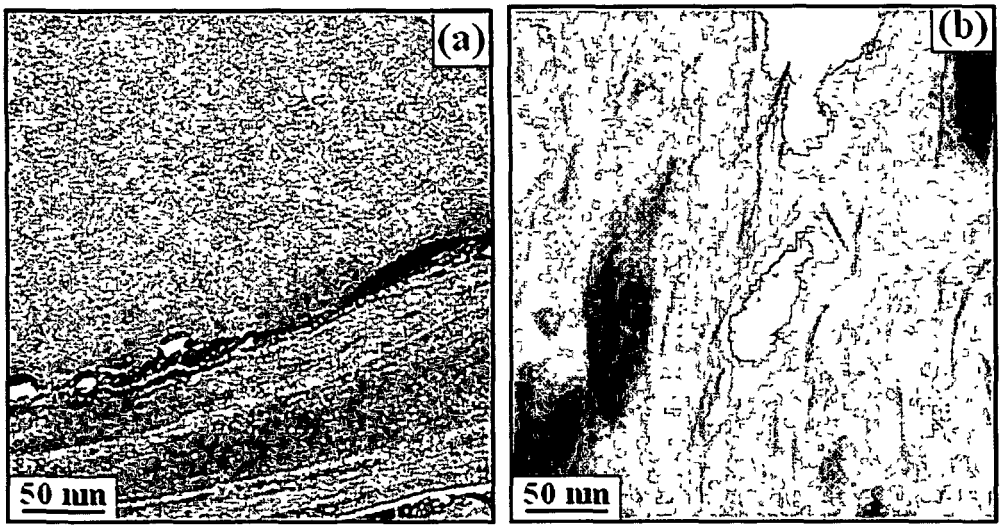

Figure 4.6.7. Transmission electron micrographs of (a) MFA/PP treated (b) MFA/PP (3 phr)/DMDHEU/nanoclay.

4.6.6. Effect of variation of plant polymer (PP) on polymer loading (WPG %), volume increase and hardness

Table 4.6.1 shows the results of variation of PP on polymer loading (WPG %), volume increase and hardness.The properties like polymer loading (WPG %), volume increase and hardness improved on impregnation with polymer. The void spaces and capillaries of wood were occupied by polymer on treatment with MFA/PP. The deposition of polymer was enhanced when DMDHEU was added. DMDHEU could form a crosslinked structure by reacting with the hydroxyl group of wood and plant polymer [41]. Addition of MMT further improved its properties. The polymer chains were intercalated in between the layers of clay thereby restricting its mobility. With the increase in the amount of PP, the polymer loading (WPG %), volume increase and hardness was also found to increase. The

PP had abundant hydroxyl groups as its main constituents are L-arabinose, D-galactose, D-glucuronic acid, L-rhamnose, D-mannose and D-xylose. The interaction of hydroxyl groups with the polymer, MMT and wood further facilitated the deposition of polymer.

Table 4.6.1. Effect of variation of plant polymer on polymer loading (WPG %), volume increase and hardness.

Samples particulars	Weight % gain	Volume increase %	Hardness (Shore D)
Untreated wood	_	_	47(±.75)
Wood treated with			
MFA/PP (3 phr)	20.38 (±0.5)	1.52 (±0.2)	49(±0.9)
MFA/PP (1 phr)/DMDHEU/MMT	27.57 (±0.43)	2.37 (±0.7)	54 (±.81)
MFA/PP (2 phr)/DMDHEU/MMT	29.13 (±0.21)	2.67 (±0.2)	56 (±.0.6)
MFA/PP (3 phr)/DMDHEU/MMT	31.09(±0.03)	2.91(±0.34)	69 (±0.45)

4.6.7. Water absorption test

Figure 4.6.8.shows the water absorption test of untreated and treated wood samples. It was observed that water absorption was found to increase with the increase in time of

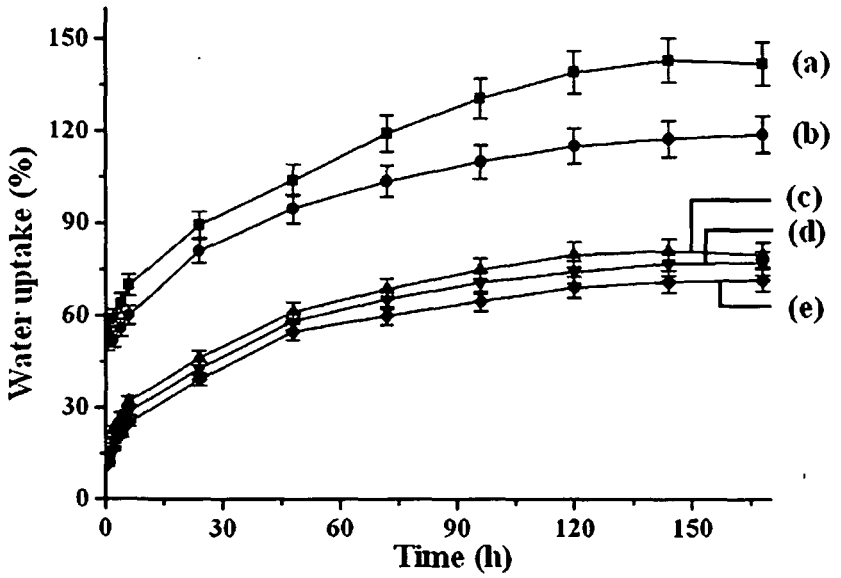

Figure 4.6.8. Water absorption test of wood (a) untreated wood and wood treated with (b) MFA/PP (3 phr) (c) MFA/ DMDHEU/nanoclay/PP (1 phr) (d) MFA/ DMDHEU/ nanoclay/PP (2 phr) (e) MFA/ DMDHEU/nanoclay/PP (3 phr).

immersion. Untreated wood showed maximum absorption capacity. Samples treated with MFA/PP showed less water absorption capacity than the untreated ones. DMDHEU could crosslink with the cellwall of wood and polymer through its hydroxyl groups leading to further decrease in water uptake capacity of the samples [41]. Addition of MMT would provide a tortuous path for the transmission of water molecules through the samples. With the increase in the amount of PP, a decreasing trend for the water uptake capacity of the samples was noticed. This was due to the formation of network structure caused by the interaction of wood, MFA, DMDHEU and MMT.

4.6.8. Chemical resistance test

The treated wood samples showed higher chemical resistance than the untreated wood samples as shown in Table 4.6.2.It was observed that higher swelling of the samples occurred in sodium hydroxide environment compared to that of acetic acid medium. This might be due to interaction of sodium hydroxide with the wood cellulose and MMT [2]. Samples treated with MFA/PP/DMDHEU/MMT showed less swelling than the samples treated with MFA/PP. This might be due to the increase in interfacial interaction provided by DMDHEU and the tortuous path provided by the silicate layers for diffusion of chemicals into the composites. With the increase in the amount of PP, the chemical resistance further enhanced due to its improved interaction with wood, polymer and MMT.

Table 4.6.2. Chemical resistance test of untreated and treated wood samples.

Medium	Time (h)	%swelling after immersion				
		Untreated wood	Wood treated with			
			MFA/PP (3phr)	MFA/PP (1phr)/ MMT/ DMDHEU	MFA/PP (2phr)/ MMT/ DMDHEU	MFA/PP (3phr)/ MMT/ DMDHEU
4% NaOH	24	11.03	5.93	4.19	3.97	3.88
	168	12.98	6.88	6.03	5.89	5.74
4% acetic acid	24	8.36	5.13	4.92	4.43	4.22
	168	10.32	7.02	5.32	5.14	5.01

4.6.9. Limiting oxygen index (LOI) study

LOI values of treated and untreated wood are summarized in Table 4.6.3. Samples treated with MFA/PP showed higher LOI values than the untreated wood samples. The nitrogen content of melamine and the presence of phosphorus (4.3 wt. %) in PP was responsible for showing higher LOI value [62]. During combustion, oxides of nitrogen and phosphorus were produced which replaced the oxygen present on the surface of the samples and hence enhanced the flame retardancy of the composites. DMDHEU could provide interaction between the polymer and wood and is also a nitrogen supplier. MMT improved the flame retardancy of the composites by providing char formation. Char protected the sample from burning and decreased the rate of mass loss [43]. When the content of PP was increased, a further improvement in flame retardancy was observed. This was due to the presence of phosphorus in PP.

4.6.10.Thermal properties

The initial decomposition temperature (T_i), maximum pyrolysis temperature (T_m), decomposition temperature at different weight loss (%) (T_D) and residual weight (RW %) for the untreated wood and WPCs are shown in Table 4.6.3. A higher T_i value was observed for the polymer treated wood samples. The value increased after incorporation of DMDHEU and MMT. DMDHEU facilitated higher interfacial interaction between the wood and polymer leading to formation of networked structure. MMT dispersed in the polymer matrix delayed the decomposition process as the silicate layers acted as a mass transport barrier for the diffusion of volatile products that were produced during decomposition throughout the composite [11].T_i value was found to increase with the increase in the amount of PP upto 3 phr. The phosphorus content of PP was responsible for showing higher T_i value [62].

Treated samples showed higher T_m and T_D values than the untreated wood samples. The interaction of MFA, DMDHEU, MMT, PP and wood led to higher thermal stability of the treated wood samples. The first stage T_m values for both the untreated and treated wood samples was due to decomposition of cellulose and hemicellulose of wood. The second stage of decomposition was due to degradation of polymer. Higher the amount of PP, higher was the thermal stability of the composites.

Samples treated with MFA/DMDHEU showed least RW value whereas highest RW value was shown by untreated wood samples. Addition of MMT would again increase the RW values of the composites.

Table 4.6.3. Thermal degradation and flammability of untreated and treated wood samples.

Sample	T_i	T_m[a]	T_m[b]	Temperature of decomposition (T_D) in °C at different weight loss (%)				RW% at 600 °C	LOI (%) (±SD)
				20	40	60	80		
Untreated wood	155	296	377	253	279	310	_	25.5	22 (±0.62)
Wood treated with									
MFA/PP(3phr)	221	319	401	278	313	335	_	7.5	27 (±0.77)
MFA/DMDHEU/PP(1phr)/MMT	242	339	426	297	323	342	422	14.1	30 (±0.26)
MFA/DMDHEU/PP(2phr)/MMT	246	345	431	304	327	357	428	13.4	32 (±0.85)
MFA/DMDHEU/PP(3phr)MMT	250	349	435	307	332	366	433	13.6	35 (±0.95)

4.6.11.Mechanical properties

Table 4.6.4. represents the tensile and flexural values of untreated wood and WPCs. The interaction between polymer and wood was accountable for improved mechanical properties of MFA/PP treated wood than the untreated wood samples. DMDHEU and MMT further improved the tensile and flexural values. DMDHEU provided improved interaction as it could crosslink with the cell wall of wood through its hydroxyl groups [41]. The polymer chains lost their mobility when MMT was added to the composites. They were intercalated in between the layers of clay and hence the composites were stiffened. The properties enhanced with the increase in the amount of PP in the composites due to higher interaction between the impregnates and wood.

Table 4.6.4. Flexural and tensile properties of untreated and treated wood.

Sample	Flexural properties		Tensile properties	
	Strength (MPa)	Modulus (MPa)	Strength (MPa)	Modulus (MPa)
Untreated wood.	116.21 (±1.25)	5855.69 (±0.53)	37.03 (±1.23)	276.64 (±5.21)
Wood treated with MFA/PP(3phr)	123.71 (±2.38)	6232.92 (±0.91)	45.25 (±2.29)	334.51(±6.61)
MFA/PP(1phr)/DMDHEU/MMT	129.21 (±1.57)	6510.41 (±1.42)	52.31 (±1.51)	387.02 (±4.55)
MFA/PP(2phr)/DMDHEU/MMT	130.28 (±0.81)	6564.76 (±1.61)	54.96 (±1.45)	406.18 (±6.15)
MFA/PP(3phr)/DMDHEU/MMT	132.12 (±1.39)	6657.31 (±1.27)	55.42 (±2.65)	410.10 (±7.25)

REFERENCES

1. Zhang, S.Y.Wood specific gravity-mechanical relationship at species level property, *Wood Sci. Technol.* **31** (3), 181-191, 1997.

2. Devi, R.R.& Maji, T.K. Preparation and characterization of wood/styrene-acrylonitrile co-polymer/MMT nanocomposite, *J. Appl. Polym. Sci.***122** (3), 2099-2109, 2011.

3. Yap, M.G.S., et al. FTIR characterization of tropical wood-polymer composites, *J. Appl. Polym. Sci.***43** (11), 2083-2090, 1991.

4. Deka, B.K.& Maji, T.K. Study on the properties of nanocomposite based on high density polyethylene, polypropylene, polyvinyl chloride and wood, *Compos. Part A***42** (6), 686-693, 2011.

5. Zhong, Y., et al. Synthesis and rheological properties of polystyrene/layered silicate nanocomposite, *Polymer***46** (9), 3006-3013, 2005.

6. Tomar, A.K., et al. Structural characterization of PMMA blended with chemically synthesized PAni, *Adv. Appl. Sci. Res.***2** (3), 327-333, 2011.

7. Lu, W.H., et al. Preparation and characterization of wood/montmorillonite nanocomposites,*For. Stud. China***8** (1), 35-40, 2006.

8. Devi, R.R., et al. Studies on dimensional stability and thermal properties of rubber wood chemically modified with styrene and glycidyl methacrylate, *J. Appl. Polym. Sci.***93** (4), 1938-1945, 2004.

9. Cai, X., et al. The impact of the nature of nanofillers on the performance of wood polymer nanocomposites,*Compos. Part A***39** (5), 727-737, 2008.

10. Devi, R.R.& Maji, T.K. Chemical modification of simul wood with styrene–acrylonitrile copolymer and organically modified nanoclay, *Wood Sci. Technol.***46** (1-3),299-315, 2012.

11. Qin, H., et al. Thermal stability and flammability of polypropylene/montmorillonite composites, *Polym. Degrad. Stab.***85** (2), 807-813, 2004.

12. Fung, K.L., et al. Interface modification on the properties of sisal fiber- reinforced polypropylene composites, *J. Appl. Polym. Sci.***85** (1), 169-176, 2002.

13. Zhu, J., et al. Thermal stability and flame retardancy of poly(methyl methacrylate)-clay nanocomposites,*Polym. Degrad. Stab.*77 (2), 253-258, 2002.

14. Cho, Y.W., et al. PVA containing chito-oligosaccharide side chain, *Polymer* **41** (6), 2033-2039, 2000.

15. Lori, J.A., et al.Structural and adsorption characteristics of carbon adsorbent synthesized from polyfurfuryl alcohol with kaolinite template,*Res. J. Appl. Sci. Eng. Technol.***3** (5), 440-446, 2011.

16. Fang, Y., et al. Facile and quick synthesis of poly(N -Methylolacrylamide)/polyhedral oligomeric silsesquioxane graft copolymer hybrids via frontal polymerization, *J. Polym. Sci. Part A: Polym. Chem.***47** (4), 1136-1147, 2009.

17. Zhao, Y., et al. Properties of poly(vinyl chloride)/wood flour/montmorillonite composites: Effects of coupling agents and layered silicate, *Polym. Degrad. Stab.***91** (12), 2874-2883, 2006.

18. Hazarika, A., et al. Studies on properties of softwood (*Ficus hispida*)/PMMA nanocomposites reinforced with polymerizable surfactant-modified nanoclay, *Polym. Bull.***68** (7), 1989-2008, 2012.

19. Lu, W.H.& Zhao, G.J. Structure and characterization of Chinese fir (*Cunninghamia lanceolata*) wood/MMT intercalation nanocomposite (WMNC), *Front. For. China***3** (1), 121-126, 2008.

20. Esteves, B., et al. Properties of furfurylated wood (*Pinus pinaster*), *Eur. J. Wood Prod.***69** (4), 521-525, 2011.

21. Qiu, R., et al. Effect of fiber modification with a novel compatibilizer on the mechanical properties and water absorption of hemp-fiber-reinforced unsaturated polyester composites, *Polym. Eng. Sci.***52** (6), 1342-1347, 2012.

22. Lee, H.& Kim, D.S. Preparation and physical properties of wood/polypropylene/clay nanocomposites, *J. Appl. Polym. Sci.***111** (6), 2769–2776, 2009.

23. Huda, M.S., et al. Wood-fiber-reinforced poly (lactic acid) composites: evaluation of the physicomechanical and morphological properties, *J. Appl. Polym. Sci.* **102** (5), 4856–4869, 2006.

24. Lin, Q., et al. Some studies on mechanical properties of wood flour/continuous glass mat/polypropylene composite, *J. Appl. Polym. Sci.* **85** (3), 536–544, 2002.

25. Camino, G., et al. Thermal and combustion behaviour of layered silicate–epoxy nanocomposite,*Polym. Degrad. Stab.***90** (2), 354-362, 2005.

26. Deka, B.K., et al. Study on properties of nanocomposites based on HDPE, LDPE, PP, PVC, wood and clay, Polym. Bull. **67** (9), 1875-1892, 2011.

27.Qin, H., et al. Thermal stability and flammability of polypropylene/montmorillonite composites, *Polym. Degrad. Stab.***85** (2), 807–813, 2004.

28. Gindl, W., et al. Impregnation of softwood cell walls with melamine-formaldehyde resin, *Bioresour. Technol.***87** (3), 325-330, 2003.

29. Zhang, Y., et al. Dimensional stability of wood–polymer composites, *J. Appl. Polym. Sci.*, **102** (6), 5085 (2006).

30. Lee, S., et al. *In situ* formation of new crosslinking agents from acrylate derivatives and bisepoxides, *J. Polym. Sci. Part A: Polym. Chem.* **28** (3), 525-549, 1990.

31. Chuang, I.S.& Maciel, G.E. Carbon-13 NMR study of curing in furfuryl alcohol resins, *Macromolecules***17** (5), 1087-1090, 1984.

32. Mercer, A.T.& Pizzi, A. A ^{13}C-NMR analysis method for MF and MUF resins strength and formaldehyde emission from wood particleboard. I. MUF resins, *J. Appl. Polym. Sci.***61** (10), 1687-1695, 1996.

33. Angelatos, A.S., et al. NMR structural elucidation of amino resins, *J. Appl. Polym. Sci.***91** (6),3504-3512, 2004.

34. Hermanns, K., et al. Identifying extractible resin fragments in durable press cotton by ^{13}C-NMR spectroscopy, *Text. Res. J.***56** (6), 343-346, 1986.

35. Baraka, A., et al. Preparation and characterization of melamine–formaldehyde–DTPA chelating resin and its use as an adsorbent for heavy metals removal from wastewater,*React. Funct. Polym.***67** (7), 585–600, 2007.

36.Kashi, T.S.J., et al. Effect of water on HEMA concersion by FT-IR spectroscopy, *J. Dent. Tehran university of Medical Sciences*, **4** (3),123-129, 2007.

37. Jang, T.R., et al. Crosslinking of cotton fabrics premercerized with different alkalis, part III: crosslinking and physical properties of DMDHEU-treated fabrics, *Text. Res. J.***63** (11), 679-686, 1993.

38. Awal, A., et al. Thermal properties and spectral characterization of wood pulp reinforced bio-composite fibers, *J.Them. Anal. Calorim.***99** (2), 695-701, 2010.

39. Deka, B.K., et al. Effect of different compatibilisers and nanoclays on the physical properties of wood (*Phragmites karka*)–polymer composites, *Polym. Renew. Resour.***2** (3), 87-103, 2011.

40. Song, C., et al. Preparation and gas separation properties of poly(furfuryl alcohol)-based C/CMS composite membranes, *Sep. Purif. Technol.***58** (3), 412-418, (2008).

41. Xie, Y., et al. Effects of chemical modification of wood particles with glutaraldehyde and 1,3-dimethylol-4,5-dihydroxyethyleneurea on properties of the resulting polypropylene composites, *Compos. Sci. Technol.***70** (13), 2003–2011, 2010.

42. Wu, W.& Yang, C.Q. Statistical analysis of the performance of the flame retardant finishing system consisting of a hydroxy-functional organophosphorus oligomer and the mixture of DMDHEU and melamineformaldehyde resin,*Polym. Degrad. Stab.***85** (1), 623-632, 2004.

43. Gilman, J.W., et al. Flammability properties of polymer-layered-silicate nanocomposites: Polypropylene and polystyrene nanocomposites, *Chem. Mater.***12** (7), 1866-1873, 2000.

44. Wada, M., et al. Synchrotron-radiated X-ray and neutron diffraction study of native cellulose, *Cellulose***4** (3), 221-232, 1997.

45. Marcivich, N.E., et al. Modified wood flour as thermoset fillers II. Thermal degradation of wood flours and composites, *Therm. Chem. Acta***372** (1-2), 45-57, 2001.

46. Shiraishi, N., et al. Preparation of higher aliphatic acid esters of wood in an N_2O_4–DMF cellulose solvent medium, *J. Appl. Polym. Sci.***24** (12), 2347-2359, 1979.

47. Grigoriadou, I., et al. Effect of different nanoparticles on HDPE UV stability, *Polym. Degrad. Stab.***96** (1), 151-163, 2011.

48. Patachiaa, S., et al. Effect of UV exposure on the surface chemistry of wood veneers treated with ionic liquids, *Appl. Surf. Sci.* **258** (18), 6723– 6729, 2012.

49. Dieste, A., et al. Physical and mechanical properties of plywood produced with 1.3-dimethylol-4.5-dihydroxyethyleneurea (DMDHEU)-modified veneers of *Betula sp.* and *Fagus sylvatica, Holz Roh Werkst***66**(4),281–287, 2008.

50. Islam, M.S., et al. Tropical wood polymer nanocomposite (WPNC): The impact of nanoclay on dynamic mechanical thermal properties, *Compos. Sci. Technol.* **72** (16), 1995-2001, 2012.

51. Romanzini, D., et al. Influence of fiber content on the mechanical and dynamic mechanical properties of glass/ramie polymer composites, *Mater. Des.***47**, 9–15, 2013.

52. Hristov, V.& Vasileva, S. Dynamic mechanical and thermal properties of modified wood fiber poly(propylene) composites, *Macromol. Mater. Eng.***288** (10), 798-806, 2003.

53. Saiter, A., et al. Cooperative rearranging regions in polymeric materials: Relationship with the fragility of glass-forming liquids, *Eur. Polym. J.***42** (1), 213–219, 2006.

54. Roudaut, G., et al. Can dynamical mechanical measurements predict brittle fracture behaviour?*Rheol. Acta***44** (1), 104-111, 2004.

55. Ornaghi, H.L., et al. Mechanical and dynamic mechanical analysis of hybrid composites molded by resin transfer moulding, *J. Appl. Polym. Sci.***118** (2), 887–896, 2010.

56. Clausen, C. A. Bacterial associations with decaying wood: a review, *Int. Biodeter. Biodegr.***37** (1-2), 101-107, 1996.

57. El-Hanafy, A.A., et al. Molecular characterization of two native Egyptian ligninolytic bacterial strains, *J. Appl. Sci. Res.***4** (10), 1291-1296, 2008.

58. Karak, N. Polymer (epoxy) clay nanocomposites, *J. Polym. Mater.***23** (1), 1-20, 2006.

59. Alvarez, V.A., et al. Degradation of sisal fibre/Mater Bi-Y biocomposites buried in soil, *Polym. Degrad. Stab.***91** (12), 3156-3162, 2006.

60. Deka, B.K. & Maji, T.K. Effect of coupling agent and nanoclay on properties of HDPE, LDPE, PP, PVC blend and phargamites karka nanocomposite, *Compos. Sci. Technol.***70** (12), 1755-1761, 2010.

61. Jana, T., et al. Biodegradable film modification of the biodegradable film for fire retardancy, *Polym. Degrad. Stab.***69** (1), 79-82, 2000.

62. Ghosh, S.N.& Maiti, S. Adhesive performance, flammability evaluation and biodegradation study of plant polymer blends, *Eur. Polym. J.***34** (5-6), 849-854, 1998.

63. Qin, H., et al. Thermal stability and flammability of polypropylene/montmorillonite composites,*Polym. Degrad. Stab.***85** (2), 807–813, 2004.

64. Doh, G.H., et al. Thermal behavior of liquefied wood polymer composites (LWPC), *Compos. Struct.***68** (1), 103–108, 2005.

65. Kim, H.J.& Eom, Y.G. Thermogravimetric analysis of rice husk flour for a new raw material of lignocellulosic fiber-thermoplastic polymer composites, *Mokchae Konghak***29** (1), 59-67, 2001.

66. Yao, F., et al. Thermal decomposition kinetics of natural fibers: Activation energy with dynamic thermogravimetric analysis, *Polym. Degrad. Stab.***93** (1), 90-98, 2008.

67. Kim, H.S., et al. Thermogravimetric analysis of rice husk flour filled thermoplastic polymercomposites, *J. Therm. Anal. Calorim.***76** (2), 395–404, 2004.

68. Hsiue, G.H., et al. Chemical modification of dicyclopentadiene-based epoxy resins to improve compatibility and thermal properties, *Polym. Degrad. Stab.***73** (2), 309–318, 2001.

69. Vyazovkin, S.& Sbirrazzuoli, N. Isoconversional method to explore the mechanism and kinetics of multi-step epoxy cures,*Macromol. Rapid Commun.***20** (7), 387–389, 1999.

70. Angelatos, A.S., et al. NMR structural elucidation of amino resins,*J. Appl. Polym. Sci.***91** (6), 3504-3512, 2004.

71. Ghosh, S.N., et al. Characterization of a flame retardant plant polymer and its Influence on the properties of rubber vulcanizate,*Int. J. Polym. Mater.***48** (1), 79-97, 2000.

CHAPTER V

RESULTS & DISCUSSION

CHAPTER V

RESULTS & DISCUSSION

Section A: Effect of ZnO and nanoclay on the properties of softwood chemically modified with melamine formaldehyde-furfuryl alcohol/plant polymer.

Zinc oxide (ZnO) is a widely used metal oxide nanoparticles that enhances mechanical, thermal, UV resistance along with other physical properties of the composites. The literatures based on wood polymer clay nanocomposites are available. However far less are available on the study of the combined effect of clay and metal oxide nanoparticles. The present work is aimed to prepare wood polymer nano composites (WPNC) by impregnating nano ZnO and nanoclay by impregnation of melamine formaldehyde-furfuryl alcohol (MFFA) copolymer, 1,3-dimethylol 4,5-dihydroxy ethylene urea (DMDHEU), a crosslinking agent and a renewable polymer obtained as a gum from the plant *Moringa oleifera* under vacuum condition. The present work is focused on the study of the effect of ZnO, plant polymer (PP) and nanoclay on the physical mechanical, flame retardancy, thermal and ultraviolet (UV) resistance properties of wood composites. Various parameters like vacuum, time of impregnation, monomer concentration, initiator concentration, amount of crosslinking agent, nanoclay, PP were varied to obtain optimum properties. The conditions, at which highest enhancement of properties were obtained, were 500mm Hg vacuum, 6 h time of impregnation, 5:1 (MFFA:FA-water) prepolymer concentration, 1% (w/w) maleic anhydride, 3 ml DMDHEU, 3 phr nanoclay and 3 % (w/v) PP.

5.1. RESULTS AND DISCUSSION

5.1.1. Fourier transform infrared (FTIR) spectroscopy study

Figure 5.1.1. represents the FTIR analysis of (a) MFFA (b) DMDHEU (c) PP (d) nanoclay (e) ZnO (f) N-Cetyl-N,N,N-trimethyl ammonium bromide (CTAB) modified ZnO. MFFA copolymer (curve a) showed bands at 3404 cm^{-1} (-OH stretching), 1566 cm^{-1} and 1508 cm^{-1} (furan ring vibration), 1186 cm^{-1} (C-N stretching) and 813 cm^{-1} (out plane trisubstitution of triazine ring) [1]. The absorption bands exhibited by DMDHEU (curve b) at 3418, 1702, 1245, 1021 cm^{-1} were for -OH stretching, C=O stretching, -CHOH stretching, $-CH_2OH$ stretching respectively [2]. The PP (curve c) showed bands at 3431 cm^{-1} (-OH

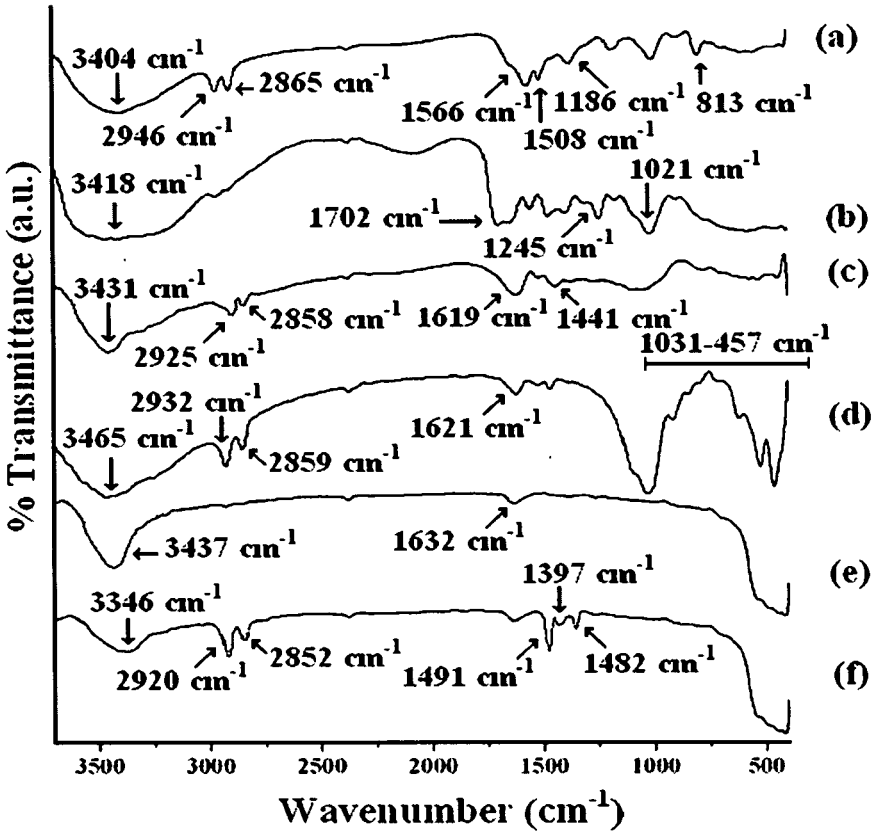

Figure 5.1.1. FTIR spectra of (a) MFFA (b) DMDHEU (c) PP (d) nanoclay (e) ZnO (f) CTAB modified ZnO.

stretching), 2925 cm^{-1}, 2858 cm^{-1} (–CH_2 asymmetric and symmetric stretching), 1619 cm^{-1} (–OH bending), 1441 cm^{-1} (C-H bending in lignin and carbohydrates, O-H in plane bending of cellulose) and 1376 cm^{-1} (-CH bending in cellulose and hemicelluloses, C-H bond in -O(C=O)-CH_3 group). In the spectrum of nanoclay (curve d), peaks appeared at 3465, 2932 and 2859, 1621, 1031–457 cm^{-1} were for –OH stretching, –CH stretching of modified hydrocarbon, –OH bending and oxide bands of metals like Si, Al, Mg, etc. The absorption peaks at 3437 and 1632 cm^{-1} in the spectrum of unmodified ZnO (curve e) could be assigned to -OH (-stretching) and -OH (-bending) vibrations and the peaks appeared at around 424 cm^{-1} was due to the vibration of metal–oxygen (M–O) bond. Curve f represents the FTIR spectrum of CTAB modified ZnO. The intensity of the peak assigned for -OH group was found to decrease and shifted to wave number 3346 cm^{-1}. Moreover, two new peaks at 2920 and 2852 cm^{-1} due to the presence of -CH_2 group of CTAB were appeared. Other notable peaks were appeared at 1491 and 1482 cm^{-1} (asymmetric CH_3-N^+ deformation mode of the CTAB head group) and 1397 cm^{-1} (symmetric CH3-N^+ deformation mode of CTAB head

group) [3]. This indicated the incorporation of long chain of CTAB on the surface of the ZnO nanoparticles.

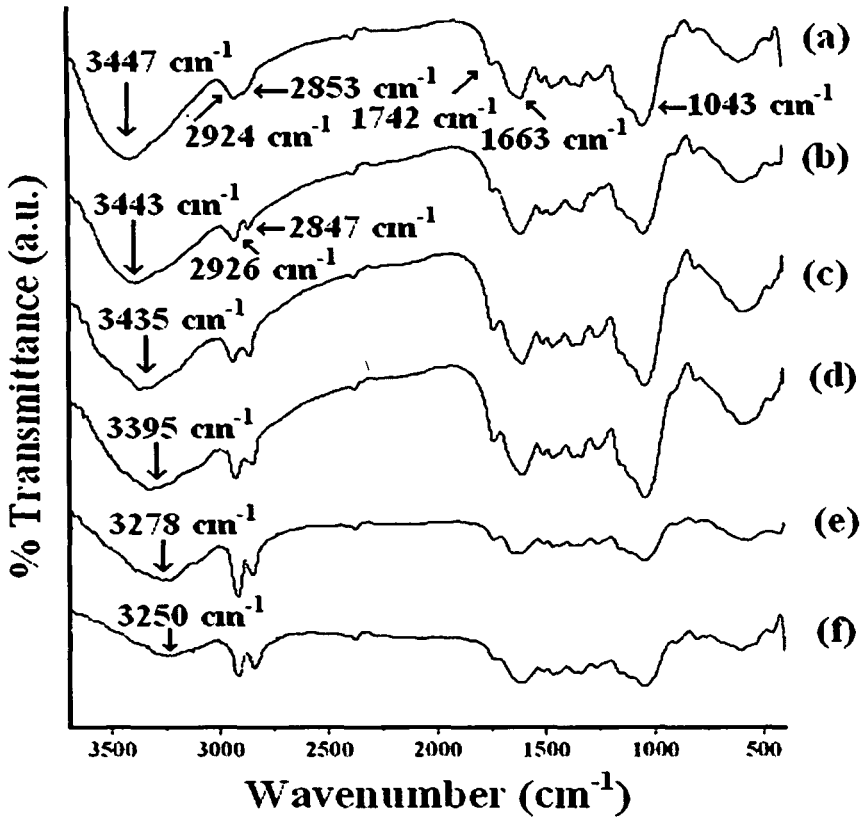

Figure 5.1.2. FTIR spectra of wood (a) untreated and treated with (b) MFFA/DMDHEU (c) MFFA/DMDHEU/nanoclay/ZnO (1 phr) (d) MFFA/DMDHEU/nanoclay/ZnO (2 phr) (e) MFFA/DMDHEU/nanoclay/ZnO (3 phr) (f) MFFA/DMDHEU/nanoclay/ZnO (3 phr)/PP.

Figure 5.1.2 represents the FTIR analysis of wood (a) untreated and treated with (b) MFFA/DMDHEU (c) MFFA/DMDHEU/nanoclay/ZnO (1 phr) (d) MFFA/DMDHEU/ nanoclay/ZnO (2 phr) (e) MFFA/DMDHEU/nanoclay/ZnO (3 phr) (f) MFFA/DMDHEU/ nanoclay/ZnO (3phr)/PP. Untreated wood (curve a) shows absorption bands at 3447 cm^{-1} (–OH stretching), 2924 cm^{-1}, and 2853 cm^{-1} (–CH_2 asymmetric stretching in alkyl groups due to both cellulose and lignin), 1742 cm^{-1} (C=O stretching of hemicelluloses), 1663 cm^{-1} (–OH bending), 1509 cm^{-1} (aromatic skeletal vibration by lignin), 1258 and 1043 cm^{-1} (C–O stretching) and 1000–646 cm^{-1} (out of plane C–H bending vibration). In the curves (b-f), it was observed that intensity of the peak corresponding to -OH stretching was decreased and shifted to 3443 cm^{-1} (curve b), 3435 cm^{-1} (curve c), 3395 cm^{-1} (curve d), 3278 cm^{-1} (curve e).

The decrease in intensity of hydroxyl group and shifting of the peak to lower wave number might be attributed to the participation of hydroxyl groups of clay and ZnO in the crosslinking reaction between wood, MFFA and DMDHEU. Dhoke et al. studied the interaction between nano-ZnO particles and alkyd resin by FTIR analysis and found similar decrease in the intensity of hydroxyl group of alkyd resin [4]. In the spectrum of PP treated wood/MFFA/DMDHEU/nanoclay/ZnO composite (curve f), the intensity of the –OH stretching peak was found to decrease further and shifted to lower wave number (3250 cm^{-1}). This further confirmed the participation of PP in the crosslinking reaction. Moreover, in all the cases, the intensity of the peak for the –CH stretching at 2924 cm^{-1} was found to increase compared to that of peak of untreated wood. Similar observation pertaining increase in peak intensity was reported by Deka and Maji while studying the FTIR analysis of wood polymer composite (WPC) treated with clay and ZnO [5].

5.1.2. X-ray diffraction (XRD) study

Figure 5.1.3. represents the X-ray diffraction pattern of (a) unmodified ZnO (b) CTAB modified ZnO nanoparticles (c) nanoclay. All the characteristic crystalline peaks for

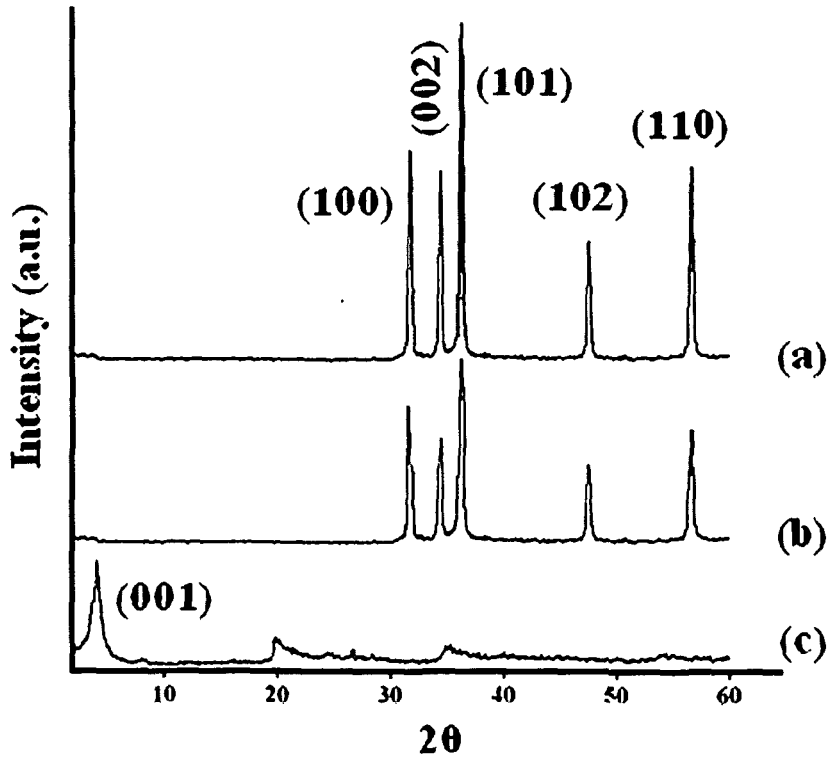

Figure 5.1.3. X-ray diffraction of (a) Unmodified ZnO (b) CTAB modified ZnO (c) nanoclay.

both unmodified and modified ZnO appeared above $2\theta = 30^{\circ}$ (curve a and b). The crystalline peaks appeared at $2\theta = 31.9^{\circ}$ (100), 33.3° (002), 36.4° (101), 47.7° (102) and 56.7° (110) [6]. It was observed from curve b that position of the characteristic peaks of ZnO remained unchanged after modification. This suggested that the crystalline structure of ZnO was not influenced by the cetyl group [7]. The organically modified nanoclay (curve c) shows a sharp peak at $2\theta = 4.3^{\circ}$. The gallery distance calculated by using Bragg's equation was found to be 2.05 nm.

Figure 5.1.4. shows the X-ray diffraction pattern of (a) untreated wood (b) MFFA/DMDHEU/nanoclay/ZnO (1 phr) treated (c) MFFA/DMDHEU/nanoclay/ZnO (2 phr) treated (d) MFFA/DMDHEU/nanoclay/ZnO (3 phr) treated (e) MFFA/DMDHEU/nanoclay/ZnO (3 phr)/PP treated wood samples. A wide diffraction peak at 22.98° due to the (002) crystal plane of cellulose was appeared for the untreated wood (curve a). Additional small peaks appeared at 37.68° and 15.02° might be ascribed to the 040 and 101 crystal plane of cellulose I respectively. The diffraction peak for the 040 crystal plane was much weaker than the peak for 002 crystal plane as the molecular plane of glucose found in cellulose was parallel to the 002 crystal plane [8]. Curves b-d represent the X-ray diffractogram of WPNC treated with different percentages of ZnO (1-3 phr) and PP. It was observed that the intensity of the crystalline peak of wood appearing at $2\theta = 22.98^{\circ}$ decreased in the wood composites and the first diffraction peak of nanoclay for $2\theta = 4.3^{\circ}$ disappeared. This suggested that either it was not possible to detect it by XRD or the nanoclay layers became delaminated and no crystal diffraction peak appeared [9]. The peak corresponding to 37.68° disappeared and the peak appearing at 15.02° became dull. Thus, the crystallinity of wood cellulose decreased in the case of composites as some nanoparticles were inserted into the amorphous region of cellulose of wood cell walls [8]. The characteristics peaks of ZnO appeared in diffractogram of WPNC loaded with ZnO. Higher the percentage of ZnO in the composites, higher was the intensity of the characteristics peaks of ZnO. This indicated the distribution of ZnO nanoparticles in the amorphous region of the WPNC. Similar increase in the intensity of ZnO was reported by Deka and Maji while studying the XRD pattern of WPC treated with ZnO [10]. The addition of PP did not significantly change the diffractogram of WPNC. Thus it could be concluded that the nanoclay layers were delaminated and the ZnO nanoparticles were incorporated into the wood.

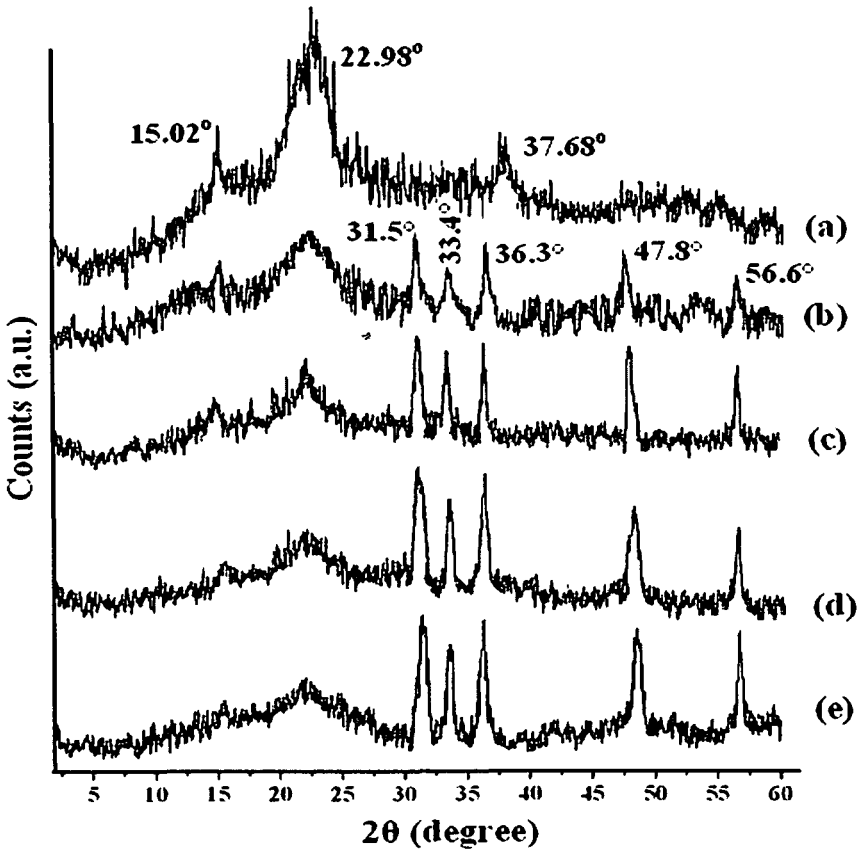

Figure 5.1.4. X-ray diffraction of (a) untreated wood (b) MFFA/DMDHEU/nanoclay/ZnO (1 phr) treated (c) MFFA/DMDHEU/nanoclay/ZnO (2 phr) treated (d) MFFA/DMDHEU /nanoclay/ZnO (3 phr) treated (e) MFFA/DMDHEU/nanoclay/ZnO (3 phr)/PP treated wood samples.

5.1.3. Crystallinity determination from FTIR and XRD

Related results are shown in Table 5.1.1. Although different functions were used to analyze the diffraction peaks, fitting with the Voigst functions resulted in the best fit [11]. The recorded diffractograms were deconvoluted using Voigst function.

FTIR study was employed to find out the crystallinity index. Figure 5.1.4. shows no lattice transformation of cellulose I to cellulose II as the peaks appearing at 15.02° and at 22.98° representing 101 and 002 plane of cellulose I were not replaced by 2θ = 12° and 21° due to prevention of transformation caused by lignin [12]. A reduction in crystallinity index values was observed for the treated wood samples. The cellulose of untreated wood showed the highest crystallinity index while the lowest value was shown by the wood samples treated with MFFA/DMDHEU/nanoclay/ZnO (3 phr)/PP. The inter-molecular and

intramolecular -OH bonds were busted by the MFFA, DMDHEU, nanoclay, ZnO, PP. They formed bonds with cellulose through their hydroxyl groups and thereby lowering the rigidity of cellulose. A major fraction of cellulose remained as crystallites with interspersed amorphous region of low extent of order [13]. The structures of the crystallites were distorted when chemical grafting reaction took place. It was difficult for the polymers to disseminate into the crystalline region of cellulose and thus the chemical reaction occurred in the amorphous region as described by Shiraishi et al. [14]. The opening of some hydrogen bonded cellulose chains occurred by reacting the polymers at the chain end on the surface of the crystallites. Thus some new amorphous cellulose was produced and it continued with the progress of reaction [13]. Crystallinity index determined from XRD analysis was also shown in Table 5.1.1. The results were in good agreement with the values obtained from FTIR studies. This indicated a clear reduction in crystallinity of cellulose due to treatment with DMDHEU, nanoclay, ZnO and PP.

5.1.4. Morphological studies of the nanocomposites

The energy dispersive X-ray spectroscopy (EDS) of the PP and the composite are represented in Figure 5.1.5. It was observed from the spectrum (Figure 5.1.5.a) that PP contained C, O, P and Ca. The occurrence of phosphorus in the PP contributed to its flame retarding behavior. Ghosh et al. found similar results while studying the EDS analysis of PP [15]. The spectrum of wood treated with MFFA/DMDHEU/nanoclay/ZnO (3 phr)/PP is shown in Figure 5.1.5.b. The composite contained C, O, N, Na, Mg, Al, Si, Zn and P. It was evident from the spectrum that all the components were successfully impregnated into the wood. The presence of nitrogen from MFFA and DMDHEU; phosphorus from the PP significantly contributed the flame retarding characteristics of the composites.

The scanning electron micrographs (SEM) of untreated and treated wood samples are shown in Figure 5.1.6. The vacant cell wall, pits and parenchymas seen in untreated wood (Figure 5.1.6.a) were filled up by MFFA/DMDHEU (Figure 5.1.6.b). The nanoclay and ZnO were traced as some white spots located either in cell lumen or cell wall (Figure 5.1.6.c-f).

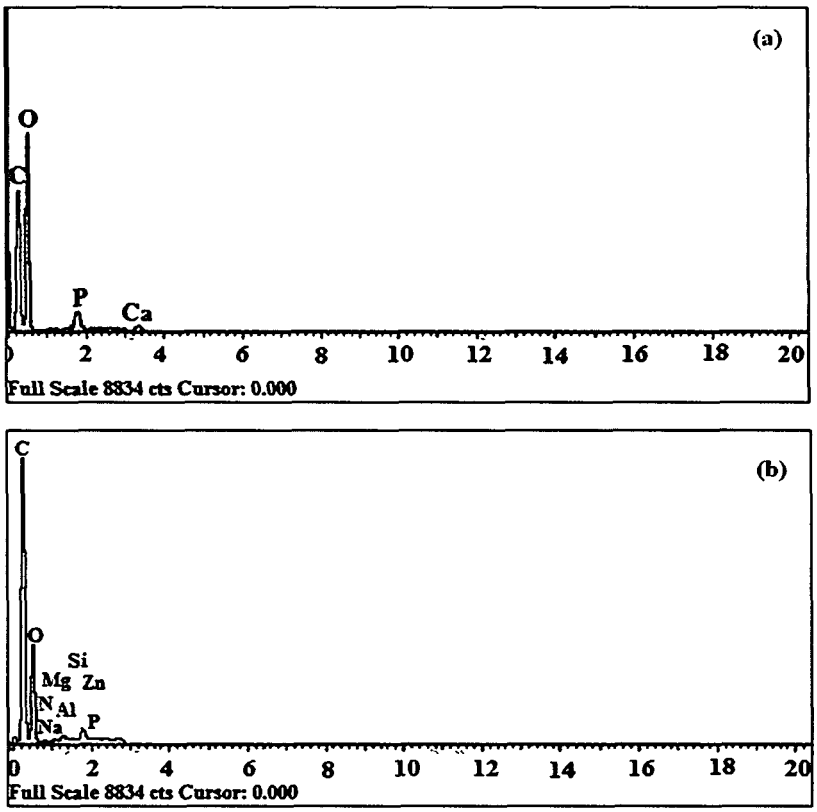

Figure 5.1.5. EDS of (a) PP (b) wood treated with MFFA/DMDHEU/nanoclay/ZnO (3 phr)/PP.

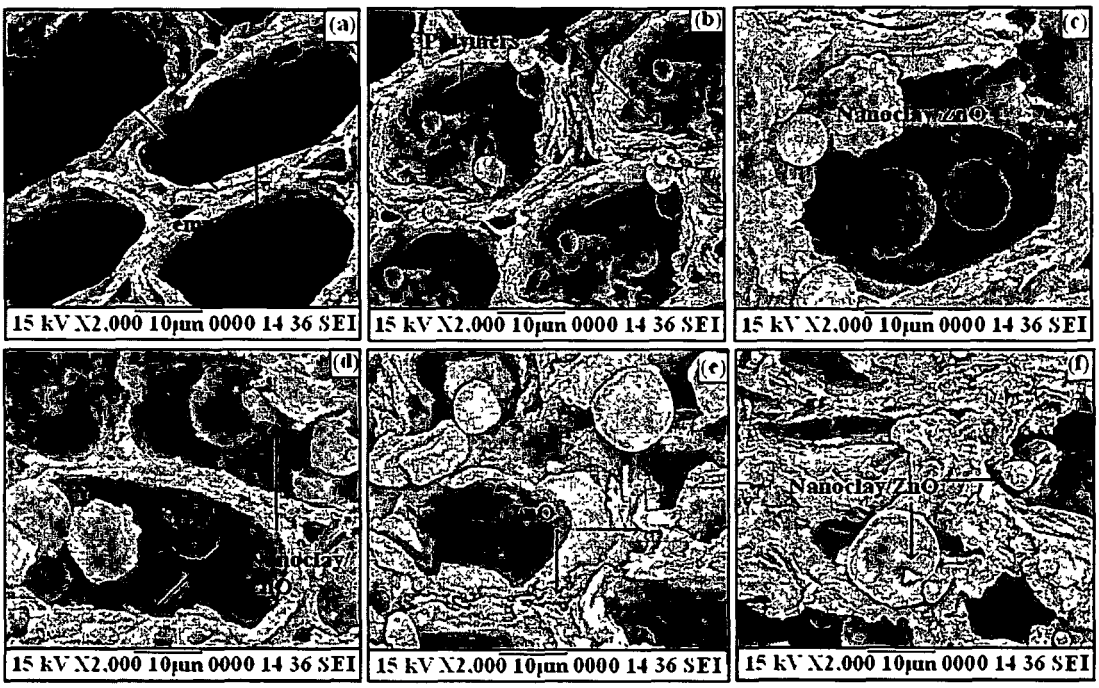

Figure 5.1.6. Scanning electron micrographs of wood (a) untreated and treated with (b) MFFA/DMDHEU (c) MFFA/DMDHEU/nanoclay/ZnO (1 phr) (d) MFFA/DMDHEU /nanoclay/ZnO (2 phr) (e) MFFA/DMDHEU/nanoclay/ZnO (3 phr) (f) MFFA/DMDHEU/nanoclay/ZnO (3 phr)/PP.

Figure 5.1.7. shows the Transmission electron microscope (TEM) micrographs of untreated and treated wood samples. There was no observation of the orientation of cell wall components in untreated wood (Figure 5.1.7.a). The nanoclay and ZnO nanoparticles, which were dispersed in the cell wall or lumen along with polymer matrix, could be seen as black slices and black spots respectively. (Figure 5.1.7.b-e).

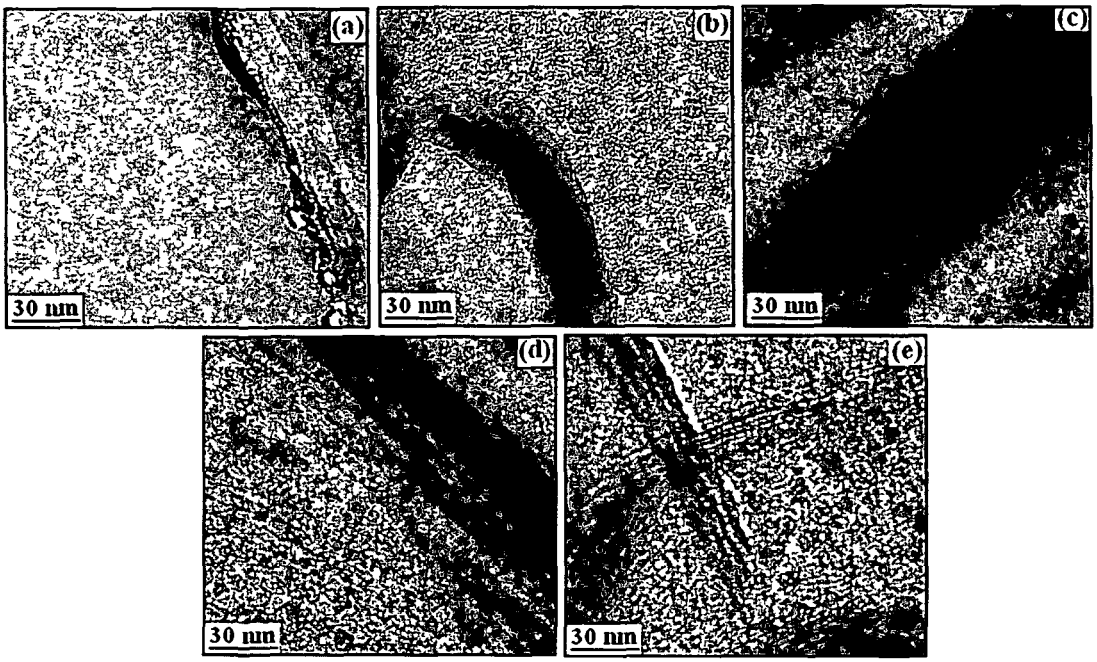

Figure 5.1.7. Transmission electron micrographs of (a) untreated (b) MFFA/DMDHEU /nanoclay/ZnO (1 phr) treated (c) MFFA/DMDHEU/nanoclay/ZnO (2 phr) treated (d) MFFA/DMDHEU/nanoclay/ZnO (3 phr) treated (e) MFFA/DMDHEU/nanoclay/ZnO (3 phr)/PP treated wood samples.

5.1.5. UV Resistance Study

Figure 5.1.8. represents the weight loss of untreated and treated wood samples exposed to an UV environment for different time periods. At the early stage of exposure time, a small increase in weight was found for all the samples due to the moisture uptake. This early increase in weight was higher than the material loss induced by the degradation. The maximum weight loss (%) was shown by untreated wood samples followed by the treated ones after 60 days of irradiation. With the increase in the amount of ZnO the rate of weight loss decreased. Minimum weight loss was shown by the samples when PP was added to the system.

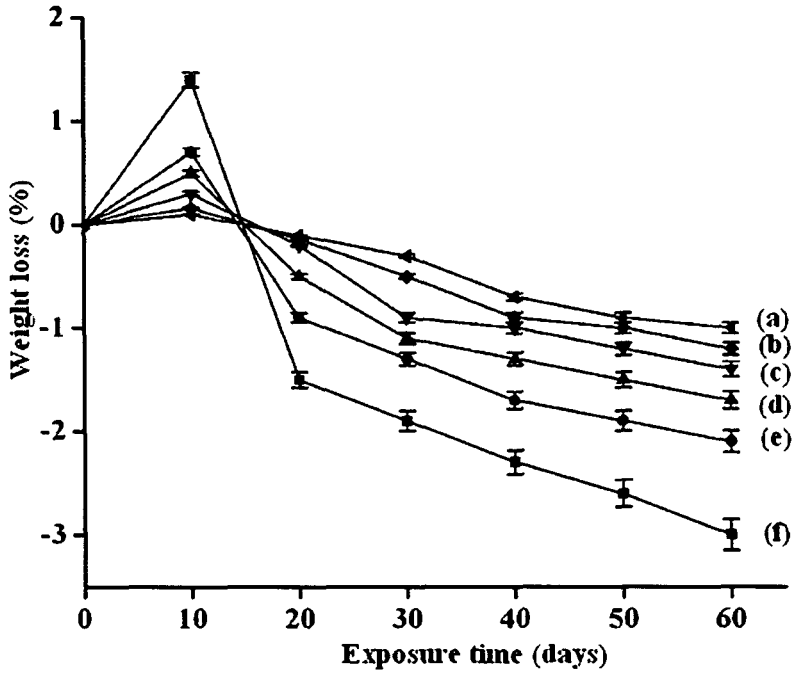

Figure 5.1.8. Weight losses versus exposure time of (a) untreated wood and treated with (b) MFFA/DMDHEU (c) MFFA/DMDHEU/nanoclay/ZnO (1 phr) (d) MFFA/DMDHEU/nanoclay/ZnO (2 phr) (e) MFFA/DMDHEU/nanoclay/ZnO (3 phr) (f) MFFA/DMDHEU/nanoclay/ZnO (3 phr)/PP.

Figure 5.1.9. shows the change of carbonyl index values with time for untreated and treated wood samples. The increase of carbonyl index values was due to chain scission of the polymer and wood. The chain scission decreased the density of entanglement of the polymer chains and hence a decrease in weight was observed. Untreated wood (curve 5.1.9.a) has the highest carbonyl index values due to higher oxidation of wood cellulose. The samples treated with MFFA/DMDHEU/nanoclay/ZnO (3 phr)/PP showed the lower carbonyl index value (curve 5.1.8.f). The incorporation of MFFA/DMDHEU decreased the carbonyl index value. The crosslinking provided by DMDHEU might be responsible for delayed photodegradation of the composites. The value decreased further when nanoclay and ZnO was added along with MFFA/DMDHEU to the wood (curve 5.1.9.c- curve 5.1.9.e). The higher the amount of ZnO, the lower was the carbonyl index value. Both nanoclay and ZnO stabilized the composite by providing a barrier to UV radiation and hence delayed the photo degradation process; and improved the UV resistance. Similar UV stability of polypropylene nanocomposite was reported by Zhao and Li after the incorporation of ZnO [16]. Grigoriadou et al. reported an increase in UV stability on addition of montmorillonite clay in high density polyethylene [17]. The PP enhanced the interaction among wood,

MFFA, clay, ZnO through its hydroxyl groups resulting in decrease of the photodegradation process. This in turn showed the lower carbonyl index value.

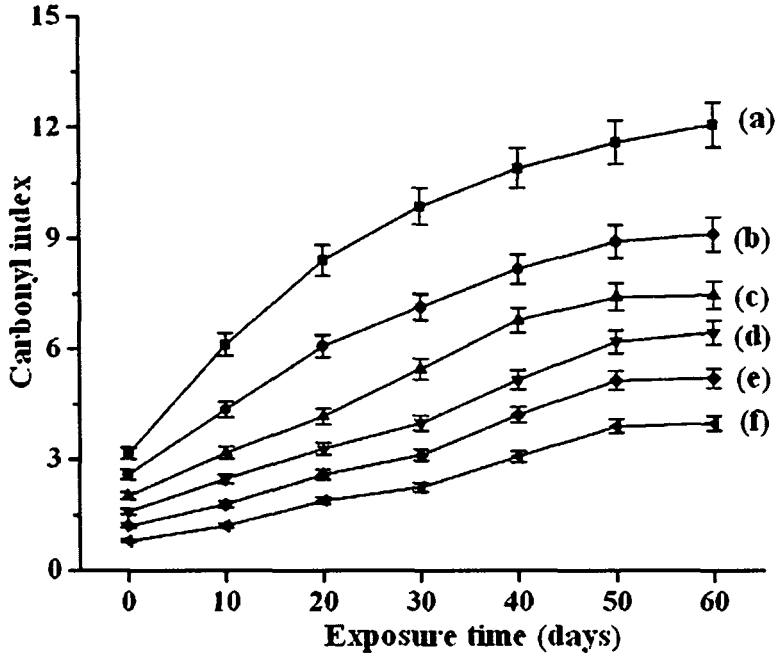

Figure 5.1.9. Carbonyl index values of (a) untreated wood and treated with (b) MFFA/DMDHEU (c) MFFA/DMDHEU/nanoclay/ZnO (1 phr) (d) MFFA/DMDHEU/nanoclay/ZnO (2 phr) (e) MFFA/DMDHEU/nanoclay/ZnO (3 phr) (f) MFFA/DMDHEU/nanoclay/ZnO (3 phr)/PP.

Figure 5.1.10. shows the lignin index values with time for untreated and treated wood samples. Lignin index value decreased with the increase in UV exposure time. The trend of the lignin index value followed the order: MFFA/DMDHEU/nanoclay/ZnO (3 phr)/PP treated > MFFA/DMDHEU/nanoclay/ZnO (3 phr) treated > MFFA/DMDHEU/nanoclay/ZnO (2 phr) treated > MFFA/DMDHEU/nanoclay/ZnO (1 phr) treated > MFFA/DMDHEU treated > untreated wood samples. ZnO protected the lignin decay of wood from the UV radiation by preventing the formation of quinones, carbonyls or peroxides. Patachiaa et al. reported that lignin index values of ionic liquid treated wood decreased on exposure to UV [18].

Figure 5.1.11. shows the FTIR spectra of the untreated and treated wood samples upon exposure to UV rays for 60 days. Untreated wood had the highest carbonyl peak intensity and treated wood samples had lower peak intensity. It was also observed that after irradiation, the characteristic peak for lignin almost disappeared in case of untreated wood and treatment of the samples with polymer, nanoclay, ZnO enhanced the lignin stability.

Hence, the decrease of lignin peak intensity was less pronounced in case of treated wood samples.

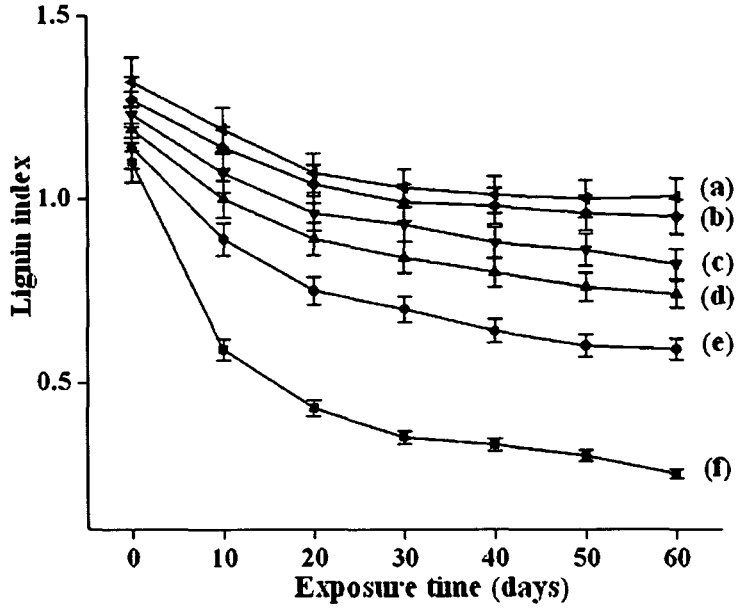

Figure 5.1.10. Lignin index values of wood treated with
(a) MFFA/DMDHEU/nanoclay/ZnO (3 phr)/PP (b) MFFA/DMDHEU/nanoclay/ZnO (3 phr) (c) MFFA/DMDHEU/nanoclay/ZnO (2 phr) (d) MFFA/DMDHEU/nanoclay/ZnO (1 phr) (e) MFFA/DMDHEU (f) untreated wood samples.

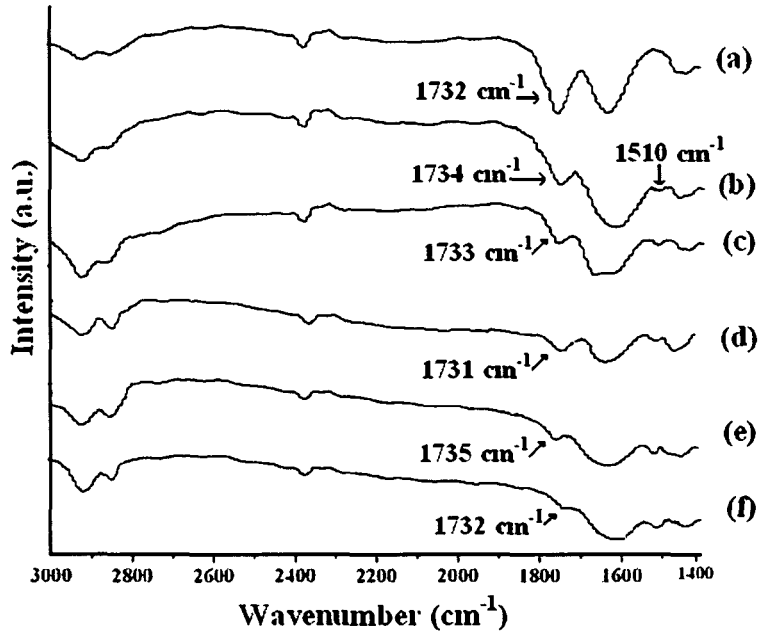

Figure 5.1.11. Change in carbonyl and lignin peak intensity of (a) untreated wood and treated with (b) MFFA/DMDHEU (c) MFFA/DMDHEU/nanoclay/ZnO (1 phr) (d) MFFA/DMDHEU/nanoclay/ZnO (2 phr) (e) MFFA/DMDHEU/nanoclay/ZnO (3 phr) (f) MFFA/DMDHEU/nanoclay/ZnO (3 phr)/PP.

Table 5.1.1. shows the variation of crystallinity index values of the untreated and treated wood samples on exposure to UV rays for different time period. The crystallinity index values were calculated from FTIR spectra (not shown). Untreated wood showed higher crystallinity index compared to treated wood samples. In both untreated and treated wood samples, crystallinity index was found to decrease with the increase in exposure time to UV light. Further the rate of decrease of crystallinity index was more in untreated wood than that of treated wood. DMDHEU, nanoclay and PP enhanced the interfacial interaction, while ZnO provided the protective barrier against UV light. Thus, the treated wood samples would undergo less degradation and hence exhibit a lower rate of decrease in crystallinity index. Similar decrease in crystallinity index values was observed by Patachia et al. while studying the UV degradation of ionic liquid treated wood [18].

Table 5.1.1 Crystallinity index values of cellulose matrix of untreated and treated wood samples calculated by the area method before and after UV exposure.

Samples		Untreated wood	MFFA/ DMDHEU treated	MFFA/ DMDHEU/ nanoclay/ ZnO (1 phr) treated	MFFA/ DMDHEU/ nanoclay/ ZnO (2 phr) treated	MFFA/ DMDHEU/ nanoclay/ ZnO (3 phr) treated	MFFA/ DMDHEU/ nanoclay/ ZnO (3 phr)/ PP treated
XRD results	Before	63.21	53.12	41.23	37.67	34.43	33.51
FTIR results	irradiation	62.53	54.22	40.56	37.81	35.62	32.65
	After irradiation						
	10 days	*60.34*	*52.33*	*39.37*	*36.58*	*34.69*	*31.45*
	20 days	57.21	49.87	36.54	35.62	33.72	28.78
	30 days	52.76	46.58	35.78	34.39	31.46	27.85
FTIR	40 days	49.88	45.32	34.28	32.47	30.57	26.98
results	50 days	47.54	43.27	32.56	31.42	29.76	26.03
	60 days	46.53	42.16	31.64	30.12	28.43	25.63

SEM micrographs of samples after 60 days of exposure are shown in Figure 5.1.12. Cracks appeared and degradation occurred on the surface of untreated wood (Figure 5.1.12.a). The surface of wood treated with MFFA/DMDHEU (Figure 5.1.12.b) was more uneven compared to samples treated MFFA/DMDHEU/nanoclay/ZnO (Figure 5.1.12.c). With the increase in the percentage of ZnO, the surface smoothness of the composites was found to increase. This indicated the shielding effect of ZnO nanoparticles to UV rays. Addition of PP to the ZnO treated samples retarded further the formation of cracks on surface of the samples. The PP facilitated the interfacial interaction between wood, ZnO, nanoclay and MFFA polymer and hence protected the composite from degradation against UV rays.

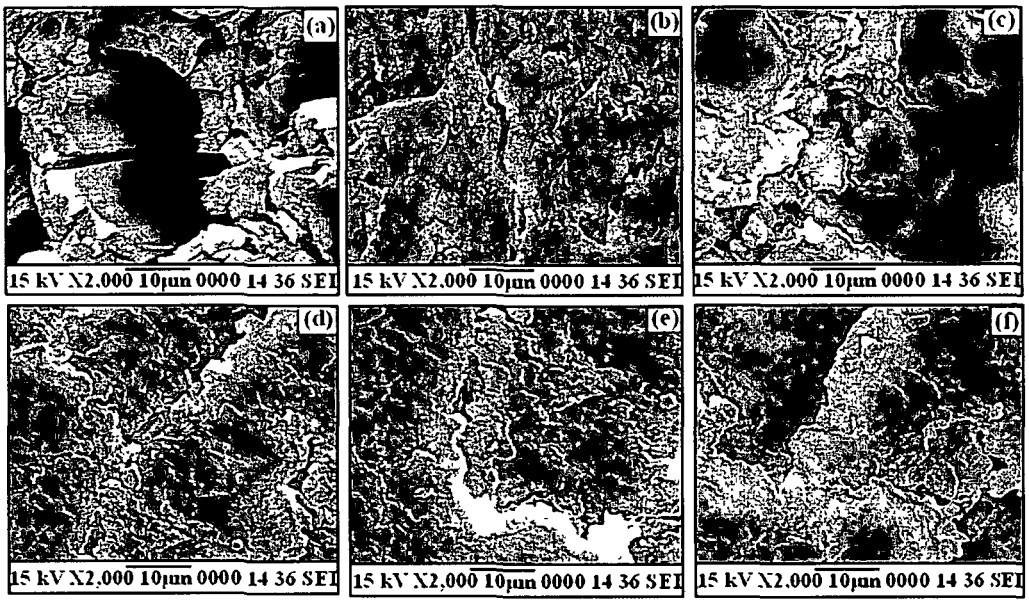

Figure. 5.1.12. SEM micrographs of UV treated samples after 60 days (a) untreated wood and treated with (b) MFFA/DMDHEU (c) MFFA/DMDHEU/nanoclay/ZnO (1 phr) (d) MFFA/DMDHEU/nanoclay/ZnO (2 phr) (e) MFFA/DMDHEU/nanoclay/ZnO (3 phr) (f) MFFA/DMDHEU/nanoclay/ZnO (3 phr)/PP.

The mechanical properties of the samples after 60 days of irradiation are shown in Table 5.1.2. Highest loss of mechanical properties was observed in case of untreated wood. However, loss was less significant when ZnO and nanoclay were added to the MFFA/DMDHEU treated wood samples. With the increase in the amount of ZnO, further reduction in loss of tensile and flexural values was noticed. ZnO shielded the composites thus, offering resistance to UV rays.

Table 5.1.2. Flexural and tensile properties of untreated and treated wood before and after UV degradation.

Sample	Flexural properties				Tensile properties			
	Before degradation		After degradation		Before degradation		After degradation	
	Strength (MPa) (±SD)	Modulus (MPa) (±SD)	Strength (MPa) (±SD)	Modulus (MPa) (±SD)	Strength (MPa) (±SD)	Modulus (MPa) (±SD)	Strength (MPa) (±SD)	Modulus (MPa) (±SD)
Untreated wood	118.07 (±0.58)	5922.54 (±0.45)	100.89 (±0.66)	5018.64 (±0.87)	41.15 (±0.76)	305.23 (±10.13)	30.11 (±0.43)	223.34 (±9.76)
Wood treated with MFFA/DMDHEU	127.64 (±0.86)	6402.58 (1.12)	119.76 (±0.53)	6009.55 (±1.01)	48.75 (±1.01)	361.62 (±9.57)	39.23 (±0.38)	290.98 (±7.87)
MFFA/DMDHEU/ nanoclay/ZnO (1 phr)	139.13 (±0.75)	6978.93 (±0.68)	132.33 (±0.47)	6639.81 (±0.26)	64.91 (±1.08)	481.46 (±12.46)	58.75 (±0.56)	435.77 (±8.43)
MFFA/DMDHEU/ nanoclay/ZnO (2 phr)	140.35 (±1.05)	7040.13 (±1.03)	135.58 (±0.28)	6803.40 (±0.92)	65.53 (±0.75)	486.06 (±16.78)	61.13 (±0.64)	453.43 (±8.98)
MFFA/DMDHEU/ nanoclay/ZnO (3 phr)	142.68 (±0.64)	7157.03 (±0.76)	139.86 (±0.51)	7018.17 (±0.54)	67.83 (±1.22)	503.12 (±8.63)	64.86 (±0.82)	481.09 (±10.21)
MFFA/DMDHEU/ nanoclay/ZnO (3 phr)/ PP (3 phr)	143.57 (±0.87)	7207.16 (±1.23)	140.63 (±0.36)	7056.81 (±1.12)	68.46 (±1.87)	507.80 (±7.84)	66.26 (±1.45)	491.48 (±11.13)

5.1.6. Mechanical properties

Table 5.1.2. shows the tensile and flexural values of untreated and treated wood samples. It was observed that the treatment of the samples with MFFA/DMDHEU enhanced the tensile and flexural values. DMDHEU enhanced the interfacial interaction between wood and MFFA resulting in increased values [19]. A perceptible improvement in tensile and flexural values was observed upon inclusion of nanoclay and ZnO to the WPC samples. At a fixed clay loading (3 phr), the higher the amount of ZnO, the higher was the tensile and flexural values. The silicate layers intercalated the polymer chains in its gallery layers and thereby stiffening the composites. The cetyl group and surface hydroxyl group present in CTAB modified ZnO enhanced its interaction between wood, MFFA, DMDHEU and clay [10]. Samples treated with MFFA/PP/DMDHEU/nanoclay/ZnO/PP had the highest improvement in properties. The abundant hydroxyl groups present in PP facilitated the interaction between wood, MFFA, DMDHEU, clay and ZnO.

5.1.7. Effect of variation of ZnO on polymer loading (WPG %), volume increase, and hardness

From Table 5.1.3., it was observed that the hardness of the composites increased due to impregnation of MFFA copolymer into wood. A significant improvement in polymer loading (WPG %), volume increase, and hardness was noticed when ZnO was impregnated along with MFFA, DMDHEU and nanoclay into the wood. The deposition of polymer, nanoclay and ZnO into the empty spaces of wood was facilitated by DMDHEU as it could interact through its hydroxyl groups [19]. Further improvement in properties was observed with the increase in percentage of ZnO. The addition of PP again enhanced the properties. The plant polymer contains mainly L-arabinose, D-galactose, D-glucuronic acid, L-rhamnose, D-mannose and D-xylose [20] which have abundant hydroxyl groups. These hydroxyl groups facilitated interaction between the hydroxyl groups of wood, polymer and nanoparticles.

5.1.8. Limiting oxygen index (LOI)

The LOI values of treated and untreated wood are shown in Table 5.1.4. Treated wood samples showed higher LOI values than the untreated ones. Higher LOI value of MFFA/DMDHEU treated samples was due to the synergistic effect of MFFA and

DMDHEU [21]. Both contains nitrogen and on combustion oxides of nitrogen were produced which displaced the oxygen present on the surface of the composites. Nanoclay promoted char formation. The char produced an insulated layer over the samples and thus increased its flame resistance property [22]. With the increase in the amount of modified ZnO, the flame retardancy would increase as it could protect the samples from heat and oxygen. Addition of PP would amplify the flame retardancy of the composites to a considerable amount because of its phosphorus content. [23,24].

Table 5.1.3. Effect of variation of CTAB-ZnO on weight % gain (WPG %), volume increase and hardness.

Samples particulars	Weight % gain (WPG %)	Volume increase %	Hardness (Shore D)
Untreated		-	46 (±1.07)
Samples treated with MFFA/FA-water/DMDHEU/ nanoclay/CTAB-ZnO/PP			
100/20/3/0/0/0	28.13 (±0.47)	2.12 (±0.82)	62 (±0.76)
100/20/3/3/1/0	43.53 (±0.63)	3.32 (±0.28)	75 (±1.06)
100/20/3/3/2/0	46.88 (±0.49)	3.54 (±0.38)	77 (±0.57)
100/20/3/3/3/0	49.86 (±0.81)	3.98 (±1.03)	78 (±0.43)
100/20/3/3/3/3	50.91 (±0.75)	4.01 (±0.93)	79 (±0.37)

5.1.9. Thermal stability

Table 5.1.4. shows the initial decomposition temperature (T_i), maximum pyrolysis temperature (T_m), and residual weight (%) (RW) for untreated and polymer-treated wood samples. Non combustible material and moisture are produced in the temperature range between 100-200°C. T_i values improved after treatment of the samples with MFFA/DMDHEU. The incorporation of nanoclay and ZnO in the samples further enhanced the T_i values. Maximum T_i value was observed for MFFA/DMDHEU/nanoclay/ZnO (3 phr)/PP (3 phr) treated wood samples.

Table 5.1.4. Thermal degradation and flame retardancy of untreated and treated wood samples.

Sample	T_i	T_m[a]	T_m[b]	Temperature of decomposition (T_D) in °C at different weight loss (%)				RW% at 600°C	LOI (%)(±SD)
				20%	40%	60%	80%		
Untreated wood	161	302	395	267	294	332	--	27.82	21(±0.33)
Wood treated with									
MFFA/DMDHEU	238	338	431	304	330	360	424	8.2	26 (±0.25)
MFFA/DMDHEU/ nanoclay/ZnO (1 phr)	268	366	455	341	357	390	459	20.41	37 (±0.67)
MFFA/DMDHEU/ nanoclay/ZnO (2 phr)	271	369	458	343	359	394	461	21.23	38 (±0.43)
MFFA/DMDHEU/ nanoclay/ZnO (3 phr)	274	372	461	346	361	396	463	22.02	40 (±0.41)
MFFA/DMDHEU/ nanoclay/ZnO (3 phr)/PP	276	375	463	348	364	398	466	22.04	42 (±0.72)

T_i: value for initial degradation; [a]T_m: value for 1st step; [b]T_m: value for 2nd step.

T_m values were also higher for the treated wood than untreated ones. T_m values for the first stage of pyrolysis was due to the depolymerization of hemicellulose, glycosidic linkage of cellulose, thermal decomposition of cellulose and disintegration of interunit linkages and condensation of aromatic rings during pyrolytic degradation of lignin [13]. The second stage of pyrolysis was due to the degradation of polymers. Improvement of thermal stability of wood treated with MFFA/DMDHEU was associated with the formation of crosslinked structure with cell wall of wood. The combined effect of nanoclay and ZnO had a significant effect on enhancing the thermal stability of the composites. The silicate layers of nanoclay provided a meandering path and thus delaying the diffusion of volatile product through the prepared composites [25]. ZnO interacted with the wood, nanoclay and polymer through its surface hydroxyl groups and cetyl groups. Laachachi et al. found an improvement in thermal stability of PMMA composite after addition of organo-MMT and ZnO into PMMA [26]. Incorporation of PP would further improve the thermal stability of the composites due to the presence of phosphorus (4.34%, w/w) [23].

RW (%) value of untreated wood was highest while the value for treated wood with MFFA/DMDHEU was lowest. The volatile components diffused out and the lignin present in the wood contributed to char formation. The addition of nanoclay and ZnO would increase the char formation and thus would further prevent the thermal degradation by forming a protective insulating layer.

5.1.10. Water uptake test

Figure 5.1.13. shows the water uptake capacity of untreated and treated wood samples. Untreated wood showed the highest water absorption capacity. Wood consists of native cellulose which has a rigid structure and the rest components present in wood are amorphous substance accessible to water molecules. MFFA/DMDHEU was impregnated into the cell wall of wood and impeded the water penetration by a bulk effect. DMDHEU could form crosslink with the cell wall, and prevented water incursion into the composite [19]. MFFA/DMDHEU/nanoclay/ZnO treatment offered higher water repellence. With the increase in the amount of ZnO, the water repellency increased. ZnO in combination with nanoclay occupied the void spaces in wood and made the cell wall more bulky. The plant polymer contained a plenty of available hydroxyl groups which enhanced the interaction with wood, MFFA, DMDHEU, nanoclay and ZnO; thus improved the water resistance.

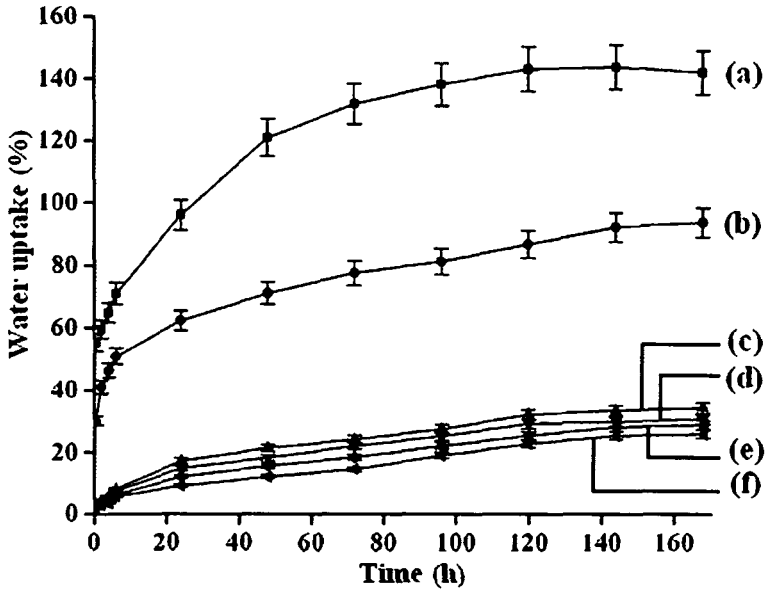

Figure 5.1.13. Water absorption test of wood (a) untreated and treated with (b) MFFA/ DMDHEU (c) MFFA/DMDHEU/nanoclay/ZnO (1 phr) (d) MFFA/DMDHEU/nanoclay/ ZnO (2 phr) (e) MFFA/DMDHEU/nanoclay/ZnO (3 phr) (f) MFFA/DMDHEU/nanoclay /ZnO (3 phr)/PP.

Section B: Properties of softwood polymer composites impregnated with nanoparticles and melamine formaldehyde furfuryl alcohol copolymer.

Among the different nanofillers used in polymer composites, silicon dioxide (SiO_2) nano particles are an attractive nano material for enhancing polymer properties. It can improve the mechanical as well as thermal properties of the composite. The synergistic effect of SiO_2 nano particles with the organoclay can result in improved performance of the composites. Keeping this in view, wood polymer composites (WPC) based on nano SiO_2 and nanoclay were prepared by the impregnation of MFFA copolymer, DMDHEU, a crosslinking agent and a renewable polymer into wood. The main objective of this article is to study the synergistic effect of CTAB modified SiO_2 nanoparticles and nanoclay on the various properties of the wood polymer nanocomposites and the effect of PP on flame retarding and other properties of the composites.

Maximum improvement in properties was checked by variation of parameters like vacuum, time of impregnation, monomer concentration, initiator concentration, amount of crosslinking agent, nanoclay, PP, modified SiO_2 nanoparticles. The optimum conditions, at which enhancement of properties were obtained: 500 mm Hg vacuum, 6 h time of impregnation, 5:1 (MFFA:FA-water) prepolymer concentration, 1% (w/w) maleic anhydride, 3 mL DMDHEU, 3 phr nanoclay, 3 % (w/v) PP and 1.0-3.0 phr modified SiO_2 nanoparticles.

5.2. RESULTS AND DISCUSSION

5.2.1. FTIR study

Figure 5.2.1. shows the FTIR spectra of MFFA copolymer, DMDHEU, nanoclay, PP, unmodified and CTAB modified SiO_2 and nanoclay. MFFA copolymer (curve a) could be characterized by the presence of bands at 3420 cm^{-1} (-OH stretching), 2924 cm^{-1} and 2853 cm^{-1} (-CH_2 asymmetric and symmetric stretching), 1569 cm^{-1} and 1501 cm^{-1} (furan ring vibration), 1189 cm^{-1} (C-N stretching), 815 cm^{-1} (out plane trisubstitution of triazine ring) [1]. The main characteristic absorption bands for DMDHEU (curve b) were at 3422 cm^{-1} (-OH stretching), 1703 cm^{-1} (C=O stretching), 1247 cm^{-1} (-CHOH stretching), 1022 cm^{-1} (CH_2OH stretching) [2]. In the spectrum of PP (curve c), appearance of bands at 3434, 2923, 2855, 1622, 1443 and 1378 cm^{-1} could be assigned to the -OH stretching, –CH_2

asymmetric and symmetric stretching, –OH bending, C-H bending in lignin and carbohydrates, O-H in plane bending of cellulose, -CH bending in cellulose and hemicelluloses and C-H bond in -O(C=O)-CH_3 group respectively. The absorption bands shown by the spectrum of unmodified SiO_2 (curve d) at 3426 cm^{-1}, 1630 cm^{-1} and 1085-462 cm^{-1} were for -OH group stretching, -OH bending and Si-O-Si stretching respectively [27]. Peaks appearing at 3427, 2930 and 2854, 1631, 1473, 1084-464 cm^{-1} could be attributed to –OH stretching, -CH_2 stretching of the modifying hydrocarbon, -OH bending, Si-O-Si stretching (curve e). In the spectrum of CTAB modified SiO_2, the intensity of the hydroxyl peaks of SiO_2 was found to decrease due to its interaction with CTAB. In the absorption spectrum of nanoclay (curve f), the presence of peaks at 3438, 2931 and 2857, 1623, 1033–455 cm^{-1} were for –OH stretching, –CH stretching of modified hydrocarbon, –OH bending and oxide bands of metals like Si, Al, Mg, etc respectively.

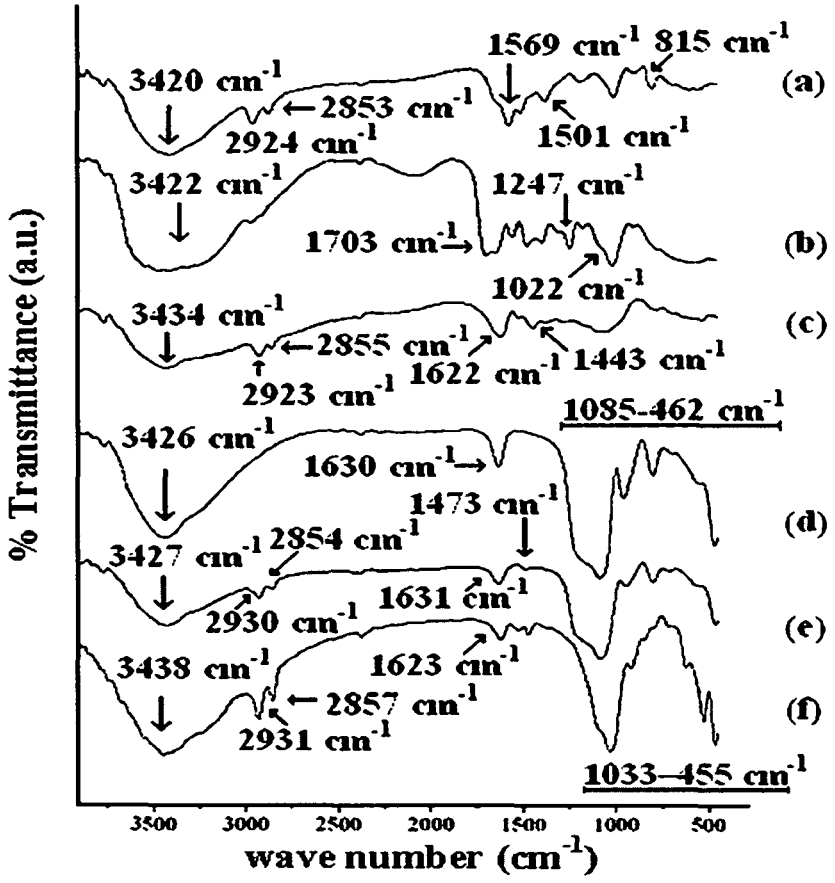

Figure. 5.2.1. FTIR spectra of (a) MFFA copolymer (b) DMDHEU (c) PP (d) unmodified SiO_2 (e) CTAB modified SiO_2 (f) nanoclay.

Figure 5.2.2. shows the FTIR spectra of untreated and treated wood samples. Untreated wood (curve a) is characterized by the absorption bands at 3447 cm^{-1} (–OH stretching), 2924 cm^{-1}, and 2853 cm^{-1} (–CH_2 asymmetric stretching in alkyl groups due to both cellulose and lignin), 1742 cm^{-1} (C=O stretching of hemicelluloses), 1663 cm^{-1} for (–OH bending), 1509 cm^{-1} (aromatic skeletal vibration by lignin), 1258 and 1043 cm^{-1} (C–O stretching) and 1000–646 cm^{-1} (out of plane C–H bending vibration). A decrease in the wavenumber for the hydroxyl peak was observed in the case of the treated wood samples (curve b-f). The hydroxyl peak at 3447 cm^{-1} for untreated wood shifted to 3343 (curve b), 3336 (curve c), 3329 (curve d), 3323 (curve e), and 3315 cm^{-1} (curve f) due to treatment. There was a decrease in the intensity of the hydroxyl group and carbonyl group with the increase in the amount of nano SiO_2 in the composites. The intensities of the peak corresponding to –CH stretching was more pronounced in treated wood samples compared to that of untreated wood samples. These indicated the participation of hydroxyl group and carbonyl group of wood in the crosslinking reaction between MFFA, DMDHEU, nano SiO_2 and PP. The intensity of carbonyl group decreased due to the formation of hydrogen bonds with the hydroxyl groups on the silica surface as reported by Motaung and Luyt while studying the FTIR analysis of low density polyethylene/wax/SiO_2 nanocomposite [28].

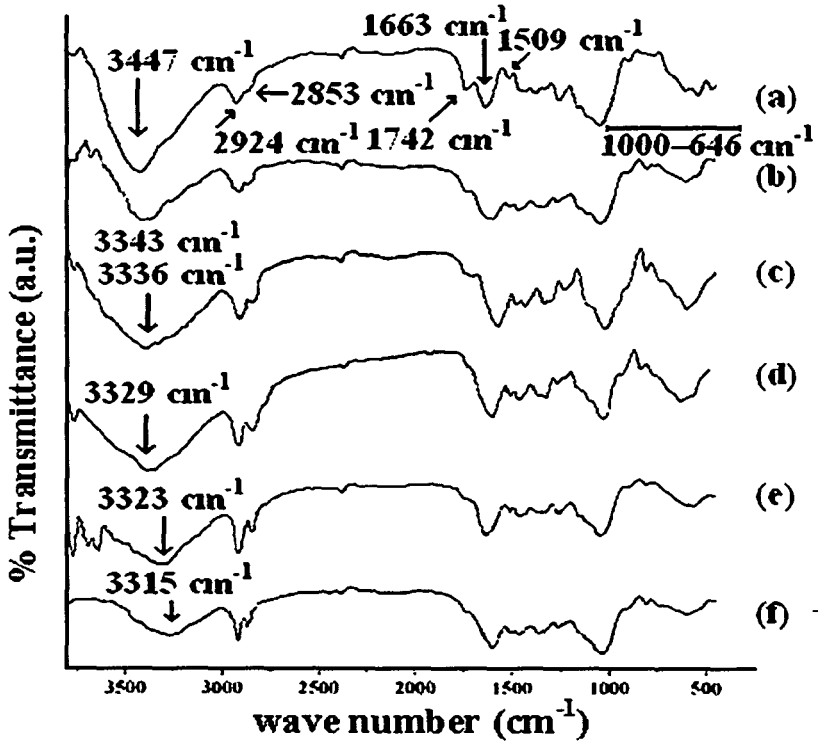

Figure. 5.2.2. FTIR spectra of wood (a) untreated and treated with (b) MFFA/DMDHEU (c) MFFA/DMDHEU/nanoclay/SiO_2 (1 phr) (d) MFFA/DMDHEU/nanoclay/SiO_2 (2 phr) (e) MFFA/DMDHEU/nanoclay/SiO_2 (3 phr) (f) MFFA/DMDHEU/nanoclay/SiO_2 (3phr)/PP.

5.2.2. XRD analysis

XRD analysis of (a) nanoclay (b) CTAB modified SiO_2 (c) untreated wood (d) MFFA/DMDHEU/nanoclay composite and wood treated with (e) MFFA/DMDHEU/nanoclay/modified SiO_2 (1 phr) (f) MFFA/DMDHEU/nanoclay/modified SiO_2 (2 phr) (g) MFFA/DMDHEU/ nanoclay/modified SiO_2 (3 phr) (h) MFFA/DMDHEU/nanoclay/modified SiO_2 (3 phr)/PP are shown in Figure 5.2.3. A sharp diffraction peak appeared at 4.3° in the diffractogram of nanoclay (curve a). CTAB modified SiO_2 showed a broad peak at 23.2° which was due to its amorphous nature [29]. The diffraction pattern of SiO_2 did not change due to modification suggesting its amorphous nature (curve b). This was in agreement with the observation made by Ahmed et al. [30]. Untreated wood shows a wide diffraction peak at 22.7° due to 002 crystal plane of cellulose. Two additional small peaks appeared at 15.3° and 37.7° were due to the 101 and 040 planes respectively (curve c). In the XRD diffractogram of MFFA/nanoclay/DMDHEU (curve d), the sharp diffraction peak of nanoclay at $2\theta = 4.3°$ disappeared. From this, we might conclude that either there was full expansion of gallery layers of nanoclay which could not be detected by XRD or the layers became delaminated. Further it showed a broad diffraction peak at $2\theta = 22.8$ due to MFFA copolymer. In the case of the wood samples treated with MFFA/DMDHEU/nanoclay/SiO_2, there was a decrease in peak intensity of 002 crystal plane of cellulose. Peaks at 15.3° and 37.7° disappeared which indicated a decrease in crystallinity of wood cellulose (curve e-g) [8]. There were no such noticeable differences in the diffractogram of WPC on addition of PP (curve h).

5.2.3. Crystallinity determination from FTIR and XRD

The crystallinity index value was shown in Table 5.2.1. The recorded diffractograms were deconvoluted using Voigst function. Analysis of the diffraction peaks were performed by using different functions but fitting the curves with the Voigst functions resulted in the best fit [11]. The cellulose of untreated wood showed the highest crystallinity index while the lowest value was shown by the wood samples treated with MFFA/DMDHEU/nanoclay/SiO_2 (3 phr)/PP. The intermolecular and intra molecular hydrogen bonds of cellulose were broken down as they participated in the bond formation between MFFA, DMDHEU, nanoclay, SiO_2 and PP. Thus the rigidity of wood cellulose is reduced. When chemical grafting reaction took place, the structures of crystallites of wood cellulose became nebulous [13]. The distribution of the polymer chains in the crystallites

region of cellulose became difficult. Shiraishi et al. reported that chemical grafting reaction took place in the amorphous region of wood cellulose [14]. The polymers reacted on the surface of the crystallites thereby opening of some hydrogen bonded cellulose chains. As the reaction continued, more amorphous cellulose were produced. The crystallinity index values were determined from both FTIR and XRD and the results found were in good agreement with each other. Popescu et al. determined the crystallinity index values of acetylated kraft pulp fibers by using both the FTIR and XRD techniques. Both the methods produced similar results [31]. Thus, a reduction in crystallinity index values was observed for the treated wood samples.

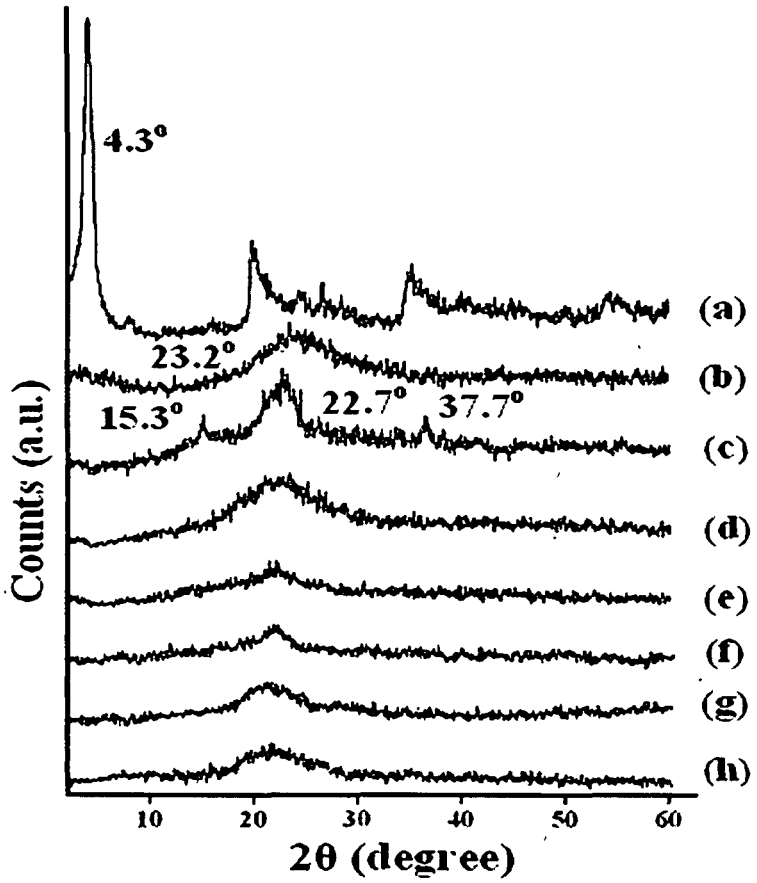

Figure 5.2.3. X-ray diffraction of (a) nanoclay (b) CTAB modified SiO_2 (c) untreated wood (d) MFFA/DMDHEU/nanoclay composite and wood treated with (e) MFFA/DMDHEU/ nanoclay/modified SiO_2 (1 phr) (f) MFFA/DMDHEU/nanoclay/modified SiO_2 (2 phr) (g) MFFA/DMDHEU/ nanoclay/modified SiO_2 (3 phr) (h) MFFA/DMDHEU/nanoclay/ modified SiO_2 (3 phr)/PP.

Table 5.2.1. Crystallinity index values of cellulose matrix of untreated and treated wood samples calculated by the area method.

Samples	Untreated wood	MFFA/ DMDHEU treated wood	MFFA/ DMDHEU/ nanoclay/ SiO_2 (1 phr) treated	MFFA/ DMDHEU/ nanoclay/ SiO_2 (2 phr) treated	MFFA/ DMDHEU/ nanoclay/ SiO_2 (3 phr) treated	MFFA/ DMDHEU/ nanoclay/ SiO_2 (3 phr)/ PP treated
XRD results	63.83	53.54	38.65	35.47	32.21	30.86
FTIR results	62.74	54.68	38.02	34.98	32.78	30.23

5.2.4. Scanning electron microscopy

Figure 5.2.4. shows the scanning electron micrograph of untreated and treated wood samples. Untreated wood had void spaces and empty cell wall (Figure 5.2.4.a). The deposition of polymer in the cell wall and cell lumen was observed on MFFA/DMDHEU treated wood samples. (Figure 5.2.4.b) [32]. The presence of traces amount of nanoclay/SiO_2 could be detected by some white patches located either in cell wall or cell lumen (Figure 5.2.4.c-f).

5.2.5. Transmission electron microscopy

Figure 5.2.5. shows the transmission electron micrograph of untreated and treated wood samples. The radial fracture patterns perpendicular to the compound middle lamella were regularly observed in the case of untreated wood. No orientation of cell wall component was observed in the case of untreated wood (Figure 5.2.5.a). The silicate layers of nanoclay and nano SiO_2 were observed as some black slices and black spots in the micrograph. The dispersion of nanoclay and nanoparticles in the cell wall with the MFFA polymer matrix was clearly visible from the micrograph from which we could confirm that nanoclay and nano SiO_2 were successfully impregnated into the composites (Figure 5.2.5.b-

e). The uniform distribution of silica nanoparticles in epoxy nanocomposites was reported in the literature [33].

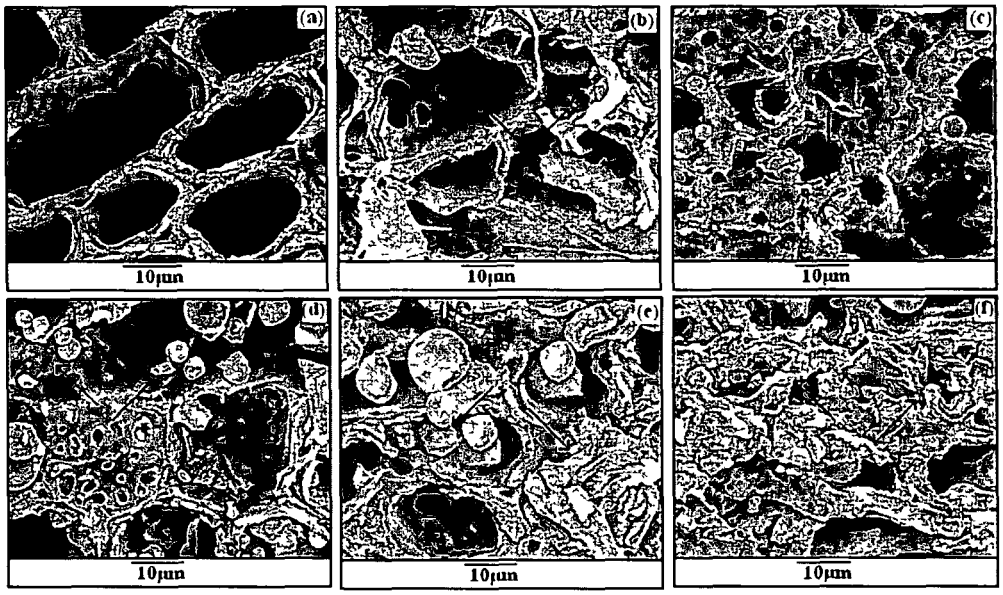

Figure 5.2.4. SEM micrographs of wood (a) untreated and treated with (b) MFFA/DMDHEU (c) MFFA/DMDHEU/nanoclay/SiO_2 (1 phr) (d) MFFA/DMDHEU/nanoclay/SiO_2 (2 phr) (e) MFFA/DMDHEU/nanoclay/SiO_2 (3 phr) (f) MFFA/DMDHEU/nanoclay/SiO_2 (3 phr)/PP.

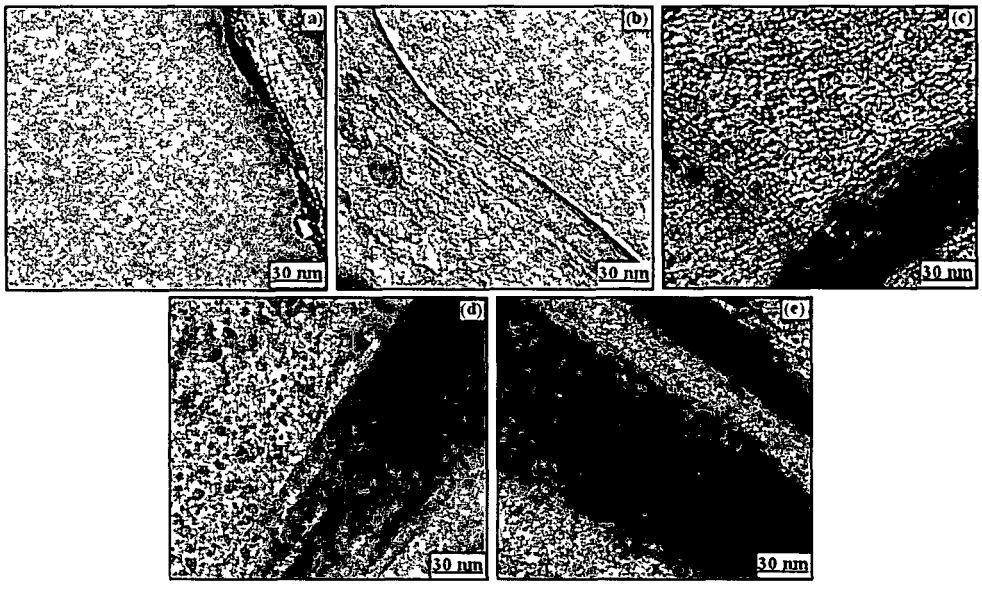

Figure 5.2.5. TEM micrographs of (a) untreated (b) MFFA/DMDHEU/nanoclay/SiO_2 (1 phr) treated (c) MFFA/DMDHEU/nanoclay/SiO_2 (2 phr) treated (d) MFFA/DMDHEU /nanoclay/SiO_2 (3 phr) treated (e) MFFA/DMDHEU/nanoclay/SiO_2 (3 phr)/PP treated wood samples.

5.2.6. Effect of treated SiO_2 content on polymer loading (WPG %), volume increase and hardness

Polymer loading (WPG %), volume increase, and hardness of wood were found to increase on impregnation with polymer, crosslinker and SiO_2. The higher the concentration of SiO_2, the higher was the improvement in properties. Wood contains void spaces, empty pits and parenchymas. When wood was impregnated with MFFA, the polymer would fill the empty pits and parenchymas resulting in increased polymer loading (WPG %), volume increase, and hardness. Impregnation of wood with melamine formaldehyde resulted in increased hardness of the solid [34]. When DMDHEU was added to MFFA prepolymer, an improvement in properties of wood composites was observed. DMDHEU facilitated the deposition of polymer by interacting with wood and polymer through its hydroxyl groups [19]. With the increase in the amount of nano SiO_2, an improvement in properties was observed as the void spaces and capillaries of wood were occupied by the nanoparticles. PP would further improve its properties because of its enhanced interaction caused by the presence of abundant hydroxyl groups with the wood, MFFA, DMDHEU, SiO_2 and nanoclay.

Table 5.2.2. Effect of variation of CTAB modified SiO_2 on weight % gain (WPG %), volume increase and hardness.

Samples particulars	Weight % gain (WPG %)	Volume increase %	Hardness (Shore D)
Untreated	--	--	47 (±0.97)
Samples treated with MFFA/FA-water/DMDHEU/ nanoclay/CTAB- SiO_2/PP			
100/20/3/0/0/0	27.89 (±0.96)	2.08 (±0.78)	61 (±0.82)
100/20/3/3/1/0	41.86 (±0.73)	3.19 (±0.44)	71 (±0.48)
100/20/3/3/2/0	44.38 (±0.54)	3.38 (±1.02)	73 (±0.63)
100/20/3/3/3/0	46.93 (±0.65)	3.67 (±0.86)	76 (±1.03)
100/20/3/3/3/3	49.21 (±0.82)	3.91 (±0.89)	78 (±0.54)

5.2.7. Water absorption test

The water absorption capacities for the untreated and treated wood samples are shown in Figure 5.2.6. In all the samples, there was an increase in absorption with the increase in time. Void spaces, empty pits and parenchymas made wood easy accessible to water. Highest water absorption capacity was shown by the untreated wood samples due to its hydrophilic nature. The water absorption capacity of wood samples decreased on impregnation with MFFA/DMDHEU. This was due to decrease in available void spaces. Moreover, DMDHEU could crosslink with the cell wall of wood and increase dimensional stability of the composites [19]. Further incorporation of nanoclay and SiO_2 would fill the void spaces of wood thereby decreasing its water absorption capacity. Samples treated with MFFA/DMDHEU/nanoclay/SiO_2 showed more reduction in water absorption capacity since the layers of nanoclay provided a tortuous path for diffusion of water molecules [32]. It was observed from the figure that with the increase in the amount of SiO_2, there was a noticeable improvement in properties as SiO_2 decreased the available sites for water absorption. Addition of PP would enhance the interaction between wood, MFFA, DMDHEU, SiO_2 and surface hydroxyl group of nanoclay through its available hydroxyl groups and hence it showed least water absorption. The results of volumetric swelling of the samples showed similar trend as those of samples for water absorption.

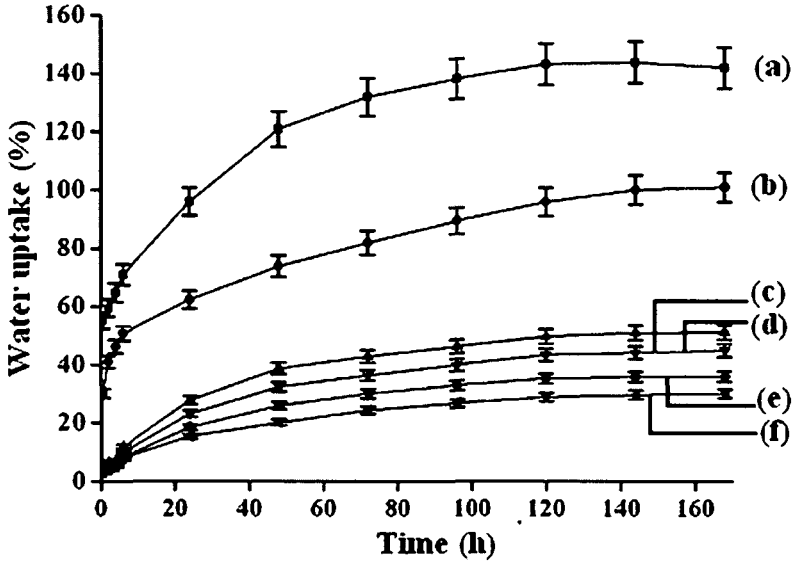

Figure 5.2.6. Water absorption test of wood (a) untreated and treated with (b) MFFA/DMDHEU (c) MFFA/DMDHEU/nanoclay/ SiO_2 (1 phr) (d) MFFA/DMDHEU/ nanoclay/ SiO_2 (2 phr) (e) MFFA/DMDHEU/nanoclay/SiO_2 (3 phr) (f) MFFA/DMDHEU /nanoclay/SiO_2 (3 phr)/PP.

5.2.8. Chemical resistance test

Table 5.2.3. shows the chemical resistance of untreated and treated wood samples. Both untreated and treated wood samples were kept immersed in 4% acetic acid and 4% NaOH solution. Tajvidi et al. compared the chemical resistance properties of rice hulls /polypropylene composites in different chemical reagents and found that maximum weight loss of composite occurred due to treatment with NaOH [35]. Treated wood samples showed less swelling than the untreated ones. MFFA could interact with wood through its hydroxyl and methylol groups. This interaction was improved after the addition of DMDHEU as it could crosslink with the cell wall of wood and the polymer. Further addition of nanoclay and SiO_2 decreased the swelling of wood samples as clay layers acted as barrier for the diffusion of chemical into the composite. Further the void spaces in wood were filled by the polymer, crosslinker, nanoclay and SiO_2. The addition of PP further reduced the swelling of the samples as it could augment the interaction between wood, MFFA, DMDHEU, nanoclay and SiO_2 through its available hydroxyl groups. Samples immersed in NaOH swelled more compared to those of samples immersed in acetic acid. This might be due to the better interaction of clay layers, wood cellulose and sodium hydroxide [36].

Table 5.2.3. Chemical resistance test of the WPC samples.

Samples	Volumetric swelling Time			
	24 h		168 h	
	NaOH solution (4%)	Acetic acid (4%)	NaOH solution (4%)	Acetic acid (4%)
Untreated	12.57 (±0.82)	8.27 (±0.68)	13.83 (±0.65)	10.68 (±0.46)
MFFA treated	8.41 (±0.51)	5.28(±0.38)	11.27 (±0.46)	6.21 (±0.72)
MFFA/DMDHEU treated	6.39 (±0.77)	4.23 (±0.54)	7.78 (±0.22)	5.28 (±0.48)
MFFA/DMDHEU/nanoclay/ SiO_2 (1.0 phr) treated	3.03 (±0.38)	2.02 (±0.79)	4.58 (±0.83)	2.98 (±0.41)
MFFA/DMDHEU/nanoclay/ SiO_2 (2.0 phr) treated	2.87 (±0.53)	1.93 (±0.77)	4.39 (±0.94)	2.72 (±0.52)
MFFA/DMDHEU/nanoclay/ SiO_2 (3.0 phr) treated	2.68 (±0.84)	1.82 (±0.43)	4.19 (±0.47)	2.59 (±0.56)
MFFA/DMDHEU/nanoclay/ SiO_2 (3.0 phr)/PP treated	2.36 (±0.55)	1.70 (±0.34)	4.04 (±0.89)	2.31 (±0.95)

5.2.9. Mechanical properties

Flexural and tensile values of untreated and treated wood samples are shown in Table 5.2.4. Untreated wood samples showed the least flexural and tensile values whereas samples treated with MFFA/DMDHEU/nanoclay/SiO_2 (3 phr)/PP showed the highest values. Samples treated with MFFA/DMDHEU had higher values than the untreated wood samples. Melamine formaldehyde (MF) resin is one of the stiffest polymeric resins and DMDHEU could form crosslink structure with cell wall of wood and polymer [19,34]. Nanoclay and SiO_2 could significantly improve its properties. With the increase in the amount of SiO_2, there was a notable enhancement in properties. The uniform distribution of SiO_2 nanoparticles in the composites was also responsible for improvement in the properties. The interaction of wood with SiO_2 and nanoclay could stiffen the composites. The polymer chains were inserted in between the gallery layers of nanoclay thereby losing its mobility. Thus, a crosslinked structure might form which enhanced the tensile and flexural values. PP further facilitated the interaction between wood, MFFA, DMDHEU, nanoclay and SiO_2 through its hydroxyl groups.

Table 5.2.4. Flexural and tensile properties of untreated and treated wood.

Sample	Flexural properties		Tensile properties	
	Strength (MPa)(±SD)	Modulus (MPa)(±SD)	Strength (MPa)(±SD)	Modulus (MPa)(±SD)
Untreated wood	117.79 (±0.65)	5907.50 (±0.45)	39.39 (±2.10)	292.17 (±9.22)
Wood treated with MFFA/DMDHEU	125.44 (±0.58)	6292.23 (±1.32)	46.73 (±1.16)	346.62 (±8.78)
MFFA/DMDHEU/ nanoclay/SiO_2 (1 phr)	135.42 (±0.75)	6792.84 (±1.21)	62.33 (±0.96)	462.33 (±10.98)
MFFA/DMDHEU/ nanoclay/SiO_2 (2 phr)	139.87 (±0.97)	7017.06 (±1.19)	64.28 (±0.84)	476.80 (±11.12)
MFFA/DMDHEU/ nanoclay/SiO_2 (3 phr)	142.53 (±0.43)	7149.48 (±0.86)	67.37 (±1.73)	499.72 (±9.23)
MFFA/DMDHEU/ nanoclay/SiO_2 (3 phr)/PP (3 phr)	145.67 (±0.87)	7307.01 (±1.27)	69.54 (±2.02)	515.81 (±8.32)

5.2.10. Limiting oxygen index (LOI)

Table 5.2.5. shows the limiting oxygen index values of untreated and treated wood samples. Wood samples treated with MFFA and DMDHEU showed higher LOI values due to the combined effect of MFFA and DMDHEU. Both were the supplier of nitrogen and when the samples were subjected to combustion, oxides of nitrogen were produced. These oxides of nitrogen displaced oxygen present on the surface of the samples [21]. Samples treated with MFFA/DMDHEU/nanoclay/SiO_2 showed higher LOI values than MFFA/DMDHEU treated ones. Surface modification of SiO_2 resulted in improved adhesion between wood, MFFA, DMDHEU. Nanoclay and SiO_2 enhanced the formation of char. Higher the amount of SiO_2, higher was the amount of carbonaceous-silica char on the surface. Char insulated the samples resulting in improved flame retardancy [22]. Samples treated with MFFA/DMDHEU/nanoclay/SiO_2 (3 phr)/PP showed highest LOI values due to its phosphorus content [23].

5.2.11. Thermogravimetric analysis

Table 5.2.5. shows the initial decomposition temperature (T_i), maximum pyrolysis temperature (T_m), and residual weight (%) (RW) for untreated and treated wood samples. The values for each sample were very close to each other. The datas presented (Table 5.2.5.) were the average value of three samples. Treatment of samples with MFFA/DMDHEU enhanced the T_i values. There was a decrease in weight loss (%) below 100°C which was due to moisture loss. DMDHEU played a significant role in improving the T_i values as it could improve interfacial adhesion between wood and the polymer. Samples treated with MFFA/DMDHEU/nanoclay/SiO_2/PP showed maximum T_i values. Nanoclay and SiO_2 improved thermal stability of the composites and acted as barrier for the volatile products generated during decomposition [25]. With the increase in amount of SiO_2, there was an improvement in thermal stability of the composites. Katsikis et al. also had found similar improvement in thermal properties of PMMA silica nanocomposite [37]. The presence of phosphorus in PP further improved the thermal properties of the composites.

T_m values for the first stage of pyrolysis was due to the depolymerization of hemicellulose, glycosidic linkage of cellulose, thermal decomposition of cellulose and disintegration of interunit linkages, condensation of aromatic rings during pyrolytic degradation of lignin while the second stage was due to polymer degradation [13]. T_m values for the treated samples were found higher than the untreated ones.

Untreated wood had the highest RW value. All the volatile components diffused during degradation and the lignin contributed to char formation. MFFA/DMDHEU had the lowest RW value. The values increased on addition of nanoclay and SiO_2. Moreover, as the amount of SiO_2 increased, the RW values also increased. Nanoclay and SiO_2 promoted formation of char, insulated the samples and thereby increased its thermal stability.

Table 5.2.5. Thermal degradation of untreated and treated wood samples.

Sample	T_i	T_m[a]	T_m[b]	Temperature of decomposition (T_D) in °C at different weight loss (%)				RW% at 600 °C	LOI (%)(±SD)
				20%	40%	60%	80%		
Untreated wood	160	301	393	265	295	334	--	28.12	20 (±0.87)
Wood treated with MFFA/DMDHEU	236	337	433	303	331	359	423	8.6	24 (±0.42)
MFFA/DMDHEU/ nanoclay/SiO_2 (1 phr)	270	368	458	338	359	388	449	18.11	27 (±0.53)
MFFA/DMDHEU/ nanoclay/SiO_2 (2 phr)	272	371	460	342	362	391	459	18.78	31 (±0.62)
MFFA/DMDHEU/ nanoclay/SiO_2 (3 phr)	276	375	464	344	364	394	461	19.32	33 (±0.39)
MFFA/DMDHEU/ nanoclay/SiO_2 (3 phr)/PP	278	377	466	347	366	397	464	19.44	37 (±1.01)

Section C: Synergistic effect of nano TiO_2 and nanoclay on the ultraviolet degradation and physical properties of wood polymer nanocomposites.

Titanium dioxide (TiO_2) nanopowder is increasingly being investigated to improve UV stability and durability of the composites. TiO_2 reinforcement can improve physiochemical, mechanical and abrasion resistance properties making the nanocomposites a promising category of products [38]. There are few reports addressing the enhancement in properties of wood such as weather resistance and antimicrobial activity of wood by the use

of TiO_2 sols through sol-gel methods [39]. There is scope to do further work in this area. The objective of the present work was to study the combined effect of TiO_2 nanopowder and organoclay on the different properties of wood. WPNC was prepared by impregnating MFFA copolymer, DMDHEU, a crosslinking agent, nanoclay, nano TiO_2 and a renewable polymer obtained as a gum from the plant *Moringa oleifera* into wood (*Ficus hispida*) (PP). In order to obtain optimum properties, the parameters like vacuum, time of impregnation, monomer concentration, initiator concentration, amount of crosslinking agent, nanoclay and plant polymer were varied to obtain optimum properties. The conditions, at which maximum improvement of properties were obtained, were 500 mm Hg vacuum, 6 h time of impregnation, 5:1 (MFFA:FA-water) prepolymer concentration, 1% (w/w) maleic anhydride, 3 mL DMDHEU, 3 phr nanoclay, 3 % (w/v) PP.

5.3. RESULTS AND DISCUSSION

5.3.1. Effect of variation of TiO_2 on polymer loading (WPG %), volume increase, and hardness

Related results are shown in Table 5.3.1. An enhancement in properties like polymer loading (WPG %), volume increase, and hardness were observed on impregnation of TiO_2

Table 5.3.1. Effect of variation of CTAB-TiO_2 on weight % gain (WPG %), volume increase and hardness.

Samples particulars	Weight gain (%) (WPG %)	Volume increase (%)	Hardness (Shore D)
Untreated	--	--	47 (±0.97)
Samples treated with MFFA/FA-water/DMDHEU/ nanoclay/CTAB- TiO_2/PP			
100/20/3/0/0/0	27.12 (±0.45)	2.06 (±0.23)	60 (±0.37)
100/20/3/3/1/0	43.76 (±0.79)	3.23 (±0.85)	69 (±0.76)
100/20/3/3/2/0	45.86 (±0.68)	3.63 (±0.43)	74 (±0.42)
100/20/3/3/3/0	48.12 (±0.93)	3.89 (±0.54)	77 (±0.89)
100/20/3/3/3/3	50.11 (±0.36)	3.99 (±0.61)	78 (±0.66)

along with MFFA, DMDHEU and nanoclay into wood. The higher the amount of TiO_2, the higher was the improvement. The improvement was due to deposition of polymer, crosslinker and nanoparticles into the void spaces of wood. DMDHEU enhanced the deposition by forming crosslinked structure with the cell wall of wood [19]. Devi and Maji found similar improvement in weight percent gain of wood after incorporation of styrene-acrylonitrile copolymer and ZnO nanoparticles [40]. Further incorporation of PP resulted in enhancement of properties of the composites. The key ingredients of PP are L-arabinose, D-galactose, D-glucuronic acid, L-rhamnose, D-mannose and D-xylose [20]. All of these ingredients have plentiful hydroxyl groups which increase the interaction with MFFA, DMDHEU, nanoclay and TiO_2.

5.3.2. FTIR study

The FTIR spectra of MFFA, DMDHEU, nanoclay, unmodified TiO_2, CTAB modified TiO_2 are shown in Figure 5.3.1. The characteristic bands for MFFA copolymer were appeared at 3421 cm^{-1} (-OH stretching), 2937 cm^{-1} and 2858 cm^{-1} (-CH_2 asymmetric and symmetric stretching), 1568 cm^{-1} and 1500 cm^{-1} (furan ring vibration), 1187 cm^{-1} (C-N stretching), 814 cm^{-1} (out plane trisubstitution of triazine ring) [1]. Absorption bands appearing in the spectrum of DMDHEU at 3421, 1704, 1244 and 1024 cm^{-1} (curve b) were for -OH stretching, C=O stretching, -CHOH stretching, CH_2OH stretching respectively [2]. Nanoclay (curve c) showed peaks at 3466 cm^{-1} for –OH stretching, 2929 and 2854 cm^{-1} for –CH stretching of modified hydrocarbon, 1620 cm^{-1} for –OH bending, 1032–459 cm^{-1} for oxide bands of metals like Si, Al, Mg, etc. The FTIR spectrum of plant polymer showed the presence of bands at 3422 cm^{-1} (-OH stretching), 2930 cm^{-1} and 2859 cm^{-1} (-CH_2 stretching), 1676 cm^{-1} (the α,β-unsaturated carbonyl stretching), 1368 cm^{-1} (C-H deformation), 1010 cm^{-1} (R-O-Ar linkage) (curve d). The surface hydroxyl groups of TiO_2 showed bands at 3430 and 1630 cm^{-1} due to –OH stretching and –OH bending (curve e). Moreover, it showed a strong absorption band at 1030–416 cm^{-1} due to the Ti-O-Ti stretching [41,42]. It was observed that the intensity of the peak corresponding to -OH stretching decreased in the spectrum of modified TiO_2 which indicated the interaction of the hydroxyl group absorbed on TiO_2 surface with CTAB (curve f). Some new peaks were appeared at 2920 and 2846 cm^{-1} (-CH stretching of the modifying hydrocarbon) and 1472 cm^{-1} (-CH bending) in the spectrum of modified TiO_2. Qu et al. modified TiO_2 with CTAB and suggested that the interaction of TiO_2 occurred with Br^- ion of CTAB through hydrogen bond formation or electrostatic attractions [43].

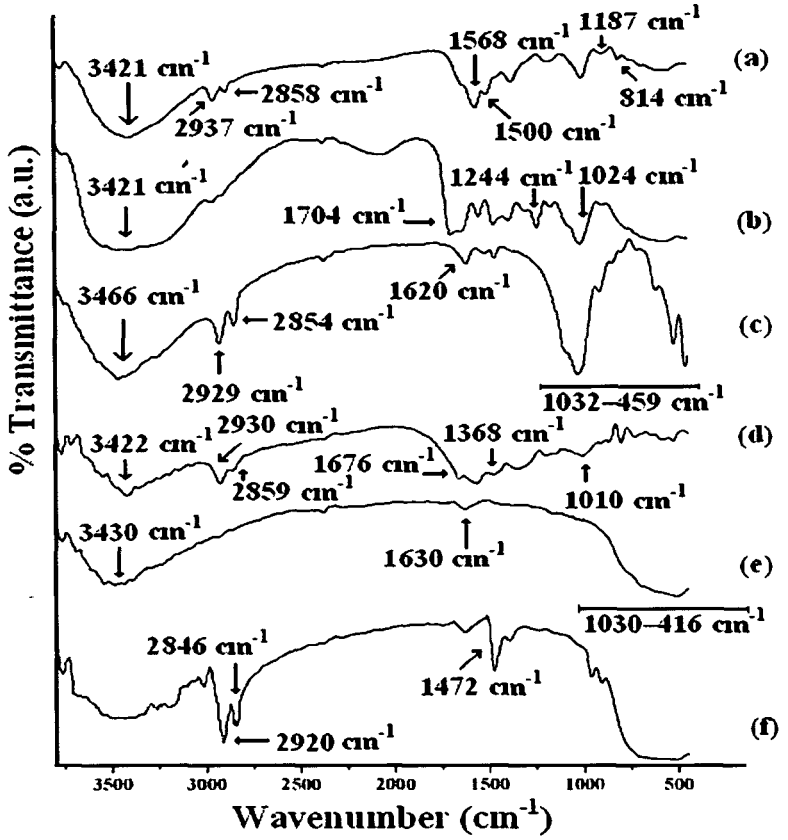

Figure 5.3.1. FTIR spectra of (a) MFFA (b) DMDHEU (c) nanoclay (d) unmodified TiO_2 (d) CTAB modified TiO_2.

Figure 5.3.2. shows the FTIR spectra of untreated and treated wood samples. Untreated wood (curve a) was characterized by the absorption bands appeared at 3448 cm^{-1} (–OH stretching), 2923 cm^{-1}, and 2855 cm^{-1} (–CH_2 asymmetric stretching in alkyl groups due to both cellulose and lignin), 1740 cm^{-1} (C=O stretching of hemicelluloses), 1661 cm^{-1} for (–OH bending), 1506 cm^{-1} (aromatic skeletal vibration by lignin), 1256 and 1041 cm^{-1} (C–O stretching) and 1000–644 cm^{-1} (out of plane C–H bending vibration). In the spectrum for the treated wood samples, the intensity of the hydroxyl peaks decreased and shifted to lower wave number. The peaks shifted to 3432 cm^{-1} (curve b), 3412 cm^{-1} (curve c), 3362 cm^{-1} (curve d), 3295 cm^{-1} (curve e), 3273 cm^{-1} (curve f) compared to 3448 cm^{-1} (curve a) of untreated wood. This confirmed the interaction between hydroxyl group of wood, MFFA, DMDHEU, nanoclay and TiO_2. The addition of PP further enhanced the interaction caused by the presence of profuse hydroxyl groups. In all the treated wood samples, the intensity of the peak corresponding to the –CH_2 stretching was found to increase.

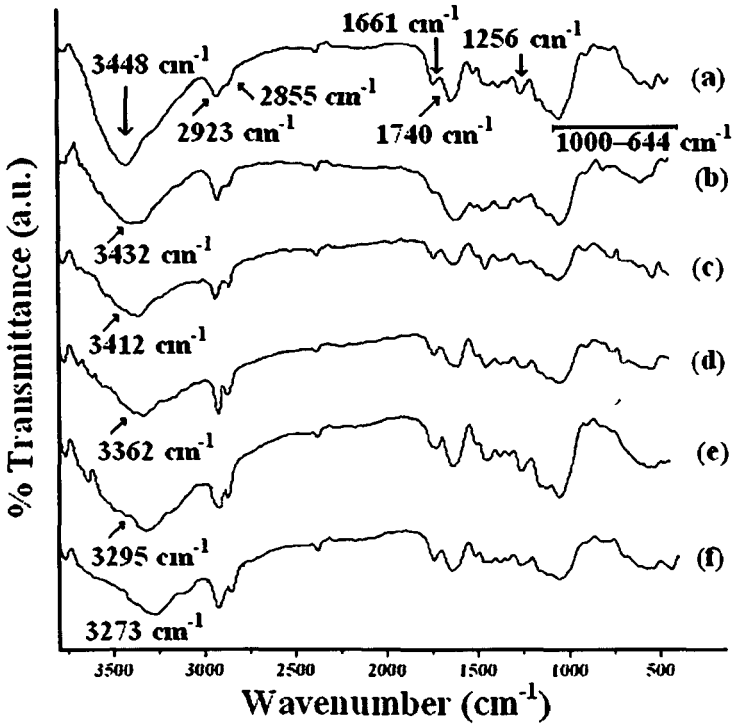

Figure 5.3.2. FTIR spectra of wood (a) untreated and treated with (b) MFFA/DMDHEU (c) MFFA/DMDHEU/nanoclay/TiO_2 (1 phr) (d) MFFA/DMDHEU/nanoclay/TiO_2 (2 phr) (e) MFFA/DMDHEU/nanoclay/TiO_2 (3 phr) (f) MFFA/DMDHEU/nanoclay/TiO_2 (3 phr)/PP.

5.3.3. XRD analysis

The X-ray diffractogram of nanoclay and nano TiO_2 are presented in Figure 5.3.3. Nanoclay showed a sharp diffraction peak at $2\theta = 4.4^\circ$ due to the 101 crystal plane with basal spacing of 2.15 nm as calculated from Bragg's equation (curve a). The crystalline portion of TiO_2 showed peaks at $2\theta = 27.37^\circ$ (110), 36.13° (200), 37.69° (111), 47.78° (210), 54.37° (211), 56.70° (220) (curve-b) [44,45].

X-ray diffractogram of untreated and treated wood samples are shown in Figure 5.3.4. As cellulose is the chief constituent of wood, it showed a wide diffraction peak at $2\theta = 22.83^\circ$ due to the 002 crystal plane of cellulose. The other crystal plane of cellulose i.e. 101 plane showed small peak at 15.02° (curve a) [8]. Curves (b-e) represent the diffractograms of WPC treated with 3 phr nanoclay, different percentages of TiO_2 (1-3 phr) and 3 phr PP. The diffraction peak for the nanoclay disappeared in the composites suggesting either the

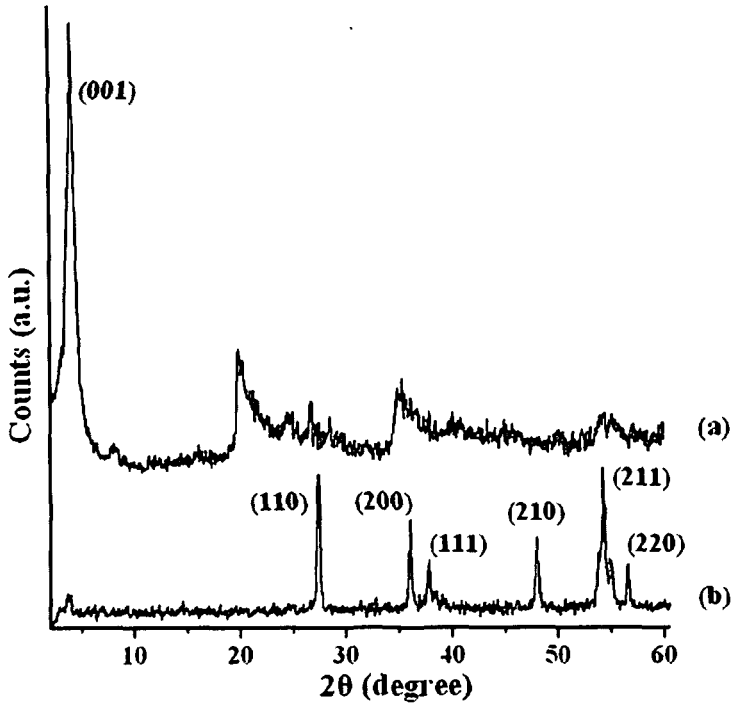

Figure 5.3.3. X-ray diffraction of (a) nanoclay (b) Nano TiO_2.

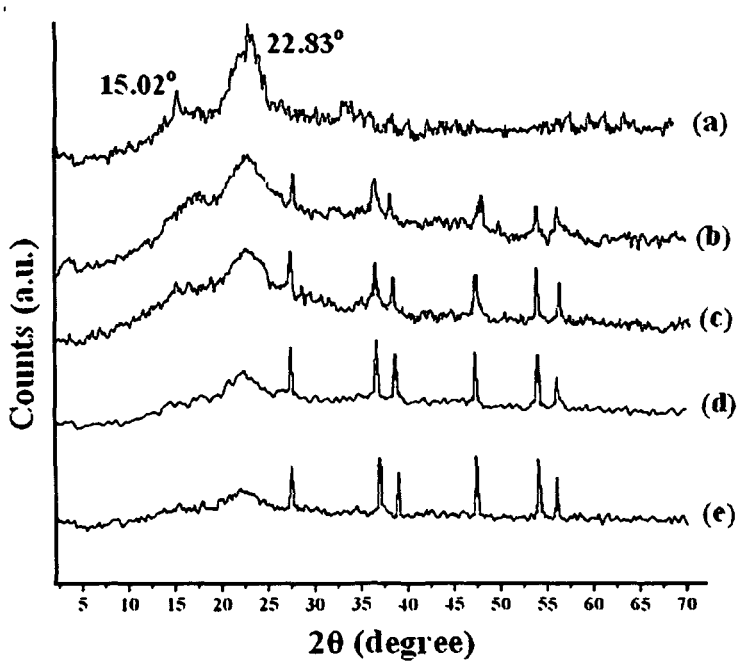

Figure 5.3.4. X-ray diffraction of (a) untreated wood (b) MFFA/DMDHEU/nanoclay/TiO_2 (1 phr) treated (c) MFFA/DMDHEU/nanoclay/TiO_2 (2 phr) treated (d) MFFA/DMDHEU/ nanoclay/TiO_2 (3 phr) treated (e) MFFA/DMDHEU/nanoclay/TiO_2 (3 phr)/PP treated wood samples.

nanoclay layers were separated so that it was not possible to detect by XRD or the nanoclay layers became delaminated. With the increase in the amount of TiO_2, it was observed that the intensity of the peak appearing at $2\theta = 22.83^{\circ}$ decreased. The peak corresponding to 15.02° became dull which indicated a decrease in crystallinity of wood cellulose. The decrease in crystallinity of cellulose of wood was due to insertion of silicate nanolaminae and TiO_2 nanoparticles into the amorphous region of wood cellulose [8]. Mina et al. studied the X-ray diffraction pattern of polypropylene/titanium dioxide composite and reported a similar increase in peak intensity of TiO_2 in the composites [46]. The addition of PP did not bring about any significant change in the diffractogram of WPNC (curve e).

5.3.4. Crystallinity determination from FTIR and XRD

Deconvolution of the diffractograms was done by using Voigst function. Varied functions were used to analyze the diffraction peaks, but fitting with the Voigst functions resulted in the best fit [11]. The results for the crystallinity index determination are shown in Table 5.3.2. Figure 5.3.4 shows no lattice transformation of cellulose I to cellulose II as the peaks appearing at 15.02° and at 22.98° were not replaced by the characteristics peak for the 101 ($2\theta = 12^{\circ}$) and 002 plane ($2\theta = 21^{\circ}$) of cellulose II. This was due to the presence of lignin which prevented its transformation [12]. Highest crystallinity index was shown by the untreated wood followed by the treated ones. The rigidity of cellulose of wood was reduced due to the breaking of intermolecular and intramolecular hydrogen bonds. They participated in the bond formation between MFFA, DMDHEU, nanoclay, TiO_2 and PP. The distortion of the crystallites structures of wood cellulose occurred due to chemical grafting. The chemical grafting reaction took place in the amorphous region of wood cellulose since the distribution of the polymer chains in the crystallites region of cellulose was difficult. The polymers reacted at the chain end on the surface of the crystallites and thus some of the hydrogen bonded cellulose chains were opened. More amorphous cellulose was produced with the progress of the reaction [13]. The results for the crystallinity index values were calculated from both FTIR and XRD and the values were found in good agreement with each other. Least crystallinity index value was shown by the samples treated with MFFA/DMDHEU/nanoclay/TiO_2 (3 phr)/PP.

5.3.5. Morphological Studies of the nanocomposites

Figure 5.3.5. shows the energy dispersive X-ray spectroscopy (EDS) of the PP and CTAB modified TiO_2. It was evident from the EDS spectrum that the PP contained C, O, P and Ca (Figure 5.3.5. a). The presence of phosphorus was responsible for its flame retardant behavior. Similar results were reported by Ghosh et al. while studying the EDS analysis of PP [15]. Traces amount of nitrogen was also found in modified TiO_2 as shown in the EDS spectrum of CTAB modified TiO_2. This traces amount of nitrogen did not have a significant contribution in governing the flame retardancy behavior of the composites. This spectrum indicated the grafting of alkyl chain of CTAB onto the surface of TiO_2.

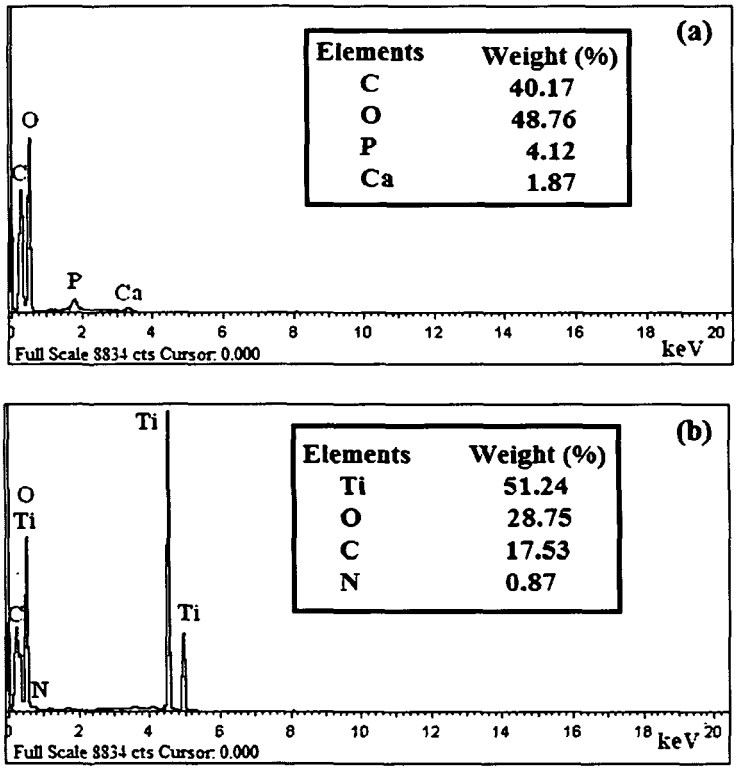

Figure 5.3.5. EDS of (a) PP (b) CTAB modified TiO_2.

Scanning electron micrographs for the untreated and treated wood samples are shown in Figure 5.3.6. The empty cell lumens of untreated wood (Figure 5.3.6.a) were occupied by the polymer and crosslinker (Figure 5.3.6.b). The presence of nanoclay and TiO_2 were appeared as white spots and black spots which were located either in the cell walls or in the cell lumen (Figure 5.3.6.c-f).

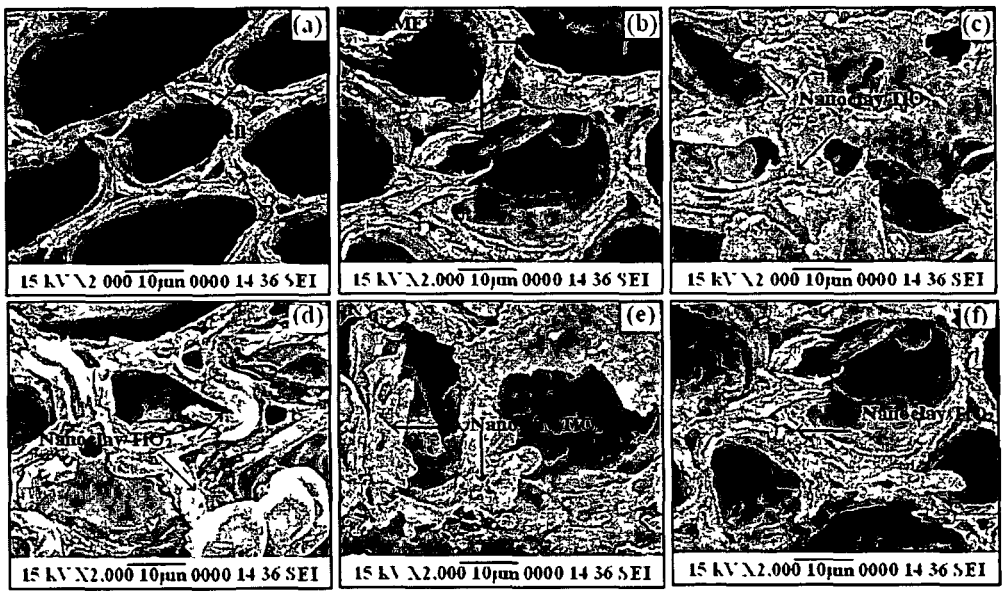

Figure 5.3.6. SEM micrographs of wood (a) untreated and treated with (b) MFFA/DMDHEU (c) MFFA/DMDHEU/nanoclay/TiO_2 (1 phr) (d) MFFA/DMDHEU/ nanoclay/TiO_2 (2 phr) (e) MFFA/DMDHEU/nanoclay/TiO_2 (3 phr) (f) MFFA/DMDHEU/ nanoclay/TiO_2 (3 phr)/PP.

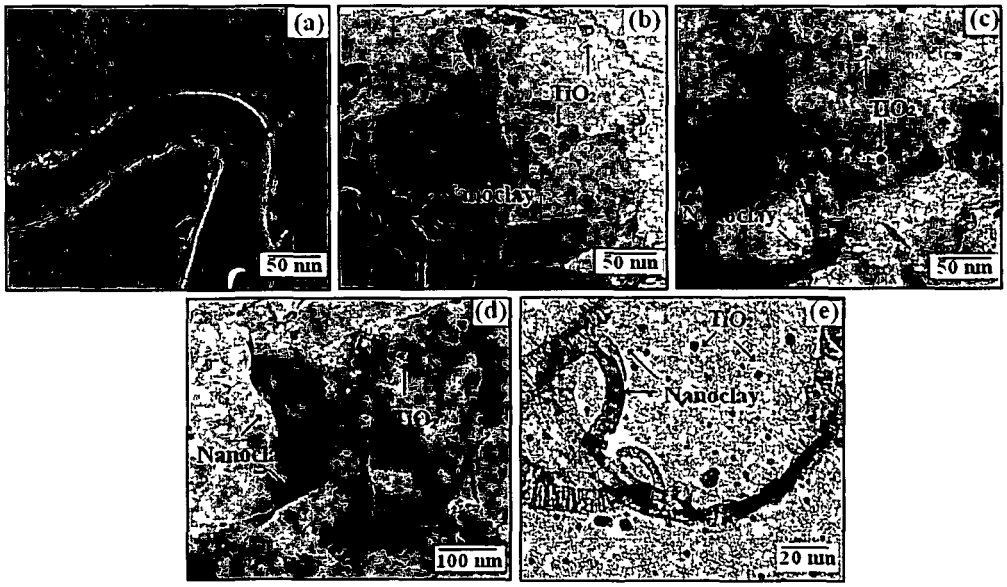

Figure 5.3.7. Transmission electron micrographs of (a) untreated (b) MFFA/DMDHEU /nanoclay/TiO_2 (1 phr) treated (c) MFFA/DMDHEU/nanoclay/ TiO_2 (2 phr) treated (d) MFFA/DMDHEU/nanoclay/TiO_2 (3 phr) treated (e) MFFA/DMDHEU/nanoclay/TiO_2 (3 phr)/PP treated wood samples.

Transmission electron micrographs of untreated and treated wood samples are shown in Figure 5.3.7. Untreated wood showed no such orientation of its cell wall components (Figure 5.3.7.a). The presence of nanoclay could be seen in the micrograph as some dark lines while that of TiO_2 was seen as dark spots. A homogenous distribution of nanoclay and TiO_2 was observed in the cell wall of wood (Figure 5.3.7.b-e).

5.3.6. UV resistance study

Five specimens of each composition were used for both untreated and treated wood samples. The variation of crystallinity index values of the untreated and treated wood samples calculated from FTIR spectra on exposure to UV rays for different time period are shown in Table 5.3.2. The rate of decrease of crystallinity index was more in untreated wood than that of treated wood. DMDHEU and PP enhanced the interfacial interaction between wood and polymer. TiO_2 and nanoclay shielded the composite by acting as a barrier for the UV rays. Thus the crystallinity of the composite was least affected by the UV rays.

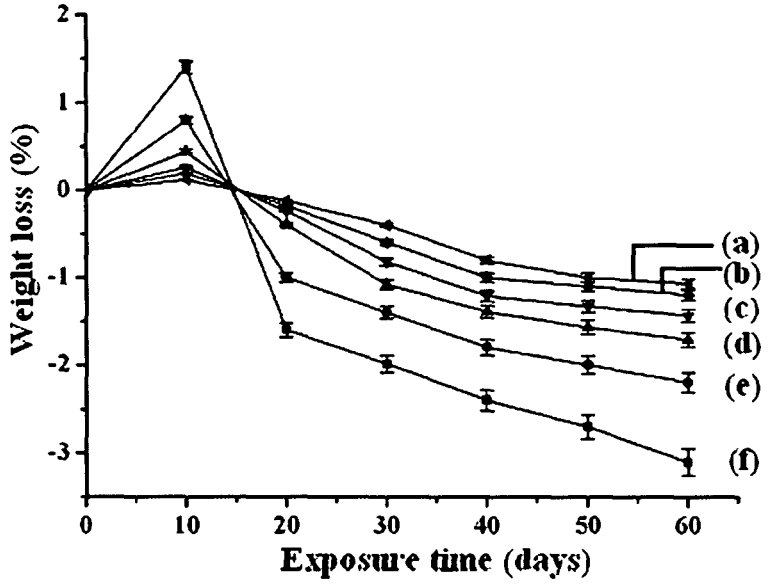

Figure 5.3.8. Weight losses versus exposure time of (a) MFFA/DMDHEU/nanoclay/TiO_2 (3 phr)/PP treated (b) MFFA/DMDHEU/nanoclay/TiO_2 (3 phr) treated (c) MFFA/DMDHEU /nanoclay/TiO_2 (2 phr) treated (d) MFFA/DMDHEU MFFA/DMDHEU/nanoclay/TiO_2 (1 phr) treated (e) MFFA/DMDHEU treated (f) untreated wood samples.

Table 5.3.2. Crystallinity index values of cellulose matrix of untreated and treated wood samples calculated by the area method before and after UV exposure.

Samples		Untreated wood	MFFA/ DMDHEU treated	MFFA/ DMDHEU/ nanoclay/ TiO_2 (1 phr) treated	MFFA/ DMDHEU/ nanoclay/ TiO_2 (2 phr) treated	MFFA/ DMDHEU/ nanoclay/ TiO_2 (3 phr) treated	MFFA/ DMDHEU/ nanoclay/ TiO_2 (3 phr)/ PP treated
XRD results		62.87	53.23	40.12	38.67	33.92	32.48
FTIR results	Before irradiation	62.26	53.41	41.89	38.88	34.31	32.31
	After irradiation						
	10 days	59.14	50.66	39.12	37.58	33.54	32.97
	20 days	56.32	49.43	39.83	38.86	32.32	33.62
	30 days	54.27	47.67	38.78	37.48	31.11	32.86
FTIR results	40 days	50.38	46.87	37.63	36.98	31.87	31.17
	50 days	46.65	45.23	36.33	36.53	30.28	31.78
	60 days	44.32	45.76	36.92	36.13	30.64	32.03

The weight loss of untreated and treated wood samples exposed to UV irradiation for different time periods are shown in Figure 5.3.8. An early increase in weight was observed for both the untreated and treated wood samples which were due to moisture uptake. The material loss induced by the degradation was lower than the early increase in weight loss. Untreated wood samples showed highest weight loss (%). With the increase in the amount of TiO_2, a decrease in the rate of weight loss was observed after 60 days of exposure. The weight loss was lowest in case of samples treated with MFFA/DMDHEU/nanoclay/TiO_2/PP.

The change of carbonyl index value with time is shown in Figure 5.3.9. Highest carbonyl index value was shown by the untreated wood samples due to higher oxidation of cellulose of wood. After 60 days of exposure to an UV environment, there was an increase in carbonyl index value for all the samples. The increase in the values was ascribed due to chain scission of the polymer and wood. As the chain scission occurred, the density of entanglements of polymer chain decreased and thus a reduction in weight loss was observed. Treatment of the samples with MFFA/DMDHEU showed lower carbonyl index values than the untreated ones. The crosslinked structure formed by DMDHEU with the hydroxyl group of cellulose delayed the photodegradation process. Addition of nanoclay and TiO_2 further decreased the carbonyl index value. The higher the TiO_2 concentration, the lower was the carbonyl index value. Both nanoclay and TiO_2 played a significant role in stabilizing the composites. They acted as a screen for the UV rays. Hence the intensity of UV rays required for oxidation of the samples decreased and as a consequence the rate of the photo degradation process delayed. An increase in UV stability was reported by Grigoriadou et al. due to addition of montmorillonite clay in high density polyethylene [17]. Du et al. observed an increase in UV stability of TiO_2 treated wood flour/high density polyethylene composite [47]. PP enhanced the interaction through its hydroxyl groups between wood, polymer, crosslinker, nanoclay and TiO_2 and thus decreased the degradation process.

The lignin index values with time for untreated and treated wood samples are shown in Figure 5.3.10. Nanoclay and TiO_2 prevented the degradation of lignin present in wood from the formation of quinones, carbonyls or peroxides and thus enhanced the UV stability of composites. The values for the lignin index decreased with the increase in UV exposure time. Treated samples showed higher lignin index values than untreated wood samples. Ionic liquid treated wood showed similar decrease in the lignin index values on exposure to UV radiation [18].

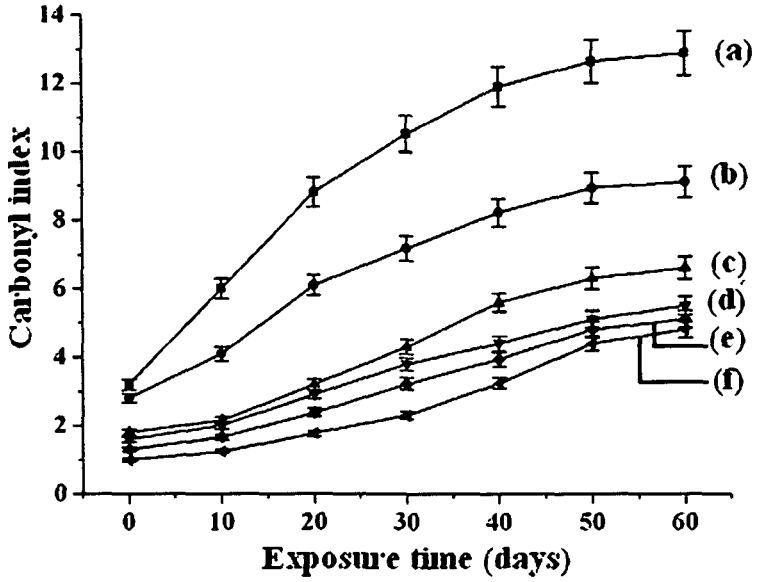

Figure 5.3.9. Carbonyl index values of (a) untreated wood and treated with (b) MFFA/DMDHEU (c) MFFA/DMDHEU/nanoclay/TiO_2 (1 phr) (d) MFFA/DMDHEU/nanoclay/TiO_2 (2 phr) (e) MFFA/DMDHEU/nanoclay/TiO_2 (3 phr) (f) MFFA/DMDHEU/nanoclay/TiO_2 (3 phr)/PP.

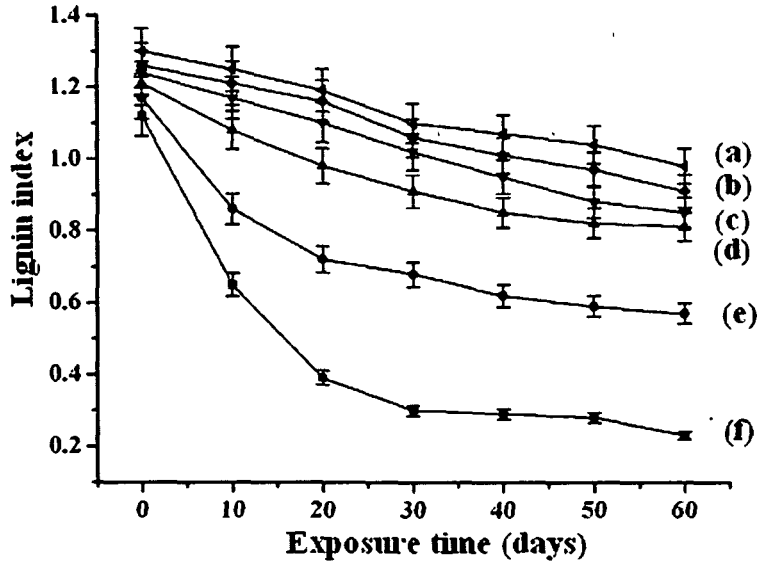

Figure 5.3.10. Lignin index values of wood treated with (a) MFFA/DMDHEU/nanoclay/ TiO_2 (3 phr)/PP (b) MFFA/DMDHEU/nanoclay/TiO_2 (3 phr) (c) MFFA/DMDHEU/ nanoclay/TiO_2 (2 phr) (d) MFFA/DMDHEU/nanoclay/TiO_2 (1 phr) (e) MFFA/DMDHEU (f) untreated wood samples.

The change in carbonyl peak (1733 cm^{-1}) and lignin peak (band at 1510 cm^{-1}) intensity was evident from the FTIR spectra of the untreated and treated wood samples upon exposure to UV rays for 60 days (Figure 5.3.11.).

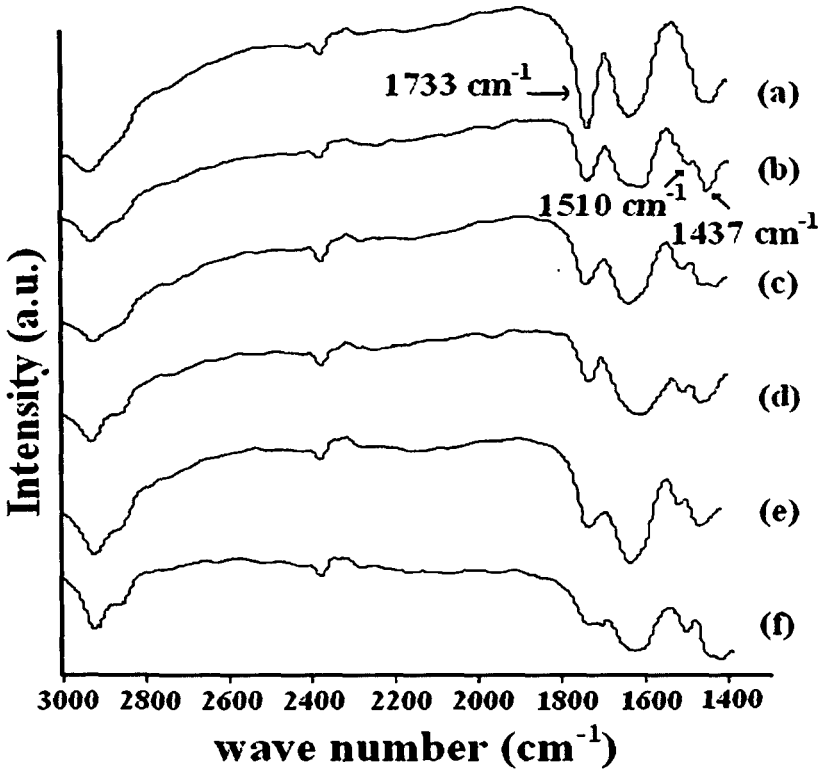

Figure 5.3.11. Change in carbonyl and lignin peak intensity of (a) untreated wood and treated with (b) MFFA/DMDHEU (c) MFFA/DMDHEU/nanoclay/TiO_2 (1 phr) (d) MFFA/DMDHEU/nanoclay/TiO_2 (2 phr) (e) MFFA/DMDHEU/nanoclay/TiO_2 (3 phr) (f) MFFA/DMDHEU/nanoclay/TiO_2 (3 phr)/PP.

Scanning electron micrographs of samples after 60 days of exposure to UV irradiation are shown in Figure 5.3.12. Surface morphology of the samples changed due to exposure to UV radiation. Degradation occurred and cracks appeared on the surface of untreated wood. MFFA/DMDHEU treatment further reduced the formation of cracks on the surface. The surface smoothness of the composites was found to increase with the increase in the amount of TiO_2. Thus nanoclay and TiO_2 shielded the composite and retarded the formation of cracks. Addition of PP further enhanced its surface smoothness as it protects the composites from the UV rays by increasing the interaction between wood, TiO_2, nanoclay and MFFA polymer.

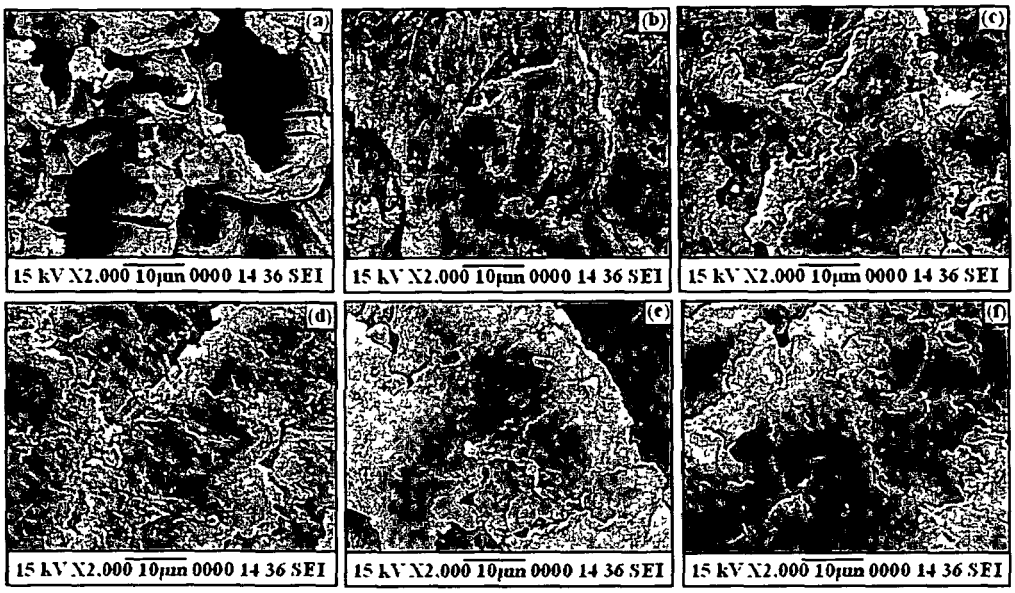

Figure 5.3.12. SEM micrographs of wood (a) untreated and treated with (b) MFFA/ DMDHEU (c) MFFA/DMDHEU/nanoclay/TiO_2 (1 phr) (d) MFFA/DMDHEU/nanoclay /TiO_2 (2 phr) (e) MFFA/DMDHEU/nanoclay/TiO_2 (3 phr) (f) MFFA/DMDHEU/nanoclay/ TiO_2 (3 phr)/PP.

The changes in mechanical properties after 60 days of UV exposure are presented in Table 5.3.3. Loss of mechanical properties was highest in the case of untreated wood while loss of properties was less in WPC treated with nanoclay and TiO_2. With the increase in the amount of TiO_2, WPC showed a less reduction in mechanical properties due to UV shielding effect provided by TiO_2.

5.3.7. Mechanical properties

Table 5.3.3. shows the tensile and flexural values of untreated and treated wood samples. Wood treated with MFFA/DMDHEU showed higher tensile and flexural values compared to untreated wood because of the presence of stiff MF resin. DMDHEU formed a crosslinked structure with cell wall of wood and polymer resulting in enhanced properties [19]. Incorporation of nanoclay and TiO_2 influenced the mechanical properties of the composites to a significant amount. At a fixed clay loading (3 phr), the tensile and flexural values of the WPC increased with the increase in the amount of TiO_2. The polymer chains were fastened in the gallery layers of nanoclay. This restricted the mobility of the polymer

Table 5.3.3. Flexural and tensile properties of untreated and treated wood before and after UV degradation.

Sample	Flexural properties				Tensile properties			
	Before degradation		After degradation		Before degradation		After degradation	
	Strength (MPa) (±SD)	Modulus (MPa) (±SD)	Strength (MPa) (±SD)	Modulus (MPa) (±SD)	Strength (MPa) (±SD)	Modulus (MPa) (±SD)	Strength (MPa) (±SD)	Modulus (MPa) (±SD)
Untreated Wood	118.82 (±0.74)	5960.14 (±0.58)	100.36 (±0.54)	5034.04 (±0.75)	40.76 (±0.42)	302.33 (±8.64)	31.32 (±0.72)	232.31 (±10.12)
Wood treated with MFFA/DMDHEU	127.24 (±0.64)	6382.51 (±0.36)	119.16 (±0.82)	5977.05 (±0.77)	48.13 (±1.21)	357.02 (±10.23)	40.66 (±0.45)	301.58 (±8.87)
MFFA/DMDHEU/nanoclay/ TiO_2 (1 phr)	136.73 (±1.02)	6858.54 (±0.71)	134.85 (±1.16)	6764.06 (±1.15)	65.75 (±1.17)	487.70 (±9.64)	58.34 (±0.68)	432.72 (±9.23)
MFFA/DMDHEU/nanoclay/ TiO_2 (2 phr)	138.87 (±0.94)	6965.89 (±0.97)	136.97 (±0.37)	6870.40 (±0.58)	66.65 (±0.32)	494.37 (±13.21)	61.35 (±1.14)	455.05 (±11.12)
MFFA/DMDHEU/nanoclay/ TiO_2 (3 phr)	141.39 (±1.05)	7092.30 (±1.14)	138.62 (±0.48)	6953.18 (±1.11)	68.65 (±2.01)	509.21 (±7.87)	65.31 (±0.92)	484.42 (±8.65)
MFFA/DMDHEU/nanoclay/TiO_2 (3 phr)/PP (3 phr)	142.68 (±0.65)	7157.01 (±1.03)	139.88 (±1.02)	7016.36 (±0.83)	69.54 (±1.87)	515.81 (±8.74)	67.65 (±1.31)	501.78 (±12.45)

chains and hence stiffened the composites. The cetyl group and surface hydroxyl group present in CTAB modified TiO_2 enhanced its interaction between wood, MFFA, DMDHEU and nanoclay. PP further enhanced its mechanical properties as they facilitated bond formation with the wood, MFFA, DMDHEU, nanoclay and TiO_2 through its available hydroxyl groups.

5.3.8. Water uptake test

Five specimens of each composition were used for both untreated and treated wood samples. The water uptake capacities for the untreated and treated wood samples are shown in Figure 5.3.13. With the increase in time of immersion, there was an increase in water uptake capacity for all the samples. Void spaces in untreated wood were responsible for showing the highest water absorption capacity. As DMDHEU facilitated the deposition of

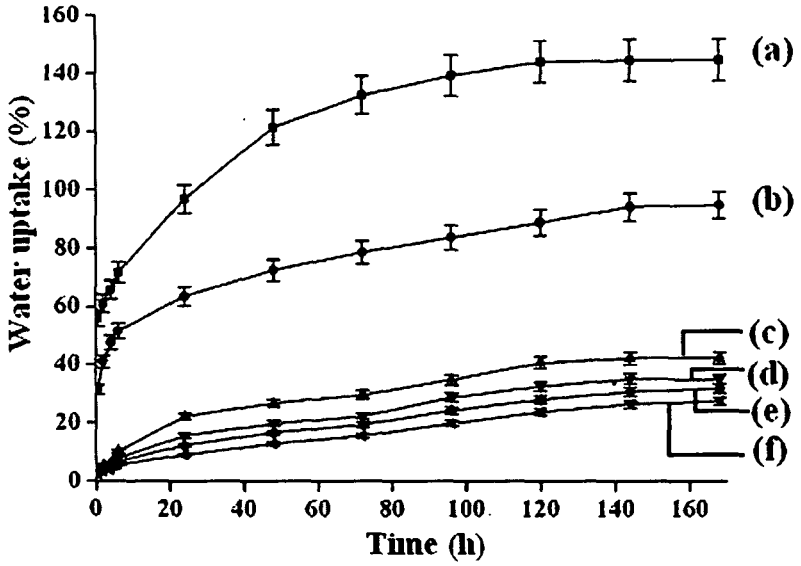

Figure 5.3.13. Water absorption test of wood (a) untreated and treated with (b) MFFA/DMDHEU (c) MFFA/DMDHEU/nanoclay/TiO_2 (1 phr) (d) MFFA/DMDHEU/nanoclay/TiO_2 (2 phr) (e) MFFA/DMDHEU/nanoclay/TiO_2 (3 phr) (f) MFFA/DMDHEU/nanoclay/TiO_2 (3 phr)/PP.

MFFA into its void spaces by forming crosslinked structure, a reduction in water uptake capacity was observed [19]. Nanoclay and TiO_2 further reduced its water uptake capacity. The layers of silica provided a meandering path for diffusion of water molecules. It was observed that with the increase in the amount of TiO_2, the water uptake capacity of the

samples decreased. TiO_2 in combination with nanoclay would make the cell wall of wood bulky by filling its empty spaces and thus a reduction in water uptake capacity was observed. The interaction between wood, MFFA, DMDHEU, nanoclay and TiO_2 was enhanced by the incorporation of PP through its available hydroxyl groups and hence a further decrease in water uptake capacity was noticed.

5.3.9. LOI study

Table 5.3.4. shows the LOI values of treated and untreated wood samples. The symbiotic effect of MFFA and DMDHEU was responsible for higher LOI values of the treated wood samples. Nitrogen is present in both MFFA and DMDHEU, and on combustion oxides of nitrogen were produced. These oxides displace oxygen present on the surface of the material and thus, increased the fire resistance properties of the composites [21]. Addition of nanoclay and TiO_2 promoted char formation. With the increase in the amount of TiO_2, there was an improvement in flame retardancy. The formation of char improved the flame retardancy by insulating the composites [22]. Higher the amount of TiO_2, higher was the char formation. Highest LOI value was observed for the samples treated with MFFA/DMDHEU/nanoclay/TiO_2/PP because of the presence of oxides of phosphorus formed by burning of PP [23].

5.3.10. Thermal stability

The initial decomposition temperature (T_i), maximum pyrolysis temperature (T_m), and residual weight (%) (RW) for untreated and treated wood samples are shown in Table 5.3.4. In all the cases, an initial weight loss (%) below 100 °C was observed due to removal of moisture. On incorporation of DMDHEU, the T_i value enhanced significantly due to improvement in interfacial adhesion between wood and MFFA caused by the formation of cross-linked structure. Nanoclay and TiO_2 further improved the T_i values. The silicate layers of nanoclay provided a tortuous path for the diffusion of decomposed volatile products throughout the composite [25]. The heat shielding effect of TiO_2 was responsible for enhanced thermal stability. The dispersion of nanoparticles inside the composite provided a thermal barrier releasing of combustible volatiles during decomposition. Higher the amount of TiO_2, higher was the insulating effect. The thermal stability of PMMA nanocomposite was significantly enhanced after the incorporation of nanoclay and TiO_2 as reported by

Laachachi et al. [26]. The presence of phosphorus in the PP further amplified its thermal stability.

T_m values for the first stage of pyrolysis was due to the depolymerization of hemicellulose, glycosidic linkage of cellulose, thermal decomposition of cellulose and disintegration of interunit linkages and condensation of aromatic rings during pyrolytic degradation of lignin [13]. The second stage of pyrolysis was due to the degradation of polymers. Higher T_m values were observed for all the treated wood samples.

RW (%) value of untreated wood was more due to the formation of char contributed by the lignin present in the wood. Samples treated with MFFA/DMDHEU showed the lowest RW value. Addition of nanoparticles would increase its value again as they fostered char formation.

Table 5.3.4. Thermal degradation and LOI test of untreated and treated wood samples.

Sample	T_i	T_m[a]	T_m[b]	Temperature of decomposition (T_D) in °C at different weight loss (%)				RW% at 600 °C	LOI (%) (±SD)
				20%	40%	60%	80%		
Untreated wood	160	303	396	266	295	331	--	27.32	21 (±0.73)
Wood treated with MFFA/DMDHEU	237	337	432	303	331	359	425	8.5	26 (±0.43)
MFFA/DMDHEU/ nanoclay/TiO_2 (1 phr)	272	369	457	344	355	392	457	21.56	36 (±0.58)
MFFA/DMDHEU/ nanoclay/ TiO_2 (2 phr)	275	372	459	347	358	396	459	22.58	37 (±0.36)
MFFA/DMDHEU/ nanoclay/ TiO_2 (3 phr)	277	375	462	349	361	398	462	23.03	39 (±0.29)
MFFA/DMDHEU/ nanoclay/ TiO_2 (3 phr)/PP	279	377	464	352	363	400	465	23.05	43 (±0.53)

T_i: value for initial degradation; [a]T_m: value for 1st step; [b]T_m: value for 2nd step.

Section D: Strain sensing behavior and dynamic mechanical properties of carbon nanotubes/nanoclay reinforced wood polymer nanocomposite.

The application of nano materials such as nanoclay and carbon nanotubes (CNT) to reinforce polymer composites has drawn the attention in recent years. CNT has been gaining attraction because of its excellent mechanical and thermal properties. WPNC was prepared consisting of multiwalled carbon nanotubes (MWCNT) and nanoclay by vacuum impregnation of MFFA copolymer and DMDHEU, a crosslinking agent. The main aim of the work is to study the synergistic effect of MWCNT and nanoclay on Raman peak shift due to the strain sensing behavior of the composites under loading, dynamic mechanical analysis (DMA), tensile, flexural and water repellent properties of the prepared composites.

Highest enhancement in properties was obtained by optimizing various parameters like vacuum, time of impregnation, monomer concentration, initiator concentration, amount of crosslinking agent, MMT and MWCNT. The final optimized impregnating conditions were 500mm Hg vacuum, 6 h time of impregnation, 5:1 (MFFA:FA-water) prepolymer concentration, 1% (w/w) maleic anhydride, 3 mL DMDHEU, 3 phr nanoclay and 0.5-1.5 phr MWCNT.

5.4. RESULTS AND DISCUSSION

5.4.1. XRD study

The XRD pattern of MWCNT-OH, nanoclay, untreated wood and WPC is shown in Figure 5.4.1. A sharp diffraction peak for MWCNT-OH appeared at 25.85° (002 crystal plane graphite). Appearance of peaks of medium intensity at 42.87° and 44.82° could be attributed to the 002, 100 and 101 reflections of graphite (curve a) [48]. The organically modified nanoclay (curve b) showed a sharp peak at $2\theta = 4.3°$. The gallery distance calculated by using Bragg's equation was found to be 2.05 nm. Other peaks appeared at 21.01° and 35.54° were due to the presence of alkyl chain of the surfactant [49]. As cellulose is the chief constituent of wood, it showed a wide diffraction peak at $2\theta = 22.88°$ due to the 002 crystal plane of cellulose. The other crystal plane of cellulose i.e. 101 plane showed small peak at 15.02° (curve c) [8]. WPC treated with MWCNT showed a decrease in the intensity of the crystallinity peak of cellulose at 22.88°. The peak at 15.02° corresponding to 101 plane of cellulose became dull. The characteristic peaks of MWCNT at $2\theta = 42.87°$ and

44.82° were appeared in the diffractograms of the composites (curve d). Curve (e-g) represents the X-ray diffraction pattern of WPC treated with 3 phr nanoclay, different percentages of MWCNT (0.5-1.5 phr). The disappearance of the first diffraction peak for the nanoclay in the composites indicated that either the nanoclay layers became delaminated or layers of nanoclay were separated so that it was not possible to detect by XRD. The intensity of the peak appearing at 22.88° of wood cellulose was found to decrease with the increase in the amount of MWCNT and the small peak at 15.02° became dull. The nanoparticles were inserted into the amorphous region of wood cellulose suggesting a decrease in the crystallinity of wood cellulose due to incorporation of nanoparticles into the composites [8]. However, the characteristic peaks of MWCNT at 42.87° and 44.82° were found in the diffractograms of the WPC and the intensity became more pronounced as the amount of MWCNT was increased.

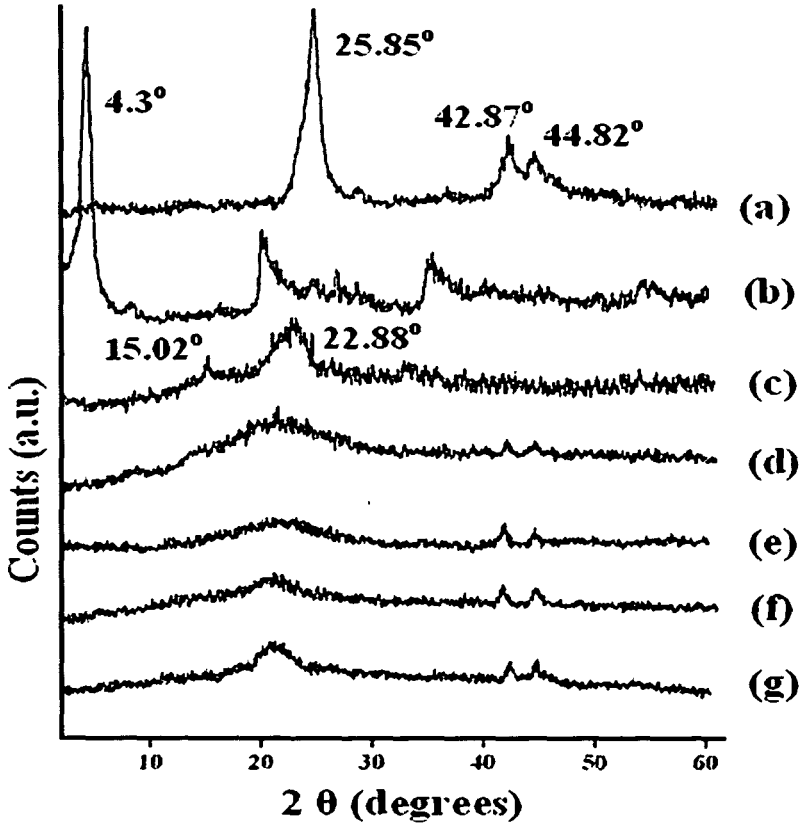

Figure 5.4.1. X-ray diffraction of (a) modified MWCNT (b) nanoclay (c) untreated wood and wood treated with (d) MFFA/DMDHEU/MWCNT (1.5 phr)
(e) MFFA/DMDHEU/nanoclay/MWCNT (0.5 phr) (f) MFFA/DMDHEU/MWCNT (1.0 phr) (g) MFFA/DMDHEU/nanoclay/MWCNT (1.5 phr).

5.4.2. Raman study

The functionalization of the MWCNT was investigated by use of Raman spectroscopy. The hydroxyl functionalized MWCNT (Figure 5.4.2.) showed an enhanced area ratio of D-band to G-band compared to the pristine MWCNT which could be attributed to the microstructural changes in the tubes (Figure 5.4.2.). The ratio between the intensity of D-band (I_D) and G-band (I_G) peaks is used to indicate the degree of crystallinity and is typically taken as a standard measurement of the surface defects of CNTs [50], purity of the CNTs [51] and hence the structural modification of the sidewall. An increase in the intensity ratio of the bands I_D to I_G due to MWCNT surface functionalization was reported in the literature [52]. The surface modification of MWCNT was reported by the visible increase of the I_D/I_G ratio. The D band indicates the multi crystal or amorphous carbon-based materials, whereas the G band indicated the graphite crystal structure in the carbon-based materials. Further, it was observed from the spectra of WPC loaded with MWCNT that the I_D/I_G ratio increased with the increase in the amount of MWCNT. This was due to interaction of polymer and wood with hydroxyl group of MWCNT.

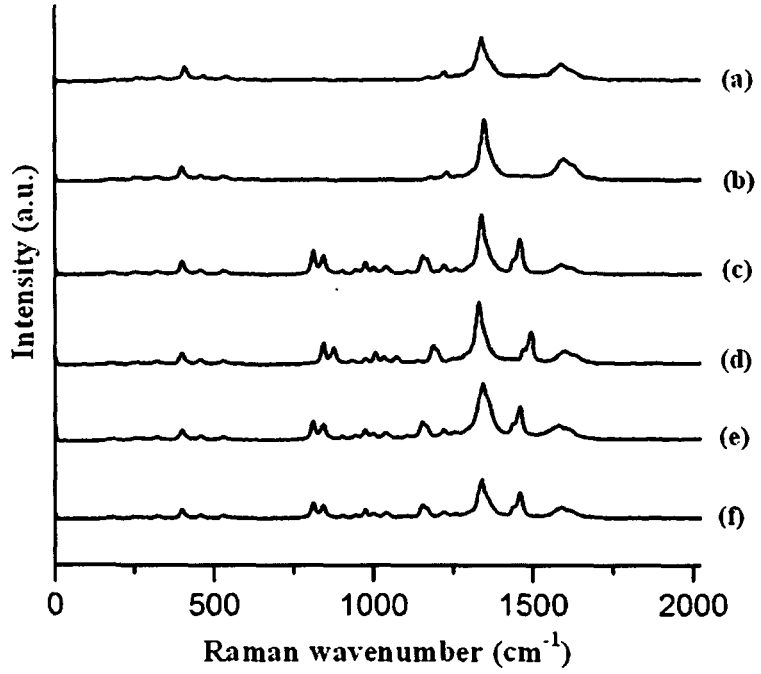

Figure 5.4.2. Raman spectra of (a) unmodified MWCNT (b) MWCNT-OH and wood treated with (c) MFFA/DMDHEU/nanoclay/MWCNT (0.5 phr) (d) MFFA/DMDHEU/ nanoclay/MWCNT (1.0 phr) (e) MFFA/DMDHEU/MWCNT (1.5 phr)
(f) MFFA/DMDHEU/nanoclay/MWCNT (1.5 phr).

A change in both interatomic distance and vibrational frequencies of some of the normal modes of a material caused the shifting of Raman peak under an applied strain [53]. When strain was applied, the C-C bond vibration of MWCNT was changed due to transfer of load from wood/polymer to MWCNT. With the increase in the amount of strain, a significant shift of the G'-band of MWCNT was observed (Figure 5.4.3.). The defect functionalized MWCNT enhanced the interfacial interaction between MWCNT, polymer and wood through its hydroxyl groups. It was observed from Figure 5.4.3. that there was a linear relationship (with a negative slope) between the G'-band shift and the applied strain for the WPC samples loaded with MWCNT. The higher the applied strain, the higher was

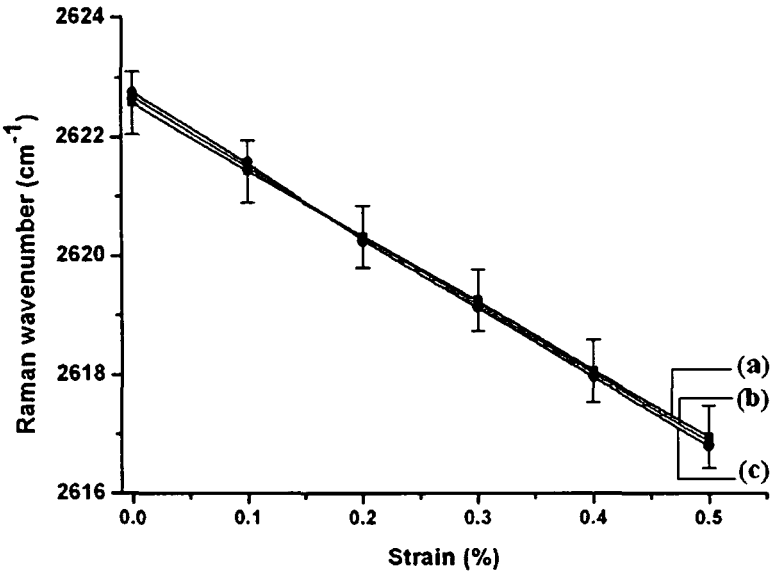

Figure 5.4.3. G'-band shift as a function of strain (%) for wood treated with (a) MFFA/ DMDHEU/nanoclay/MWCNT (0.5 phr) (b) MFFA/DMDHEU/nanoclay/MWCNT (1.0 phr) (c) MFFA/DMDHEU/nanoclay/MWCNT (1.5 phr).

the G'-band shift indicating a good interfacial interaction between the MWCNT and the MFFA/wood. At a fixed loading of nanoclay, WPC treated with 0.5, 1 and 1.5 phr MWCNT showed slopes of 11.2, 12.1 and 13.3 cm^{-1}/strain%, respectively calculated from the G'-band shift rates. Wood treated with MFFA/DMDHEU/MWCNT (1.5 phr) showed shifting of G'-band similar to those of samples treated with MFFA/DMDHEU/nanoclay/MWCNT (1.5 phr) (not shown). The effectiveness of load transfer in the composites was determined by the slope of the G'-band shift versus the strain curve. From Figure 5.4.3., it was further observed that the slope became steeper with the increase in the content of MWCNT in the composites.

Load transfer occurred more effectively to the composites having a steeper slope [54]. The higher the amount of MWCNT, the more efficient was the load transfer from wood/polymer to MWCNT. The increase in slope (20 %) with the increase in MWCNT content indicated better stress transfer at the interface by the distributed MWCNT in the composites.

5.4.3. Morphological studies of the WPC

Scanning electron microscopy

The scanning electron micrographs of untreated and treated wood samples are shown in Figure 5.4.4. Untreated wood samples have empty pits and parenchymas (Figure 5.4.4.a) which were filled up by the MFFA/DMDHEU due to treatment with polymer (Figure 5.4.4.b). In the micrograph of samples treated with MFFA/DMDHEU/MWCNT, a homogenous dispersion of MWCNT was observed (Figure 5.4.4.c). Addition of nanoclay and MWCNT could be seen as some white spots and cylindrical structures (Figure 5.4.4.d-f).

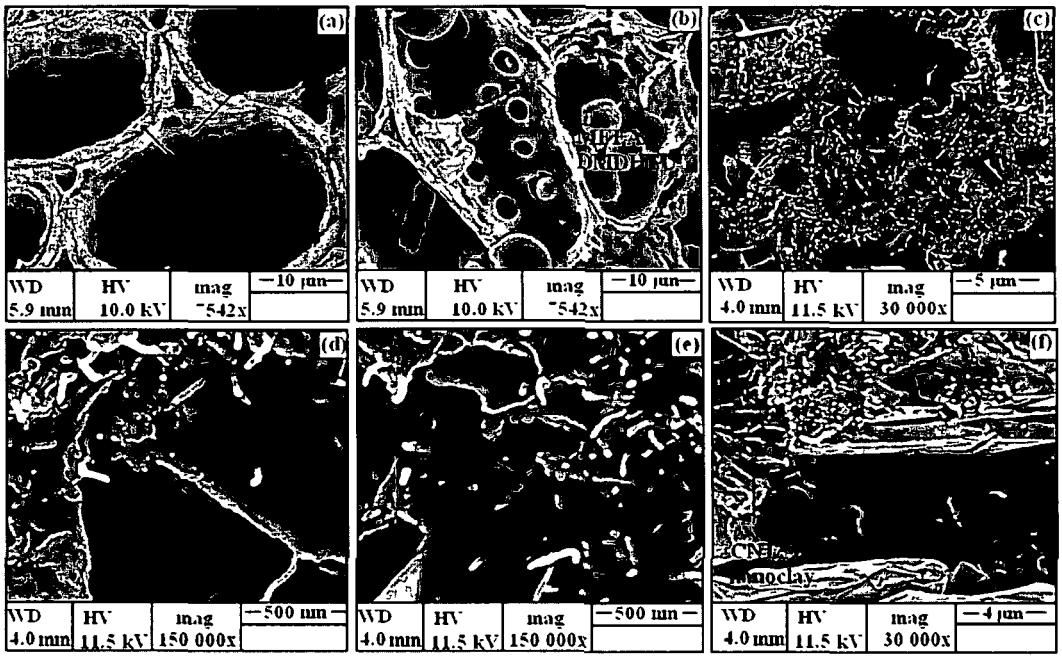

Figure 5.4.4. SEM micrograph of (a) untreated wood and wood treated with (b) MFFA/ DMDHEU (c) MFFA/DMDHEU/nanoclay/MWCNT (0.5 phr) (d) MFFA/DMDHEU /nanoclay/MWCNT (1.0 phr) (e) MFFA/DMDHEU/MWCNT (1.5 phr) (f) MFFA/ DMDHEU/nanoclay/MWCNT (1.5 phr).

Transmission electron microscopy

TEM micrographs of untreated and treated wood samples are shown in Figure 5.4.5. No orientation of cell wall components were observed in untreated wood (Figure 5.4.5.a). The dispersion of MWCNT and nanoclay was observed as some cylindrical and dark slices in the micrograph. It was observed that the MWCNT was dispersed uniformly in the wood samples treated with MFFA/DMDHEU/MWCNT as revealed by the TEM study (Figure 5.4.5.b). The dispersion of nanoclay along with MWCNT was also found to be distributed homogenously in the micrograph of the samples treated with MFFA/DMDHEU/MWCNT/nanoclay. In order to improve some certain properties of WPC addition of clay to MWCNT is very relevant.

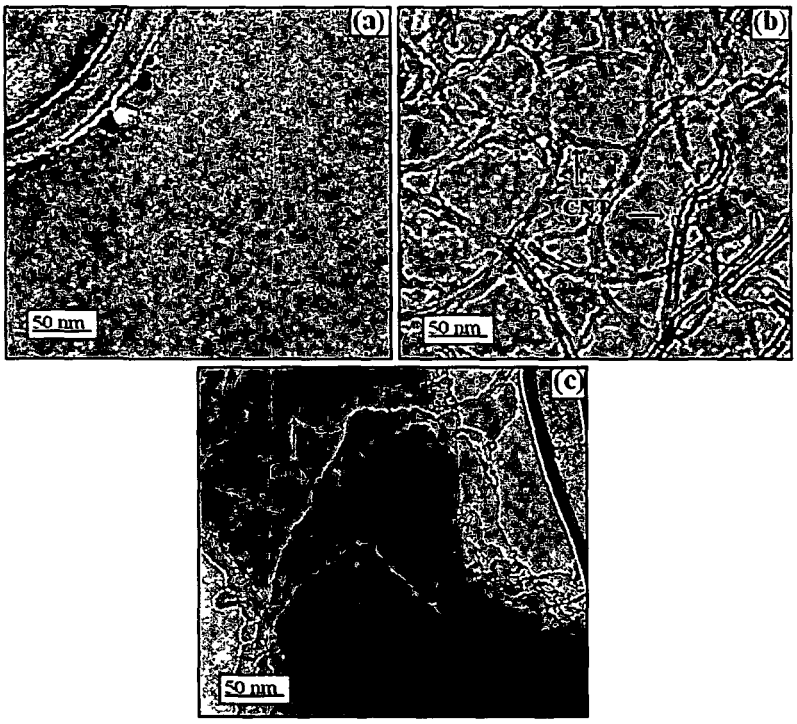

Figure 5.4.5. TEM micrographs of (a) untreated wood and wood treated with (b) MFFA/ DMDHEU/MWCNT (1.5 phr) (c) MFFA/DMDHEU/MWCNT (1.5 phr)/nanoclay.

5.4.4. Effect of variation of MWCNT on polymer loading (WPG %), volume increase and hardness

It was observed from Table 5.4.1. that polymer loading (WPG %), volume increase, and hardness were found to increase for the samples treated with MFFA/DMDHEU. The deposition of polymer into the void spaces of wood was enhanced by DMDHEU due to its

interaction with wood and polymer through its hydroxyl groups [19]. Addition of MWCNT to MFFA/DMDHEU did not significantly influence its WPG % and the volume increase but a remarkable enhancement in hardness was observed. When nanoclay was added to the composites treated with MFFA/DMDHEU/MWCNT, an overall improvement in properties was observed. At fixed nanoclay loading (3 phr), a slight increase in WPG (%) and volume increase (%) were observed with the increase in the amount of MWCNT. The hardness value was found to increase appreciably. A significant increase in hardness value was reported by Uddin et al. after incorporation of MWCNT into copper matrix composite [55]. The increased hardness value was due to interfacial interaction of surface hydroxyl groups of MWCNT with the hydroxyl groups of wood, MFFA, DMDHEU and nanoclay.

Table 5.4.1. Effect of variation of MWCNT on weight % gain (WPG), volume increase, hardness and activation energy.

Samples particulars	Weight gain (%) (WPG)	Volume increase (%)	Hardness (Shore D)	Activation energy (E_a kJ/mol)
Untreated	--	--	47 (±0.93)	118.84
Samples treated with MFFA/FA-water/DMDHEU/ nanoclay/MWCNT				
100/20/3/0/0	28.34 (±0.56)	2.07 (±0.43)	61 (±0.53)	129.43
100/20/3/3/0	35.02 (±0.38)	2.71 (±0.54)	72 (±0.28)	-
100/20/3/0/1.5	31.12 (±0.64)	2.32 (±0.75)	92 (±0.43)	273.56
100/20/3/3/0.5	35.63 (±0.36)	2.78 (±0.75)	88 (±0.72)	243.32
100/20/3/3/1.0	36.52 (±0.41)	2.86 (±0.67)	91 (±0.83)	260.43
100/20/3/3/1.5	37.58 (±0.78)	2.98 (±0.48)	95 (±0.48)	282.32

5.4.5. Dynamic mechanical Analysis

5.4.5.1. Storage modulus

The storage moduli of untreated and treated wood samples are represented in Figure 5.4.6. (A). The storage modulus decreased steeply near the glass transition temperature (T_g) of wood (50-120°C) due to the viscoelastic behavior of wood. In all the cases, the storage modulus was found to decrease with the increase in temperature because of increased chain

mobility of the wood cell wall polymeric components. MFFA copolymer and DMDHEU interacted with hydroxyl groups of wood cell wall forming a networked structure. The higher interfacial adhesion between wood, polymer and crosslinker promoted better load transfer at the interface. Addition of MWCNT to the MFFA/DMDHEU enhanced the interaction through its surface hydroxyl groups which resulted in higher stress transfer at the interface. Samples treated with MFFA/DMDHEU/nanoclay/MWCNT exhibited an improvement in storage modulus of the composites as the silicate layers restricted the mobility of the polymer chains by fastening them into its gallery layers. At fixed loading of nanoclay, with the increase in the amount of MWCNT concentration, a further improvement in storage modulus value was observed.

5.4.5.2. Loss modulus

The loss moduli of untreated and treated wood samples are shown in Figure 5.4.6. (B). All the loss modulus curves reached a maximum and then it decreased with the increase in the temperature because of the maximum dissipation of energy which occurred due to the free movement of the polymeric chains. MWCNT treated wood composites exhibited higher loss modulus than the untreated or the polymer treated wood composites. Nanoclay enhanced the interfacial interaction between wood and polymer resulting in improved E'' value. With the increase in the amount of MWCNT, an increase in the peak height for the loss modulus was observed. This occurred due to energy dissipation and inhibition of the relaxation process within the composite which contributed to an increase in internal friction.

5.4.5.3. Damping parameter (tan δ)

The variation of tan δ as a function of temperature is shown in Figure 5.4.6. (C). A reduction in peak height and broadening of the peak was observed for MFFA/DMDHEU treated samples in comparison with the untreated wood sample. A broader peak suggested that more time was needed for the relaxation of molecules due to lower polymeric chains movement resulting from formation of higher crosslinking density in the composites [56]. Further shifting of the peak to higher temperature was observed when MWCNT was added to the composite. MWCNT improved the interfacial adhesion that further reduced the peak intensity and shifted the peak to higher temperature [57]. The synergistic effect of nanoclay and MWCNT enhanced the interaction between wood and polymer through their surface hydroxyl groups leading to a more shifting of the peak. MWCNT in combination with

nanoclay left a small part to deform at the interface and carried out a greater part of the force. Therefore, energy dissipation was less at the interface due to stronger interaction. The restriction in polymeric chain movement occurred in between the silicate layers. Higher the percentage of MWCNT, higher was the amount of shifting as well as decrease in peak height.

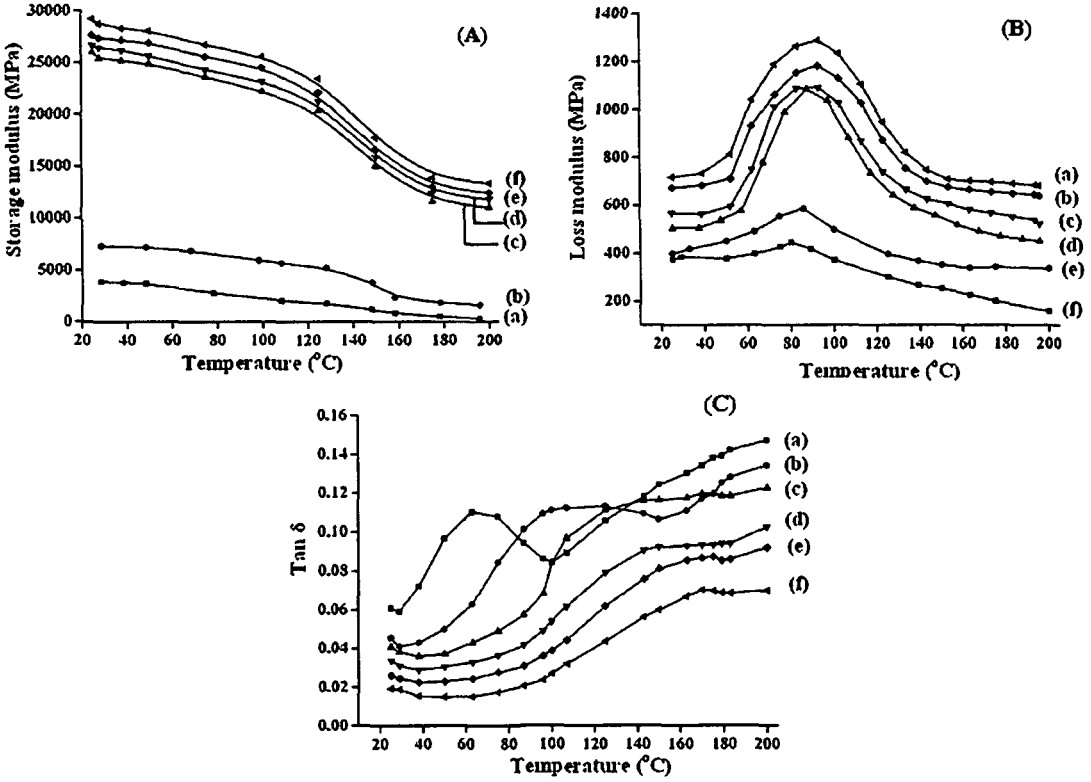

Figure 5.4.6. (A). Storage modulus of (a) untreated wood and wood treated with (b) MFFA/DMDHEU (c) MFFA/DMDHEU/nanoclay/MWCNT (0.5 phr) (d) MFFA/DMDHEU/nanoclay/MWCNT (1.0 phr). (e) MFFA/DMDHEU/MWCNT (1.5 phr) (f) MFFA/DMDHEU/nanoclay/MWCNT (1.5 phr).

(B). Loss modulus of wood treated with (a) MFFA/DMDHEU /nanoclay/MWCNT (1.5 phr) (b) MFFA/DMDHEU/MWCNT (1.5 phr) (c) MFFA/ DMDHEU/nanoclay/MWCNT (1.0 phr) (d) MFFA/DMDHEU/nanoclay/ MWCNT (0.5 phr) (e) MFFA/DMDHEU (f) untreated wood samples.

(C). Tan δ of (a) untreated wood and wood treated with (b) MFFA/DMDHEU (c) MFFA/DMDHEU/nanoclay/MWCNT (0.5 phr) (d) MFFA/DMDHEU/nanoclay/ MWCNT (1.0 phr) (e) MFFA/DMDHEU/MWCNT (1.5 phr) (f) MFFA/DMDHEU/ nanoclay/MWCNT (1.5 phr).

5.4.5.4. Effect of frequency

The viscoelastic properties of a material depend upon temperature and frequency. An increase in modulus values was obtained when frequency was varied as a function of temperature [58]. The variation of tan δ values with frequency is represented in Figure 5.4.7. An increase in peak height and shifting of glass transition temperature values were observed

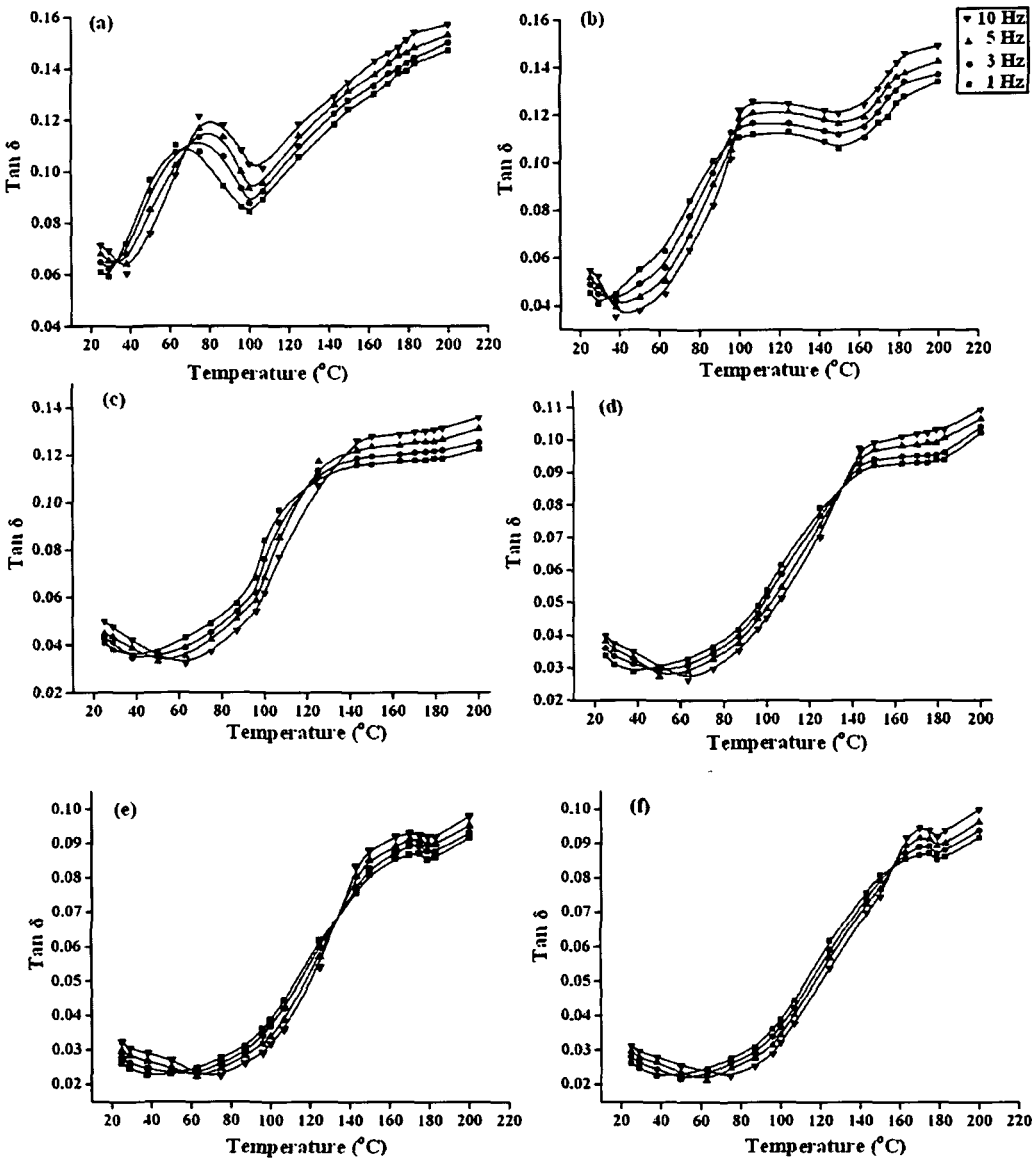

Figure 5.4.7. Tan δ at different frequency range (a) untreated wood and wood treated with (b) MFFA/DMDHEU (c) MFFA/DMDHEU/nanoclay/MWCNT (0.5 phr) (d) MFFA/DMDHEU/nanoclay/MWCNT (1.0 phr) (e) MFFA/DMDHEU/MWCNT (1.5 phr) (f) MFFA/DMDHEU/nanoclay/MWCNT (1.5 phr).

with the increase in frequency. The activation energy of the relaxation process for each composite can be calculated from the Arrhenius equation

$$\log f = \log f_o - E_a/2.303RT$$

where 'f', 'f_o', E_a, R and T denote the measured frequency, the frequency when the temperature approaches infinite, activation energy, universal gas constant and tan δ maximum temperature respectively. Table 5.4.1. shows the activation energy for the relaxation process calculated from the slope of the plot of log f vs reciprocal of temperature. Higher value of activation energy was obtained for the treated wood samples. Nanoclay and MWCNT restricted the polymeric chain movement by increasing the interfacial interaction and stiffening the composites. Higher the amount of MWCNT, higher was the activation energy. Activation energy in the glass transition region was associated with the energy required for promotion of the initial movement of some molecular segments [59]. Higher activation required higher energy for initiation of polymer chain movement.

5.4.6. Tensile and flexural properties

Table 5.4.2. shows the tensile and flexural values of untreated and treated wood samples. Wood samples treated with MFFA/DMDHEU showed higher tensile and flexural values than the untreated wood samples. MF resin is one of the toughest polymeric resins that can enhance mechanical properties significantly and further DMDHEU could form a crosslinked structure with wood cell wall and polymer through its hydroxyl groups [19]. The incorporation of MWCNT enhanced the strength properties, MOE and modulus of rupture (MOR) of the composites. The surface hydroxyl groups present in modified MWCNT interacted with hydroxyl and methylol groups of wood, crosslinker and prepolymer resulting in enhanced properties. The MOE, MOR values improved further as nanoclay was added to the samples treated with MFFA/DMDHEU/MWCNT. The nanoclay layers restricted the mobility of the polymer chains as they were fastened in between its gallery layers and hence stiffened the composites. At a fixed clay loading, the values enhanced remarkably with the increase in the amount of MWCNT.

5.4.7. Water uptake test

The water uptake test of untreated and treated wood samples is represented in Figure 5.4.8. Untreated wood showed highest water absorption capacity as shown in curve a. The hydrophilic nature of wood was responsible for its highest water absorption capacity.

Table 5.4.2. Flexural and tensile properties of untreated and treated wood.

Sample	Flexural properties		Tensile properties	
	Strength (MPa)	Modulus (MPa)	Strength (MPa)	Modulus (MPa)
Untreated wood	120.35 (±2.83)	6047.56 (±3.34)	41.43 (±0.48)	307.77 (±11.86)
Wood treated with MFFA/DMDHEU	127.58 (±0.85)	6410.86 (±0.73)	52.35 (±0.63)	338.74 (±11.32)
MFFA/DMDHEU/ MWCNT (1.5 phr)	154.87 (±0.83)	7764.34(±0.65)	85.04 (±1.21)	631.74 (±9.67)
MFFA/DMDHEU/ nanoclay/MWCNT (0.5 phr)	147.76 (±1.23)	7424.89 (±2.76)	78.65 (±1.17)	584.26 (±12.32)
MFFA/DMDHEU/ nanoclay/MWCNT (1.0 phr)	152.47 (±1.03)	7661.46 (±4.33)	81.84 (±0.87)	607.95 (±10.43)
MFFA/DMDHEU/ nanoclay/MWCNT (1.5 phr)	156.23 (±0.92)	7850.40 (±1.12)	86.32 (±1.33)	641.22 (±8.65)

Impregnation of wood with MFFA/DMDHEU would fill up its void spaces thereby decreasing its water uptake capacity. The hydroxyl groups present in DMDHEU could react with the methylol as well as hydroxyl groups of MFFA and the hydroxyl groups of wood cell wall forming a networked structure [19]. Samples treated with MFFA/DMDHEU/nanoparticles showed improved repellence to water. With the increase in the amount of MWCNT there was a further decrease in water absorption capacity. The surface hydroxyl groups of MWCNT would interact with nanoclay, MFFA, DMDHEU and wood with their hydroxyl groups and facilitates their deposition into the empty cell wall of wood and would make it more bulky.

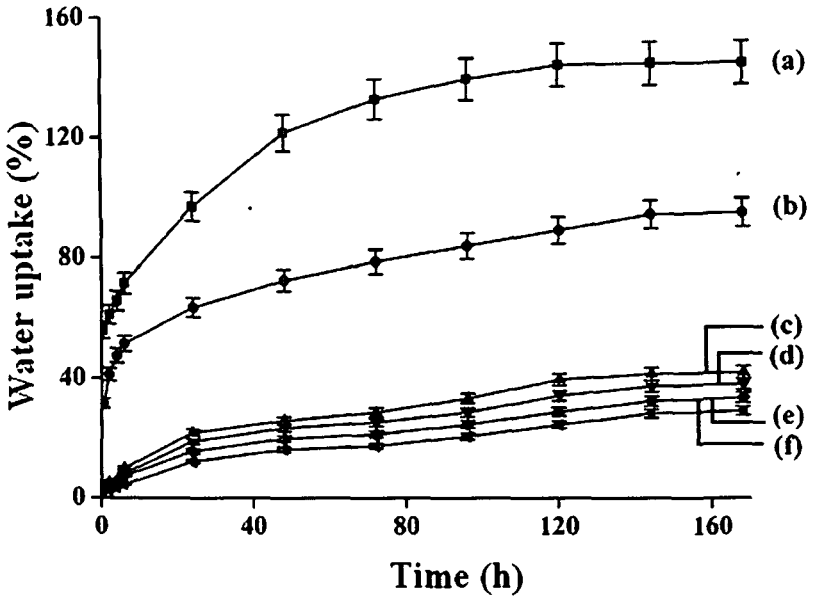

Figure 5.4.8. Water uptake capacity of (a) untreated wood and wood treated with (b) MFFA/DMDHEU (c) MFFA/DMDHEU/nanoclay/MWCNT (0.5 phr) (d) MFFA/DMDHEU/nanoclay/MWCNT (1.0 phr) (e) MFFA/DMDHEU/MWCNT (1.5 phr) (f) MFFA/DMDHEU/nanoclay/MWCNT (1.5 phr).

REFERENCES

1. Lori, J.A., et al. Structural and adsorption characteristics of carbon adsorbent synthesized from polyfurfuryl alcohol with kaolinite template, *Res. J. Appl. Sci. Eng. Technol.* **3** (5), 440-446, 2011.

2. Jang, T.R., et al. Crosslinking of cotton fabrics premercerized with different alkalis, part III: crosslinking and physical properties of DMDHEU-treated fabrics, *Text. Res. J.* **63** (11), 679-686, 1993.

3. Li, H. & Tripp, C.P. Spectroscopic identification and dynamics of adsorbed cetyltrimethylammonium bromide structures on TiO_2 surfaces, *Langmuir* **18** (24), 9441-9446, 2002.

4. Dhoke, S.K., et al. Effect of nano-ZnO particles on the corrosion behavior of alkyd-based waterborne coatings, *Prog. Org. Coat.* **64** (4), 371-382, 2009.

5. Deka, B.K. & Maji, T.K. Effect of coupling agent and nanoclay on properties of HDPE, LDPE, PP, PVC blend and phargamites karka nanocomposite, *Compos. Sci. Technol.* **70** (12), 1755–1761, 2010.

6. Leung, Y.H., et al. Zinc oxide ribbon and comb structures: synthesis and optical properties, *Chem. Phys. Lett.* **394** (4-6), 452-457, 2004.

7. Hong, J.H., et al. Synthesis, surface modification and photocatalytic property of ZnO nanoparticles, *Powder Technol.* **189** (3), 426–432, 2009.

8. Lü, W.H., et al. Preparation and characterization of wood/montmorillonite nanocomposites, *For. Stud. China* **8** (1), 35–40, 2006.

9. Devi, R.R. & Maji, T.K. Preparation and characterization of wood/styrene-acrylonitrile copolymer/MMT nanocomposite, *J. Appl. Polym. Sci.* **122** (3), 2099-2109, 2011.

10. Deka, B.K. & Maji, T.K. Effect of nanoclay and ZnO on the physical and chemical properties of wood polymer nanocomposite, *J. Appl. Polym. Sci.* **124** (4), 2919-2929, 2012.

11. Wada, M., et al. Synchrotron-radiated X-ray and neutron diffraction study of native cellulose, *Cellulose* **4** (3), 221-232, 1997.

12. Ishikura, Y., et al. Bending properties and cell wall structure of alkali-treated wood, *Cellulose*, **17** (1), 47-55, 2010.

13. Marcivich, N.E., et al. Modified wood flour as thermoset fillers II. Thermal degradation of wood flours and composites, *Therm. Chem. Acta* **372** (1-2), 45-57, 2001.

14. Shiraishi, N., et al. Preparation of higher aliphatic acid esters of wood in an N_2O_4–DMF cellulose solvent medium, *J. Appl. Polym. Sci.* **24** (12), 2347-2359, 1979.

15. Ghosh, S.N., et al. Characterization of a flame retardant plant polymer and its influence on the properties of rubber vulcanizate, *Int. J. Polym. Mater.* **48** (1), 79-97, 2001.

16. Zhao, H. & Li, R.K.Y. A study on the photo-degradation of zinc oxide (ZnO) filled polypropylene nanocomposites, *Polymer* **47** (9), 3207-3217, 2006.

17. Grigoriadou, I., et al. Effect of different nanoparticles on HDPE UV stability, *Polym. Degrad. Stab.* **96** (1), 151-163, 2011.

18. Patachiaa, S., et al. Effect of UV exposure on the surface chemistry of wood veneers treated with ionic liquids, *Appl. Surf. Sci.* **258** (18), 6723-6729, 2012.

19. Xie, Y., et al. Effects of chemical modification of wood particles with glutaraldehyde and 1,3-dimethylol-4,5-dihydroxyethyleneurea on properties of the resulting polypropylene composites, *Compos. Sci. Technol.* **70** (13), 2003-2011, 2010.

20. Bhattacharya, S.B., et al. Chemical investigations on the gum exudates from Sajna (*Moringa oleifera*), *Carbohydr. Res.* **102** (1), 253-262, 1982.

21. Wu, W., & Yang, C.Q. Statistical analysis of the performance of the flame retardant finishing system consisting of a hydroxy-functional organophosphorus oligomer and the mixture of DMDHEU and melamine formaldehyde resin, *Polym. Degrad. Stab.* **85** (1), 623-632, 2004.

22. Gilman, J.W., et al. Flammability properties of polymer-layered-silicate nanocomposites: polypropylene and polystyrene nanocomposites, *Chem. Mater.* **12** (7), 1866-1873, 2000.

23. Ghosh, S.N. & Maiti, S. Adhesive performance, flammability evaluation and biodegradation study of plant polymer blends, *Eur. Polym. J.* **34** (5-6), 849-854, 1998.

24. Jana, T., et al. Biodegradable film modification of the biodegradable film for fire retardancy, *Polym. Degrad. Stab.* **69** (1), 79-82, 2000.

25. Qin, H., et al. Thermal stability and flammability of polypropylene/montmorillonite composites, *Polym. Degrad. Stab.* **85** (2), 807–813, 2004.

26. Laachachi, A., et al. Effect of ZnO and organo-modified montmorillonite on thermal degradation of poly(methyl methacrylate) nanocomposites, *Polym. Degrad. Stab.* **94** (4), 670-678, 2009.

27. Kang J.S., et al. Effect of silane modified SiO_2 particles on poly(MMA-HEMA) soap-free emulsion polymerization, *Iran. Polym. J.* **18** (12), 927-935, 2009.

28. Motaung T.E. & Luyt, A.S. Effect of maleic anhydride grafting and the presence of oxidized wax on the thermal and mechanical behavior of LDPE/silica nanocomposites, *Mater. Sci. Eng. A* **527** (3), 761-768, 2010.

29. Wa, X., et al. The anti-superconducting effect of surface modified nano scaled SiO_2 in hydrated salts phase transition system, *J. Phys: Conference Series* **188 (1)**, 012046-012053, 2009.

30. Ahmad, S., et al. Synthesis and characterization of in situ prepared poly (methyl methacrylate) nanocomposites, *Bull. Mater. Sci.* **30** (1), 31-35, 2007.

31. Popescu, C.M., et al. Spectroscopic study of acetylated kraft pulp fibers, *Carb. Pol.* **88** (2), 530-536, 2012.

32. Cai, X., et al. The impact of the nature of nanofillers on the performance of wood polymer nanocomposites, *Compos: Part A* **39** (5), 727-737, 2008.

33. Zhang, H., et al. Property improvements of in situ epoxy nanocomposites with reduced interparticle distance at high nanosilica content, *Acta Mater.* **54** (7), 1833-1842, 2006.

34. Gindl, W., et al. Impregnation of softwood cell walls with melamine-formaldehyde resin, *Bioresour. Technol.* **87** (3), 325-330, 2003.

35. Tajvidi, M. Effect of chemical reagents on the mechanical properties of natural fiber polypropylene composites, *Polym. Compos.* **27** (5), 563-569, 2006.

36. Deka, B.K. & Maji, T.K. Effect of nanoparticles on flammability, UV resistance, biodegradability, and chemical resistance of wood polymer nanocomposite, *Ind. Eng. Chem. Res.* **51** (37), 11881-11891, 2012.

37. Katsikis, N., et al. Thermal stability of poly(methyl methacrylate)/silica nano- and microcomposites as investigated by dynamic-mechanical experiments, *Polym. Degrad. Stab.* **92** (11), 1966-1976, 2007.

38. Mirabedini, S.M., et al. Effect of TiO_2 on the mechanical and adhesion properties of RTV silicone elastomer coatings, *Colloids Surf. A: Physicochem. Eng. Aspects* **317** (1-3), 80-86, 2008.

39. Tshabalala, M.A., et al. Photostability and moisture uptake properties of wood veneers coated with a combination of thin sol-gel films and light stabilizers, *Holzforschung* **65** (2), 215-220, 2010.

40. Devi, R.R. & Maji, T.K. Effect of nano-ZnO on thermal, mechanical, UV stability, and other physical properties of wood polymer composites, *Ind. Eng. Chem. Res.* **51** (10), 3870-3880, 2012.

41. Xu, L. & Yang, M. In situ compatibilization between polystyrene-grafted nanosized TiO_2 and polypropylene with friedel–crafts catalyst, *J. Appl. Polym. Sci.* **114** (5), 2755-2763, 2009.

42. Zhang, S.L., et al. Morphological structure and physicochemical properties of nanotube TiO_2, *Chinese Sci. Bull.* **45** (16), 1533-1536, 2000.

43. Qu, Y., et al. Surface modification of nanocrystalline anatase with CTAB in the acidic condition and its effects on photocatalytic activity and preferential growth of TiO_2, *Appl. Surf. Sci.* **257** (1), 151-156, 2010.

44. Sham, E.L., et al. Zirconium titanate from sol–gel synthesis: thermal decomposition and quantitative phase analysis, *J. Solid State Chem.* **139** (2), 225-232, 1998.

45. Wang, H., et al. Effect of surfactants on synthesis of TiO_2 nano-particles by homogeneous precipitation method, *Powder Technol.* **188** (1), 52-54, 2008.

46. Mina, F., et al. Improved performance of isotactic polypropylene/titanium dioxide composites: effect of processing conditions and filler content. *Polym. Degrad. Stab.* **94** (2), 183-188, 2009.

47. Du, H., et al. Effects of pigments on the UV degradation of wood-flour/HDPE composites, *J. Appl. Polym. Sci.* **118** (2), 1068-1076, 2010.

48. Cao, A.Y., et al. X-ray diffraction characterization on the alignment degree of carbon nanotubes, *Chem. Phy. Lett.* **344** (1-2), 13-17, 2001.

49. Zhu, J., et al. Arrangement models of alkylammonium cations in the interlayer of HDTMA+ pillared montmorillonites, *Chinese Sci. Bull.* **48** (4), 368-372, 2003.

50. Shanmugharaj, A.M., et al. Physical and chemical characteristics of multiwalled carbon nanotubes functionalized with aminosilane and its influence on the properties of natural rubber composites, *Compos. Sci. Technol.* **67** (9), 1813-1822, 2007.

51. Tan, P., et al. Comparative raman study of carbon nanotubes prepared by D.C. arc discharge and catalytic methods, *Raman Spectr.* **28** (5), 369-372, 1997.

52. Sahoo, N.G., et al. Effect of functionalized carbon nanotubes on molecular interaction and properties of polyurethane composites, *Macromol. Chem. Phys.* **207** (19), 1773-1780, 2006.

53. Schadler, L.S., et al. Load transfer in carbon nanotube epoxy composites, *Appl. Phys. Lett.* **73** (26), 3842-3844, 1998.

54. Liu, L., et al. Strain-sensitive raman spectroscopy and electrical resistance of carbon nanotube-coated glass fibre sensors, *Compos. Sci. Technol.* **72** (13), 1548-1555, 2012.

55. Uddin, S.M., et al. Effect of size and shape of metal particles to improve hardness and electrical properties of carbon nanotube reinforced copper and copper alloy composites, *Compos. Sci. Technol.* **70** (16), 2253-2257, 2010.

56. Saiter, A., et al. Cooperative rearranging regions in polymeric materials: relationship with the fragility of glass-forming liquids, *Eur. Polym. J.* **42** (1), 213-219, 2006.

57. Hernandez-Perez, A., et al. Effective properties of multiwalled carbon nanotube/epoxy composites using two different tubes, *Compos. Sci. Technol.* **68** (6), 1422-1431, 2008.

58. Roudaut, G., et al. Can dynamical mechanical measurements predict brittle fracture behaviour? *Rheol. Acta* **44** (1), 104-111, 2004.

59. Ornaghi, H.L., et al. Mechanical and dynamic mechanical analysis of hybrid composites molded by resin transfer molding, *J. Appl. Polym. Sci.* **118** (2), 887-896, 2010.

CHAPTER VI

SUMMARY & CONCLUSIONS

CHAPTER VI

SUMMARY AND CONCLUSIONS

6.1. Summary and Conclusions

The notable aspect that emanates from the present study could be summarized as follows-

In the present investigation, a lower grade wood was made value added through the formation of wood polymer composites (WPC). The vacuum impregnation technique combined with the nanotechnology opens up a new dimension to improve numerous properties of wood like surface hardness, dimensional stability, mechanical properties, weatherability etc.

Wood polymer nanocomposites (WPNC) were prepared by vacuum impregnation of water insoluble monomer methylmethacrylate (MMA) and water soluble monomers viz. melamine formaldehyde-furfuryl alcohol (MFFA) copolymer and melamine formaldehyde-acrylamide (MFA) copolymer in combination with different crosslinkers, flame retardant and nanofillers into Fig wood (*Ficus hispida*). The conditions at which optimum enhancement in properties were obtained for the water insoluble system are vacuum: 508 mm Hg, time of impregnation: 4 h, catalyst (AIBN): 0.5 phr, MMA (mL):100, tetrahydrofuran (THF) (mL): 20 and for the water soluble system are vacuum: 508 mm Hg, time of impregnation: 6 h, catalyst (maleic anhydride/$K_2S_2O_8$): 1.0 phr/0.5 phr, MFFA/MFA (mL):100, FA-H_2O/H_2O (mL): 20 mL.

Initially, WPNC were prepared by the impregnation of MMA prepolymer, glycidyl methacrylate (GMA) cross-linker and montmorillonite (MMT) modified with either a mixture of surfactants 2-acryloloxy ethyl trimethyl ammonium chloride (ATAC) and cetyl trimethyl ammonium bromide (CTAB) (1:1) or 2-acryloloxy ethyl trimethyl ammonium chloride (ATAC). Fourier transform infrared (FTIR) spectroscopy confirmed surface modification of MMT and indicated that there was some interaction between wood, MMA, GMA and clay. X-ray diffraction (XRD) studies revealed that gallery distance in clay layer increased due to treatment with CTAB and ATAC. XRD studies also showed that the crystallinity in WPNC decreased. Scanning electron microscopy (SEM) study showed the existence of polymer, clay within the cell wall or lumen of wood. The improvement in properties like weight percent gain (WPG %), volumetric swelling, hardness, water uptake (%), water repellent efficiency (WRE %), dimensional stability, chemical resistance, thermal

stability and mechanical properties was more in WPNC treated with ATAC/CTAB modified clay compared to WPNC treated with ATAC modified clay.

The influence of unmodified MMT, MMT modified with ATAC and a mixture of surfactants ATAC and CTAB on the various properties of wood impregnated with melamine formaldehyde-furfuryl alcohol (MFFA) prepolymer, n-methylol acrylamide (NMA) crosslinker was investigated. Successful modification of MMT and formation of nanocomposites were confirmed by XRD and FTIR analysis. SEM study revealed the presence of polymer, crosslinker and clay in the cell wall or cell lumen. Transmission electron microscopy (TEM) study indicated the dispersion of clay in the MFFA polymer. Addition of MMT imparted significant improvement in WPG (%), volumetric swelling, hardness, water uptake (%), dimensional stability, and chemical resistance. Inclusion of clay improved thermal stability, flammability and mechanical properties. Treatment of wood polymer samples with (ATAC+CTAB) modified MMT showed maximum improvement in properties than those of either ATAC modified MMT or unmodified MMT treated samples.

The effect of different crosslinkers on the final properties of the composites was studied. The synthesized MFFA copolymer and the NMA and 1,3-dimethylol 4,5-dihydroxy ethylene urea (DMDHEU) crosslinkers were characterized by NMR and FTIR spectroscopy. Mixed crosslinkers and MMT treated samples showed maximum interaction as revealed by FTIR. X-ray diffraction study showed that the incorporation of MMT decreased the crystallinity of wood composites. SEM and TEM study indicated that MMT was incorporated in the composites. A considerable improvement in properties such as weight percent gain (%), hardness, dimensional stability, water uptake (%) resistance, chemical resistance, mechanical properties, flame retardancy and thermal stability were observed for the MMT reinforced WPC crosslinked with 1:1:1 (NMA, HEMA, DMDHEU) mixed crosslinker in comparison with either polymer, NMA, HEMA or DMDHEU treated WPC. The improvement in overall properties was more in samples treated with MFFA/(NMA+HEMA+DMDHEU)/MMT followed by samples treated with MFFA/DMDHEU, MFFA/HEMA and MFFA/NMA respectively.

The effect of procured organically modified nanoclay (Nanomer, surface modified by 15-35 wt% octadecylamine and 0.5-5 wt% amino propyl triethoxy silane) on the final properties of resultant WPNC was also studied. FTIR study showed the evidence of incorporation of nanoclay into the WPC. The exfoliation of the nanoclay layers and the uniform distribution of the nanoparticles were studied by XRD and TEM study. The

improved properties of wood could be ascribed to inherent properties as well as better interphase interactions between the wood, MFFA, DMDHEU and nanoclay. The trace of nanoclay and MFFA polymer located on the cell wall, pit and cell lumen, were observed by SEM study. The elements present in the WPNC due to incorporation of nanoclay were further investigated by energy dispersive X-ray spectroscopy (EDS) of the samples used for SEM study. Dimensional stability, chemical resistance, flammability, thermal stability and mechanical properties were found to increase with the inclusion of nanoclay to the composite. UV resistance of the composites improved significantly as observed from the measurement of weight loss, carbonyl index, lignin index, crystallinity index values, SEM and mechanical properties. Treated samples showed an improvement in elastic modulus, loss modulus and damping index as indicated by dynamic mechanical analysis (DMA). The calculated activation energy for the relaxation process in the glass transition region enhanced for the treated wood samples indicating an improvement in interfacial interaction. The nanoclay impregnated wood polymer composite showed higher biodegradation compared to MFFA polymer impregnated wood composites. Loss in mechanical properties, weight loss, and hardness were observed for both untreated and treated wood samples due to degradation caused by the growth of bacteria in the composites. Untreated wood showed maximum loss in properties and biodegradability followed by the samples treated with MFFA/DMDHEU/nanoclay and MFFA/DMDHEU. SEM analysis of the composites also revealed similar findings. Untreated wood showed maximum growth of actinomycetes, fungi and bacteria compared to wood treated with MFFA/DMDHEU as shown by soil burial test.

The incorporation of a renewable polymer, collected as gum from a local plant (*Moringa oleifera*) as flame retardant along with MFFA copolymer, DMDHEU, a crosslinking agent and nanoclay into Fig wood improved thermal stability and flame retardancy of the composites to a considerable extent. FTIR and XRD study confirmed the incorporation of polymers into the wood composite. SEM and TEM study indicated the presence of polymers and nanomer in the cell lumen or cell wall of wood. The weight percent gain (%), hardness, dimensional stability, mechanical properties and water repellency were improved after the addition of plant polymer. The activation energy of all samples was determined by using Ozawa-Flynn-Wall's and Vyazovkin methods. The activation energy of the composites decreased upto a certain decomposed fraction thereafter it remained invariable. Higher the plant polymer content higher was the activation energy of the prepared composites which indicated a better interfacial adhesion and thermal stability.

In this study, wood polymer nanocomposites were prepared by the impregnation of melamine formaldehyde-acrylamide copolymer (MFA), plant polymer (PP) obtained from a local plant *Moringa oleifera* as flame retardent, DMDHEU as crosslinking agent and VTCS modified MMT. The formation of MFA and DMDHEU was confirmed from NMR and FTIR analysis. FTIR and XRD study were employed to confirm the surface modification of MMT and formation of WPNC. SEM and TEM study confirmed the impregnation of polymer and MMT into the cell wall of wood. The various properties of the composites like hardness, water uptake, chemical resistance, mechanical properties improved after the treatment. The thermal stability and flame retardancy enhanced remarkably after inclusion of PP in the composites.

Surface modified metal oxide nanoparticles in combination with nanoclay also played a significant role in further improvement in the properties of wood polymer nanocomposites. The effect of ZnO and nanoclay on the properties of WPNC impregnated with MFFA copolymer, DMDHEU and PP has been studied. The surface modification of ZnO by CTAB was confirmed by FTIR. XRD and FTIR studies indicated the formation of the composites and a decrease in crystallinity of cellulose was determined from crystallinity index. The morphology of the nanocomposites was studied by SEM and TEM. An enhanced UV resistance property was shown by the treated wood samples as judged by the lower weight loss, carbonyl index, lignin index, and cellulose crystallinity index values, mechanical properties loss compared to the untreated wood samples. The composites resulted in improved water repellency, mechanical, thermal, flame retardant properties.

The synergistic influence of SiO_2 nanoparticles and nanoclay on the final properties of the WPNC was studied. FTIR study confirmed the modification of SiO_2 nanoparticles by CTAB and showed the incorporation of modified SiO_2 and nanoclay into wood/MFFA/PP composite. A decrease in crystallinity of the composites was revealed by XRD. SEM was used for morphological characterization. TEM showed uniform distribution of nano SiO_2 and nanoclay in the composites. PP improved thermal stability and flame retardancy of the composites. There was a reduction in water uptake capacity, enhanced chemical resistance, mechanical properties of the resultant composites. WPNC loaded with 3 phr each of SiO_2, nanoclay and PP resulted in enhanced properties.

In another study, WPNC was prepared by impregnation of MFFA copolymer, DMDHEU, a crosslinking agent, nanoclay, nano TiO_2 and PP. Surface modification of TiO_2 and the formation of the composites were studied by FTIR and XRD analysis. The

crystallinity of cellulose of wood was decreased due to impregnation of polymer and nanomaterials as judged by X ray diffraction and FTIR analysis. The presence of TiO_2 nanoparticles in the composites and that of phosphorus in the PP was analyzed by EDS. Remarkable improvement in ultraviolet resistance properties was observed as manifested by lower weight loss, carbonyl index, lignin index, crystallinity index values, SEM study and lower loss in mechanical properties. WPNC treated with 3 phr each of nanoclay, TiO_2 and PP enhanced significantly the mechanical, flame retardancy, thermal stability and decreased water uptake capacity.

WPNC was prepared consisting of multiwalled carbon nanotubes (MWCNT) and nanoclay by vacuum impregnation of MFFA copolymer and DMDHEU, a crosslinking agent. XRD study demonstrated a reduction in crystallinity of wood cellulose as nanoclay and MWCNT was impregnated along with MFFA/DMDHEU into the composites. Raman spectroscopic analysis indicated surface modification of MWCNT and the formation of the composites. Load transfer was found efficient from the wood/polymer to the nanotubes as evidenced by strain dependent Raman spectroscopy signifying better interfacial interaction. The surface morphology of the composites was studied by scanning electron microscope. Dynamic mechanical analysis showed an enhancement in elastic modulus, loss modulus and damping index for the WPNC. At a fixed nanoclay loading, the apparent activation energy for the relaxation process in the glass transition region increased with the increase in the content of MWCNT in the composites. The other properties like tensile, flexural, hardness and water repellence properties improved appreciably after inclusion of MWCNT into the composites.

6.2. Future scope

The formation of WPC using polymers and different nanofillers results in overall improvement in properties of the nanocomposites. The laboratory study of the composites exhibits a remarkable improvement in properties of the composites. But a thorough investigation has to be done on a large scale for commercial utilization of the product. Maximum improvement in properties can be achieved by fine tuning in the ratio of clay with different nanofillers. The use of cellulose nanofibrils either alone or in combination with other nanofillers and their effect on various properties of the wood composites may be tried. The combined use of both vacuum and pressure may help in better penetration of

polymer/nanofillers into the porous structure of wood and results in further improvement in properties. The inclusion of pigments into impregnation solutions like supercritical fluid e.g. SC-CO_2 as the medium of impregnation may be studied extensively to investigate diversified value added uses for modified wood, particularly for flooring and other value-added applications. As government is more concerned for assuring resource sustainability and promoting green technology, therefore, a thorough investigation of composites in terms of the biodegradability, fire resistance, pest resistance and low emission of volatile organic compound is also required. The monomer/polymers which are used for impregnation are mainly derived from petrochemical resources which are nonrenewable and moreover on degradation or decomposition most of them emit volatile organic compounds. Consequently they are harmful for the environment. Therefore bio-based resins may be attempted as they are obtained from renewable resources and have least harmful effects from environmental concern. During processing on a large scale in industrial applications, the use of water as a solvent can help to minimize all the hazardous effects of petrochemicals diluents. WPNC can be prepared from bio-based resins such as starch, polylactic acid, polyhydroxyalkanoates and soya flour etc. Starch is one of the most outstanding raw materials which is produced from a great variety of crops and is a natural renewable polysaccharide. It is of lower cost as compared to other synthetic plastics and is readily available. However the drawbacks of starch-based materials are that they have limited long-term stability. Therefore grafting of starch with other vinyl monomers may be tried in order to achieve superior properties of the composites. Research on preparation of WPCs by using techniques like gamma radiation, electron beam (EB) or radio-frequency (RF) to polymerize the monomer(s) within the composite, is nearly instantaneous. This may lead to high volume throughout and enable other manufacturing operations to be performed immediately after EB or RF exposure.

List of Publication

In Journals

1. **A. Hazarika,** R.R. Devi & T.K. Maji. Studies on properties of softwood (*Ficus hispida*)/ PMMA nanocomposites reinforced with polymerizable surfactant-modified nanoclay, Polymer Bulletin 68 (7), 1989–2008, 2012.

2. **A. Hazarika** & T.K. Maji. Study on the properties of wood polymer nanocomposites based on melamine formaldehyde-furfuryl Alcohol copolymer and modified clay, Journal of Wood Chemistry and Technology 33 (2), 103–124, 2013.

3. **A. Hazarika** & T.K. Maji. Effect of different crosslinkers on properties of melamine formaldehyde-furfuryl alcohol copolymer/montmorillonite impregnated softwood (*Ficus hispida*), Polymer Engineering and Science 53 (7), 1394-1407, 2013.

4. **A. Hazarika** & T.K. Maji. Synergistic effect of nano-TiO_2 and nanoclay on the ultraviolet degradation and physical properties of wood polymer nanocomposites, Industrial and Engineering Chemistry Research 52 (38), 13536−13546, 2013.

5. A. Hazarika, T.K. Maji. Properties of softwood polymer composites impregnated with nanoparticles and melamine formaldehyde furfuryl alcohol copolymer, Polymer Engineering and Science 54 (5), 1019-1029, 2014.

6. **A. Hazarika** & T.K. Maji. Thermal decomposition kinetics, flammability, and mechanical property study of wood polymer nanocomposite, Journal of Thermal Analysis and Calorimetry 115 (2), 1679-1691, 2014.

7. **A. Hazarika** & T.K. Maji. Dynamic mechanical analysis, biodegradability and thermal stability of wood polymer nanocomposites, Composites: Part B 60, 568-576, 2014.

8. **A. Hazarika** & T.K. Maji. Strain sensing behavior and dynamic mechanical properties of carbon nanotubes/nanoclay reinforced wood polymer nanocomposite, Chemical Engineering Journal, 247, 33-41, 2014.

9. **A. Hazarika** & T.K. Maji. Modification of softwood by monomers and nanofillers : a review. Defense Science Journal, 64 (3), 262-272, 2014

10. **A. Hazarika,** B.K. Deka & T.K. Maji. Melamine formaldehyde-acrylamide and gum polymer impregnated wood polymer nanocomposite, (manuscript submitted).

11. **A. Hazarika** & T.K. Maji. Studies on the properties of wood polymer nanocomposites impregnated with melamine formaldehyde-furfuryl alcohol copolymer and nanoclay (manuscript submitted).

12. **A. Hazarika** & T.K. Maji. Effect of ZnO/nanoclay/plant polymer on the ultraviolet resistance and other physical properties of softwood polymer composite (manuscript submitted).

13. **A. Hazarika** & T.K. Maji. Bio based wood polymer nanocomposites: A sustainable high performance material for future (Book chapter communicated).

In Conferences

1. **A. Hazarika** & T.K. Maji. Study on dimensional and mechanical properties of chemically modified soft wood (*Ficus Hispida*), "*National Seminar on Recent Challenges for chemical research and Practices*" organized by the Department of Chemistry, Darrang College, 9-10 November (2012).

2. **A. Hazarika** & T.K. Maji. Study on properties on melamine formaldehyde-furfuryl alcohol impregnated soft wood (*Ficus hispida*), "*100th Session of Indian Science Congress*" organized by Calcutta University, Kolkata, 03-07 January (2013).

3. **A. Hazarika,** R.R. Devi & T.K. Maji. Studies on properties of organoclay reinforced softwood/PMMA nanocomposites, "*National Conference on Chemistry, Chemical Technology and Society*" organized by Tezpur university, Assam, 11-12 November (2011).

****

I&EC research
Industrial & Engineering Chemistry Research

Article

pubs.acs.org/IECR

Synergistic Effect of Nano-TiO_2 and Nanoclay on the Ultraviolet Degradation and Physical Properties of Wood Polymer Nanocomposites

Ankita Hazarika and Tarun K. Maji*

Department of Chemical Sciences, Tezpur University, Assam 784028, India

Supporting Information

ABSTRACT: A wood polymer nanocomposite (WPNC) was prepared by impregnating melamine formaldehyde–furfuryl alcohol copolymer, dimethylol dihydroxyethylene urea, a cross-linking agent, nanoclay, nano-TiO_2, and a renewable polymer obtained as a gum from the plant *Moringa oleifera* into wood (*Ficus hispida*). Fourier transform infrared spectroscopy and X-ray diffractometry were used to confirm the surface modification of TiO_2 and interfacial interaction between wood, polymer, cross-linker, and nanoparticles. The uniform distribution of nanoclay and TiO_2 was evidenced by transmission electron microscopy and scanning electron microscopy (SEM) Remarkable improvement in the ultraviolet resistance properties was observed, as manifested by lower weight loss, carbonyl index, lignin index, and crystallinity index values, SEM study, and lower loss in mechanical properties. WPNC treated with 3 phr each of nanoclay, TiO_2, and the plant gum enhanced significantly the mechanical properties, flame retardancy, and thermal stability and decreased the water uptake capacity.

1. INTRODUCTION

The modification of wood by the formation of nanocomposites through in situ polymerization has been studied comprehensively in recent years.[1] The cell wall of wood is mainly composed of biopolymers, i.e., cellulose, hemicellulose, and lignin. The glucose units of cellulose and hemicellulose are linked by a glycosidic linkage, and the free hydroxyl groups in cellulose help in the easy formation of hydrogen bonding with water, which causes swelling of wood.[2] However, lignin is an aromatic compound, polymers of a phenyl propane unit, and has the least tendency to absorb water.[3] All of the components of wood are susceptible to UV degradation. However, lignin is the primary component of wood responsible for degradation because of the presence of chromophoric functional groups.[4] These groups absorb light, generate long-lived triplet states, and thus assist in its degradation. Moreover, lignin can form free radicals as intermediates upon UV exposure, and the process of degradation is stimulated by moisture and atmospheric oxygen.[5]

Chemical treatment such as the formation of wood polymer composites (WPCs) is one potential way to overcome the drawbacks allied with the properties of wood.[6] Nanofiller-based WPC as in situ nanoreinforcement offers new opportunities in the overall properties of the composites. Wood modified with nanoclay has been reported to improve the dimensional stability, water repellency, surface hardness, and modulus of elasticity (MOE).[7] The combination of nanoclay with other metal nanoparticles will influence the properties of the composites considerably, as reported by Laachachia et al. while studying the properties of poly(methyl methacrylate) (PMMA) nanocomposites prepared with TiO_2 and nanoclay.[8]

The ultraviolet (UV)-resistant property is one of the desirable properties of WPC because it is mainly used for outdoor applications. Among the different nanofillers, TiO_2 nanopowder is increasingly being investigated to improve the UV stability and durability of the composites. TiO_2 reinforcement can improve the physiochemical, mechanical, and abrasion-resistance properties, making the nanocomposites a promising category of products.[9] Most of the reports have addressed the enhancement in the properties of wood such as weather resistance and antimicrobial activity of wood by the use of TiO_2 sols through sol–gel methods.[10,11]

Using water as a solvent instead of using a petroleum-based organic solvent has rejuvenated the awareness for a sustainable environment. Furfuryl alcohol (FA) derived from renewable feedstock improves the durability, dimensional stability, and hardness of wood.[12] However, it cannot influence the bending strength and MOE of the treated wood. Melamine formaldehyde (MF) is one of the important thermoset resins because of its advantageous properties such as high hardness, stiffness, and low flammability.[13] Mantanis et al.[14,15] have reported that the cell wall of wood is permanently swelled by low-molecular-weight monomers that are capable of forming hydrogen bonds. Similarly, melamine formaldehyde–furfuryl alcohol (MFFA), which is a low-molecular-weight and low-viscosity prepolymer, has the capacity to swell the cell wall of wood, and hence the prepolymer penetrates easily into the cell wall. The prepolymer contains abundant hydroxyl groups, polymerizes in the cell wall, and can be grafted permanently into the cell wall of wood through their hydroxyl groups.

Flame retardants are incorporated in WPC to achieve fire resistance, which is one of the most desired properties of wood Polymeric flame retardants obtained from a renewable resource, i.e, from a local plant, *Moringa oleifera*, can diminish the leaching problem and are also ecofriendly.[16] Very few reports

Received: May 19, 2013
Revised: August 22, 2013
Accepted: August 26, 2013
Published: August 26, 2013

Chemical Engineering Journal 247 (2014) 33–41

Contents lists available at ScienceDirect

Chemical Engineering Journal

journal homepage: www.elsevier.com/locate/cej

Strain sensing behavior and dynamic mechanical properties of carbon nanotubes/nanoclay reinforced wood polymer nanocomposite

Ankita Hazarika, Tarun K. Maji *

Department of Chemical Sciences Tezpur University Assam 784028 India

HIGHLIGHTS

- Wood polymer nanocomposites (WPNC) were prepared by impregnation method
- Modification of MWCNT was studied by Raman spectroscopy
- Efficient load transfer was found from MWCNT to wood/polymer
- WPNC exhibited an improvement in dynamic mechanical properties
- Activation energy for the relaxation process increased for the composites

GRAPHICAL ABSTRACT

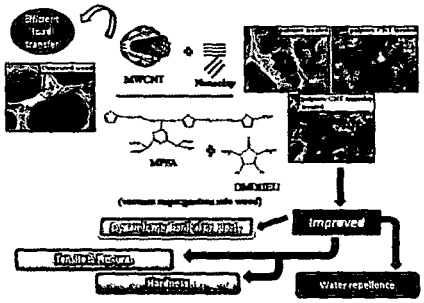

ARTICLE INFO

Article history
Received 30 September 2013
Received in revised form 21 January 2014
Accepted 21 February 2014
Available online 12 March 2014

Keywords
Wood
Nanocomposites
Multiwalled carbon nanotubes
Raman spectroscopy
Mechanical properties

ABSTRACT

Wood polymer nanocomposites (WPNC) was prepared consisting of multiwalled carbon nanotubes (MWCNT) and nanoclay by vacuum impregnation of melamine formaldehyde furfuryl alcohol copolymer and 1,3-dimethylol 4,5-dihydroxy ethylene urea, a crosslinking agent. X-ray diffraction study indicated a decrease in crystallinity of wood cellulose in the composites. Strain dependent Raman spectroscopy showed efficient load transfer from the wood/polymer to the nanotubes indicating better interfacial interaction. The surface morphology of the composites was studied by scanning electron microscope. Dynamic mechanical analysis showed an enhancement in elastic modulus, loss modulus and damping index for the WPNC. At a fixed nanoclay loading, with the increase in the content of MWCNT in the composites, the apparent activation energy for the relaxation process in the glass transition region increased. Tensile, flexural, hardness and water repellence properties improved significantly after incorporation of MWCNT into the composites.

1. Introduction

Wood polymer composites (WPC) have gained significant popularity in the recent years as it can be a replacement for solid wood due to its advantageous properties for different construction purposes and outdoor applications. The service life of wood can be enhanced through chemical modification by the use of suitable chemicals [1]. Fig. wood (*Ficus hispida*), a type of softwood, is not appropriate for structural applications due to its poor dimensional, mechanical and other physical properties. This wood can be made value added by forming composites with polymers. WPC prepared by vacuum impregnation of polymers are suitable for various applications like outdoor deck floors, railings, fences, cladding and siding, park benches, window and door frames and indoor furnitures [2,3]. The application of vacuum during the process of impregnation evacuates air from the pores of the wood samples and helps in penetration of monomers and nanofillers into its empty spaces. However, the simultaneous use of the combination of vacuum and pressure leads to better penetration of polymer/

* Corresponding author. Tel: +91 03712 267007x5053; fax: +91 03712 267005.
E-mail address: tkm@tezu.ernet.in (T.K. Maji).

http://dx.doi.org/10.1016/j.cej.2014.02.069
1385-8947/

Composites Part B 60 (2014) 568–576

Contents lists available at ScienceDirect

Composites: Part B

journal homepage www.elsevier.com/locate/compositesb

Dynamic mechanical analysis, biodegradability and thermal stability of wood polymer nanocomposites

Ankita Hazarika [a], Manabendra Mandal [b], Tarun K. Maji [a,*]

[a] Department of Chemical Sciences Tezpur University, Assam, India
[b] Department of Molecular Biology and Biotechnology Tezpur University Assam, India

ARTICLE INFO

Article history
Received 25 July 2013
Received in revised form 5 November 2013
Accepted 22 December 2013
Available online 31 December 2013

Keywords
A. Wood
B Mechanical properties
D Electron microscopy
MFFA

ABSTRACT

Melamine formaldehyde-furfuryl alcohol copolymer (MFFA) and 1,3-dimethylol 4,5-dihydroxy ethylene urea (DMDHEU) were synthesized and vacuum impregnated into wood with nanoclay to prepare wood polymer nanocomposite (WPNC) MFFA, DMDHEU and WPNC were characterized by Fourier Transform Infrared Spectroscopy (FTIR) Transmittance Electron Microscopy (TEM) study confirmed impregnation of nanoclay into the composites Treated samples showed an improvement in elastic modulus, loss modulus and damping index as indicated by dynamic mechanical analysis (DMA) The incorporation of nanoclay improved the thermal stability of the composites The apparent activation energy for the relaxation process in the glass transition region increased with the increase in the amount of nanoclay Untreated wood exhibited maximum biodegradability whereas polymer treated wood showed minimum biodegradability Addition of nanoclay improved the biodegradability of the polymer treated wood samples as evidenced by decay evaluation, soil burial and scanning electron microscopy (SEM) study

1. Introduction

Wood modification has been expedited in the last decade due to increased environmental awareness, availability of tropical hardwood species and rise in demand for a high quality timber for various engineering and structural applications so as to enhance its service life It is, naturally available composite, composed of cellulose fiber embedded in an amorphous matrix of lignin The carbohydrate polymeric constituents of wood contain abounding hydroxyl groups which render wood with some unfavorable properties like poor dimensional stability, mechanical strength, susceptible to rot caused by wet weather and humid condition etc

The drawbacks associated with the properties of wood can be overcome through the formation of wood polymer composites (WPC) [1–3] Chemical modification of wood involves bond formation between the reagents and the polymeric constituents of wood cell wall. Modification with both thermosetting resin as well as thermoplastic brings out some changes in the chemical and physical properties of the wood to a great extent Therefore, the substrate is difficult to be recognized by the enzymes responsible for metabolizing the cell wall polymers The moisture content of the cell wall is not enough for fungal attack due to reduction in the accessible hydroxyl groups [4,5]

Nanobased treatment of WPC offers it with potentially effective products to meet its end-use applications [6] WPC treated with layered silicate nanoclays as in situ reinforcement has been reported to enhance its properties significantly [7] Cai et al has reported that WPC modified with aluminosilicate nanofillers can significantly improve the wood properties, including surface hardness, modulus of elasticity, dimensional stability and water repellence [8]

The replacement of petroleum-derived raw materials with renewable ones is very worthy and challenging The utilization of water as a solvent instead of petroleum based diluents is of special interest from environmental point of view Furfuryl alcohol, obtained from sugarcane bagasse, has been reported to enhance significantly the dimensional stability and durability of the treated wood [9,10] But, the bending strength and the modulus of elasticity (MOE) of the furfuryl alcohol based composites are same as that of untreated wood [11] The important feature of melamine formaldehyde (MF) is their ability to form hydrogen bonds which leads to dimensional, mechanical and thermal properties [12] It is also one of the hardest polymeric resins. Therefore furfuryl alcohol can be copolymerized with MF resin to get overall improvement in the properties of the composites

As the wood polymer nanocomposites (WPNC) can be subjected to various types of dynamic stressing during service, studies regarding the structures and viscoelastic behavior of these materials for determining their relevant stiffness and damping character-

* Corresponding author Tel +91 3712267007x5053 fax +91 03712 267005
E-mail address tkm@tezu ernet in (T K. Maji)

1359-8368/$ - see front matter © 2014 Elsevier Ltd All rights reserved
http //dx doi org/10 1016/j compositesb 2013 12 046

Effect of Different Crosslinkers on Properties of Melamine Formaldehyde-Furfuryl Alcohol Copolymer/ Montmorillonite Impregnated Softwood (*Ficus hispida*)

Ankita Hazarika, Tarun K. Maji
Department of Chemical Sciences, Tezpur University, Assam 784028, India

Melamine formaldehyde-furfuryl alcohol (MFFA) copolymer was prepared and impregnated into softwood *Ficus hispida* in combination with crosslinking agent and montmorillonite (MMT) under vacuum condition. Different crosslinkers namely *n*-methylol acrylamide, (NMA), 2-hydroxyethyl methacrylate (HEMA) and 1,3-dimethylol-4,5-dihydroxyethyleneurea (DMDHEU) were used for evaluation of properties of the prepared composites. Nuclear magnetic resonance (NMR) and fourier transform infrared spectroscopy (FTIR) studies confirmed the formation of MFFA copolymer, NMA, and DMDHEU crosslinkers. X-ray diffractometry (XRD) and FTIR studies were used to characterize the nanocomposites. The incorporation of MMT decreased the crystallinity of wood composites as revealed by XRD study. Maximum interaction was found in wood samples treated with MFFA/(NMA+HEMA+DMDHEU)/MMT as shown by FTIR study. The incorporation of MMT into the wood polymer composite was revealed by transmission electron microscopy study. Thermal stability and flammability were checked by thermogravimetric analyzer and limiting oxygen index instrument. Wood treated with MFFA, blended crosslinker and MMT exhibited higher dimensional stability, lower water uptake (%), enhanced chemical resistance, and better mechanical properties (flexural, tensile, and hardness). SEM study indicated the presence of polymer and MMT in the void spaces of wood. POLYM. ENG. SCI., 00:000–000, 2012. © 2012 Society of Plastics Engineers

INTRODUCTION

Wood is a renewable resource and has a wide range of applicability [1]. Wood, as a natural composite, is also very sensitive to moisture and fungal decay. Softwoods are generally not considered for construction purpose due to their poor dimensional and mechanical properties. Attention has been drawn worldwide to substitute of the high quality timbers, which are rapidly depleting of the world forest resource, by improving the abundantly available low quality woods through wood polymer composite (WPC) formation [2]. Chemical modification of wood is one of the potential ways to improve the properties of wood. Wood can be impregnated with either vinyl monomers followed by *in situ* polymerization [3, 4], or water soluble thermoset resins [5, 6]. Gao and Li [7] have reported that poplar wood can be chemically modified with foaming polyurethane resins for the improvement of dimensional stability and mechanical properties.

The utilization of water soluble monomers will provide a potential advantage from environmental concern. Since, water act as a solvent and dispersing medium, it can greatly reduce the harmful effect of using hazardous solvents.

The applicability of furfuryl alcohol (FA) in wood modification has been known for a long time [8, 9]. Petroleum-based chemicals can be widely replaced by some sustainable solution of vegetable biomass. In particular, hemicellulose constitutes an important source of monomers such as FA. FA is usually converted into furanic resin prepolymers and these represent excellent eco-friendly precursors for wood impregnation [10]. The drawback of zinc chloride associated with the process of furfurylation is its disparaging effect on cellulose degradation and thereby on the long-term strength properties of the modified wood. In the furfurylation process, cyclic carboxylic system is found to be superior catalytic system than the zinc chloride system, out of which maleic anhydride is the most suitable one [11].

It has been found that dimensional stability of wood treated with bio-derived FA has increased with the increase in weight percent gain (WPG) [12]. Furfurylated wood is an environmentally acceptable product and its degradation do not release any volatile organic compounds [13]. Though furfurylated wood shows a decrease in equilibrium moisture content, increase in dimensional stability but it cannot enhance the thermal stability and mechanical properties of wood efficiently. The furfurylation does not improve the bending strength and the modulus of elasticity (MOE) is same as that of untreated wood [14].

Melamine-formaldehyde (MF) represents one of the hardest and stiffest isotropic polymeric materials used in different adhesives, coatings, decorative laminates for

Correspondence to: T.K. Maji; e-mail: tkm@tezu.ernet.in
DOI 10.1002/pen.23391
Published online in Wiley Online Library (wileyonlinelibrary.com).

Properties of Softwood Polymer Composites Impregnated with Nanoparticles and Melamine Formaldehyde Furfuryl Alcohol Copolymer

Ankita Hazarika, Tarun K. Maji
Department of Chemical Sciences, Tezpur University, Assam 784 028, India

Wood polymer composites (WPC) based on nano SiO_2 and nanoclay were prepared by the impregnation of melamine formaldehyde-furfuryl alcohol copolymer, 1,3-dimethylol 4,5-dihydroxy ethylene urea, a crosslinking agent, and a renewable polymer. Surface modification of SiO_2 and formation of composites were characterized by Fourier Transform Infrared Spectroscopy (FTIR). X-ray diffractometry (XRD) studies indicated a decrease in crystallinity of the composites. The crystallinity index value of wood cellulose decreased from 63.8 to 30.8 as determined from FTIR and XRD studies. Scanning Electron Microscopy was used for morphological characterization. Transmission Electron Microscopy (TEM) showed uniform distribution of nano SiO_2 and nanoclay in the composites. Remarkable reduction in water uptake capacity was observed for the treated wood samples. It was found to reduce from 142.2% to 30.2%. Both tensile and flexural properties increased upto 76.5% and 23.6%, respectively in the WPCs. An improvement in chemical resistance, flame retardancy and thermal stability were observed in the composites as a result of treatment.
POLYM. ENG. SCI., 00:000–000, 2013.

INTRODUCTION

Wood is a heterogeneous material composed of cellulose, hemicellulose, and lignin. The glucose units in wood cellulose are attached by glycosidic linkage and the free OH groups absorb atmospheric moisture that causes swelling of wood. Though it has a pivotal role in human society, yet some unfavorable properties restrict its widespread applications. Fig wood, a kind of softwood, is widely used for fuel purposes. This wood can be made value added product by modification with polymers.

Chemical modification is one of the potential ways to overcome the disadvantages associated with its properties [1, 2]. Petroleum based chemicals can be replaced with biobased renewable feedstocks such as furfuryl alcohol (FA), which is derived from sugarcane bagasse, an excellent eco-friendly precursor used for wood modification [3]. The use of water as a solvent provides environmental benefits compared to petroleum-based diluents. Furfurylated wood has improved dimensional stability and durability [4, 5]. The cell wall of wood is permanently swelled by low molecular volume monomers that are able to form hydrogen bonds. Furfurylation of wood improves both the dimensional stability and durability but it does not bring about any change in bending strength and the modulus of elasticity (MOE) compared to the untreated wood [5].

Melamine formaldehyde (MF) resin is one of the hardest and stiffest polymers that can enhance mechanical and thermal properties of wood [6]. Therefore MF-FA (MFFA) copolymer is expected to enhance overall properties of the wood composites.

Flame retardancy is a desirable property of wood polymer composites (WPC) and therefore various flame retardants are incorporated into the composites to meet its specific requirements. The flame retardancy and biodegradability of starch-based film has been enhanced by using the gum obtained from the plant *Moringa Oleifera* [7]. Similar improvement in flame retardancy and adhesiveness has been reported by Ghosh and Maiti by blending polymer derived from *M. Oleifera* with various rubbers [8]. The high molecular weight polymeric flame retardant obtained from renewable resource will minimize leaching problem and improve the service life of the composite. Moreover it is ecofriendly. The use of gum as a flame retardant is reported in few literatures. There is sufficient scope to do work using the Moringa gum.

Polymer composites loaded with clay are known for remarkable enhancement in thermal, physical, and other properties. Various literatures based on polymer clay nanocomposites are available [9]. The fabrication of WPC based on nanofillers shows a prospective approach in obtaining a product having superior properties [10, 11]. WPC treated with aluminosilicate nanofillers has been reported to enhance the properties of melamine urea formaldehyde and phenol formaldehyde impregnated wood [12, 13]. Cai et al. has reported that nanoclay modified WPC can significantly improve the wood properties, including surface hardness,

Correspondence to: T.K. Maji; e-mail: tkm@tezu.ernet.in
DOI 10.1002/pen.23643
Published online in Wiley Online Library (wileyonlinelibrary.com).

Polym. Bull. (2012) 68:1989–2008
DOI 10.1007/s00289-012-0706-1

ORIGINAL PAPER

Studies on properties of softwood (*Ficus hispida*)/ PMMA nanocomposites reinforced with polymerizable surfactant-modified nanoclay

A. Hazarika · R. R. Devi · T. K. Maji

Received: 19 October 2011 / Revised: 15 November 2011 / Accepted: 15 January 2012 /
Published online: 25 January 2012

Abstract Soft wood (*Ficus hispida*) was chemically modified by impregnation of methyl methacrylate monomer, glycidyl methacrylate (GMA), a cross-linking agent, and montmorillonite (MMT) using catalyst heat treatment. MMT was modified by using a polymerizable surfactant 2-acryloloxy ethyl trimethyl ammonium chloride (ATAC) and a mixture of surfactants ATAC and cetyl trimethyl ammonium bromide (CTAB) in a molar ratio of (1:1). A comparative study on different properties of the prepared wood polymer nanocomposite (WPNC) based on impregnation of intercalating mixture containing MMA/GMA/clay modified by both the surfactants (ATAC and CTAB) and MMA/GMA/clay modified by only surfactant ATAC were done. FTIR, XRD, and TGA studies were employed for the characterization of clay and WPNC. WPNC prepared by using combined surfactant-modified clay along with MMA/GMA exhibited improved dimensional stability, chemical resistance, thermal stability, mechanical properties, and lower water uptake than that of WPNC prepared by using single surfactant-modified clay and MMA/GMA system.

Keywords Soft wood · MMA prepolymer · Organo-MMT · Preparation · Characterization

Introduction

Wood is a cellular polymeric composite material abundantly available in nature. It is used, not only as a fuel but also as a versatile material for domestic purposes like shed and other structures, furniture, tools, vehicles, and decorative objects because of its accessibility. Though it has aesthetic appearance and is used widely in engineering applications, it has certain disadvantages like susceptible to shrinking, swelling, attack by fungi, insects, etc.

A. Hazarika · R. R. Devi · T. K. Maji (✉)
Department of Chemical Sciences, Tezpur University, Tezpur 784 028, Assam, India
e-mail: tkm@tezu.ernet.in

Journal of Wood Chemistry and Technology, 33:103–124, 2013

ISSN: 0277-3813 print / 1532-2319 online
DOI: 10.1080/02773813.2012.751428

Taylor & Francis
Taylor & Francis Group

Study on the Properties of Wood Polymer Nanocomposites Based on Melamine Formaldehyde-furfuryl Alcohol Copolymer and Modified Clay

ANKITA HAZARIKA AND TARUN K. MAJI

Department of Chemical Sciences, Tezpur University, Assam, India

Abstract: *A wood polymer nanocomposite was prepared by impregnating a melamine formaldehyde-furfuryl alcohol (MFFA) copolymer, n-methylol acrylamide (NMA), a crosslinking agent, and montmorillonite (MMT) into wood (*Ficus hispida*) by using a catalyst heat treatment. MMT was modified by using a polymerizable surfactant 2-acryloloxy ethyl trimethyl ammonium chloride (ATAC) and a mixture of surfactants ATAC and cetyl trimethyl ammonium bromide (CTAB) in a molar ratio of 1:1. FTIR and XRD studies confirmed the formation of the MFFA copolymer, NMA, and modification of MMT. These studies also indicated an interaction between wood, polymer, crosslinker, and MMT. Wood treated with modified MMT exhibited lower water uptake, higher dimensional stability, enhanced chemical resistance, thermostability, flame retardancy, and better mechanical properties than wood samples treated with unmodified clay. Samples treated with combined surfactant (ATAC+CTAB) modified clay exhibited better property compared to those samples treated with single surfactant (ATAC) modified clay.*

Keywords Fig wood, wood polymer nanocomposites, MFFA copolymer, organo-clay, characterization

Introduction

Wood has many desirable characteristics required for a variety of end uses, such as construction, furniture, and tools. It is a natural polymeric composite material, made up mainly of cellulose, hemicellulose, and lignin. All of these polymers have abundant hydroxyl groups. These hydroxyl groups are responsible for the hygroscopic nature of wood, which attracts moisture through hydrogen bonding. Despite its various useful properties, wood also possesses some disadvantages, such as poor dimensional stability, susceptibility to wood worm and decay, and poor mechanical and thermal properties, preventing it from being utilized more widely.

Fabrication of wood-polymer composites (WPC) is one of the promising techniques used to improve the properties of wood by impregnating a polymer through *in situ* polymerization. Various types of vinyl monomers and low-molecular-weight resins are impregnated in wood for enhancement of properties.[1,2,3]

Address correrspondence to Tarun K. Maji, Department of Chemical Sciences, Tezpur University, Assam 784028, India. E-mail: tkm@tezu.ernet.in

J Therm Anal Calorim (2014) 115:1679–1691
DOI 10.1007/s10973-013-3394-7

Thermal decomposition kinetics, flammability, and mechanical property study of wood polymer nanocomposite

Ankita Hazarika · Tarun Kumar Maji

Received: 22 February 2013 / Accepted: 30 August 2013 / Published online: 9 October 2013

Abstract Melamine formaldehyde-furfuryl alcohol copolymer was impregnated into softwood in combination with 1,3-dimethylol-4,5-dihydroxy ethyleneurea, a cross-linking agent, nanoclay, and a renewable polymer, collected as gum from a local plant (*Moringa oleifera*) under vacuum condition and polymerized by catalyst heat treatment. Fourier-transform infrared spectroscopy, X-ray diffractometry, and scanning electron microscopy were used to characterize the nanocomposites. Transmission electron microscopy showed uniform distribution of nanoclay in the composites. The mechanical properties were improved after the addition of plant polymer. The plant polymer had a marked influence on the flammability and thermal stability of the prepared composites. The apparent activation energy was determined by Ozawa-Flynn-Wall's and Vyazovkin methods. The activation energy of the composites decreased up to a certain decomposed fraction thereafter it remained constant. Higher the plant polymer content higher was the activation energy of the prepared composites which indicated a better interfacial adhesion and thermal stability.

Keywords Nanocomposites · Plant polymer · Flammability · Thermal stability · Activation energy

Introduction

Wood polymer composites (WPC) have evoked considerable interest as one of the rapidly growing industries in recent years. The hydrophilic nature of polymer constituents of cell wall of wood is responsible for exhibiting hygroscopic behavior. Excessive moisture can lead to shrinking and swelling of wood and results in fungal attack causing changes of color and finally degradation of wood. To enhance the long-term service life, chemical modification of wood can be made with various monomers and thermoset resins [1, 2].

Increased awareness of wood preservatives on environmental effect has rendered special importance to furfuryl alcohol as an eco-friendly agent for wood modification. Furfuryl alcohol causes wood cell wall to swell and sufficiently polar so that they enter wood cell walls [3]. Mantanis et al. [4, 5] have reported that low molecular volume monomers that are capable of forming hydrogen bonds swell the cell wall of wood permanently. Impregnation of wood with furfuryl alcohol would lead to considerable improvement in properties such as hardness, density, equilibrium moisture content, dimensional stability, and durability [6, 7]. Nevertheless, furfurylation does not have marked influence on the bending strength and the modulus of elasticity (MOE) of wood [8].

Modification of wood with melamine formaldehyde resin can significantly improve the mechanical properties of wood [9]. Besides, it contains nitrogen and as a result it can influence thermal properties and flammability of the prepared composites. A copolymer of melamine formaldehyde and furfuryl alcohol (MFFA) has been prepared with the intend of getting overall benefits of the properties.

There is a continuous effort to enhance thermal stability and flame retardancy of wood to expand its utility. Flame retardancy can be achieved by the use of organohalogen, organophosphorus, organoantimony compounds, various silicates and borates compounds [10, 11]. While

A. Hazarika · T. K. Maji (✉)
Department of Chemical Sciences, Tezpur University,
Tezpur 784028, Assam, India
e-mail: tkm@tezu.ernet.in

Defence Science Journal, Vol. 64, No. 3, May 2014, pp. 262-272, DOI : 10.14429/dsj.64.7325

REVIEW PAPER

Modification of Softwood by Monomers and Nanofillers

Ankita Hazarika and Tarun K. Maji*

Department of Chemical Sciences, Tezpur University, Assam-784 028, India
**E-mail: tkm@tezu.ernet.in*

ABSTRACT

Technological development of wood polymer composites (WPC) is a very promising approach to overcome most of the disadvantageous properties of wood products, for example their poor mechanical strength, poor dimensional stability, susceptibility to fungal attack, weathering and the like. To find the substitute for costly items of hard wood, suitable technologies have been developed to modify softwood to meet specific end-use requirements. Various vinyl monomers and/or copolymers or thermosetting resin in combination with different types of cross linking agents, flame retarding agents have been used to improve the properties of wood. Nanotechnology is a new area of science and technology which opens up new opportunities to develop wood based products with desired properties. Now-a-days government is making strict legislations to promote green technology for the protection of environment worldwide. With the depletion of petroleum resources at alarming rate, it is high time to replace petroleum-based products by some sustainable alternative products based on vegetable biomass. The bio-based resins obtained from renewable feedstock have been widely utilized by taking the advantages of easy availability, renewable nature and low cost. The green route of modification of wood is widely encouraged. With the progress of technological development, now it is possible to avoid the hazardous influence of organic solvents by using water as solvent or diluents for modification of wood. WPC has got tremendous scope for use in diverse areas of applications.

Keywords: Nanocomposites, green technology, wood, renewable resource, environment, characterization of properties

1. INTRODUCTION

Wood is a unique and renewable resource material that has been an important substance since time immemorial of human civilization because of its easy availability unique aesthetic look and useful properties[1]. It can be reaped sustainably at a constant rate without depleting the existing resource pool. Because of the influence of increasing human activities on the environment, awareness of the society on the environment is rapidly increasing, thus environmental considerations have given due attention to effect a change in the way of utilization of materials for various purposes. Thus, chemical industries are seeking to manufacture products with minimal environmental impact. Scientists have been working to improve the utilization of raw material, reduce production inefficiencies and develop more sustainable industrial practices. The widespread occurrence, stability, hardness, lightness, elasticity and as perspective potential renewable material make wood an important raw material sources[2]. Natural look and versatility make wood a class of material for various purposes of applications. It has wide range of applications to make items like paper, pulp, construction of materials and as resource material for energy generation[3].

Wood is a natural polymeric composite consisting of cellulose, hemicelluloses and phenolic polymers of lignin. The cellulose is a polymer of D-glucopyranose units linked together by β(1→4) glycosidic bonds. Hemicelluloses are heteropolysaccharides having a lower degree of polymerization (DP) than cellulose of about 100-300. Cellulose is more ordered than hemicellulose, although some hemicellulose can form crystalline units. Water present in atmospheric moisture can easily form hydrogen bonding with the free hydroxyl groups in cellulose resulting in shrinking and swelling of wood depending upon its moisture content. Lignins have the least water sorption tendency and are amorphous, highly complex, mainly aromatic, polymers of phenylpropane units[4]. Lignin is associated with hemicelluloses through covalent bond forming lignin-carbohydrate complexes but there is no evidence of their association with cellulose. Thus, the hydroxyl groups present in the cell wall of wood are the most abundant reactive and vulnerable chemical site[3].

Mechanical anisotropy arises in wood due to its highly heterogeneous structure. Among the numerous applications, the utilization of wood in particular for flooring and hard wearing wood surfaces preferably need an improvement of strength and elasticity in the direction normal to the grain. Hence strength in lateral direction is most desirable. The success of trees as

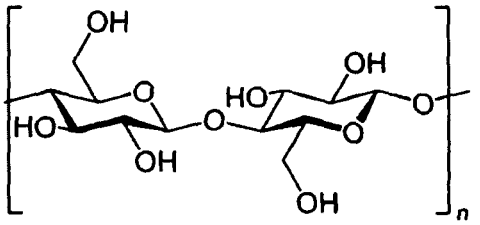

Figure 1. Chemical structure of cellulose.

Received 5 December 2013, revised 24 February 2014, online published 20 May 2014